

AD 691974

# U.S. ARMY FOREIGN SCIENCE AND TECHNOLOGY CENTER



THERMOELECTRIC COOLING DEVICES

SEP 2 1969

COUNTRY: USSR

## TECHNICAL TRANSLATION

This document has been approved  
for public release and sale;  
its distribution is unlimited.  
It may be released to the  
Clearinghouse, Department of  
Commerce, for sale to the  
general public.

Reproduced by the  
CLEARINGHOUSE  
for Federal Scientific & Technical  
Information Springfield Va 22151

# NOTICE TO USERS

Portions of this document have been judged by the Clearinghouse to be of poor reproduction quality and not fully legible. However, in an effort to make as much information as possible available to the public, the Clearinghouse sells this document with the understanding that if the user is not satisfied, the document may be returned for refund.

If you return this document, please include this notice together with the IBM order card (label) to:

Clearinghouse  
Attn: 152.12  
Springfield, Va. 22151

**BEST**

**AVAILABLE**

**COPY**

TECHNICAL TRANSLATION

FSTC-HT-23- 435-68

THERMOELECTRIC COOLING DEVICES

by

Ye. A. Kolenko

SOURCE: TERMOELEKTRICHESKIYE CKHLAZHDAYUSHCHIYE  
PRIBORY  
pp. 1-257, 1967  
USSR

Translated for FSTC by ACSI

This translation is an unedited rendition of the original foreign text. Statements or theories advocated or implied are those of the source and do not reflect the position or opinion of the US Army Foreign Science and Technology Center. This translation is published with a minimum of copy editing and graphics preparation in order to expedite the dissemination of information. Requests for additional copies of this document should be addressed to the Defense Documentation Center, Cameron Station, Alexandria, Virginia, ATTN: OSR-2.



Cyrillic	Transliteration	Page
онr	opt	7
р	cr	17
э	el	17
б	b	17
	d	18
ср	AV	88
ст	Sta	90
мин	min	101
в	wa	103

## TABLE OF CONTENTS

PREFACE	1
INTRODUCTION	3
PART I.	
THE THEORY OF THERMOELECTRIC COOLING	
Chapter I. The Basic Energy Relationships	
§1. Maximum Temperature Reduction	5
§2. The Coefficient of Performance	11
§3. Multi-Stage Thermopiles	13
Chapter II. Materials for Thermoelements	
§1. The Conditions of Maximum Thermoelement Effectiveness	17
§2. The Choice of Materials for the Arms of Thermoelements	22
§3. Bismuth Telluride as a Material for Thermoelements	27
Chapter III. The Consideration of Additional Factors	
§1. A Consideration of Electron Heat Conductivity	33
§2. A Consideration of Thompson Heat in the Thermoelement Energy Balance	35
§3. Deviations from Optimum Conditions	39
Chapter IV. Thermogalvanometric Methods of Cooling	
§1. Thermoelectric Cooling at Low Temperatures	43
§2. Thermoelectric Cooling in a Magnetic Field	45
§3. Thermomagnetic Cooling (the Ettinghausen Effect)	47
PART II	
ENGINEERING PROBLEMS IN THERMOELECTRIC COOLING TECHNOLOGY	
Chapter V. The Fundamentals of the Design of Thermoelectric Cooling Devices	
§1. Thermopile Operating Conditions	53
§2. Thermopile Design	56
§3. The Design of a Radiator for Heat Extraction	60
Chapter VI. The Construction Elements of Thermoelectric Cooling Devices	
§1. An Individual Thermoelement	62
§2. Multi-stage Thermoelement	64
§3. A Thermoelectric Pile	67
§4. The Heat Coupling of the Thermopile	71
§5. The Design of Heat Transfer Systems	77
§6. The Operating Chamber of the Device	81
Chapter VII. Methods of Heat Removal From Thermocooling Devices	
§1. A Radiator System with Natural Convection Heat Exchange	84

§2. A Radiator System with Forced Heat Removal	88
§3. Spike Radiator Systems	92
§4. A Liquid System with Natural Circulation	95
§5. Employment of the Latent Heat of Fusion	99
§6. Utilization of the Latent Heat of Vaporization	101
§7. A Heat Transfer System Utilizing Specific Heat	104
§8. The Utilization of Solutions with a Low Cryohydrate Temperature	106
Chapter VIII. Power Supplies for Thermoelectric Cooling Devices	
§1. Rectifiers	111
§2. Storage Batteries	118
§3. Current Converters	121
§4. Thermoelectric Generators	123
Chapter IX. Several Problems in the Technology of the Manufacture of Thermo-Cooling Devices	
§1. The Manufacture of Thermoelement Arms	127
§2. The Tinning of Thermoelement Arms	131
§3. Thermopile Connections	134
§4. Other Technological Considerations	137
PART III.	
THERMOELECTRIC COOLING IN PRACTICE	
Chapter X. High-Vacuum Collectors With Thermoelectric Cooling	
§1. Purpose	144
§2. Thermoelectric Collectors for the Unified Series of Pumps	149
§3. A Thermoelectric Collector for Mercury-Vapor Pumps	160
§4. Thermoelectric Collectors for Automatic Evacuation Devices	162
Chapter XI. Thermoelectric Coolers for Radiant Energy Receivers	
§1. Microthermostat Systems for Cooling Photoconductive Cells	167
§2. A Microthermostat System for Bolometer Cooling	176
§3. A Thermoelectric Cooler for Radiation Balance-Meters	178
§4. Thermoelectric Coolers for Photomultipliers	180
Chapter XII. Thermoelectric Cooling Devices for Medicine	
§1. A Thermoelectric Cataract Cryoextractor	190
§2. A Device for Thermal Stimulation of the Skin--A Thermod	196
§3. A Microrefrigerator for the Treatment of Skin Diseases	200
§4. Microtomic Stages with Thermoelectric Cooling	202
§5. A Cooler For Plastic Surgery	205
Chapter XIII. Thermoelectric Devices for Radioelectronics	
§1. A Microthermostated Device for Radioelectronic Devices	210
§2. A Thermoelectric Ultrathermostat System	215
§3. A Thermoelectric Cooler for a Parametric Amplifier	219
§4. A Thermoprobe	221

Chapter XIV. General Purpose Thermoelectric Refrigerators.	
§1. Microrefrigerators for Laboratory Purposes	225
§2. Experimental Thermoelectric Microchambers	233
§3. Thermoelectric Condensation Hygrometers	237
§4. A Device for Thermometer Calibration	246
§5. Thermoelectric Null-Thermostat Systems	248
§6. Microscope Stages with Regulated Temperatures	254
Chapter XV. Thermoelectric Conditioners and Domestic Refrigerators	
§1. Conditioners for Official Purposes	262
§2. Conditioners for Domestic Purposes	267
§3. High-Capacity Domestic Refrigerators	269
§4. A Low-Volume Domestic Refrigerator	277
Chapter XVI. Devices for Various Purposes	
§1. Refrigerators for Stock-Raising	281
§2. A Thermostat System for the Coke-Oven Gas Industry	289
§3. A Refrigerator With A Detachable Thermopile	293
§4. A Thermoelectric Temperature Stabilizer for Photographic Solutions	295
§5. Thermoelectric Devices for the Determination of the Pour Points of Petroleum Products	297
§6. A Thermoelectric Milk Cooler	305
§7. A Thermoelectric Drinking-Water Cooler	310
BIBLIOGRAPHY	312

## THERMOELECTRIC COOLING DEVICES

### PREFACE

The development of science and technology during recent years has been characterized by wide-spread usage of artificial cooling methods. Comparatively recently artificial cold was most effectively produced by Freon refrigerating machines which completely fulfilled practically all requirements. During the past ten years, however, qualitatively new demands have been made on refrigerators which cannot be met by Freon installations. The choice of a refrigerator will also determine overall dimensions and weight characteristics, power requirements, the possibility of reliable operation under the influence of static and dynamic overloads, the length of service life and a series of other factors. Many of these factors cannot be satisfied by compressor refrigerators.

Therefore, the great amount of interest which the new branch of refrigeration engineering--the technique of thermoelectric cooling--has attracted, is fully understandable. If several years ago thermo-electric cooling devices were only pictorial representations of a new method of obtaining cold, then at the present time numerous organizations both in the USSR and abroad are engaged in the development and industrial manufacture of various types of thermo-electric cooling devices. Numerous articles appear in the press every year devoted to the technique of thermo-electric cooling. However, there is not a single textbook which generalizes the experience in engineering design, construction and the technology of manufacturing thermo-electric devices.

The author's book "Thermoelectric Cooling Devices", published in 1963, was an attempt to fill an existing omission in the reference materials on thermoelectric cooling. The basis of the book was work accomplished mainly at the Institute of Semiconductors of the Academy of Sciences of the USSR and at several organizations during the period from 1956 to 1961. Considering the large amount of interest in thermoelectric instruments manufactured on the part of numerous organizations,

the decision was made to reprint the book "Thermoelectric Cooling Devices." Included in the second edition, significantly revised and expanded, are the results in investigations and developments prior to 1966.

In the first part of the book, which is devoted to the physical nature of thermoelectric cooling, chapters have been added concerning thermogalvanomagnetic cooling methods concerning materials for thermoelements and other materials. The third part contains a significantly expanded description of thermoelectric devices intended for use in various sectors of scientific and production activity.

Many of the devices described were developed by the author with the outstanding creative participation of P. S. Vinogradov, G. M. Voronov, A. M. Ivanov, I. I. Komarov, V. S. Kutogribov, I. V. Enken, B. I. Tsirkel, M. A. Zakrevska.

A visual hygrometer was developed by V. P. Rybal'schenko. A refrigerator for stock-raising with liquid heat removal was created by M. A. Kaganov, Ye. A. Kolenko, I. G. Mushkin, and A. F. Chudnovskiy. Thermoelectric null-thermostats were constructed by A. N. Voronin, E. M. Shero, and A. G. Shcherbina. The inventors of a thermostat for the determination of naphthalene in coke-oven gasses were A. N. Voronin, and A. G. Shcherbina. A thermostat for photographic solutions was developed by A. N. Voronin, E. M. Shero, and A. G. Shcherbina. A thermoelectric refrigerator for cooling milk on dairy farms was created by S. P. Bardeyeva, I. A. Ioffe, M. A. Kaganov and A. S. Chudnovskiy. A thermoelectric cooler for radiation balance meters was designed by V. P. Rybal'chenko. A refrigerator with a detachable battery was developed by I. S. Lisker and A. S. Chudnovskiy. The author takes this opportunity to express his gratitude to numerous people for materials courteously presented for this work. The author also expresses his sincere gratitude to I. D. Gusenkova for selection and formulation of the materials of the book and to T. N. Dunayeva, who took upon herself the labor of checking the manuscript.

## INTRODUCTION

The effect of thermoelectric cooling was first discovered and described in 1834 by the French physicist Jean Peltier. This phenomenon, having obtained the name of the Peltier effect, consists of the fact that during the flow of the constant electrical current in a certain direction through an electrical circuit consisting of diverse conductors, a certain quantity of heat is absorbed at the junction of the conductors, and the junction is, therefore, cooled.

The subsequent work of investigators, in attempting to explain the nature of the Peltier effect, revealed that the quantity of the heat absorbed at the junction of the conductors is proportional to the strength of the current, to the duration of the flow, and to a certain coefficient which depends on the physical-chemical properties of the circuit conductor material.

Notwithstanding the fact that since the time of the discovery of the effect of thermoelectric cooling more than 130 years have passed, its practical application has become possible only during recent years. This situation finds an explanation in the fact that a great deal of importance was not attached to this effect earlier since the cooling effect, generated at the junction of the diverse metals, was quite small.

In 1911 the German physicist Altenkirch, in attempting to formulate a theory of thermoelectric cooling for metallic thermocouples, came to the conclusion that the practical use of this phenomenon would not be advantageous.

As a result of many years of work, the academician A. F. Ioffe and his colleagues in 1950 formulated a theory of power application of thermoelectricity, having established the conditions and having indicated the path for the creation of highly-effective transformers on the basis of semiconductor materials. At the present time, intermetallic alloys serve as materials for this purpose on the basis of bismuth telluride and several of its solid solutions. The creation of highly-effective semiconductor materials for the arms of the thermoelements permitted an approach to be made toward the technical realization of the Peltier effect.

For the first time in world practice, engineering designs for thermoelectric cooling devices were formulated in 1957 at the Institute of Semiconductors of the Academy of Sciences of the USSR. Recently more than 100 thermoelectric devices, of various design and for various

purposes, were developed at the institute. Among these were devices intended for use in astronomy and botany, nuclear physics and agriculture, vacuum technology, and archeology, meteorology and medicine, electronics, and a whole series of other fields of science. Many of the devices developed in the course of several years are now being produced by native industry, which has laid a foundation for a new branch of refrigeration engineering--that of thermoelectric instrument manufacture.

Such high interest in this new branch of technology is explained by the fact that thermoelectric cooling has opened qualitatively new methods in the creation of small-sized devices, intended for the reduction and stabilization of temperature in small areas or for the creation of local, strictly regulated sources of cold, which if applied through the utilization of previously existing methods of artificial cooling would not be economically advantageous or technically feasible.

In thermoelectric devices it is possible by changing the value of the supply current to change smoothly the temperature and rate of cooling, and by changing the direction of current flow to convert the apparatus from a cooling to a heating cycle, which permits changing the temperature in accordance with an established program.

The theory and practice of thermoelectric cooling was first developed in the USSR. Our priorities in this area are protected by 68 foreign patents.

The reader who is interested in the development of the technology of thermoelectric instrument manufacture abroad may find corresponding references in the list of references at the end of the book.



## PART I. THE THEORY OF THERMOELECTRIC COOLING

### Chapter I. The Basic Energy Relationships

#### Section I. Maximum Temperature Reduction

The basis of any thermoelectric cooling device is the elementary thermoelement, which is a series connection of two semiconductor arms (figure 1), one of which possesses electron (n) conductivity, and the other, p-type conductivity.<sup>1</sup>

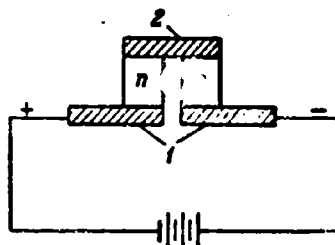


Figure 1. Diagram of an Elementary Thermoelement.

During the passage of a direct electric current through the thermoelement in the direction indicated on the drawing, a difference in temperature is generated between the connecting slabs 1 and 2, which form the junction of the thermoelement, and which is caused by the release (at junction 1) and by the absorption (at junction 2) of Peltier heat.

If, in this connection, as a result of heat transfer, the temperature of junction 1 is maintained at a constant level, the temperature of junction 2 is reduced to a certain defined value. With a given current, the value of the temperature reduction depends on the heat load on it. This load is composed of the heat influx from the surrounding medium, from the heat passing from junction 1, due to heat transfer from the thermoelements comprising the arms, and from Joule heat, released in the arms of the thermoelement during the passage of current through them.

<sup>1</sup> In further discussion of the relationships characterizing the operation of thermal cooling devices, we shall not examine the thermopile, which consists of a group of series or parallel connected thermoelements, but the individual thermoelements, which from a qualitative point of view does not change the main point.

Joule heat substantially influences the operation of the thermoelement. In fact, if the Peltier heat absorption is proportional to the first stage of the current intensity, i.e.

$$-Q_{pe1} = III_1,$$

then the heat released in the thermoelement due to the Joule effect is proportional to the square of the current intensity:

$$+Q_{JO} = I^2 R l.$$

Calculation reveals that in a first approximation, approximately half of the Joule heat passes to the cold junction of the thermoelement, which correspondingly decreases the cooling effect. Figure 2 shows the dependence of the heat which passes to the cold junction of the thermoelement due to the Joule ( $Q_1$ ) effect and subtracted from the junction as a result of the Peltier ( $Q_2$ ) effect on the value of current  $I$  supplied to the thermoelement.

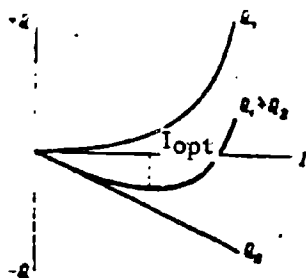


Figure 2. Dependence of Joule ( $Q_1$ ) and Peltier ( $Q_2$ ) Heat Quantity Released at the Cold Junction of the Thermoelement on Current ( $I$ ).

Since both effects take place in one electrical circuit, in combining them algebraically, we obtain a resultant curve which characterizes the heat balance of the thermoelement at various values of supply current.

The current has a minimum which corresponds to optimum current  $I_{opt}$ , at which the maximum temperature reduction is obtained at the cold junction of the thermoelement. Due to the amount of slope of the curve minimum, the maximum cooling created by the thermoelement does not show a marked dependence of the value of the current supplied. In operating designs of thermal cooling devices, a change in current intensity by  $\pm 10\%$  from the optimum value has practically no influence on the degree of cooling.

However, a noticeable increase in current intensity above the optimum value leads to a decrease in the cooling effect as a result of an increase in Joule heat. A further increase in current intensity may cause the Joule heat to exceed Peltier heat, and cooling of the junction in this case would be transformed into heat.

In order to find the optimum current value we shall write an equation for the sum of the Joule and Peltier heats, appearing at and being absorbed at the cold junction of the thermoelement per unit time.

$$Q = -\Pi_{1,2}J + \frac{1}{2}IR^2, \quad (1)$$

Where  $\Pi_{1,2}$  is the Peltier coefficient of the thermoelement, consisting of semiconductors 1 and 2 ( $R$  is the resistance of the thermoelement, defined by link  $l$ , by specific resistance  $\rho_1$  and  $\rho_2$  and by sections  $S_1$  and  $S_2$  of the arms of the thermoelement, as follows:

$$R = l \left( \frac{\rho_1}{S_1} + \frac{\rho_2}{S_2} \right). \quad (2)$$

After differentiation (1), we find that  $Q$  achieves a maximum with optimum current

$$I_{opt} = \frac{\Pi_{1,2}}{R}, \quad (3)$$

from which

$$Q_{max} = \frac{\Pi_{1,2}^2}{2R}. \quad (4)$$

From (4) it follows that the lower the resistance of the thermoelement, the higher the heat quantity  $Q_{\max}$ , which may be absorbed on the cold junction, i.e., the higher the refrigeration capacity. From this it is possible to conclude that by increasing the section or by decreasing the length of the arms of the thermoelement, it would be possible to obtain lower temperatures. In fact, this is not exactly right, since an increase in heat conductivity in the thermoelement is accompanied by a proportional heat flux increase in the arms. Calculation reveals that the optimum current and refrigeration capacity depends on the geometric dimensions of the thermoelement, or more exactly on the ratio of the section of the arms to the length; the maximum temperature reduction, as will be apparent from further discussion, as a whole is determined by the Peltier coefficient, by the specific heat conductivity and by the electrical conductivity of the arms of the thermoelement.

Thus it follows from formula (4), that the quantity of heat absorbed at the cold junction of the thermoelement, or, as it is convenient to term it, the refrigerating capacity, is inversely proportional to the resistance of the thermoelement arms.

We shall determine the conditions under which the thermoelement creates a maximum temperature reduction.

Heat absorbed at the cold junction of the thermoelement which is in a steady-state condition must be equal to the heat load, which is made up, as has been pointed out earlier, of the heat flux from the hot junction of the thermoelement as a result of heat conductivity  $Q_x$  of the semiconductors and heat flux  $Q_0$  on the cold junction from the surrounding medium, i.e.,

$$Q = Q_x + Q_0$$

In order to simplify the reasoning involved, we shall consider that the cold junction of the thermoelement is thermally isolated, i.e., that  $Q_0 = 0$ . Then,

$$Q = Q_x = \tau(T_0 - T)$$

or,

$$T_0 - T = \frac{Q}{\tau} \quad (5)$$

where  $x$  is the heat conductivity of the thermoelement.

$$x = \frac{1}{l} (x_1 S_1 + x_2 S_2); \quad (6)$$

$x_1$  and  $x_2$  represent the specific heat conductivity of the arms. Therefore, in agreement with (4) and (5),

$$(T_0 - T)_{\max} = \frac{Q_{\max}}{x} = \frac{M_{1,2}}{2xR}. \quad (7)$$

Substituting in (7) the value for  $R$  and  $x$  from (2) and (6) and considering that

$$M_{1,2} = (a_1 - a_2) T,$$

where  $a_1$  and  $a_2$  are the coefficients of the thermoelectromotive forces of the materials of the thermoelements arms; we obtained

$$(T_0 - T)_{\max} = \frac{1}{2} \cdot \frac{(a_1 - a_2)^2 T^2}{(x_1 S_1 + x_2 S_2) \left( \frac{l_1}{S_1} + \frac{l_2}{S_2} \right)}. \quad (8)$$

We shall insert the symbols

$$\frac{S_2}{S_1} = m$$

and

$$\frac{(a_1 - a_2)^2}{(x_1 + x_2 m) \left( \frac{l_1}{m} + l_2 \right)} = \frac{(a_1 - a_2)^2}{x_2} = \frac{(a_1 - a_2)^2}{x} = z,$$

where

$$x_2 = (x_1 + x_2 m) \left( \frac{l_1}{m} + l_2 \right) = \frac{x}{z}.$$

Then, substituting these symbols in (8), we obtain

$$(T_0 - T)_{\max} = \frac{1}{2} z T^2. \quad (9)$$

Equation (8) reveals that the maximum temperature reduction is determined by the parameters  $\alpha$ ,  $\rho$  and  $x$  of the materials of the thermoelement arms, by the temperature  $T$  of the cold junction and by the ratio of the section  $m$  of the arms; simple calculations show that quantity  $z$  reaches a maximum value for the definite ratio of the arms:

$$m_0 = \left( \frac{s_2}{s_1} \right)_{\max} = \sqrt{\frac{s_1 b}{s_2}}; \quad (10)$$

Here,

$$z = \left[ \frac{(s_1 - s_2)}{\sqrt{s_1 s_2} + \sqrt{s_2 s_1}} \right]^2. \quad (11)$$

From (9) we may obtain the temperature of the cold junction in the form

$$T_{\max} = \frac{\sqrt{1 - 2T_0^2 z} - 1}{z}. \quad (12)$$

Figure 3 shows the dependence of the temperature difference  $(T_0 - T)$ , which is provided by the thermoelement, on value  $z$  of the substances utilized. The importance of this search for new thermoelectric materials with higher values of  $z$  is readily apparent from the movement of the curve.

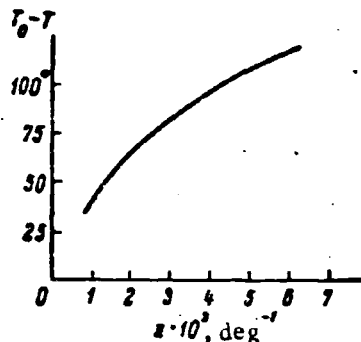


Figure 3. The Dependence of Maximum Temperature Difference  $(T_0 - T)$ , Furnished by the Thermoelement, on Value  $z$ .

## Section 2. The Coefficient of Performance

During our examination of conditions in which the thermoelement provided for a maximum temperature difference, the assumption was made that the heat load  $Q_0$  on the cold junction from the surrounding medium was lacking. However, under actual conditions a heat transfer occurs between the cold junction of the thermopile and the surrounding medium, the value of which is determined by the purpose and design of the thermal cooling device. In some cases, the heat load on the thermopile is furnished by those objects which must be reduced in temperature. In other words, the thermoelectric pile must carry off a certain quantity of heat  $Q_0$ , which enters its cold junctions.

In this case, the most important parameter which characterizes the effectiveness of the operation of the thermal cooling device is the coefficient of performance  $\epsilon$ , which is determined by the ratio of the quantity of heat drawn off per unit time by the thermopile to the electrical energy  $W$  expended:

$$\epsilon = \frac{Q_0}{W}. \quad (13)$$

With the presence of additional heat flux  $Q_0$ , which appears at the cold junctions, equilibrium occurs at temperature  $T$ , at which the full quantity of heat arriving at the cold junction, i.e. the sum of  $Q_0$ , the Joule heat and the heat flux occurring as a result of heat conductivity along the arms of the thermoelement balance the Peltier heat absorbed at the junction. Therefore, the conditions of equality may be written in the following form:

$$Q_{\text{Pel}} = (\alpha_1 - \alpha_2)II = \frac{1}{2}I^2R + \kappa(T_0 - T) + Q_0.$$

From which

$$Q_0 = (\alpha_1 - \alpha_2)II - \frac{1}{2}I^2R - \kappa(T_0 - T). \quad (14)^1$$

<sup>1</sup> The Thompson effect may be disregarded if the difference  $\alpha_1 - \alpha_2$  is an average value at temperature  $T = \frac{T_0 - T}{2}$ .

The power  $W$ , which is required by the thermoelement is made up of two parts: the Joule heat  $I^2R$  and the power expended in overcoming the thermoelectromotive forces generated in the thermoelement as a result of the Seebeck effect and opposite in polarity to the voltage supply to the thermoelement and are equal to

$$(\alpha_1 - \alpha_2)(T_0 - T)I,$$

i.e.,

$$W = I^2R + (\alpha_1 - \alpha_2)(T_0 - T)I. \quad (15)$$

Substituting the value  $Q_0$  and  $W$  (13), we have

$$\epsilon = \frac{(\alpha_1 - \alpha_2)TI - \frac{1}{2}I^2R - \epsilon(T_0 - T)}{I^2R + (\alpha_1 - \alpha_2)(T_0 - T)I}. \quad (16)$$

In this manner the coefficient of performance depends on the value of the current feeding the thermoelement.

It can be shown that the maximum value of the coefficient of performance is obtained when the current is

$$I = \frac{(\alpha_1 - \alpha_2)(T_0 - T)}{R[1 + 0.5z(T_0 - T) - 1]} \quad (17)$$

and the corresponding voltage drop equals

$$V = \frac{(\alpha_1 - \alpha_2)(T_0 - T)\sqrt{1 + 0.5z(T_0 - T)}}{\sqrt{1 + 0.5z(T_0 - T)} - 1}. \quad (18)$$

In this connection,

$$\epsilon_{\max} = \frac{T}{T_0 - T} \frac{\sqrt{1 + 0.5z(T_0 - T)} - \frac{T_0}{T}}{\sqrt{1 + 0.5z(T_0 - T)} + 1}. \quad (19)$$



It is important to note that the coefficient of performance depends on temperature difference  $T_0 - T$ , which is created by the thermoelectric battery and by value  $z$ , which characterizes the properties of the semiconductor substances utilized. With low temperature differences the coefficient of performance has a high value and when  $(T_0 - T) \rightarrow 0$  approaches infinity, and vice versa, with significant temperature differences the coefficient of performance approaches 0.

In many cases maximum refrigerating capacity  $Q_{\max}$  is demanded from thermoelectric cooling devices, sometimes even to the detriment of economy.

The maximum refrigerating capacity of the thermopile, in agreement with (3) is achieved when the current is

$$I_{\text{opt}} = \frac{(z_1 - z_2) T}{R}$$

and the voltage is

$$V_{\text{opt}} = I_{\text{opt}} R \div (z_1 - z_2) (T_0 - T) = (z_1 - z_2) T_0$$

and, in agreement with (4), equals

$$Q_{\max} = \frac{(z_1 - z_2)^2 T_0^2}{2R} \quad (20)$$

In a state involving the maximum coefficient of performance, the temperature difference which is created by the thermopile and in the presence of a heat load will equal

$$T_0 - T = (T_0 - T)_{\max} = \frac{Q_0}{z} \quad (21)$$

### Section 3. Multi-Stage Thermopiles

As we have pointed out earlier, a temperature difference is created between the cold and hot junctions of the thermoelement under the influence of a constant current. It is apparent that the temperature on the cold junction will depend on the temperature of the hot junctions. By lowering the temperature of the hot junctions by one method or another, we may achieve a lower temperature on the cold junction. One possible method of solving this problem is by using multi-stage thermopiles.

We shall examine as an example a principle construction involving a three-stage pile. The hot junctions of the upper stage of the thermoelement rest on the cold junctions of the thermoelements of the second stage. The hot junctions of the thermoelements of the second stage rest on the cold junction of the first stage. The thinnest possible electrically-insulated washers are placed between the thermoelements. Every thermoelement forms an independent electrical circuit. With this arrangement, the cold junction of the lower thermoelement accepts heat from the hot junction of the middle element, and the cold junction of the middle thermoelement cools the hot junction of the upper thermoelement. Here the refrigerating capacity of each stage must be able to provide an effective heat takeoff from the overlying stages.

One of the basic parameters of a multi-stage thermoelement--the coefficient of performance--is determined in the following manner. Let  $Q_1$  represent the refrigerating capacity of the first stage,  $\epsilon_1$  the coefficient of performance, and  $W_1$  the required power from the source. Corresponding values for the second stage are designated by  $Q_2$ ,  $\epsilon_2$ , and  $W_2$ , etc. Then, in agreement with (13), the power required for the first stage will equal

$$W_1 = \frac{Q_1}{\epsilon_1}.$$

The second stage must have the refrigerating capacity

$$Q_2 = Q_1 + W_1 = Q_1 \left(1 + \frac{1}{\epsilon_1}\right),$$

and for the third stage

$$Q_3 = Q_2 + W_2 = Q_2 \left(1 + \frac{1}{\epsilon_2}\right) = Q_1 \left(1 + \frac{1}{\epsilon_1}\right) \left(1 + \frac{1}{\epsilon_2}\right) \quad (22)$$

and for  $n + 1$  stage,

$$Q_{n+1} = Q_1 \left(1 + \frac{1}{\epsilon_1}\right) \left(1 + \frac{1}{\epsilon_2}\right) \dots \left(1 + \frac{1}{\epsilon_n}\right).$$

But  $\epsilon^{(n)}$  is made up of two parts--the power required by the entire thermopile  $W = W_1 + W_2 + \dots + W_n$ , and its refrigerating capacity  $Q_1$ :

$$Q_{n+1} = W + Q_1 = Q_1 \left(1 + \frac{1}{\epsilon^{(n)}}\right). \quad (23)$$

where  $\epsilon^{(n)}$  is the coefficient of performance of the entire pile as a whole. A comparison of (22) and (23) gives us an equation for the coefficient of performance of the multi-thermopile:

$$1 + \frac{1}{\epsilon^{(n)}} = \prod_{i=1}^n \left(1 + \frac{1}{\epsilon_i}\right) \quad (24)$$

or

$$\epsilon^{(n)} = \frac{1}{\prod_{i=1}^n \left(1 + \frac{1}{\epsilon_i}\right) - 1} \quad (25)$$

The coefficients of performance  $\epsilon_i$  of the last stages may be different, since the effectiveness  $\epsilon$  of the thermoelement, generally speaking, depends on temperatures; in addition, the temperature drops at the various stages may also differ from each other; a steady-state condition is achieved for such a temperature difference at each stage when its refrigerating capacity becomes equal to the quantity of heat passing to the stage from the preceding stage.

An analysis of equation (25), however, reveals that with a given number of stages ( $n$ ) and a temperature differential for the entire thermopile

$$\Delta T = \Delta T_1 + \Delta T_2 + \dots + \Delta T_n$$

The coefficient of performance of the entire thermopile ( $\epsilon^{(n)}$ ) achieves a maximum, if

$$\epsilon_1 = \epsilon_2 = \dots = \epsilon_n = \epsilon_0. \quad (26)$$

The coefficient of performance  $\epsilon_i$  of the  $i$ -th stage is determined by the temperature differential  $\Delta T_i$  at this stage, but the temperature differential at a given (with a preceding stage) refrigerating capacity is determined by the dimensions of a given thermopile; they must, therefore, be chosen in order to fulfill the conditions (26). Here the conditions are

$$\epsilon^{(n)} = \frac{1}{\left(1 + \frac{1}{\epsilon_0}\right)^n - 1}. \quad (27)$$

In particular, for a two-stage pile, (27) gives:

$$\epsilon_2 = \frac{1}{\frac{1}{\epsilon_1} + \frac{2}{\epsilon_0}} = \frac{\epsilon_1 \epsilon_0}{2\epsilon_0 + \epsilon_1} \quad (28)$$

Figure 4 shows the dependence of the coefficient of performance on the temperature difference for a one- and two-stage pile.

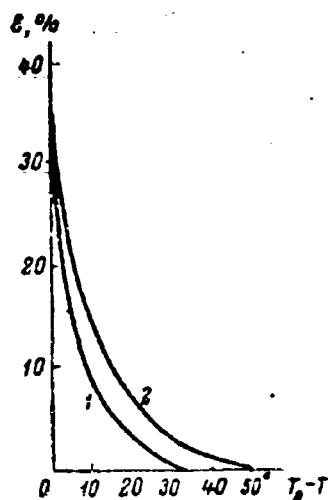


Figure 4. The Dependence of Coefficient of Performance ( $\epsilon$ ) on Temperature Difference ( $T_0 - T$ ) for Single-Stage (1) and Two-Stage (2) Thermoelements.

It is apparent from the graph that the superiority of the two-stage thermoelement in comparison to the single-stage element is particularly noticeable with small values of  $\epsilon$ . However, when it is desired to obtain the maximum temperature reduction without considering thermoelement power requirements, it is possible to utilize two-stage and rarely three-stage thermoelements. The employment of thermoelements with a number of stages higher than three is considered to be impractical, since the refrigeration

capacity of the third stage would already be so low that the utilization of such a thermoelement under actual conditions would not be possible. In addition, it is necessary to keep in mind that due to the temperature dependence  $z$ , the temperature differential created by the separated states decreases in proportion to the square of the increase in the quantity of stages.

If we add to this the fact that the creation of three-stage thermoelements is connected with significant design difficulties then it becomes clear why thermoelements consisting of less than three stages are widely employed.

## Chapter II. Materials for Thermoelements

### Section 1. The Conditions of Maximum Thermoelement Effectiveness

The parameters of the matter determining the quantity  $z$ , such as the thermoelectromotive force coefficient  $\alpha$ , specific electrical conductive  $\sigma$  and specific heat conductivity  $\kappa$  are functions of the concentrations of free electrons (or holes). This dependence is represented qualitatively in figure 5. Electrical conductivity is proportional to  $n$ ; the thermoelectromotive force, on the other hand, approaches 0 with an increase in the number of carriers. Heat conductivity is made up of two parts: the heat conductivity  $\kappa_{cr}$  of the crystal lattice and electron heat conductivity  $\kappa_{el}$ , therefore,  $\kappa = \kappa_{cr} + \kappa_{el}$ . In a first approximation, lattice conductivity does not depend on  $n$ , but  $\kappa_{el}$  is proportional to  $n$ .

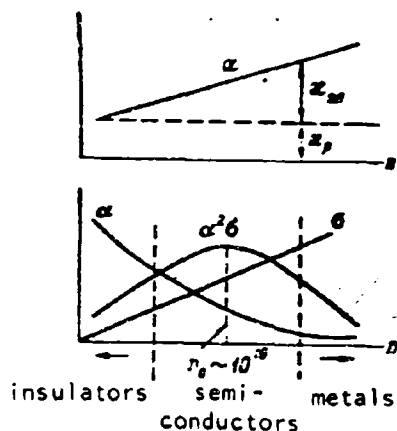


Figure 5. Qualitative Dependence of Electrical Conductivity ( $\sigma$ ) Thermoelectromotive Force Coefficient ( $\alpha$ ) and  $\alpha^2 \sigma$  on the Value of Carrier Concentration ( $n$ ).

In metals and metallic alloys the value  $z$  is very small as a result of a low thermoelectromotive force coefficient, and in dielectrics it approaches 0 due to insignificantly small electrical conductivity; in the area of semiconductors the carrier concentrations  $z$  reach a maximum value. These qualitative considerations permit us to understand why the effectiveness of metallic thermocouples is very low; this also explains why thermoelectric generators and refrigerators up until recent times found no widespread application in technology. If we employ semiconductors (or more exactly semimetals) (see below) as materials for the arms of thermocouples and select among these in a corresponding fashion a concentration of electrons (or holes, if we are dealing with a positive arm), we may increase the effectiveness of thermoelements by ten times.

In order to establish a quantitative formulation of these considerations, we must employ equations for the thermoelectromotive force coefficient, for electrical conductivity and heat conductivity and place these in an equation for  $z$  and for the extreme condition

$$\frac{dz}{dn} = 0$$

to find the optimum carrier concentration (electrons or holes)  $n_0$ , at which  $z$  attains a maximum.

We must obtain a solution in analytical form, and for this purpose we shall make two assumptions, which will simplify solving the problem.

1. It is apparent from figure 5 that the maximum numerical expression for  $z$  lies in the area of carrier concentration of the order of  $10^{19} \text{ cm}^{-3}$ . i.e., it is approximately 1,000 times less than the concentration of free electrons in metals. That part of the electron conductivity which refers to the thermoconductivity of the crystal lattice under these conditions (usually) is no longer very great (whereas in metals  $\kappa_{el}$  plays a predominant role); therefore, in a first approximation, we may replace in the equation for  $z$  the full heat conductivity ( $\kappa = \kappa_{cr} + \kappa_{el}$ ) with the heat conductivity  $\kappa_{cr}$  of the crystal lattice;

$$z = \frac{A_2}{T_1}$$

and assuming that  $\kappa_{cr}$  does not depend on  $n$ , to find the maximum  $\alpha^2 \sigma$  (as a function of  $n$ ), and not  $z$ . The assumption that the heat conductivity of the lattice does not depend on the concentration of free carriers is, generally speaking, not very firm; in the first place, a change in the concentration of carrier (at a given temperature) always demands the introduction of impurities, and the latter cause additional scattering of phonons and reduce the heat conductivity of the lattice; secondly, the phonons scatter directly to the free electrons and holes; for this reason the heat conductivity of the crystal lattice of metals is significantly low. However, with carrier concentrations of the order of  $10^{19} \text{ cm}^{-3}$ , both these factors play a minor role, and we may, therefore consider  $\kappa_{cr}$  independent of  $n$ .

2. Let us assume further that with a carrier concentration corresponding to maximum value  $\alpha^2 \sigma$ , they (the carriers) are in a nondegenerate state, and therefore classical statistics are applicable to them. In this case, the fermi distribution function is replaced by the Maxwell distribution function

$$f \approx e^{-\frac{\epsilon - \mu^*}{kT}} \quad (29)$$

In the equations for the thermoelectromotive force, for the carrier concentration, electrical conductivity and heat conductivity are considerably simplified:  $\mu^*$ ,  $\alpha$ ,  $\sigma$  and  $\kappa_{el}$  may be expressed in the obvious form functions of  $n$ :

$$\mu^* = \ln \frac{k^3 n}{2(2\pi m k T)^{3/2}} \quad (30)$$

$$\alpha \approx \frac{k}{e} (r + 2 - \mu^*) = \pm \frac{k}{e} \left[ r + 2 + \ln \frac{2(2\pi m k T)^{3/2}}{k^3 n} \right], \quad (31)$$

$$\sigma = enU, \quad (32)$$

$$\kappa_{el} = (r + 2) \left( \frac{k}{e} \right)^2 T \sigma = AT \sigma, \quad (33)$$

Here  $\mu^* = \frac{\mu}{kT}$  is a so-called reduced chemical potential.

where

$$A = \frac{r}{r_c} = \left(\frac{k}{e}\right)^2 (r + 2).$$

Under these conditions, the problem of finding the optimum carrier concentration  $n_0$  and the maximum value  $\alpha^2 \sigma$  corresponding to it may be solved in a comparatively simple manner.

In the following discussions we shall make the assumption that the electron mobility does not depend on  $n$ , which strictly speaking, is not completely correct, since: 1) with an increase in  $n$ , the number of ionized donors simultaneously increases, and they are supplementary sources for electron scattering; 2) at large electron concentrations an increase in  $n$  (as a result of degeneration) results in an increase in electron energy which also influences  $U$  (since  $U$  is an energy function  $U = \frac{e\phi(\eta)}{mV}$ ). However, for a qualitative analysis, which is the purpose of our calculations, we may for the time being disregard these dependencies (the question of degeneration will be examined below).

In agreement with (31) and (32),

$$\alpha^2 \sigma = \frac{k^2}{e} \left[ r + 2 + \ln \frac{2(2\pi mkT)^{3/2}}{h^3 n} \right]^2 n U$$

The condition  $\frac{\partial (\alpha^2 \sigma)}{\partial n} = 0$  gives optimum carrier concentration  $n$  which corresponds to electrical conductivity  $\sigma_0$ ,

$$n_0 = \frac{2(2\pi mkT)^{3/2}}{h^3} e^{\eta}, \quad \sigma_0 = e U n_0 \quad (34)$$

and optimum thermoelectromotive force

$$\alpha_0 = 2 \frac{k}{e} = 172 \quad (35)$$

and here the equation for maximum value  $\alpha^2 \sigma$  assumes the following form

$$\alpha^2 \sigma_{\max} \approx 1.2 \cdot 10^{-2} \cdot U^2 \left( \frac{m}{m_0} \cdot \frac{T}{T_0} \right)^{3/2} e^{\eta} \quad (36)$$



and correspondingly the maximum value  $z$  has the form

$$z_{\max} \approx 1.2 \cdot 10^{-7} \frac{U}{T_0} \left( \frac{m}{m_0} \cdot \frac{T}{T_0} \right)^{1/2} e, \quad (37)$$

where  $m_0$  is the mass of the free electron, equal to  $9 \cdot 10^{-28}$  g, and  $T_0 = 300^\circ \text{ K}$ .

It is apparent from (34), that the optimum carrier concentration depends on a series of factors: the effective mass  $m$ , temperature  $T$  and maximum scattering  $r^2$ .

The optimum thermoelectromotive force ( $\alpha$ ), in agreement with (35), remains a constant for all substances and under all conditions. Therefore in the selection of the required carrier concentration, it is convenient to direct our attention to the value of the thermoelectromotive force, since its measurement is considerably simpler than measurement of the free electron concentration.

In agreement with (34), the optimum carrier concentration at which  $z$  achieves a maximum value is a function of temperature; therefore, the carrier concentration must be selected in agreement with the operating temperature range. From this point of view the most advantageous material for the construction of thermocouples would be a substance in which the electron concentration changed with temperature in accordance with the principle  $n_0 \sim T$  and thus the optimum condition (34) would be

satisfied in the entire operating temperature range of the thermocouple for any differential segment of its arm. Unfortunately, such substances do not exist in nature. In ordinary similar conductors in the region of impurity conductivity, the carrier concentration increases exponentially

in accordance with the law  $n \sim e^{-\frac{\Delta \epsilon_1}{kT}}$ , where  $\Delta \epsilon_1$  is the activation energy of the impurity levels, i.e., it is much more rapid than condition (34) requires.

Fortunately, to some extent nature does help us. The fact is that the activation energy ( $\Delta \epsilon_1$ ) of the impurities is not a constant, but as a general rule decreases with concentration  $N$  and usually when

<sup>2</sup>  $r$  is a value which reflects the nature of current carrier scatter: for atomic lattices  $r = 0$ , for ion lattices  $r = \frac{1}{2}$  to 1, and for scattering on impurity atoms,  $r = 2$ .

$N \sim 10^{18} \text{ -- } 10^{19}$  is reduced to 0. In this connection a semiconductor is transformed into a so-called semimetal: even close to absolute 0 all impurities are ionized, and the carrier concentrations remain constant ( $n = N$ ) down to the temperature at which characteristic conduction begins to appear.

Thus, if we employ semimetals with a sufficiently broad forbidden zone as materials for the arms of a thermocouple, then we may consider that the carrier concentration remains constant. In this connection, the condition (34) is not strictly fulfilled for the whole extent of the arm of the thermoelement and this leads to a certain reduction in effectiveness. However, since the temperature differential on the cooling thermocouple, as a rule, does not exceed several dozen degrees, the deviation from (34) and the corresponding losses in effectiveness usually do not exceed 10-20%. In this connection multi-stage piles acquire still another advantage: if the total operating drop is divided into small temperature differentials, then in each stage, the condition (34) may be satisfied in better agreement with the corresponding choice of impurity concentrations. This condition could also be fully fulfilled if a continuous change in the concentration of the impurities along the arms of the thermocouple were provided; however, this presents a great deal of technical difficulty, which, even up to the present time has not yet been overcome.

In agreement with (37), thermocouple ( $z$ ) effectiveness is proportional to the ratio of carrier mobility to crystal lattice heat conductivity;  $z$  has a maximum value with a certain carrier concentration. Thus, the analysis cited above reveals that the development of materials for the arms of thermoelements is reduced to the solution to the solution of the following basic problems:

- 1) the search for materials with a maximum ratio of carrier mobility to crystal lattice heat conductivity;
- 2) the creation in these substances of a carrier concentration corresponding to (34).

## Section 2. The Choice of Materials for the Arms of Thermoelements

The means of discovering materials with optimum properties, i.e., with a maximum ratio of carrier mobility to the crystal lattice heat conductivity, to a certain extent remains unclear, even at the present time. This is partly explained by a lack of experimental data, and partly by the lack of developed theory which might have predicted the substances in which a high degree of mobility of electrical carriers might be found.

However, contemporary electron solid-state theory still gives us certain indications in this regard, which we will attempt to set forth here.

As is known, electrons in their movement in an ideal periodic field experience no collisions. Such a field must exist in an ideal (i.e., having no structural defects) crystal at a temperature of absolute 0; in such a crystal electron mobility and hole mobility would be infinite. In existing crystals and in temperatures differing from absolute 0, the electrons are scattered by heat fluctuations and lattice defects; these scattering effects limit the length of the free path of the electrons and their mobility. We shall now digress from the existence of defects, since to a certain degree we may decrease their number, and therefore their influence on mobility by a corresponding choice in the technology of the preparation of materials<sup>3</sup> (the cleaning of initial materials, the growth of single crystals, annealing, etc.), and we shall examine a scattering of the carriers in lattice heat fluctuations.

In this connection, we must keep in mind that the electron scattering is not caused by thermofluctuations of the atoms themselves, but is due to their periodic potential breakdown. The more strongly the relief of the periodic potential is expressed, the stronger will be local fields generated as a result of heat fluctuations. Therefore, carrier mobility, as a rule, is low in ion crystals, in which potential relief is expressed most forcefully. On the other hand, in crystals with a covalent bond (in which there is no interchange of positively and negatively charged ions), carrier mobility is significantly higher. Among the latter type are the crystals of elementary semiconductors--silicon, germanium, gray tin in a series of intermetallic compounds--InSb, GaSb, AlSb, ZnSb, CdSb, etc.

We must note here that a sharp line does not exist between the covalent and ionic compounds. In fact, let us imagine that one of the atoms forming a binary compound gave up a certain quantity of electrons to the second atom and in this manner an ion molecule was formed. But, here the electron cloud of the negative ion will be deformed under the influence of the positive field and its center of gravity will be displaced in the direction of the latter. If the polarizability of the negative ion is high and the cloud is deformed sufficiently far to capture a positive ion with its edge, the bond will have a partially covalent character.

---

<sup>3</sup> This, by the way, does not refer to those defects which unavoidably arise when we introduce into the substance a certain quantity of donors or acceptors required to provide an optimum concentration of carriers.

In the same way, if one of the elements forming a covalent compound has an electron affinity greater than the second, then the center of gravity of the electron cloud which forms the covalent bond will be displaced toward the direction of the first element and the compound will be partially ionic.

A whole series of chalcogenides of metals of the fourth and fifth groups belong to this type of compound with an "almost" covalent bond ( $\text{PbS}$ ,  $\text{PbSe}$ ,  $\text{PbTe}$ ,  $\text{Bi}_2\text{Te}_3$ ,  $\text{Sb}_2\text{Te}_3$ ,  $\text{Bi}_2\text{Se}_3$ ); in these compounds carrier mobility also achieves rather high values.

A comparison of carrier mobility in a series of isomorphic crystals, for example  $\text{PbS}$ ,  $\text{PbSe}$ ,  $\text{PbTe}$ , reveal that here also a definite relationship is observed, namely that the mobility of both electrons and holes increases from lead sulfide to lead telluride, i.e., with the replacement of one of the components of the compound with its heavier analog. In this case it might be possible to think that the reason for the mobility increase was the decrease in the ionicity of the compound, since the electron affinity of tellurium is considerably less than that of sulfur.

But in fact, a decrease in ionicity only partly explains the relationship indicated above, since it is also observed in diamonds, silicon, germanium and gray tin, in which naturally there can be no consideration for ionicity.

A second reason for the increase in mobility during the passage to a heavier element is the fact that the polarizability of atoms (and ions) which are in the same sub-group of the periodic system, increases with an increase in their periodic number (i.e., with an increase in the dimensions of the electron shell of the atom and the number of electrons included within it). The heavier atoms are more strongly polarized under the influence of electrical fields (therefore the dielectric constant of germanium is approximately four times greater than for a diamond). But this pertains not only to external fields, but also to the inherent periodic field of the crystal; the electron clouds of the heavier atoms are to a large extent deformed under its influence, and in this manner the change in the periodic potential in the crystal is flattened out. The heavier the atoms forming the covalent crystal, the less directed and more diffused is the character of the covalent bonds, and the less positively expressed the potential relief in the direction perpendicular to the bond. It may be said that during the transition to the heavier atoms, "metallization" of the covalent bonds gradually occurs.

Free electrons in metals are also not distributed uniformly throughout the volume of the crystal, but move principally along "bridges" which connect neighboring atoms. Therefore, between the metallic and covalent bond there is no sharp line, as there is between the covalent and ionic. However, a fundamental difference in ionic and covalent crystals, on the one hand, and metallic ones, on the other, consists of the fact that in the latter case we are dealing with unfilled electron shells; therefore, electrons in metal may freely "jump" from one bridge to another and change the direction of their movement under the influence of an electrical field; this, roughly speaking, facilitates metallic conductivity. Another difference between the covalent crystals and metals is the small coordination number (i.e. the number of close neighbors of the atom). In covalent crystals, this fluctuates from two to four, and in metals from six to twelve.

In summing up what has been said above, it may be stated that high mobility values may be expected in covalent or "almost covalent" crystals, consisting of heavy atoms.

Let us explain now to what extent  $z$  depends on the effective mass of the carriers. The effective mass enters into the equation for  $z$  (37) first, obviously:  $z \sim m^{2/2}$  as a result of the dependence of the thermoelectromotive force on  $m$  (see equation (31)), and secondly, indirectly, since the mobility of the carriers also depend on their effective mass. In agreement with the theory, in crystals with an ionic bond,  $U \sim m^{-3/2}$ ,  $z$ , therefore, do not depend on effective mass. More importantly, in the case of covalent crystals  $U \sim m^{-3/2}$  and  $z$ , in agreement in (37), is inversely proportional to the effective mass.

This is about all that can be said at the present time concerning the choice of materials with a high degree of mobility. Even the qualitative conclusions made above, for example, concerning the dependence of  $U$  on  $m$ , cannot be considered to be conclusive, since the theoretical considerations at their base are not completely firm and experimental data thus far collected is too limited.

The situation concerning the search for materials with a low crystal lattice heat conductivity is somewhat better. Although a complete theory still does not exist at the present time which will give us a quantitative prediction concerning the heat conductivity of crystals, the qualitative theory developed by academician A. F. Ioffe permits us to make the following conclusions.

1. The heat conductivity of the crystal lattice is accomplished through the distribution of elastic waves and is limited by the scattering of these waves a) against each other and b) against crystal defects.

Just as in our examination of mobility, at first we shall consider that the number of defects in the crystal is relatively low and that we may disregard the scattering of heat waves by these defects.

If the forces connecting the atoms of the crystal conform strictly to Hooke's law, i.e. the force  $F$  would be directly proportional to the displacement of the atom from the position of equilibrium ( $x$ ), and the potential energy  $U$  to the square of the displacement:  $F = -fx$ ,  $U = \frac{1}{2}fx^2$ , within the oscillations of the atoms in the elastic waves would display a strictly harmonic (sinusoidal) character. Such waves, in the process of their propagation, do not interact with each other, and the heat conductivity of such a crystal would be infinite. In fact, however, atomic interaction has a more complex character; the potential energy as a function of displacement is described by the infinite series:

$$U = \frac{1}{2}fx^2 + \frac{1}{3}gx^3 + \dots \quad (38)$$

and the force is

$$F = -\frac{\partial U}{\partial x} = -fx - gx^2 - \dots \quad (38a)$$

The coefficient  $g$  in formulas (38, 38a) is called the coefficient of anharmonic oscillations. The higher the coefficient  $g$  and the amplitudes of oscillation  $x$ , the higher the value of the second element in (38), the more the oscillation deviates from the simple harmonic rule and interact with each other, the lower the crystal heat conductivity. In crystals with ionic bond, the anharmonicity of the oscillations is considerably greater than in covalent crystals, therefore, the heat conductivity in the former case is usually lower than in the latter.<sup>4</sup> The amplitude of the atomic heat oscillations increases with an increase in the heat content of the crystal or, in other words, with an increase in the number of phonons. The lower the Debye temperature of a given

<sup>4</sup> Anharmonicity of heat oscillation also appears in heat expansion crystals. Therefore, the value of the coefficient  $g$  may be judged also from the linear coefficient of heat expansion.

crystal, the higher its heat content at a given temperature and the lower the heat conductivity. But Debye temperature ( $\theta$ ) is linked with the mass (M) of the atoms forming the crystal and with the coefficient  $f$  in the expansion (38) by the relationship:

$$\theta \sim \sqrt{\frac{T}{M}}.$$

Therefore, low values of heat conductivity must be expected for substances consisting of atoms which are heavy and loosely bonded to each other. The value of the coefficient  $f$  may be determined from the Young modulus or, more directly, from the value from the heat of the formation of the crystal. In summarizing the foregoing, it may be stated that the heat conductivity of the crystal is proportional to the value of the Young modulus of the substance forming the crystal, and is inversely proportional to the atomic mass of the substance and its coefficient of heat expansion.

2. In any semiconductor substance, the ratio of carrier mobility to the heat conductivity of the crystal lattice may be increased through the introduction of neutral impurities. These impurities increase the effectiveness of the scattering of elastic waves, which leads to a decrease in the heat conductivity of the crystal. On the other hand, these neutral impurities need not exert any significant influence on the scattering of basic carriers. Many isomorphic compounds may serve as neutral impurities; they form solid solutions with the basic substance of the thermoelement.

### Section 3. Bismuth Telluride as a Material for Thermoelements

In recent years the most wide-spread material for the manufacture of thermoelement arms has been bismuth telluride ( $\text{Bi}_2\text{Te}_3$ ) and several of its solid solutions with such isomorphic compounds as bismuth selenide ( $\text{Bi}_2\text{Se}_3$ ) and tellurium antimonide ( $\text{Sb}_2\text{Te}_3$ ). Bismuth telluride may be obtained in both p and n types. With a surplus of bismuth,  $\text{Bi}_2\text{Te}_3$  of the p-type is formed, and with a surplus of tellurium,  $\text{Bi}_2\text{Te}_3$  of the n-type is formed.

In order to increase the ratio of the mobility of basic carriers to the heat conductivity of the crystal lattice, solid solutions  $\text{Bi}_2\text{Te}_3$ -- $\text{Bi}_2\text{Se}_3$  and  $\text{Bi}_2\text{Te}_3$ -- $\text{Sb}_2\text{Te}_3$  are employed.

Figure 6 shows the dependence of the heat conductivity of the lattice and electron mobility in a solid solution of  $\text{Bi}_2\text{Te}_3$ -- $\text{Bi}_2\text{Se}_3$  of the n-type as a function of  $\text{Bi}_2\text{Se}_3$  content. It is apparent from the movement of the curves, that with an increase in the content of bismuth selenide in a solid solution, electron mobility at first decreases significantly, and then increases sharply. At the same time the value of the heat conductivity of the lattice with a composition of 50%  $\text{Bi}_2\text{Te}_3$ --50%  $\text{Bi}_2\text{Se}_3$  decreases by almost 1.5 times. The increase in electron mobility in the given case is caused by the fact that the effective mass of the electrons in bismuth selenide is almost 3 times less than in bismuth telluride (figure 7). It is apparent from this figure that an increase in mobility as a result of a decrease in the effective mass does not always favorably affect the thermoelectric effectiveness of the material. This is caused by the fact that with an increase in electron mobility and a decrease in the effective mass, the value of the thermoelectromotive force coefficient decreases, which in turn leads to a decrease in the value  $\alpha^2\sigma$ .

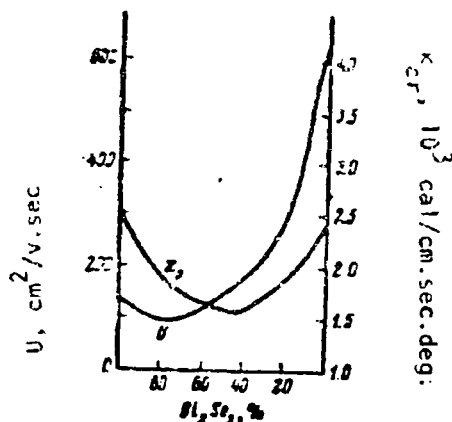


Figure 6. Heat Conductivity of the Lattice ( $\kappa_{cr}$ ) and Carrier Mobility ( $u$ ) in a  $\text{Bi}_2\text{Te}_3$ -- $\text{Bi}_2\text{Se}_3$  Solid Solution as a Function  $\text{Bi}_2\text{Se}_3$  Content.



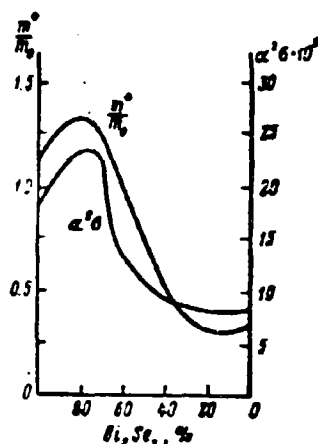


Figure 7. The Dependence of Effective Mass ( $\frac{m^*}{m_0}$ ) and ( $\alpha^2 \sigma$ ) for a  $\text{Bi}_2\text{Te}_3$ -- $\text{Bi}_2\text{Se}_3$  Solid Solution on  $\text{Bi}_2\text{Se}_3$  Content.

These considerations were confirmed for the material for the positive arm of the thermoelement-p-type bismuth telluride. By means of replacing this with a solid solution of  $\text{Bi}_2\text{Te}_3$ -- $\text{Sb}_2\text{Te}_3$ ,  $z$  was raised by more than 2 times. However, the  $\text{Bi}_2\text{Te}_3$ -- $\text{Sb}_2\text{Te}_3$  system (in which either hole or electron conductivity may be created by a suitable choice of impurities), proved to be an ineffective material for the negative arm of the thermoelement: its effectiveness in this case proved to be not only significantly lower than the solid solution indicated above, but also lower than simple bismuth telluride. A detailed study of this question revealed that from the standpoint of carrier mobility an important consideration was which of the components of the compound was partially replaced by its analog; thus, in the crystal lattice when a part of the anions are replaced, the electron mobility changes little, but hole mobility drops sharply; on the other hand, a partial change of the cations results in a decrease in electron mobility, while hole mobility changes very little.

Figure 8 shows the dependence of electron and hole mobility in a  $\text{Bi}_2\text{Te}_3$ -- $\text{Sb}_2\text{Te}_3$  solid solution on the  $\text{Sb}_2\text{Te}_3$  content. In the case given, a change in the  $\text{Sb}_2\text{Te}_3$  content in a solid solution from 0 to 50%, electron mobility decreased by 2 times, whereas hole mobility increased and showed a maximum corresponding to a composition of 67%  $\text{Bi}_2\text{Te}_3$  and 33%  $\text{Sb}_2\text{Te}_3$ . This composition corresponds to the formation of an ordered solid solution.

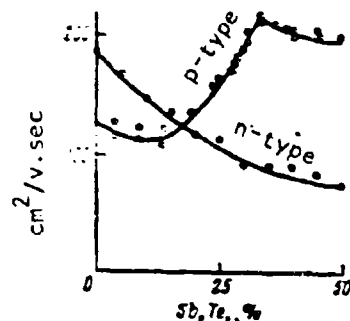


Figure 8. Carrier Mobility in a  $\text{Bi}_2\text{Te}_3$ -- $\text{Sb}_2\text{Te}_3$  Solid Solution (p and n-types) as a Function of  $\text{Sb}_2\text{Te}_3$  Content.

The facts presented above permit us to come to the conclusion that in semiconductors even with weakly expressed ion bonds, the basic carriers do not move in the entire volume of the crystal, but predominantly along "bridges," which are formed between the ions. The electrons move along a sub-lattice, which is formed by positively charged ions, and the hole along a sub-lattice, which is formed of negatively charged ions. Therefore, distortion of a "positive" lattice greatly reduces electron mobility, and "negative" distortion has the same effect on hole mobility. It follows that in the case when we wish to reduce the heat conductivity of the compound which is employed as the material for the positive arm of the thermoelement, while not decreasing the hole mobility, we must partially replace the cations; in the negative arm material, on the other hand, we must replace the anions.

It has been pointed out above that in order to provide an optimum concentration of carriers in the thermoelement material, we must introduce impurity atoms (donors or acceptors). In bismuth telluride, donor or acceptor action of the impurity atom as a whole is determined by its valence. The elements of the seventh and sixth groups (including a surplus of tellurium with respect to the stoichiometric composition)

gives donor levels, but elements with a lower number of electrons (including a surplus of bismuth with respect to the stoichiometric composition) are acceptors. If we compare the influence of a given impurity on the concentration of carriers in their mobility, then we will be able to come to a more or less convincing conclusion with respect to how the impurity atoms are distributed in the crystal lattice.

Thus, for example, surplus bismuth: 1) furnishes one acceptor level per atom, 2) significantly reduces the hole mobility, 3) exerts little influence on electron mobility. All of these three facts indicate that surplus bismuth atoms partially replace tellurium in the anion sub-lattice. For example, surplus tellurium: 1) furnishes one electron per atom, 2) significantly reduces electron mobility and 3) exerts little influence on hole mobility, i.e., judging from everything, is localized in the cation sub-lattice. Surplus iodine furnishes 1.5 electrons per atom and almost identically influences hole and electron mobility; it may therefore be assumed that iodine atoms are distributed more or less uniformly between both sub-lattices and, replacing bismuth, furnish two electrons, and in replacing tellurium, one. Lead, apparently, partially replaces bismuth, since its atoms are acceptors and sharply reduce electron mobility. Silver as a donor exerts an identical influence on hole and electron mobility, and possesses an unusually large diffusion capability; this testifies in favor of the fact that silver atoms are distributed in the areas between the lattice points of bismuth telluride.

In conclusion, it is necessary to remind ourselves of the dependence of thermoelectric material effectiveness on temperature.

In agreement with (37),

$$z \sim \frac{U}{\kappa_{cr}} T^{n_1}$$

Therefore, temperature dependence  $z$  is determined by the temperature dependencies of the mobility and the heat conductivity of the crystal lattice.

In the solid solutions  $\text{Bi}_2\text{Te}_3\text{--Bi}_2\text{Se}_3$  and  $\text{Bi}_2\text{Te}_3\text{--Sb}_2\text{Te}_3$ , which at the present time are the best materials for thermoelements, heat conductivity of the crystal lattice in a wide range of temperatures changes

very little, and carrier mobility at low temperatures ( $T \sim 250^{\circ} \text{K}$ ) is usually inversely proportional to temperature  $\mu \sim T^{-1}$ , at high values of  $\mu \sim T^{-1}$ .

Therefore, in the range of low temperatures,  $z \sim \sqrt{T}$ , in the range of high values  $z \sim \frac{1}{\sqrt{T}}$  and close to  $250^{\circ} \text{K}$   $z$  achieves the maximum value.

It is necessary to note that temperature movement considerations pertaining to  $\mu$  and  $z$ , cited above, bear a qualitative character. In fact, these movements vary within rather wide limits, and depend on a series of factors; the arguments cited above concerning temperature dependencies and figures of merit must be considered to be tentative.

## CHAPTER III

### The Consideration of Additional Factors<sup>1</sup>

The basic relationships outlined previously, which characterize the operation of the thermoelement, were formulated with a series of assumptions, which, however, do not affect the qualitative substance of the arguments. For a more exact analysis of the processes which occur in the thermoelement, we must supplement the theory examined, while considering a series of factors.

#### §1. A Consideration of Electron Heat Conductivity

In equations (34) and (35), which define the optimum carrier concentration and optimum thermoelectromotive force value in the value of a figure of merit  $z$ , the total heat conductivity was, for simplicity, replaced by the crystal lattice heat conductivity. Let us now consider the heat conductivity of electron gas. In agreement with (31) and (32), the equation for  $z$  assumes the form

$$z = \frac{z^2}{\kappa_{cr} - \kappa_{el}} = \frac{k^2 T}{e \kappa_{cr}} \cdot \frac{(C - \ln n)^2}{1 - Bn}, \quad (39)$$

$$\text{where} \quad C = r - 2 \div \ln \frac{2(2 - mkT)^2}{k^2}, \quad (40)$$

(40)

<sup>1</sup>The author of this chapter is L. S. Stil'bais (see *Semiconductors in Science and Technology*, Vol. II, Chapter XVII, AN USSR Press, M.-L., 1957).

and

$$B = \frac{(r-2) \cdot \frac{k^2}{e} U_e}{k_{cr}} \quad (41)$$

The condition  $\frac{ds}{dn} \equiv 0$  results in a transcendental equation for the determination of optimum  $n$ , which we have designated as  $n_1$ :

$$\ln n_1 = \ln n_0 - 2Bn_1 \quad (42)$$

or

$$\ln \left( 1 + \frac{n_1 - n_0}{n_0} \right) = -2Bn_1 \quad (43)$$

Since when  $n = n_0$ ,  $Bn_0 = \frac{k_{el}}{k_{cr}}$  is usually less than unity, we can expand the left side of equation (43) in a series and limit the expansion by the first term (the error involved here will not exceed several %). Therefore,

$$\frac{n_1 - n_0}{n_0} \approx -2Bn_0$$

and

$$n_1 \approx \frac{n_0}{1 + 2Bn_0} \quad (44)$$

Equation (42) may be solved with accuracy by means of a graph. For this purpose it is convenient to rewrite, with the use of (31), this in the following form:

$$a_1 = a_0 + 1 \cdot \frac{k}{e} \cdot \frac{k_{el}}{k_{cr}} = 172(1 + Bn_1) \quad (45)$$

Having plotted  $a$  in agreement with (31) and the right side of equation (45) as a function of  $n$ , we shall find  $n_1$  as the abscissa of the intersecting point of these curves.

It is apparent that the correction will be larger, the larger the ratio of mobility to heat conductivity of the lattice.

## §2. A Consideration of Thompson Heat in the Thermoelement Energy Balance

As we have seen from (34) and (35), the best materials for semiconductor thermoelements are those in which the thermoelectromotive force coefficient is constant:

$$\alpha = 2 \frac{k}{e} = 172 \text{ } \mu\text{V/deg}$$

and the carrier concentration changes in accordance with the law

$$n \sim T^n.$$

In the theory set forth in Chapters I and II, ideal conditions were examined in which the Thompson coefficient is

$$\tau = T \frac{d\alpha}{dT} = 0.$$

In practice, as we have pointed out above, the materials employed for thermoelectric arms are ordinary semimetals, i.e., they are materials in which the carrier concentration is constant, and the thermoelectromotive force increases with an increase in temperature. In this case the Thompson coefficient differs from zero and is expressed in the following form:

$$\tau = \frac{3}{2} \cdot \frac{k}{e} = 129 \text{ } \mu\text{V/deg} \quad (46)$$

We must now take into consideration the influence of Thompson heat on the heat balance of the thermoelement. This influence first of all affects the temperature distribution along the arms of the thermoelement. Up to this point we have assumed that the temperature gradient along the arms of the thermoelement is a constant and that the heat flux density on the cold junction of the thermoelement, in agreement with this, is expressed by the equation

$$Q_T = \tau \frac{T_0 - T}{l}. \quad (47)$$

The influence of Joule heat on the temperature distribution was roughly considered; it was assumed that half appears on the hot junction of the thermoelement and half on the cold junction. In order to obtain a more exact solution to this problem, we must find the temperature distribution along the arm of the thermoelement well considering Joule and Thompson heat, and then heat flux density in accordance with the following equation:

$$Q_T = -\kappa \nabla T. \quad (48)$$

We shall direct the axis  $x$  along the arm of the thermoelement and combine the beginning of the coordinates with the cold junction of the thermoelements; then (48) assumes the following form:

$$Q_T = -\kappa \frac{dT}{dx} = 0. \quad (49)$$

In order to calculate  $Q_T$  in accordance with (49), we must determine the temperature distribution along the arm of the thermoelement:

$$T = f(x).$$

Here, as before, we shall not consider temperature dependence of heat conductivity and electrical conductivity, replacing their true values as functions of temperature with average values in the operating temperature range. In a thermoelectric generator both electrons and holes move from the hot junction to the cold; here in the entire volume of the thermoelement arm, Thompson heat is released in addition to the Joule heat; in thermoelectric refrigerators both electrons and holes move in the opposite direction, and therefore the Thompson heat is subtracted from the Joule heat. Therefore, a steady state condition for a unit of volume of the arm of the thermoelement in the case under examination will have the form

$$\kappa \frac{d^2 T}{dx^2} - j \frac{dT}{dx} + j^2 \rho = 0, \quad (50)$$

where  $j$  is current density.



The solution to the differential equation (50) with boundary conditions ( $T = T_1$  when  $x = 0$  and  $T = T_0$  when  $x = l$ ) has the form

$$T = T_1 - \frac{T_1 - T_0 + \frac{w_p}{w_r} \left(1 - e^{\frac{x}{l}}\right)}{1 - e^{\frac{x}{l}}} + \frac{w_p}{w_r} x, \quad (51)$$

where the following designations are introduced:  $j_0 = w_0$  and  $j_l = w_l$ . Therefore, in agreement with (49) and (51), heat flux on the cold junction is

$$Q_r = -x \left( \frac{T_1 - T_0 + \frac{w_p}{w_r} \cdot l}{1 - e^{\frac{x}{l}}} \cdot \frac{w_r}{x} + \frac{w_p}{w_r} \right). \quad (52)$$

Expanding the exponent in equation (52) in a series and limiting the expansion by the first two terms, we obtain

$$Q_r \approx x \frac{T_0 - T_1}{l} + \frac{1}{2} j_l l - \frac{1}{2} j (T_0 - T_1). \quad (53)$$

Thus we have proved that in fact, in this first approximation, half of the Joule heat passes to the cold junction; by means of (53) we may now consider the effect of Thompson heat on the coefficient of performance  $\epsilon$  of the thermoelement. Equation (14) for the refrigerating capacity of the thermoelement, taking into consideration (53), has the following form:

$$Q_0 = \Pi I - x(T_0 - T_1) - \frac{1}{2} I^2 R - \frac{1}{2} j (T_0 - T_1) I, \quad (54)$$

where  $\Pi = 2\alpha_1 T_1$ , and  $\alpha_1$  is the value of the thermoelectromotive force coefficient at temperature  $T_1$ . Therefore, expression (54) may be rewritten as follows:

$$Q_0 = 2\alpha_1 T_1 I - x(T_0 - T_1) - \frac{1}{2} I^2 R, \quad (55)$$

where the following designation is introduced

$$z = z_1 + \frac{1}{2} \cdot \frac{T_0 - T_1}{T_1}. \quad (56)$$

We shall show that  $\bar{z}$  is equal to the average value of the thermoelectromotive force coefficient in the temperature range  $T_0 - T_1$ . In accordance with Thompson's second principle,

$$z = T \frac{d\alpha}{dT} \approx \frac{\alpha_0 - \alpha_1}{T_0 - T_1} T_1. \quad (57)$$

substituting (57) in (56), we obtain

$$\bar{z} = z_1 + \frac{1}{2} (\alpha_0 - \alpha_1) = \frac{\alpha_1 + \alpha_0}{2}.$$

With the same degree of accuracy, we may consider that the thermoelectromotive force is

$$E = \int_{T_1}^{T_0} z dT \approx \bar{z} (T_0 - T_1). \quad (58)$$

Therefore, equation (16) for the coefficient of performance of the thermoelement, considering (58) and (65) assumes the form

$$z = \frac{2\alpha_1 T_1 - \frac{1}{2} I^2 R - z (T_0 - T_1)}{I [2z (T_0 - T_1) + I R]}. \quad (59)$$

Equation (59) has the same form as in (16), the only difference being that the coefficient  $\alpha$  of the thermoelectromotive force, which earlier we considered to be independent of temperature, is replaced by its average value ( $\bar{z}$ ) within the operating temperature range. Therefore, while not repeating the calculations which we have completed earlier, we may now write the equation for the maximum coefficient of performance as follows:

$$z = \frac{T_1}{T_0 - T_1} \cdot \frac{\sqrt{1 + \frac{1}{2} (T_0 + T_1) z - \frac{T_0}{T_1}}}{\sqrt{1 + \frac{1}{2} (T_0 + T_1) z + 1}}, \quad (60)$$

where  $z = \frac{e^2}{\kappa T}$ .

It may also be shown that the temperature dependence of the electrical conductivity and heat conductivity may, in the first approximation, be taken into consideration by replacing in the equation for  $z$  the product  $\kappa \rho$  by its average value in the operating temperature range:

$$z = \frac{e^2}{\bar{\kappa \rho}}$$

where

$$\frac{1}{\bar{\kappa \rho}} = \frac{1}{T_0 - T_1} \int_{T_1}^{T_0} \frac{1}{\kappa \rho} dT.$$

### 53. Deviations from Optimum Conditions

Previously we found the ratio of the sections of the thermoelement arms at which  $z$  achieves a maximum value; we also determined the optimum electrical conductivity, the optimum current, etc.

In practice, by virtue of deviations from the technological process and which are difficult to control, not one of these conditions is fulfilled exactly. Therefore it is important to establish to what extent deviations from optimum conditions influence the effectiveness of the operation of the cooling device.

#### Deviations from the Optimum Ratio of the Arm Sections

It has been shown previously that  $z$  is inversely proportional to the product of the resistance to the thermoelement and the heat conductivity:

$$z = \frac{(x_1 - x_2)^2}{\kappa \rho} \quad (61)$$

where

$$\kappa \rho = (x_1 + x_2 n) \left( \frac{\rho_1}{m} + \rho_2 \right) \quad (62)$$

achieves a minimum value with a definite ratio of the sections  $m$  of the branches:

$$m_0 = \left( \frac{S_2}{S_1} \right)_0 = \sqrt{\frac{z_1 z_2}{z_1^2 + z_2^2}}; \quad (63)$$

here

$$z_{\min} = (\sqrt{z_1^2} + \sqrt{z_2^2})^2. \quad (64)$$

Let us clarify how the deviations from (63) influence  $z$ . In agreement with (62) and (64),

$$\frac{z - z_{\min}}{z_{\min}} = \frac{\left( \sqrt{\frac{z_1 z_2}{m}} - \sqrt{\frac{z_1 z_2}{m_0}} \right)^2}{(\sqrt{z_1^2} + \sqrt{z_2^2})^2}; \quad (65)$$

having divided the numerator and the denominator of the right side of (65) by  $\sqrt{\frac{z_1 z_2}{m_0}}$ , we obtain

$$\frac{z - z_{\min}}{z_{\min}} = \frac{1}{C^2} \frac{(m - m_0)^2}{m m_0}; \quad (66)$$

where the coefficient

$$C = \sqrt{\frac{z_1^2}{z_1^2 + z_2^2}} + \sqrt{\frac{z_2^2}{z_1^2 + z_2^2}} \geq 2$$

in the overwhelming majority of cases, and with a high degree of accuracy, equals 2.

Thus,

$$\frac{|\Delta z|}{z} = \frac{z - z_{\min}}{z_{\min}} \approx \frac{1}{4} \frac{(m - m_0)^2}{m m_0}; \quad (67)$$

assuming, for example, that  $m_0 = 1.5$  and  $m = 1$ , we obtain

$$\frac{\Delta z}{z} = 4\sigma$$

(68)

#### Deviation from the Optimum Carrier Concentration

In agreement with (34), the numeral  $\alpha^2\sigma$  of the equation for  $z$  has a maximum value with a specific carrier concentration and electrical conductivity. We shall clarify by how much the effectiveness of the thermoelement is reduced if the electrical conductivity of the branches differs somewhat from the optimum value.

Simple calculations which we have omitted here give the following result:

$$\frac{(\alpha^2\sigma)_{\max} - \alpha^2\sigma}{(\alpha^2\sigma)_{\max}} \approx \frac{1}{4} \left( \frac{\sigma - \sigma_0}{\sigma_0} \right)^2. \quad (69)$$

The relationship in (69) reveals that the dependents  $\alpha^2\sigma$ , and therefore, also  $z$  on  $\sigma$  close to the point  $\sigma = \sigma_0$  has the same nature as the dependents of  $z$  on  $m$  close to the point  $m = m_0$ ; for example, a change in  $\sigma$  by 20% generates a total reduction in  $z$  of 1%.

#### A Deviation from the Optimum Value of the Current Intensity

Under conditions of thermoelement operation involving complete thermal isolation of the cold junction, in agreement with (1) and (5),

$$\Delta T = \frac{II - \frac{1}{2} I^2 R}{1},$$

$$\frac{\partial \Delta T}{\partial I} = \frac{I}{1} - \frac{IR}{1}, \quad \frac{\partial^2 \Delta T}{\partial I^2} = -\frac{R}{1}.$$

Expanding  $\Delta T$  in a Taylor series close to the point  $I = I_0$ , we obtain, after simple transformations

$$\frac{\Delta T_{\max} - \Delta T}{\Delta T_{\max}} = \left( \frac{I - I_0}{I_0} \right)^2. \quad (70)$$

In agreement with (70), current density deviation from the optimum value by 20% generates a reduction in  $\Delta T$  by 4%.

### Considering the Value $z$ with Varying Arm Parameters

Solving another problem also presents some interest. Let us assume that the arm parameters of the thermoelement are not identical:

$$z_1 = \frac{a_1^2}{\alpha_1^2 \rho_1} > z_2 = \frac{a_2^2}{\alpha_2^2 \rho_2},$$

and we shall clarify by how much  $z$ , calculated in accordance with (11), is less than  $z_1$ , i.e., how the thermoelement indicators as a whole are poorer than the best indicators of the arm. We shall introduce the symbols:

$$\sqrt{z_1} = e_1, \sqrt{z_2} = e_2, \sqrt{z} = e, \sqrt{\alpha_1^2 \rho_1} = k_1 \text{ и } \sqrt{\alpha_2^2 \rho_2} = k_2;$$

then

$$e_1 - e = \frac{z_1}{k_1} - \frac{a_1 - a_2}{k_1 + k_2} = (e_1 - e_2) \frac{1}{1 + \frac{k_1}{k_2}}; \quad (71)$$

the lower the specific resistance of the given material, the lower the value  $k = \sqrt{\alpha^2 \rho}$  for the material; within limits this value approaches the constant of the Wiedemann-Franz law. Therefore, in order that the poorest arm does not significantly reduce  $z$ , we must in this way raise the carrier concentration so that the inequality  $\rho_1 \gg \rho_2$ .

## CHAPTER IV

### Thermogalvanometric Methods of Cooling

As has been pointed out above, the temperature on the cold junction of the thermoelement with an optimum current and a lack of a heat load depends on the temperature of the hot junctions and the value of  $z$  of the material employed. In the bismuth telluride, which so far is the best material for cooling thermoelements, a reduction in value  $z$  is accompanied by a reduction in temperature, which in turn involves a decrease in the temperature differential, provided by the thermoelement. As will be outlined in more detail below (Part II, Chapter I, §2), with a temperature at the hot junctions of  $-120^{\circ}\text{C}$ , the temperature differential at the thermoelement practically equals zero. In this connection there has been a great deal of discussion in published material recently concerning the possibility of the practical utilization of certain thermogalvanomagnetic effects for purposes of further reducing the temperature.

#### 51. Thermoelectric Cooling at Low Temperatures

As has been pointed out above, the effectiveness of semiconductor alloys on the basis of bismuth telluride falls with a temperature reduction in the hot junctions of the thermoelement, and they prove to be unsuitable for purposes involving extreme cooling. Investigations of bismuth-antimony alloys have revealed that in the low temperature area they possess unusual thermoelectrical properties. Thus, for example, with a temperature below  $220^{\circ}\text{K}$ , an alloy consisting of 95% (atomic) bismuth and 5% (atomic) antimony, surpasses in effectiveness alloys based on bismuth telluride. At a temperature of  $300^{\circ}\text{K}$ , the value  $z$  for the alloy indicated above is equal to  $1.8 \cdot 10^{-3} \text{ deg}^{-1}$ ; at the same time at the temperature of liquid nitrogen ( $77^{\circ}\text{K}$ ), a value  $z$  increases to  $4.8 \cdot 10^{-3} \text{ deg}^{-1}$  (Figure 9). It is not without interest to note here that at a

temperature of 77°K, the value  $z$  for bismuth-antimony alloys within a rather wide range show little dependence on the composition of the alloy (Figure 10).

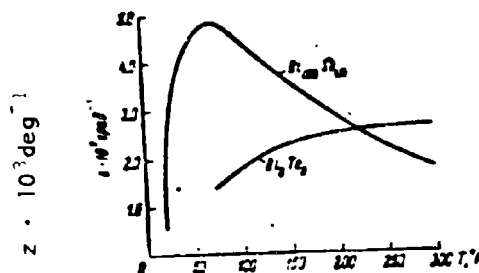


Figure 9. Dependence of value  $z$  on a 95% Bi-5% Sb alloy on temperature (the temperature gradient along the 3-fold axis of the crystal).

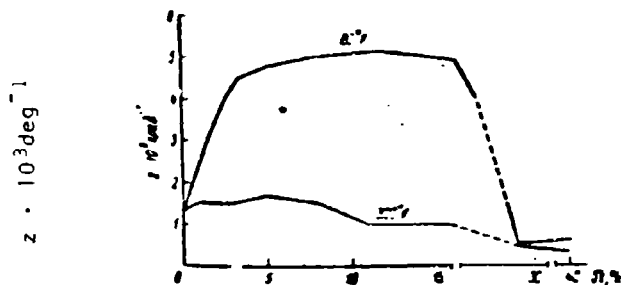


Figure 10. The dependence of value  $z$  on alloy composition at 80°K and 300°K.

Calculated temperature drops which may be provided by thermoelements of Bi-Sb (the n-arm) and  $\text{Bi}_2\text{Te}_3$  (the p-arm), at various hot junction temperatures, are shown in Figure 11. It is apparent from the slope of the curve that at 100°K the thermoelements may provide an additional temperature reduction of 10%.



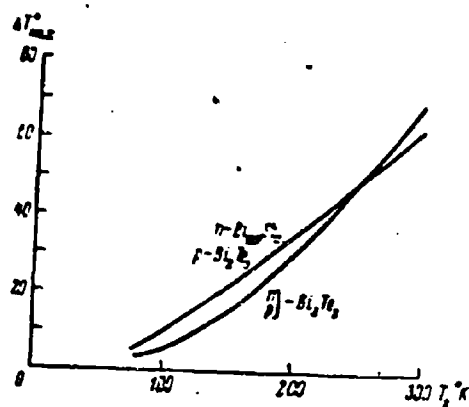


Figure 11. Maximum temperature difference provided by a thermoelement consisting of Bi<sub>(95)</sub>Sb<sub>(5)</sub> (n-arm) and Bi<sub>2</sub>Te<sub>3</sub> (p-arm).

During thermoelement operation in the extremely low temperature region (5-10°K), it is possible to employ as one of the arms a metal at this temperature in a superconducting state. In this case value  $z$  for such a thermoelement will be determined only by the parameter of the superconducting arm.

## 52. Thermoelectric Cooling in a Magnetic Field

A significant increase in value  $z$  at low temperatures was detected for bismuth-antimony alloys, placed in a magnetic field. Under the influence of a magnetic field an increase occurs in the thermoelectromotive force and simultaneously in the electrical resistance of the material. The reason for this is the influence of the magnetic field on the current carriers in the semiconductor -- the electron and holes. The greatest effect of the influence of the magnetic field on the figure of merit of the semiconductor substance proved to be with an alloy consisting of 88% bismuth and 12% antimony. Single crystals of this alloy are placed in a magnetic field which is directed in parallel to the bisecting axis of the crystal. At room temperature, without a magnetic field, the  $z$  of this material will equal  $0.8 \cdot 10^{-3} \text{ deg}^{-1}$ . At the same room temperature but in a magnetic field of 17 kilo oersteds, value  $z$  increases to  $3 \cdot 10^{-3} \text{ deg}^{-1}$ . In Bi-Sb alloys with an increase in the magnetic field as a result of an increase in the value of the thermoelectrodynamical force,  $z$  increases, however at a certain field intensity value due to an increase in the resistance,  $z$  begins to decrease, passing through a maximum. The significance of this fact is

that the maximum value of  $z$  at any temperature is always 3 times higher than when the magnetic field is lacking.

A second peculiarity in the behavior of Bi-Sb alloys in a magnetic field is an increase in  $z$  with a decrease in the surrounding temperature. Figure 12 shows a dependence of value  $z$  on temperature for various values of magnetic field intensity. With a temperature of approximately 100°K in a field of 1 kg,  $z$  has a value of  $8.6 \cdot 10^{-3} \text{ deg}^{-1}$ .

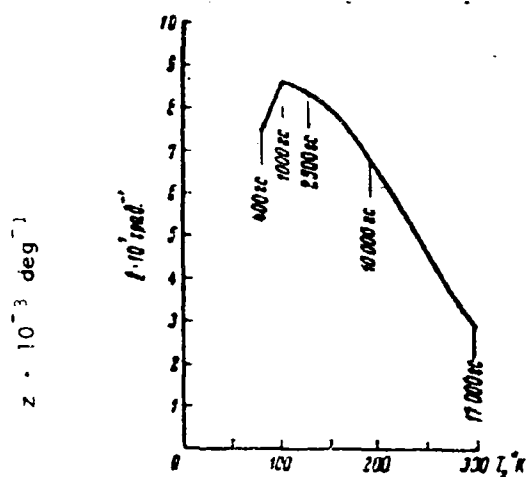


Figure 12. The dependence of value  $z$  on temperature with various magnetic field values for a Bi-Sb alloy.

All of the data cited above pertain to an alloy with N-type conductivity. Unfortunately, up to the present time we have not been successful in preparing a positive-type material with a similar dependence of properties on magnetic field and temperature, which therefore does not permit the creation of an effective low-temperature thermomagnetic element. However, the employment of bismuth telluride as the positive arm in an 800 oersted field and with a hot junction temperature of 77°K permits an additional temperature reduction of 13-15°.

We must direct our attention to the possibility of creating a combined thermoelectric-thermomagnetic cooler, in which the initial stages are thermoelectric, and the final thermoelectric, but with a magnetic field.

### 53. Thermomagnetic Cooling (the Ettinghausen Effect)

Under the influence of a magnetic field the transfer process changes in a conductor through which a constant electrical current flows. As a result of this, a whole series of so-called thermomagnetic effects arise (the transverse effects of Hall and Righi-Leduc and the longitudinal effects of Nernst and Ettinghausen). So for cooling purposes the Ettinghausen effect presents the most interest. This effect consists of the fact that when a magnetic field acts upon a conductor in a direction perpendicular to the direction of the passage of the current through the conductor, a temperature gradient is created in a third direction (Figure 13). The Ettinghausen coefficient  $P$  is determined from the relationship

$$P = \frac{\Delta T_y}{I_x H_z},$$

where  $I_x$  is the current intensity;  $H_z$  is the magnetic field strength;  $\Delta T_y$  is the temperature gradient generated.

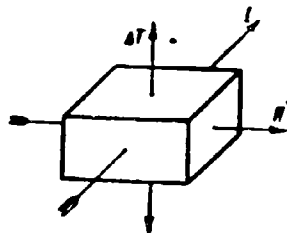


Figure 13. A diagram of the formation of the Ettinghausen effect.

Simultaneously with the Ettinghausen effect appears the Nernst effect, which pertains to the phenomenon that with a presence of a temperature gradient in a magnetic field, a transverse electrical field will be generated. The Nernst effect is thermodynamically related to the Ettinghausen effect, just as the Seebeck effect is related to the Peltier effect.

The value of the Nernst coefficient  $Q$  is determined from the equation

$$Q = \frac{E_y}{\Delta T_x H_z},$$

where  $e_y$  is the Nernst electrical field generated; and  $H_z$  is the magnetic field;  $\Delta T_x$  is the temperature gradient.

The Nernst and Ettinghausen coefficients are related to each other by the Bridgeman relation:

$$P = QT.$$

A strict analysis of the phenomena which take place in a thermomagnetic Ettinghausen refrigerator leads to an equation which is quite complex. However, for a first approximation, and with a sufficient degree of accuracy, we may simplify the problem, as a result of which the phenomenological equation of thermomagnetic cooling becomes similar to the corresponding equation for thermoelectric cooling of the Peltier effect.

Let us examine principally the possible design of an Ettinghausen refrigerator. Cooling and heating surfaces are arranged (Figure 14) above and below a rectangular section of a slug of suitable material. The width and height of the slug, and also the length of the cooling surface are designated respectively as  $a$ ,  $b$  and  $L$ . The temperature of the cold and hot sides we shall designate by  $T_{co}$  and  $T_{ho}$ . The current passing through this slug is designated as  $I_x$  and, finally, the magnetic field is  $H_z$ .

We shall assume that the value of the Nernst coefficient, and also the electrical conductivity and heat conductivity of the material of the slug do not depend on temperature. Then the Ettinghausen heat flux from the cold to the hot side of the slug will equal

$$q = \frac{PB_x I_x L k}{b},$$

where  $k$  is the coefficient of heat conductivity of the slug.

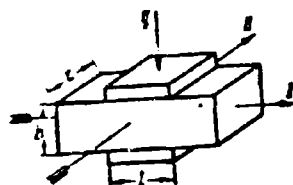


Figure 14. The principal design of a Ettinghausen refrigerator.

In agreement with the Bridgeman relation cited above, this equation may be written in the form

$$q = \frac{QH_2 I^2}{b} - k l a \frac{dT}{dy}.$$

Simultaneously with the heat flux transfer from the cold to the hot surfaces of the Ettinghausen refrigerator under the influence of the passage of the current Joule heat will be released in it, which in a layer of single thickness in a direction y equals

$$\frac{I^2 R}{2ab}.$$

With the boundary conditions

$$T = T_{co} |_{y=0} = T = T_{ho} |_{y=a}$$

the equation for the heat quantity drawn off per unit time by the Ettinghausen refrigerator will have the form

$$q = \frac{QH_2 I^2}{b} - \frac{I^2 R}{2ab} - \frac{k l a}{b} (T_{co} - T_{ho})$$

It is not difficult to note that the equation has the form as the equation for refrigerating capacity in the case of thermoelectric cooling utilizing the Peltier effect.

Here the terms  $QH_2 I^2/b$ ,  $I^2/2ab$  and  $k l a/b$  in the equation for the Ettinghausen refrigerator correspond to  $(\alpha_1 - \alpha_2) R$  and  $\kappa$  in the equation for the Peltier refrigerator. In this connection it is possible to make the very interesting conclusion that after corresponding substitutions for the various terms have been made, all relationships which characterize the operation of the Peltier refrigerator may also be employed for the Ettinghausen refrigerator. Thus, for example, the coefficient of quality of the thermoelectric refrigerator may be written in the form

$$z_0 = \frac{(QB)^2 z_0}{k},$$

in the equation for maximum temperature difference corresponds to

$$\Delta T_{\max} = \frac{Q^2 B^2 z_0 T_1}{2}.$$

The product of the Ettinghausen coefficient  $P$  and the magnetic field  $H$ , having received the designation coefficient of thermomagnetic force, replaces in thermoelectric relationships the coefficient of thermoelectromotive force  $\alpha$ . In connection with the fact that the thermomagnetic Ettinghausen refrigerator consists of 1 arm, optimization of its geometric dimensions is not required. It follows from this that it is comparatively simple to make a multi-stage refrigerator with an infinite number of stages. The shape of such a refrigerator is shown in Figure 15. It is a tetrahedral frustum of a prism, the sides of which form exponential functions. The upper area of the prism is cooled, and the lower base is heated. A similar type of cooler results from the fact that the heat flux increases in proportion to the distance from the cold surface to the hot surface. In this matter, in isothermic surfaces, formed by a prism section parallel to the base, the heat flux density remains constant. The coefficient of performance for an Ettinghausen cooler with an infinite number of stages may be calculated in accordance with the corresponding equations for a multi-stage thermoelectric pile, outlined in Chapter I, §5.

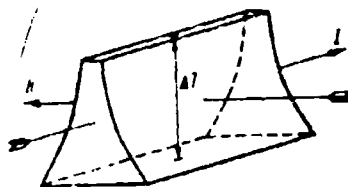


Figure 15. The geometric form of an Ettinghausen cooler with an infinite number of stages.

The Ettinghausen refrigerator described above with an infinite number of stages possesses one shortcoming; the relatively large width

of the base does not conveniently permit placing it between the poles of a magnet. In this connection another variation of this refrigerator has been proposed, but with a finite number of stages. The construction diagram is shown in Figure 16. The rectangularly shaped element consists of a series of vertically placed layers, insulated from each other. Each layer has a different thickness, governed by the refrigerating capacity which it must possess. A full analogy could be presented here with the multi-stage Peltier thermoelement.

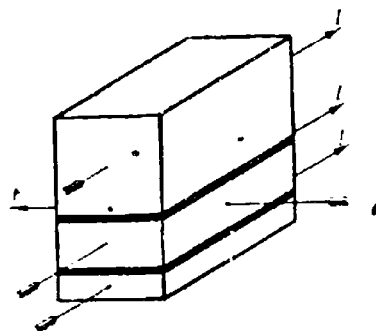


Figure 16. Diagram of an Ettinghausen refrigerating device with a finite number of stages.

Experiments in the determination of the effectiveness of the Ettinghausen refrigerator have been conducted for single-crystal models of an alloy consisting of 97% Bi and 3% Sb. The model was made in the form shown in Figure 15. The magnetic field was established parallel to the bisecting axis of the crystal. The temperature differential was generated in the direction of the binary axis. The results of measurements of dependents  $\Delta T$  on magnetic field intensity for various values of the temperature of the heat-dissipating base are shown in Figure 17. The geometric dimensions of the model were: length 25 mm, height 4.28 mm, width of the cold base 0.31 mm, and width of the hot base 3.94 mm.

In recent times there has been some discussion in publications concerning the possibility of employing for cooling purposes the thermomagnetic effect in pyrolytic graphite. A theoretical evaluation of this effect reveals that with temperatures below 100°K, one might expect an additional temperature reduction of 10°. The value of the magnetic field in this case would be  $10^4$ - $10^5$  G.

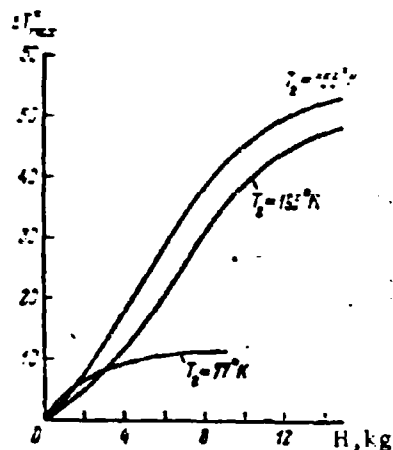


Figure 17. Temperature differential dependence in an Ettinghausen refrigerator on magnetic field intensity for various values of the hot base temperature.

Measurements conducted with pyrolytic graphite annealed at a temperature of 3500°C, have revealed that at 4.2°K value  $z$  for graphite has a maximum at a magnetic field intensity of 500 G. The value  $\Delta T$  was equal to  $2.9 \cdot 10^{-3}$  deg. Disparities in the data from published references regarding the influence of the magnetic field and the value  $z$  are connected with the fact that a decrease in  $z$  in strong magnetic fields, in all probability, is caused by non-uniformity in models or by various carrier concentrations.



## PART II. ENGINEERING PROBLEMS IN THERMOELECTRIC COOLING TECHNOLOGY

### CHAPTER V

#### The Fundamentals of the Design of Thermoelectric Cooling Devices

##### §1. Thermopile Operating Conditions

Any thermoelectric cooling device can operate under two basic conditions -- the condition of maximum coefficient of performance  $\epsilon_{\max}$  and the condition of maximum refrigerating capacity  $Q_{\max}$ . In the first case the device would most effectively transform the required electrical energy into "cold", and in the second case, to the detriment of economy, perhaps the maximum temperature reduction will be obtained. In other words, the  $\epsilon_{\max}$  condition characterizes maximum economy of operation of the thermo-cooling device, whereas the  $Q_{\max}$  condition provides for the maximum quantity of dissipated heat per unit of time. Shown in figures 18 and 19 are the graphic dependencies of the coefficient of performance and the refrigerating capacity on temperature differential on the thermoelement for cases involving conditions of maximum coefficient of performance and maximum refrigerating capacity. It must be noted that the dependencies cited refer to a thermoelement for which  $z = 2.5 \cdot 10^{-3} \text{ deg}^{-1}$  and hot junction temperature is equal to  $25^\circ\text{C}$ .

At  $\Delta T_{\max}$ , both conditions coincide, however, when  $\Delta T$  differs from the maximum value, refrigerating capacity and coefficient of performance under these conditions have different values.

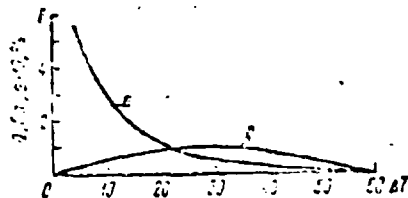


Figure 18. Dependence of the coefficient of performance ( $\epsilon$ ) and refrigerating capacity ( $Q$ ) on temperature difference ( $\Delta T$ ) for a condition of maximum coefficient of performance.



Figure 19. Dependence of the coefficient of performance ( $\epsilon$ ) and refrigerating capacity ( $Q$ ) on the difference in temperature ( $\Delta T$ ) for a condition of maximum refrigerating capacity.

Thus, for example, in the  $\epsilon_{\max}$  condition with low values of  $\Delta T$ , the coefficient of performance has a significant value, which within limits approaches infinity, whereas in the  $Q_{\max}$  condition, the value of the coefficient of performance cannot exceed 50%. In its turn the refrigerating capacity in the  $\epsilon_{\max}$  condition has a maximum at  $\Delta T = 30^\circ$  and is equal to 1w. In the  $Q_{\max}$  condition the refrigerating capacity of the thermoclement at the same  $\Delta T = 30^\circ$  is equal to 1.7 w.

From the material presented we may make the following conclusion.

In a case when the thermoelectric device must provide a small temperature differential, which occurs, for example, in air conditioning, the device must be designed in accordance with the equations for the condition of maximum coefficient of performance. When maximum cooling from the device is required at the expense of economy, it must be designed in accordance with the equations of the condition of maximum refrigerating capacity. Thus, in approaching the design of a thermoelectric cooling device, first of all it is necessary to establish the operating condition, and in agreement with this to employ design formulas for the  $\epsilon_{\min}$  or the  $Q_{\max}$  conditions. Table 1 shows the relationships required for engineering calculations of the basic parameters of thermoelectric refrigerators.

Table 1  
Design Equations for the Basic Parameters of Thermoelectric Piles

Computed Parameter	Design Equation	
	$\epsilon_{\max}$ condition	$Q_{\max}$ condition
Optimum current, $a$	$I_0 = \frac{a(T_0 - T)}{R(N+1)}$	$I_0 = \frac{aT}{R}$
Voltage drop, $v$	$V_0 = \frac{a(T_0 - T)M}{N+1}$	$V_0 = aT_0$
Coefficient of performance	$\epsilon = \frac{T}{T_0 - T} \cdot \frac{M - \frac{T_0}{T}}{M+1}$	$\epsilon = \frac{1}{2} \frac{T_0}{T} \left( T - \frac{2(T_0 - T)}{T} \right)$
Refrigerating capacity, $w$	$Q_0 = \frac{a^2 M}{R} \cdot \frac{(NT - T_0)(T_0 - T)}{(N+1)(M-1)^2} = \epsilon W$	$Q_0 = \frac{a^2}{R} \left( \frac{T^2}{2} - \frac{T_0 - T}{2} \right) = \epsilon W$
Heat released at the hot junction, $w$	$Q_r = \frac{a^2 M}{R} \cdot \frac{(MT_0 - T)(T_0 - T)}{(M+1)(M-1)^2} = Q_0 + W$	$Q_r = \frac{a^2}{R} \left[ T \left( T_0 + \frac{T}{2} \right) - \frac{T_0 - T}{2} \right] = Q_0 + W$
Power required from the source, $w$	$W = \frac{a^2 (T_0 - T)^2 M}{(M-1)^2 R} = I_0 V_0$	$W = \frac{a^2 T_0 T}{R} = I_0 V_0$

Note:  $\epsilon = \epsilon_1 + \epsilon_2$ ;  $M = \sqrt{1 + 0.5 Z(T_0 + T)}$

## §2. Thermopile Design

The engineering design of a thermo-cooling device is made up of the design for a thermoelectric pile and the heat engineering design of a system of a heat dissipation from the hot junctions of the thermopile, the heat insulation of the operating chamber of the device, calculations of the values of parasitic temperature differentials in local heat junctions, etc.

The determination of the heat-engineering parameters of the device are just as important as the design of the thermopile, since it must always be kept in mind that any thermo-cooling device is a unified construction complex in which the separate elements are closely interdependent.

In the design of a thermoelectric pile initial data usually includes the required refrigerating capacity, value of the operating voltage, the temperature differential which must be provided by the device, and the basic parameters of the substances employed ( $\alpha$ ,  $\sigma$ ,  $\kappa$ ). Proceeding from these data, first it is necessary to determine under what condition the device will be operating, and then to use the corresponding design formulas for the  $\epsilon_{\max}$  or the  $Q_{\max}$  conditions.

Further design of the thermopile, for example, for the  $\epsilon_{\max}$  condition, is carried in the following order.

1. The value of heat load  $Q$  on the thermopile is determined. This flow is made up of heat flux  $Q_1$  from the outside, which flows through the heat insulation of the operating chamber and of heat  $Q_2$  released in the operating volume by objects subject to cooling.

Heat intake through the heat insulating layer is determined in accordance with the following formula:

$$Q_1 = \frac{\lambda \Delta T}{S},$$

where  $\lambda$  is the coefficient of heat conductivity for the insulating material chosen;  $S$  is the area of the heat insulation;  $\Delta T$  is the temperature differential for the thickness of a layer of the heat insulation;  $d$  is the thickness of a layer of heat insulation.

2. The value of the coefficient of performance of the thermopile is determined in accordance with the  $\epsilon_{\max}$  condition equation.

3. The power required by the thermopile from the power source is determined as the quotient of the division of the quantity of heat passing to the thermopile by the coefficient of performance, i.e.

$$W = \frac{Q}{\epsilon}.$$

4. The voltage drop ( $v_0$ ) across 1 thermoelement is calculated, and then, proceeding from the established voltage source (V) of the thermopile, the number of thermoelements in the thermopile is determined:

$$N = \frac{V}{v_0}.$$

5. The optimum current value fed to the thermopile is determined by dividing the power required from the source by the voltage drop across the pile.

6. Thermopile resistance may be determined from the formula

$$R = \frac{\Delta TN}{1 + 0.5z(T_0 + T) - 1},$$

and the resistance of 1 thermoelement is determined in accordance with the formula

$$r = \frac{\Delta T}{1 + 0.5z(T_0 + T) - 1}.$$

7. The geometric dimensions of the arms of the thermoelement are determined in accordance with the formula

$$\frac{l}{S} = \frac{\sigma}{2},$$

where  $l$  is the thermoelement arm height;  $S$  is the arm section.

Since the geometric dimensions of the thermoelement arms are determined by the ratio of the area of the section to the height, it is possible to employ arms of any dimensions by maintaining the ratio  $l/S$ .

The choice of corresponding values for  $Z$  and  $S$  must be made with consideration for a series of design requirements imposed on a thermoelectric device, with consideration for the weight of the thermopile, for the maximum reduction in the flow rate of the semiconductor substance, and a series of other factors. However, in practice the height of the thermoelement may not be made less than 3 mm, since in this case reverse heat flow from the hot to the cold junctions would play a noticeable role. In the design of a thermopile to be employed under a condition of maximum refrigerating capacity, the determination of the optimum current value may be accomplished with the aid of an equation for an approximation, which fully satisfies practical requirements.

In the  $Q_{\max}$  condition, optimum current equals

$$I = \frac{\alpha T}{R},$$

but

$$R = \frac{2l}{\sigma S}.$$

Substituting the value  $R$  in the equation for optimum current, we obtain

$$I = \frac{\alpha T \sigma S}{2l}.$$

The value  $\frac{\alpha T \sigma}{2}$  for thermoelectric materials employed at the present time ( $\text{Bi}_2\text{Te}_3 + \text{Bi}_2\text{Se}_3$  and  $\text{Bi}_2\text{Te}_3 + \text{Sb}_2\text{Te}_3$ ) is practically constant and equals 46-50. However with the aim of reducing the power required by the thermoelement, which in turn reduces parasitic temperature drops on the element of the device, the value of this numerical coefficient is reduced to 36.

Thus optimum current may be computed in accordance with the formula

$$I = 36 \frac{S}{l}.$$

Corresponding to the optimum current, the voltage drop in 1 thermoelement will be constant and will equal 0.075 v.

The design of multi-stage thermoelements in thermopiles is conducted in the sequence described above. However in calculating the maximum temperature reduction on a multi-stage thermopile, the strongly displayed dependence of the value of the thermoelectric material electrical conductance on temperature must be kept in mind. With a decrease in the temperature of the hot junctions, which occurs in the case of multi-stage thermoelement, the electrical conductivity ( $\sigma$ ) increases and the voltage drop across the thermoelement correspondingly decreases. As a result there is a reduction in the temperature drops provided by the upper stages of the multi-stage thermoelement.

Figure 20 shows the experimentally obtained dependence of temperature drops for a single-stage thermoelement on the temperature of the hot junction. In this connection in multi-stage thermoelements it is necessary to employ materials for the upper stages, which operate at the low temperatures of the hot junctions, with a reduced (at normal temperature) electrical conductivity value, so that in the operating condition the electrical conductivity will rise to its nominal value. These considerations basically pertain to multi-stage thermoelements and thermopiles with series-fed stages.

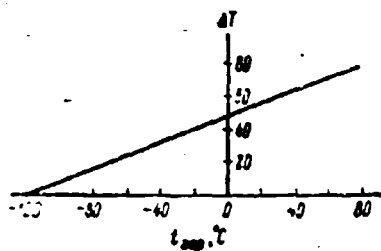


Figure 20. The dependence of the temperature drop ( $\Delta T$ ) for a single-stage thermoelement on the temperature of the hot junction ( $t_{ho}$ ).

### 53. The Design of a Radiator for Heat Extraction

The design of a system of heat dissipation from hot junctions of the thermopile is an independent problem and is examined in detail in Chapter III. However in a number of cases involving the use of air radiator systems with natural-convection or forced heat removal, it is possible to employ simplified equations in which the calculations satisfy practical requirements. The total area of the place in a radiator with natural-convection heat removal may be determined in accordance with the formula

$$F = \frac{Q}{\alpha \Delta T};$$

here  $Q$  is the quantity of heat which must be drawn off by the radiator, in kCal/h;  $\Delta T$  is the permissible drop in temperature between the radiator and the surrounding medium, °C;  $\alpha$  is the coefficient of heat transfer between the radiator and the surrounding medium, in kCal/m<sup>2</sup> · h · deg.

The quantity  $\alpha$  depends on many factors. With natural convection  $\alpha = 3$  to 5, and with forced air cooling of the radiator system to 100. In this connection in making a choice of a system for dissipating heat from the thermopile, it is worthwhile to give the preference to a radiator system with forced cooling, since this requires a radiator area of 10-15 times less, which correspondingly leads to a reduction in the overall dimensions of the device.

The geometric dimensions of the radiator place in the case of natural-convection heat removal may be determined in accordance with the equation

$$l = \frac{2Pd}{\lambda \Delta T},$$

where  $l$  is the length of the radiator plate;  $P$  is the quantity of heat delivered to the radiator, in kCal/h;  $\lambda$  is the coefficient of heat conductivity of the material from which the radiator plates are made, in kCal/m · h · deg;  $h$  is the thickness of the radiator plate, m;  $d$  is the height of the radiator plate in the direction of heat flow, m;  $\Delta T$  is the permissible temperature differential along the height of the radiator plate, °C.

It was pointed out above that the employment of radiator systems with forced cooling is considerably more defective than radiators with natural-convection heat dissipation. Problems concerning the design of



radiators with forced cooling will be examined in Chapter III, §2. Here we may employ an equation which may be used as a first approximation in evaluating the operation of a force-cooled radiator. In agreement with this equation

$$Q = WC_p \Delta T.$$

here  $Q$  is the quantity of heat supplied to the radiator,  $w$ ;  $W$  is the mass rate of flow of air through the radiator, kg/sec;  $C_p$  is the specific heat of the air at the temperature of the radiator;  $\Delta T$  is the established difference in temperature of the air at the input and the output of the radiator, °C.

## CHAPTER VI

### The Construction Elements of Thermoelectric Cooling Devices

The majority of thermoelectric cooling devices consist of three basic construction subassemblies: the thermoelectricpile, the operating chamber or surface, and the heat removal system from the thermopile. At a certain stage, the creation of each of these subassemblies is an independent problem. However, in the construction of this instrument as a whole it is necessary to consider the close interdependence of these three construction elements with each other.

With this in mind, we shall examine the basic principles of the construction of each of these sub-assemblies enumerated.

#### §1. An Individual Thermoelement

Any thermoelectricpile consists of a series of series or parallel connected thermoelements. The thermoelement itself consists of two arms, one of which possesses n-type conductivity and the other, p-type conductivity. The arms of the thermoelement are connected to each other by means of connecting plates. To a significant degree the qualitative operation of an entire thermo-cooling device depends on the correct design solution of an individual thermoelement.

The basic requirement which must be satisfied in the practical construction of a thermoelement is the elimination or the significant reduction of mechanical stresses generated in the latter as a result of the compression of cold and expansion of hot connecting plates.

In fact, the arms which make up the thermoelement are connected at the top by a connecting plate, which is soldered to the element. On the

bottom, by means of soldering, they are also joined together with connecting plates, which through electrically insulated heat junctions are soldered to the heat dissipation system. In this manner separate parts of the thermoelement, manufactured of materials with various physical properties, prove to be tightly bound to each other. We must add to this that the connecting plates are manufactured from a material with good heat and electrical conductivity and therefore possesses a high coefficient of linear expansion.

When voltage is applied to a thermoelement the upper connecting plate begins to cool and therefore to contract. The lower plate, on the other hand, begins to heat and therefore to expand. As result, a force couple is generated. As a result of these forces significant mechanical stresses are created in the thermoelement, which may lead to destruction of the element.

Since it is not possible to eliminate completely mechanical stresses, several thermoelement designs have been developed in which the mechanical stresses have been reduced to an extent that they no longer cause the thermoelement to fail. One of these provides for the utilization of the shortest possible cold connecting plate. In conformity with this system, the thermoelement arms cannot be located far from each other.

A second possible thermoelement design variation consists of manufacturing the cold connecting plate in the form of a spring (Figure 21, a). In this case, under the influence of mechanical stresses generated within the thermoelement, the spring would sag, but not exceed the limits of elastic deformation. Naturally the spring section must be such that the operating current passing through it must not release a noticeable quantity of Joule heat.

Another design for the cold connecting plate is represented in (Figure 21, c,) in which the plate is made of 2 opposed sections, separated by a thin slit. In location a a rather thin and short jumper is formed, which serves as an elastic plate. Due to the insignificant length of the jumper, no meaningful resistance is introduced into the electrical circuit of the thermoelement.

Another method of decreasing the harmful influence of mechanical stresses generated in the thermoelement involves the creation of damping layers between the arms of the thermoelement and the connecting plates. The damping material must be manufactured of a substance possessing a sufficient amount of resiliency and a small amount of ohmic resistance.

A thermoelement is shown in Figure (21, b,) in which the damper function is fulfilled by comparatively thick layers 3 and 5 of bismuth, which are

applied to arms 4 and 8 of the thermoelement. The soldering of the arms to the connecting plates 1 and 7 is provided by fusible connecting alloy elements 2 and 6.

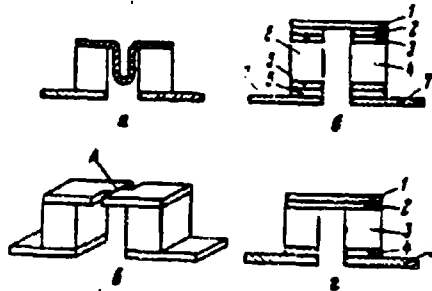


Figure 21. The construction of thermoelements with provisions for the reduction of mechanical stresses.

In the thermoelement construction examined, the thickness of the layer of bismuth must not exceed 0.2-0.3 mm, since this layer would otherwise possess noticeable electrical resistance. Thin lead washers, placed between the semi-conductor and the connecting plates, may be used as the damping layer.

A similar thermoelement is represented in Figure(21, d). To both of the arms 3, previously tinned with low-melting point connecting solder, are connected lead plates 2 and 4. Then upper and lower connecting plates 1 and 5 are soldered to them. As a result of the high ductility of the lead employed in such damping washers, the mechanical stresses generated in the thermoelement are almost completely removed.

## §2. Multi-stage Thermoelement

As we have pointed above, a multi-stage thermoelement permits us to obtain a considerably higher temperature differential than a single-stage unit. In this connection, however, the refrigerating capacity of the thermoelement decreases. In a number of devices when the heat load on the thermoelement is not great, 2-stage thermoelements are widely employed. In their construction, the basic problems are reduced to providing a current supply to the second stage and the creation of an electrically insulated junction between the hot junctions of the second

stage and the cold junction of the first stage. The provision for the current supply for the second stage of the thermoelement is a very important problem, since the current supply must satisfy two mutually exclusive conditions. On the one hand the current supply system must possess a sufficiently high cross-section to prevent the release of a significantly high quantity of Joule heat, which creates a harmful heat load on the thermoelement, and, on the other hand, the current supply system must possess high heat transfer resistance in order to reduce to a minimum the heat flux from the surrounding medium to the thermoelement.

The most efficient solution for this problem is to provide a single current for both the first and the second stages of the thermoelement. A diagram of such a system is shown in Figure 22. It provides for a parallel supply to the stages. The section of the thermoelement arms and their quantity in the first and second stages is calculated so that the current tapped off for the second stage is equal to the optimum value for this stage. In calculating the geometric dimensions of the arms of a 2-stage thermoelement with parallel feed, it must be kept in mind that the total thermoelement current passes through the outer arms of the first stage, whereas through the middle arms of the first stage and the arms of the last stage pass  $2/3$  and  $1/3$ , respectively, of the total current.

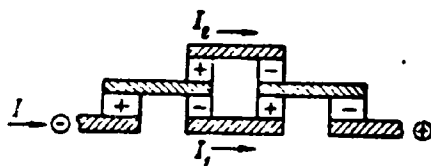


Figure 22. A 2-stage thermoelement with parallel feeding of the stages.

As has been pointed out earlier, with parallel feed the refrigerating capacity of the second stage is not very great, and because of this fact similar thermoelements may be employed in devices with a small heat load.

In a number of cases the creation of a 2-stage thermoelement is required, in which the refrigerating capacity of the second stage must be comparatively high. This is accomplished in a 2-stage thermoelement system with a series supply to the stages (Figure 23). Thermoelements 1 of the first stage are joined through electrically insulating connecting

plates 2 to the thermoelements 3 of the stage. The power supply connections to the thermoelement are made at the locations designated by arrows in the drawing. The choice of optimum operating conditions of the first and second stages is accomplished through the corresponding design of the section and height of the arms of the thermoelements.

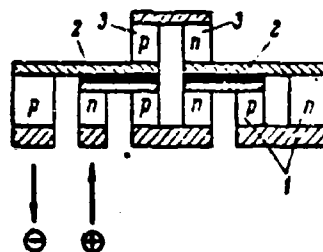


Figure 23. A 2-stage thermoelement with series feeding of the stages.

The principles of parallel and series connections of the arms in a 2-stage thermoelement may be employed also in the design of a 3-stage thermoelement with series (Figure 24 a) or series-parallel (Figure 24 b) stage connections. In particular, in a hygrometer for determining the humidity of the air at the dewpoint, a 3-stage thermoelement with series feed for all three stages was employed to cool a condensation surface 20 mm in diameter. This thermoelement provided a temperature drop of 98° and provided a temperature of -78° at the third stage. A 3-stage thermopile with series-parallel feeding of the stages, which provided for a temperature drop of 102°, was used to cool an infra-red radiation receiver.

In a design of multi-stage thermoelements and thermopiles it is necessary to pay particular attention to the refrigerating capability of the separate stages so that the underlying stages will be capable of fully accenting the heat released at the hot junctions of the upper stages. It has been established that for effective operation of a 3-stage thermopile with series feeding of the stages, the ratio of the number of thermoelements in the stages must be not less than 1 : 3, i.e., for 1 thermoelement of the third stage there must be three thermoelements in the second stage and, correspondingly, for three thermoelements of the second stage there must be 9 thermoelements in the third stage.

It must be noted that for effective multi-stage thermopile operation the design must take into consideration the dependence of the electrical

conductivity of the thermoelement material on temperature. This means that material must be employed in each stage for which the electrical conductivity will be optimum for a given stage temperature.

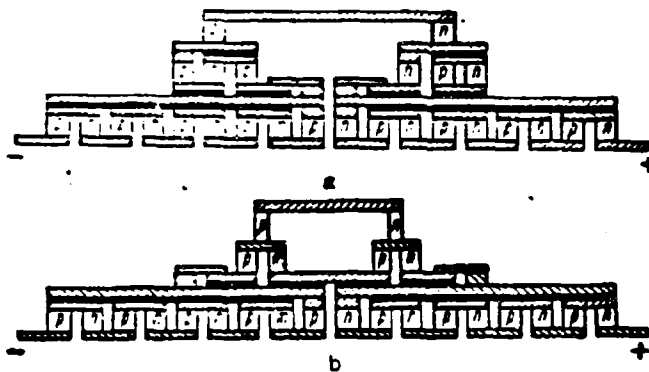


Figure 24. Diagram of the connections of a three-stage thermopile with series (a) and series-parallel (b) feeding of stages.

The creation of thermoelements and thermopiles with a number of stages above 3 is associated with significant construction complexities which are not justified by the small increase in temperature drop which a 4-stage thermoelement furnishes in comparison with a 3-stage element.

### §3. A Thermoelectric Pile

The design of a cooling device based on initial data determined by application conditions often leads to the necessity for creating a thermopile consisting of a large number of thermoelements. Often the calculated number of thermoelements may reach several hundred. This permits employing sources of relatively high voltage to supply the thermopiles and to require low operating currents from the sources.

The creation of thermopiles, consisting of many thermoelements, is linked with the necessity for manufacturing a large number of separate arms, and thermopiles assembled from these, and, what is most important, the interconnection of a large number of thermoelements. The connection of the thermopile is one of the basic operations in the technological cycle of the manufacture of a cooling device. The parameters of the

- finished article to a great extent depend on the quality of the execution of this operation.

In connection with the fact that in a majority of cases all the thermoelements are connected in a thermopile in series, the improper soldering of only one connecting plate or a breakdown in the connections during the use of the device leads to a failure of the entire apparatus.

- In addition, the necessity of employing small-dimension arms in low-current thermopiles transforms the switching process into an extremely complex operation which can only be performed by highly qualified workers. The task is simpler in the construction of a high-current pile. Rectifiers with industrially manufactured germanium or silicone diodes may serve as a source of current for a high-current pile.

Thus the choice of a feed system for a thermopile is quite an important consideration and in its solution not only operating, but also construction-technological factors must be considered. When possible one should give preference to high-current thermopiles over low-current piles.

In those cases when a thermopile is an independently constructed finished sub-assembly, the mechanical connection of separate elements is usually accomplished by means of filling the pile with epoxy compounds on the basis of ED-6 resin. The choice of this compound is governed by the fact that it possesses good adhesive properties with respect to practically all materials, it is mechanically stable and has a comparatively low coefficient of heat conductivity. The latter is particularly important, since a reverse heat flux from the hot junctions of the thermopile to the cold junctions passes through the compound, which lowers the cooling effectiveness. The best construction design is shown in the Figure 25. Epoxy compound is poured into the lower 1 and the upper 2 parts of the thermopile so that the central part (with respect to the height of the thermoelement) has a certain amount of air space. In order to prevent direct convection heat transfer between the hot and cold parts of the thermoelement this air gap 3 is filled with mipora [formaldehyde-urea foam] or foam plastic. Thermopile connections are accomplished after the compound is poured in, which permits future replacement of separate connecting plates during pile repair.

Usually arms with a rectangular section are used in thermopiles. However, in cooling devices employing liquid heat removal and annular thermoelements, proposed by A. N. Voronin, may be used.



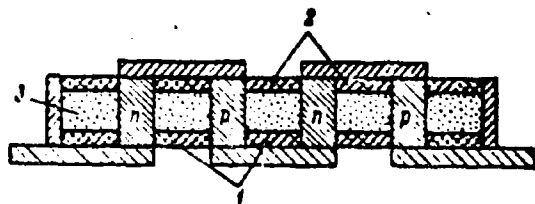


Figure 25. Diagram of a thermopile which is filled with an epoxy compound.

The design of an annular thermoelement is shown in Figure 26. Previously pressed positive and negative arms 1 and 2, manufactured in the shape of rings, are placed on metallic tubes 3 and 4, which are tinned with a connecting alloy. Tubes 3 and 4 fulfill the functions of hot connecting plates. Mica washer 5 is placed between the arms. Metallic ring 6 is placed on the outside of the thermoelement, and this forms the cold connecting plate.

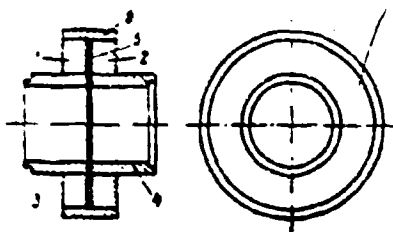


Figure 26. A section of an annular thermoelement.

The inside ring is previously tinned with a connecting alloy. Thus prepared, the intermediate product is placed in a special hot die, in which the final bonding of the semiconductors is carried out simultaneously with their connection to the external and internal rings.

The individual annular thermoelements are soldered to each other with a low-melting point solder and are assembled into a pile. Then cold radiating plates are soldered to the external rings of the thermoelements. A current of water is passed through the internal tube, which removes the heat from the hot junctions.

A section of an annular thermopile assembly is shown in Figure 27. This is one of the types employed in an everyday refrigerator with liquid heat removal. The number of thermoelements which form the annular thermopile must be such that the sum of the voltage drop on the pile is less than the difference in potential at which the electrolysis of water begins (1.8-2 v). If the number of thermoelements is so large that the total of voltage drop on the pile exceeds the value indicated above, the internal surface of the central cube must be electrically insulated from the water.

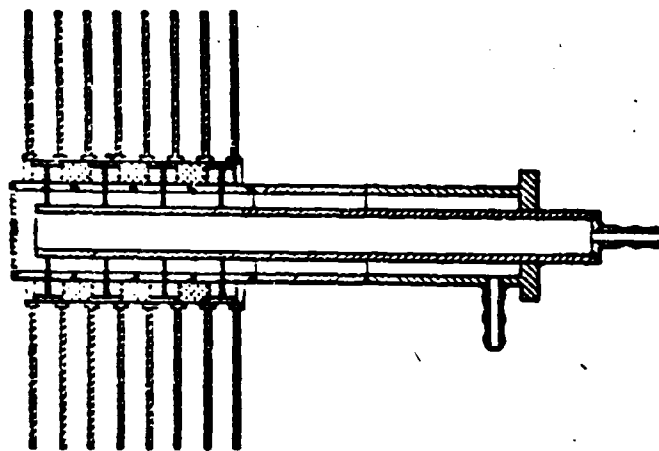


Figure 27. A section of an annular thermopile for a domestic refrigerator.

A magnetic field forms around a thermoelectric pile during operation. Sometimes this exerts a negative influence on the object undergoing cooling. The creation of special magnetic shields is not always convenient. Therefore in order to reduce the value of the magnetic field of the thermopile, the thermoelements in the latter must be distributed in a manner permitting bifilar current flow.

A similar design for the distribution of thermoelements in a linear thermopile is shown in Figure 28. Here the current passes in opposing directions through neighboring rows of thermoelements, and as a result the magnetic fields formed by this current are mutually suppressed.

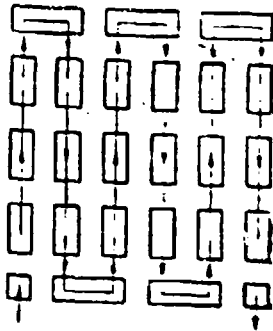


Figure 28. Diagram of the distribution of elements in a linear thermopile which provides for the partial suppression of magnetic field.

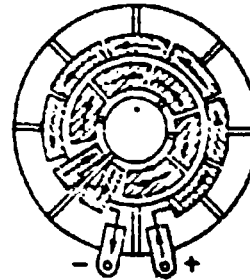


Figure 29. Bifilar distribution of elements in a thermopile. (The path of the current is shown by arrows).

Another construction variation of the bifilar thermopile is shown in Figure 29. The magnetic field of the thermoelements is distributed along the external annular circuit and is balanced by the magnetic field of the thermoelements distributed along the internal circuit, in which the current flows in the opposite direction. It must be noted that in a bifilar thermopile the magnetic field is not completely eliminated. The best compensation for the characteristic magnetic field of the thermopile may be obtained by introducing a supplementary compensating winding, which in its configuration duplicates the thermoelectric distribution in the pile. It is connected in series with the pile, but in such a manner that the direction of the current passing through it is opposite to the direction of the current flow through the pile. As a result, a magnetic field is generated in the compensating winding which has the same configuration as the field in the pile, but with an opposite sign, which results in their mutual cancellation.

#### §4. The Heat Coupling of the Thermopile

For normal operation of a thermoelectric cooling device it is necessary to provide the most effect heat coupling of the thermopile with the area or volume subject to cooling, on the one hand, and with the heat transfer system on the other hand. The heat coupling site must possess low heat transfer resistance and high electrical resistance. In addition, a practical heat coupling must also provide for reliable mechanical strength among the coupling sub-assemblies.

In the first designs of thermoelectric refrigerators (1956), the heat coupling was provided by means of mica washers 15-20  $\mu$  in thickness. The surface of the mica was covered with a thin layer of mineral oil in order to provide the best heat contact. Heat flow through the mica created a parasitic temperature drop of 10-12° with heat fluxes of 1 w/cm<sup>2</sup>. Since this method of heat coupling did not add to the mechanical strength of the device, in subsequent designs of these devices the coupling was accomplished by means of aluminum, on which a thin layer (0.5-1  $\mu$ ) of aluminum oxide ( $Al_2O_3$ ) was created in the required areas by an electrochemical method. The parts to be coupled were cemented together by means of an epoxy compound. A similar sub-assembly is shown schematically in Figure 30. Here film 1 of aluminum oxide was applied to plate 2 which is the base of radiator 3. The connecting plates of the hot junctions of the thermopile were cemented to the oxide layer, and then the thermopile 4 was assembled on the plates.

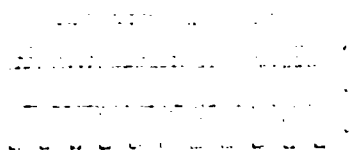


Figure 30. Diagram of the heat coupling of a thermopile with an oxidized aluminum radiating plate.

As a preliminary operation, the surfaces of the parts to be coupled were surface-lapped. Due to the epoxy compound bond, this system of coupling possessed sufficient mechanical strength. The parasitic drop on the electrically insulating layer (oxide + resin) amounted to 3.5° at a flux of 1 w/cm<sup>2</sup>. However, upon the breakdown of the electrical insulation between only 1 connecting plate and the base, disassembly of the entire thermopile was required which was an extremely time consuming operation. It became apparent that the most technically feasible thermopile heat coupling could be achieved by individual heat junctions, the dimensions of which in each specific case must be determined by the design of the thermopile. In addition, it is extremely important that the employment of individual heat junctions not require the dis-assembly of the entire thermopile whenever a separate heat junction fails. In this connection, all subsequent designs of thermo-cooling devices have been based on individual heat junctions.

Five types of heat junctions were developed, which differed from each other not only in their technical parameters, but also in the technique of their manufacture.

In 1958 heat junctions consisting of 2 copper plates of a specific dimensions, cemented together with a thermoreactive epoxy compound, began to be employed in a number of devices. Electrical insulation between the plates was provided by a thin (0.1-0.2  $\mu$ ) layer of copper oxide, obtained on the copper surface by means of processing in a water solution of potassium persulfate and sodium hydroxide.<sup>1</sup> After cementing and polymerization of the epoxy resin, the heat junction was transformed into a single part, which was soldered into place by means of low-melting point solder between the thermopile in the heat transfer system. Among the shortcomings of the cemented heat junction were the frequent occurrences of short circuits due to mechanical breakdown of the excessively thin layer of copper oxide. The creation by chemical means of a thicker oxide on the copper was not possible. In addition, the layer of resin, which was 10-15  $\mu$  in thickness, possessed relatively high heat transfer resistance as the result of which at heat flux densities of 1 w/cm<sup>2</sup> the parasitic temperature drop at the heat junction equalled 3.7°.

A subsequent design for an electrically-insulating heat junction provided again for the cementing of copper plates, but through thin (6  $\mu$ ) cable paper. This cementing was accomplished by means of a thermoreactive epoxy compound. In order to reduce the thickness of the layer of the compound between the plates, the latter were surface-lapped as a preliminary step. The electrical insulation of the cemented heat junctions through the paper was considerably higher than for the oxide junctions. Cases of short-circuits were practically not observed. This type of heat junction permits subsequent soldering to be accomplished with higher-temperature solder. The construction of a heat junction using paper as the electrically insulating layer, however, proved to be time consuming from a manufacturing standpoint, since it was necessary to carefully surface-lap the copper plates. In addition, as a result of residual mechanical stresses generated in the copper plates during their mechanical processing and lapping in the process of polymerization of the epoxy compound at a temperature of 160-180°, a certain amount of warping occurs which leads to a deterioration in the positioning of the heat junction and a corresponding increase in its heat transfer resistance.

In this connection a new heat junction system has been developed, which is free from the deficiencies enumerated above. This heat junction consisted of a copper plate surface-finished on one side with a lathe or a milling machine. Then a lead plate, surface-finished on

<sup>1</sup>The formula for the bath and the copper oxidation method are cited in Chapter IX, §4.

one side (by etching or milling) was cemented by means of a thermoreactive epoxy compound to the surface-finished copper plate, with a layer of paper 6  $\mu$  in thickness between the two. A small load is placed on the lead plate in order to provide good adhesion of the lead to the copper in the resin polymerization process. Subsequent soldering to the heat junction of the thermoelement arms is accomplished from the side of the lead plate, which in this case also serves simultaneously as a damping layer, which accepts the mechanical stresses generated in the thermoelement.

On the copper-paper-copper and copper-paper-lead heat junctions, at a flow of 1 w/cm<sup>2</sup> the parasitic temperature drop was equal to 2.3°.

A principally new system of electrical insulation of the heat junction was proposed by A. G. Shcherbina. This crimped heat junction, which is indicated schematically in Figure 31, was formed of two copper ribbons 1 and 4, 0.1 mm in thickness, with paper gasket 3, 50-80  $\mu$  in thickness, between them. This packach is formed into a "bellows" on a special machine, after which it is impregnated with thermoreactive epoxy compound 2. As a result of the large surface of the contiguous copper belts, the heat transfer resistance between them, notwithstanding the relative thickness of the paper layer, is quite small. Copper washers are soldered above and below the corrugations in order to relieve the thin copper corrugations from the necessity of carrying the current which feeds the thermopile. Soldering of the heat junction to the device is accomplished by means of these washers.

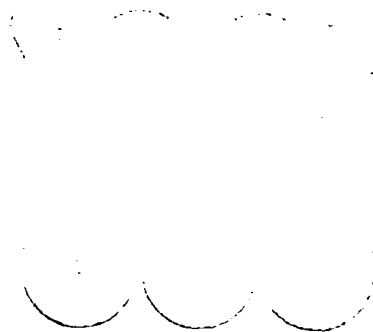


Figure 31. Diagram of a crimped heat junction design.

The crimped heat junction of copper-paper-copper will not operate in a damp atmosphere, which is characteristic of conditioners and some other type of devices, since the resistance of the heat junction falls

significantly due to the hygroscopic paper. For operation under conditions of increased moisture, strip fluoroethylene is employed as an electrical insulator in place of the paper. Heat junctions employing the fluoroethylene do not lose their electrical insulating properties even if they are fully submerged in water. However, due to the non-wettability of the fluoroethylene by the epoxy resin, air remains in the corrugations of the heat junction and causes a deterioration in the thermo and technical properties of the junction. The parasitic temperature drop, referred to the same flow of  $1 \text{ w/cm}^2$ , for a crimped heat junction with fluoroethylene was equal to  $2.1^\circ$ , whereas the value for a crimped heat junction with paper was  $1.7^\circ$ .

Among the shortcomings of crimped heat junctions, we must refer to their relatively large height ( $\approx 6 \text{ mm}$ ), which is particularly undesirable for multi-stage thermopiles, and the small reversible deformations of the junction under the influence of temperature changes. In many thermocooling devices these deformations are completely inadmissible.

Judging by all parameters, it must be acknowledged that the most advantageous heat junction is one made of ceramic material, inserted between two copper plates. The basic merits of a ceramic heat junction in comparison with others consists of its simplicity, reliability, technological effectiveness, superior electrical thermal parameters. Aluminum-oxide ceramics (alundum) are usually employed as electrical insulators in heat junctions. At room temperature the coefficient of heat conductivity for this material is practically the same as that for steel. The mechanical strength of alundum ceramic material is quite high (the ultimate tensile strength is  $1,250 \text{ kg/cm}^2$ , and ultimate compression strength  $15,000 \text{ kg/cm}^2$ ). The most essential point is that in many branches of industry -- in particular, in the capacitor industry -- the method of metalizing ceramics has been mastered long ago, which permits the subsequent soldering of ceramic materials to materials of metal. The small coefficient of linear expansion ( $\approx 6 \cdot 10^{-6}$ ) practically eliminates "creeping" of the heat junction under the influence of changing temperatures. Ceramic heat junctions permit multi-stage soldering with all soft and even hard solders with no deterioration in their properties.

It must be noted that many have the opinion that beryllium oxide ceramics have high prospects in heat junction; these opinions have no basis, since, although beryllium oxide possesses a phenomenally large coefficient of heat conductivity, its extremely high toxicity hardly permits its application in heat junctions. Alundum heat junctions possess the lowest known parasitic temperature drops. With a flux density of  $1 \text{ w/cm}^2$  the junction drop was equal to  $1.3^\circ$ . The dependencies of the experimentally obtained parasitic temperature drops for various types of heat junctions on flux density are shown in Figure 32.

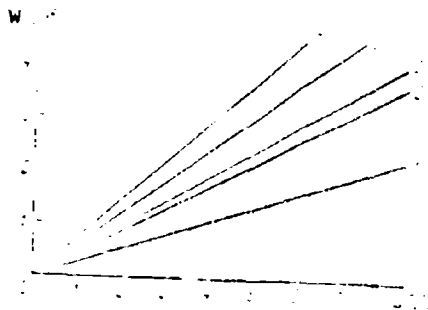


Figure 32. Parasitic temperature-drop dependence on heat flux value for various heat junctions.

- 1, oxidized cemented joints; 2, cement and paper; 3, corrugated (with fluoroethylene); 4, corrugated (with paper); 5, ceramic

It is not without interest to note that there is still another method of fabricating a ceramic heat junction. This method is as follows. First a copper base is spray-coated with a layer of aluminum oxide 0.2-0.5 mm in thickness. Then, on top of this layer, a coating of copper is sprayed to a thickness of 1-1.5 mm. After appropriate thermal normalization and mechanical processing a ceramic heat junction with sufficiently high electrical and thermal properties is obtained.

When the heat flux through a heat junction exceeds  $3 \text{ w/cm}^2$  and it is not possible to expand the surface, it is possible to employ the design schematically represented in Figure 33.



Figure 33. A section of a heat junction design for high heat flux values.



Copper plate 4 is soldered to aluminum nipple 3, which is placed in copper part 1, which contains channel 2 for the passage of heat-dissipating water. The surface of the aluminum nipple is covered with a thin coating (1-3  $\mu$ ) of aluminum oxide by the electro-chemical anodizing method, after which the nipple is filled with low melting-point alloy 5. A similar heat junction is employed in several types of high-vacuum thermoelectric collectors.

## 55. The Design of Heat Transfer Systems

The heat transfer system serves to remove heat from the hot thermopile junctions. One of three basic types of heat-transfer systems are employed in thermoelectric cooling devices; these are a radiator with natural convection heat exchange, a radiator with forced heat removal, and the liquid system. Depending on the design and the operating condition of the thermoelectric device, one of the methods enumerated above may be used. Radiator systems with natural convection are the simplest in construction, but are the least effective. These systems are employed in low-current thermopiles and utilizing thermoelements which are distributed over a relatively large area. The transfer of 1 w of heat output by means of a natural convection radiator requires approximately 2.5 cm<sup>2</sup> of plate area. As a result, such systems possess large dimensions and a great deal of weight. The best material for the fabrication of the radiator is any type of copper, or, if it is possible, pure aluminum of the "A-00" or "A-0" type.

Soldering of the plates to the base of the radiator, when copper is used, is accomplished with PSR-15 F5 hard solder (sil'fos<sup>1</sup>). An aluminum radiator is soldered with tin with the aid of 34-A flux. In any construction design the radiator fin should always be arranged vertically. A horizontal arrangement of the radiator fins is many times less effective. The surface of the fins must be blackened in order to improve the coefficient of heat exchange. The copper fins may be blackened by oxidation in potassium persulfate. Aluminum radiators are oxidized and then painted a black color with aniline pigments.<sup>2</sup>

By virtue of a large coefficient of heat transfer, air radiators with forced heat removal are significantly more compact and lighter than radiators with natural convection heat exchange. Copper or pure aluminum may again serve as materials for the radiator. In contrast to the radiator systems described above, this system does not require a linear distribution of radiator plates and is a vertical arrangement. Radiators with a blower very often have a circular shape, since the spatial

<sup>1</sup>The meaning of this term is not known. It may be a trade name for a type of hard solder. Tr.

<sup>2</sup>A method of blackening copper and aluminum is described in Chapter IX, 54.

distribution of the plates has no significance. Ventillation of the radiator system is usually accomplished by means of a small electric motor operating at high rpm (9-10 thousand rpm).

The axle of the motor is attached to a 3 or 6-bladed impeller with a blade angle of  $30^\circ$ . The direction of the rotation of the blades must be such that the fan operates not as an air injector, but as an air suction device. This requirement is established by the fact when the fan is operating at the air output, the airflow which passes over the radiator also blows on the electric motor, which creates better operating conditions for the motor. In the opposite case, when the fan is operating at the air input, heat released by the motor would pass over the radiator, lowering its efficiency. With a linear distribution of the radiator plates, their length must not be too great, since this increases the aerodynamic resistance of the radiator, causing a deterioration in the radiator parameters.

As we will discuss later in greater detail (Chapter III, §2), radiator systems with forced cooling can be constructed with a linear distribution of fins (Figure 34, 1) or, a better solution is with fins shorter in length (Figure 34, 2). If the value of the aerodynamic resistance of the radiator does not play a significant role, i.e., if the ventillator has reserve power, it is possible to recommend a radiator system in which the even rows of short plates along the airflow are inclined somewhat with respect to the plates of the uneven rows (Figure 34, 3). The angle of inclination must not exceed  $15-20^\circ$ . A radiator of this type operates very effectively.

NOT REPRODUCIBLE

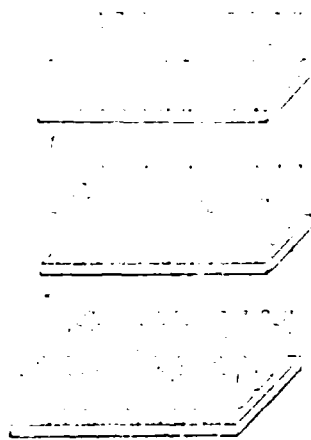


Figure 34. The design of linear radiator systems operating under a condition of forced air heat removal.

In the design of a radiator system of the annular type, it is necessary to bisect the airflow in order to decrease the air passage length, as shown in Figure 35. Here the plane of hot junctions of thermopile 1 is soldered to the body of radiator 2. Annular fins 3 are cut directly into the body of the radiator. The exterior surface of the radiator plates are covered with cylindrical casing 4, to which a pipe containing small electric motor 5 is soldered. The airflow created by impeller 6 is drawn through the opening in casing 7, flows around both sides of the radiator plates, and is exhausted through the pipe.

**NOT REPRODUCIBLE**

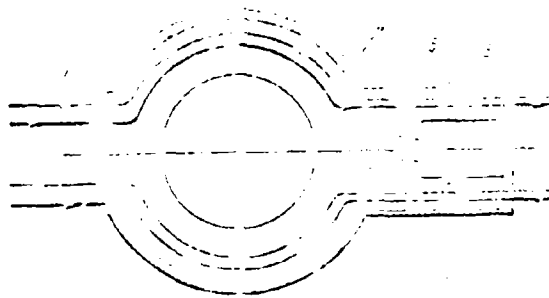


Figure 35. The design of an annular radiator system operating under a condition of forced air heat removal.

Let us examine the basic design variations of liquid heat transfer systems. In the simplest system the jacket is attached to a metallic collector of the hot junctions and circulating water flows through the jacket.

A second variation provides for the fabrication of water channels directly in the body of the collector. From the standpoint of design

in technological considerations, the most efficient method is to establish channels for the passage of the water directly within the hot connecting plates. In a number of devices described in Chapter III, liquid heat removal is accomplished in this manner.

Figure 36 shows a design for a water system of heat transfer which is employed in a microtomic stand and in a microrefrigerator for laboratory purposes. Brass slugs of square section 1 are equipped with channels 2, through which the water passes from connecting pipe 3. The slugs are electrically isolated from each other by pressboard washers 4. The washers have water passage openings in the proper places. After the sub-assembly has been prepared in this manner, it is cast in thermoreactive epoxy compound 5, and is then subject to mechanical processing.

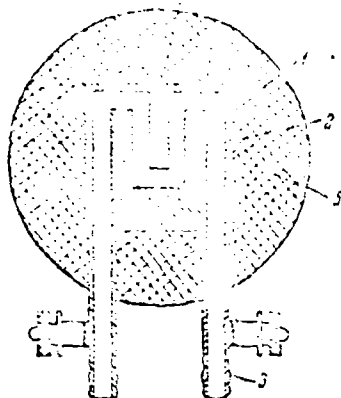


Figure 36. A system of liquid heat removal installed directly in the hot connecting plates.

The thermoelements are soldered directly to the slugs, which eliminates noticeable parasitic temperature drops. A similar heat transfer system may operate at high heat flows, up to 10-20 w/cm<sup>2</sup>.

Several types of cooling devices, according to the conditions of their operating, cannot be connected directly to the electrical and water supply systems. A number of thermoelectric cooling devices described in part III (Chapter XII) may serve as an example. In this

case the electrical supply to the device is accomplished by means of a flexible cable of PShch wire. However the necessity of delivering large currents to devices is associated with the employment of current carrying wires of large cross-section, which creates a certain amount of inconvenience in employing the devices. Moreover, in this case in addition to the current conducting wires, two hoses for water input and output must also be connected to the device.

In similar thermocooling devices a combined electrical and water supply system may be employed. The diagram for this system is shown in Figure 37. Here the current-carrying busbar 1, which is manufactured of PShch cable, is enclosed within rubber pipe 4. There is a gap between the pipe and the busbar, through which the water passes. At locations 7 the busbar is attached to terminal sub-assembly 2 and to coupling sleeve 3, which is connected to the thermopile. The water which passes through connecting pipe 5 flows around the busbar and passes through opening 6. A second cable of an analogous design is connected to the apparatus and furnishes the second pole of the electrical feed and the water output. Such a system allows a significant reduction in the cross-section of the current-carrying busbar, since the latter is constantly immersed in water. Thus, for example, in a thermoelectric cryoextractor a flexible current-carrying busbar utilizing a wire of only  $3 \text{ mm}^2$  passes a current of 90 a.

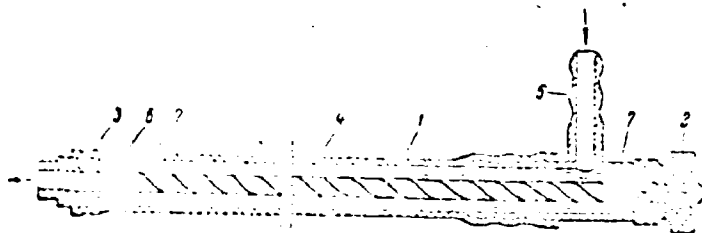


Figure 37. A section of a combined water and current supply.

#### §6. The Operating Chamber of the Device

If a thermoelectric device is intended to provide a reduction in temperature in a certain operating chamber volume, certain construction requirements must be met.

The operating chamber of the device must be constructed of material which possesses good heat conductivity (copper or aluminum). This is required in order to equalize the temperature within the chamber volume.

In order to provide good heat coupling between the operating chamber and the thermopile, the latter must be connected with electrically-insulated heat junctions, described above, and the operating chamber must be soldered to these junctions. In order to prevent heat flow from the surrounding medium into the operating chamber, the latter must be protected by a layer of heat insulation. Its thickness is determined by calculation (Chapter V, §2).

Foam plastic or some other material possessing a low coefficient of heat conductivity is employed as a heat insulating material. Basic data concerning several heat insulating materials are shown in Table 2. In specific cases it is possible to employ mipora. However, foam plastic possesses a number of advantages over mipora. But one of these consists of the fact that foam plastic is easily formed mechanically, and therefore variously shaped parts may be manufactured from it.

Table 2  
Basic Data Concerning Several Heat Insulating Materials

Heat Insulating Material	Specific Gravity, g/cm <sup>3</sup>	Coefficient of heat conductivity, kCal/m <sup>2</sup> · h · deg
Mipora	0.02	0.36 - 0.12
Foam plastic	0.005 - 0.015	0.03 - 0.08
Aerogel	0.009	0.023
Foam glass	0.5	0.1 - 0.15
Foam polystyrene	0.016	0.035
Polyurethane	0.012	0.02
Glass wool	0.04	0.07

We point out the possibility of creating a thermocooling device design in which the parasitic heat flow into the operating chamber from the surrounding medium is reduced to a significant extent. This is achieved by means of distributing a thermopile along all sides of a rectangular operating chamber. In this case the necessity for heat insulation of the chamber of the device no longer arises.

One of the variations of an experimental thermoelectric microchamber, described in chapter IX, §2, serves as an example of a chamber of this type.

In case a necessity of constructing a device possessing significant refrigerating capacity but with a relatively limited operating chamber

volume, the thermopile is constructed in several independent parts, each of which is soldered to the chamber at the appropriate place.

A second type of experimental thermoelectric microchamber (Chapter IX, §2) was constructed in exact accordance with this principle. Thermoelectric 2-stage thermopiles were soldered to the four side surfaces and to the bottom of a copper chamber. Such a design, in addition to providing a relatively high refrigerating capacity, eliminates the generation of a noticeable temperature gradients within the chamber, which is unavoidable when the thermopiles are distributed on only one side of the chamber (usually on the bottom).

## CHAPTER VII

### Methods of Heat Removal From Thermocooling Devices

It has been pointed out previously that the minimum temperature on the cold junctions of a thermobattery is achieved when the heat which is released from the hot junctions is eliminated; therefore, the normal operation of any thermocooling device depends to a great extent on the effectiveness of the heat transfer system. The selection of one or another heat transfer system depends on a series of factors, which depend on the construction of the device and the conditions surrounding its application.

Several methods of heat transfer are described in this chapter which are used in thermocooling devices operated under stationary and non-stationary conditions. Here various methods are discussed for the removal of heat from the thermocooling devices which in accordance with operating conditions must operate for a limited amount of time in a self-contained apparatus.

#### §1. A Radiator System with Natural Convection Heat Exchange

In many designs for thermoelectric cooling devices an air radiator with natural convection heat exchange is employed as the heat transfer system. Much work has been devoted to the problem of the design of suitable systems; however in a majority of these purely qualitative calculations are given. It is not always convenient to employ the relationships cited in these publications in the engineering design of a radiator system. At the same time it is known that a radiator system which satisfies practical requirements may be designed with approximation equations which significantly simplify the design method.

We shall show the design of a radiator system with *equidistant* flat fins, which is most often encountered in practice. The following



must be given as the initial design data:

- 1) the permissible temperature drop between the radiator and the surrounding air;
- 2) the heat output released at the hot thermopile junctions, which must be dissipated by the radiator;
- 3) the radiator-air heat transfer coefficient;
- 4) the coefficient of heat conductivity for the material from which the radiator plates are manufactured.

The area of a radiator system with natural convection heat removal may be determined with a sufficient degree of accuracy by the relationship

where  $F$  is the sum of the area of all heat exchange surfaces of the radiator,  $m^2$ ;  $Q$  is the heat output which the radiator must remove from the thermopile,  $kcal/h$ ;  $\alpha$  is the radiator-air heat transfer coefficient ( $kcal/m^2 \cdot h \cdot deg$ );  $\Delta T$  is the permissible temperature drop between the radiator and the surrounding air.

The numerical value of the heat transfer coefficient under conditions of natural convection heat exchange usually lies within the limits of 3-5  $kcal/m^2 \cdot h \cdot deg$ . However, the value of this coefficient depends on a number of factors; the first of these is the spatial distribution of the radiator plates. In order to calculate the numerical value of the heat exchange coefficient for radiator systems of various arrangements, we may employ the relationships shown below:

- a) for a radiator equipped with a system of horizontally distributed fins,

$$\alpha = 0.001 \sqrt{\frac{Q}{F \Delta T}}$$

- b) for a radiator with a system of vertically distributed fins, with the opening upward,

$$\alpha = 0.001 \sqrt{\frac{Q}{F \Delta T}}$$

c) for a radiator with a system of vertically distributed fins with the opening downward,

where  $\Delta t$  is the temperature difference between the radiator and the surrounding air;  $L$  is the height of the vertical surface of the radiator plates, m;  $l$  is the shortest side of the horizontal surface of the radiator plates, m.

In order to calculate the convection heat exchange of the front surfaces of the radiator plates with the surrounding medium, we may use the equation

where  $\delta$  is the thickness of the radiator plate, mm.

In calculating the effectiveness of the air radiator system, basically we must keep in mind the coefficient of the convection heat exchange between the surface of the radiator and the surrounding medium. However in addition to convection heat exchange, radiation heat exchange also plays a role in the process of heat transfer from the radiator. It was established in the work by G. N. Pokrovskaya that even at low temperatures the extent of the radiating power of the radiating surface plays a rather significant role in the heat exchange process. Conclusions were made on this basis that the surface of the fins of the air radiator system, even those operating at low temperatures (20-50°) must be fabricated in order to provide for a maximum radiation capability.

In order to calculate the coefficient of heat exchange between the radiator and the surrounding medium as a result of radiation, we may, with sufficient accuracy employ the following relationship:

$$\alpha_{\text{rad}} = \frac{\epsilon \sigma (T_{\text{r}}^4 - T_{\text{a}}^4)}{L + l}$$

here  $T$  is the average temperature of the radiator,  $^{\circ}\text{K}$ ;  $T_c$  is the temperature of the surrounding medium,  $^{\circ}\text{K}$ ;  $b$  is the distance between the fins,  $\text{m}$ ;  $h$  is the height of the fins,  $\text{m}$ ;  $\epsilon$  is the emissivity of the radiator fins.

The emissivity of various materials from which radiator systems may be constructed or with which they may be coated is shown in Table 3.

Table 3  
The Emissivity of Various Materials Employed in the Manufacture and Coating of Radiator Systems

Material	Temperature, $^{\circ}\text{C}$	Emissivity
Polished aluminum	50-100	0.04-0.06
Aluminum with a rough surface	20-50	0.06-0.07
Heavily oxidized aluminum	50-500	0.2-0.3
Aluminum paint	20	0.2-0.3
Rolled brass	20	0.06
Roughened brass	20	0.2
Polished copper	50-100	0.02
Scraped copper	20	0.02
Oxidized copper	50	0.6
Sheet steel	50	0.56
Oxidized sheet steel	50	0.88
Black Matte laquer	40-100	0.96-0.98
Glossy black laquer	20	0.87
Lamp black	20-400	0.95
Carbon black with water glass	20-200	0.96
Black glossy shellac on iron	20	0.92

As we have pointed above, the relationship shown for the calculation of a natural convection radiator system is to a certain extent an approximation; however, it does permit obtaining the required practical calculations with an error not exceeding 10-15%.

If with natural convection heat exchange, the coefficient  $\alpha$  usually equals 3-5, then with forced air cooling of the radiator system, value  $\alpha$  increases to 100. Therefore in a radiator system with forced cooling the radiator plate area may be significantly reduced. However, in a

design of radiator systems with forced heat removal a number of additional conditions arise which are determined by the distance between the fins, the height and length of the fins, the degree of roughness, the flow rate of the air and a number of other factors.

## §2. A radiator System with Forced Heat Removal

As we have already indicated above (Chapter I, §3), in radiator systems with forced heat removal (by blowing) the radiator-air heat transfer coefficient may reach a value of 100 and higher, i.e., almost 1 1/2 orders of magnitude higher than in the case of natural convection heat removal. However, due to complexity of the design of radiator systems with forced heat removal, there is practically no material on this subject in any of the textbooks in heat engineering and thermophysics. We shall employ the calculations of A. M. Ramadan, which are cited below, although these calculations cannot pretend to complete mathematical accuracy.<sup>1</sup>

In a case when the radiator system is soldered to the hot connecting plates of the thermoelectric pile through the corresponding heat junctions, and disregarding parasitic temperature drops on the heat junctions, the radiator heat removal value will be determined by the relationship:

$$Q = \alpha_{av} (F_1 + F_2) (t_1 - t_2) \quad (72)$$

Here  $Q$  is the quantity of heat subject to removal by the radiator;  $F_1$  is the radiator plate surface area;  $F_2$  is the area of the base between the ribs;  $F_3 = F_1 + F_2$  is the total heat transfer area of the radiator;  $\alpha_{av}$  is the average heat transfer coefficient;  $t_1$  is the temperature of the hot junction of the thermopile;  $t_2$  is the temperature of the surrounding medium;  $B$  is the fin coefficient, equal to the quotient of the division of the full heat exchange surface of the radiator by the total area of the base of the radiator;  $C_1$  is a coefficient which characterizes the locus of the radiator connection to the thermopile, which is defined as the quotient resulting from the division of the total area of the hot

<sup>1</sup>The materials in this paragraph have been taken from a dissertation by A. M. Ramadan, *Heat Transfer Intensification in Thermoelectric Cooling Devices*, completed at the Leningrad Technological Institute of the Refrigerating Industry in 1963.

junctions of the semiconductors by the total area of the hot connecting plates;  $C_2$  is a coefficient which characterizes the heat transfer resistance between the hot junctions of the thermopile and the base of the radiator system, equal to the quotient resulting from the division of the average temperature of the base of the fin by the temperature of the hot junction of the thermopile.

The value  $l_{av}$ , as a part of equation (72), is called the average effectiveness of the radiator fins and is defined as

$$l_{av} = \frac{t_3 - t_4}{t_3 - t_5}$$

here  $t_3$  is the average temperature of the radiator fin;  $t_4$  is the average temperature of the radiator base.

It is apparent from the formula shown that in order to increase the effectiveness of the radiator it is necessary to increase fin coefficient  $B$ , fin effectiveness  $l_{av}$  and the fin heat transfer coefficient  $\alpha_{av}$ .

The average heat transfer coefficient of the radiator system may be determined in accordance with the equation

$$\alpha_{av} = \frac{Q}{F(t_3 - t_4)}$$

where  $t_5$  is the average temperature of the base of the fin; the remaining values in this equation were explained above.

In forced air cooling, just as in radiator systems with natural convection heat removal, the basic resistance to the flow of heat from the fin to the surrounding medium is concentrated in a fin boundary layer of air near the side of the fin. The heat transfer coefficient from the surface of the fins increases with the decrease in the thickness of this boundary layer. It has been established that in tubular heat exchangers, through air is being passed, the heat exchange coefficient depends to a great extent on the ratio of the length ( $L$ ) of the pipe to its diameter ( $b$ ). With a decrease in the value of this ratio the heat transfer coefficient increases as a result of the fact that an air boundary layer of significant thickness does not form on the internal surface of a

short tube. In this connection a radiator system with forced heat removal must be constructed in the form of individual short laminated fins, which are distributed linearly with a gap between them. An important value characterizing a radiator system with forced air cooling is the hydrodynamic frictional resistance which is encountered by the air flow moving along the radiator plates. For a radiator system consisting of a linearly distributed fin with a gap along the length, the value of the hydrodynamic resistance is determined from the equation

where  $\Delta H_{sta}$  is the static pressure differential at the input and output of the radiator,  $W_y$  is the air mass flow rate ( $\text{kg/m}^2 \cdot \text{sec}$ ), which equals

where  $f$  is the sum of the area of the transfer section of the radiator,  $\text{m}^2$ ;  $G$  is the mass rate of air flow,  $\text{kg/h}$ .

The dependence of the value of the average heat exchange coefficient on the mass rate of air flow, determined for a radiator with a linear distribution of fins with a gap, is shown in Figure 38 (curve 1). Curve (2), which is shown on the same graph for comparison, was obtained for a radiator with linearly distributed ribs without a gap. The geometric dimensions of the radiators employed are shown below.

#### For a Radiator with a Gap

The length of the radiator plate along the air flow	6.25 mm
Height of the plate	30 mm
Thickness of the plate	0.2 mm
Distance between plates	1.5 mm
Size of the gap between groups of fins	1.25 mm
Number of stacks of plates in the radiator	35
Ratio $L/d_{ek}$	2

### For a Radiator Without a Gap

Length of the plate	260	mm
Height of the plate	30	mm
Thickness of the plate	0.2	mm
Distance between plates	3	mm
Ratio $L/d_{ek}$	44	

It is apparent from Figure 38 that the average heat transfer coefficient for fins with a gap is almost twice as high as for radiators without a gap in the plates. It has also been determined experimentally that the value of the gap does not significantly influence the radiator effectiveness.

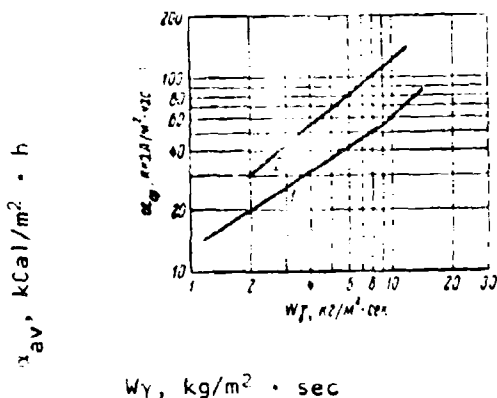


Figure 38. The dependence of the average heat exchange coefficient ( $\alpha_{av}$ ) on the mass rate of air flow ( $W_\gamma$ ) passing through the radiator.

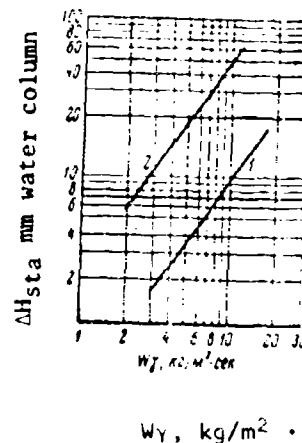


Figure 39. Static pressure differential ( $\Delta H_{sta}$ ) for air passing through the radiator as a function of mass rate of flow ( $W_\gamma$ ).

Static pressure differential dependence on mass rate of air flow is shown in Figure 39. Curve 1 corresponds to a radiator system without a gap, and curve 2 to a system with a gap. The parameters of the radiators investigated are the same as those shown above. It is apparent from this graph that the static pressure differential for a radiator with a gap is significantly higher than for a radiator without a gap. This, however, was to be expected, since in a radiator system with gaps, airflow turbulence is significantly higher than in a radiator with continuous fins. Therefore it is natural that a radiator with a gap would have a

large coefficient of friction in comparison to a radiator that is continuous. It was also established that the value of the coefficient of friction is inversely proportional to the ratio  $L/d_{ek}$  of the radiator. A change in the length of the gap between the ribs does not significantly change the coefficient of friction.

The following preliminary conclusions may be drawn on the basis of what has already been stated.

1. In utilizing a radiator with linear distribution of plates, gaps must be employed along the plates, the number of which is determined by the construction of the thermopile and the dimensions of the radiator, but the dimensions of these gaps must lie within the limits of 1-10 mm.

2. If the construction of the thermopile permits, the radiator plate must be fabricated in a manner that allows the base to serve simultaneously as the connecting plate of the thermoelement.

3. The geometry of the radiator must be such that the ratio  $L/d_{ek}$  lies within the limits of 2-5.

### §3. Spike Radiator Systems

One of the merits of thermoelectric cooling devices is a possibility of creating concentrated thermopiles in which individual thermoelements are distributed close to each other. However, a concentration of thermoelements on the small surface of the thermopile requires the creation of effective compact heat exchange surfaces from the side of the hot junctions.

The employment of radiators with natural convection heat exchange, due to low values of the heat exchange coefficient, does not permit the construction of the compact system of heat transfer. Radiator systems with forced air cooling permit attaining heat exchange coefficients from 8-10 times higher than in systems with natural convection cooling.

It is known that for these systems the heat exchange coefficient of the laminated fins depends on the rate of gas flow and on the geometry of the relative distribution of the radiator plates. In this connection, a decrease in the width of the plate in the direction of the flow of the cooling air leads to an increase in the heat exchange coefficient. However, a significant decrease in the width of the radiator plates with a given plate thickness leads to an increase in the temperature difference along the height of the fin, which during intensive heat transfer almost completely cancels the advantage gained in increasing the heat exchange coefficient.



Heat transfer effectiveness of a radiator plate equipped with forced draft may be increased to a certain extent if the plate has a large heat conducting section with respect to its perimeter. A spike is a fin of this type. Such radiator systems are called spicular.

A number of experiments were carried out in order to investigate the coefficient of heat transfer of spicular radiator systems operating under conditions of natural convection. As a result of these experiments it was established that for a system of spikes, distributed in a staggered fashion, air flow turbulence in the radiator system sharply increased its aerodynamic resistance. At the same time a noticeable increase in the coefficient of heat transfer occurred at an air flow rate of 0.04-0.05 m/sec, which corresponds to Reynolds number  $Re = 9$ . With a required temperature drop between the radiator and the surrounding medium of 4-5°, such a rate of air flow cannot be provided under conditions of natural convection.

With forced draft spicular radiator systems the heat transfer coefficients may be significantly increased and may reach values of 100-200 kCal/m<sup>2</sup> · h · deg.

Let us examine the general characteristics of the operation of a spicular radiator system operating with forced air cooling. The forced draft of an individual spike with a circular section with  $Re = 0.25$  is characterized by a smooth flow around the spike. When  $Re = 2$ , a noticeable flow disturbance begins at the intake side of the spikes, and when  $Re = 9$ , this type of disturbance has reached its full development. With an increase in an air flow turbulence near the spike, the heat exchange coefficient between the spike and the moving air increases. With an increase in the  $Re$  value, the radiator resistance to the air flow increases. The relative distribution of individual spikes in the radiator is very important. With straight line order of the spikes, the air flow has a *laminar* nature and the heat transfer coefficient increases slightly. With a staggered distribution of spikes, the air flow proves to be quite turbulent, which leads to a sharp increase in the heat transfer coefficient.

It must be noted that the heat transfer coefficient has various values around the outside of the cylinder which forms the radiator spikes.

Figure 40 shows the dependence of the heat transfer intensity around the circumference of the spike cooled by an air flow, for 2 Reynolds numbers:  $Re = 10$  (curve 1) and  $Re = 4 \cdot 10^4$  (curve 2). From the shape of the curves it is apparent that for effective operation of the spicular radiator it is necessary to choose the corresponding

direction of the air flow which cools the spike. The optimum parameters of a spicular radiator system with spikes located in a staggered fashion will occur with the following spike arrangement:

$$\frac{S_1}{d} = 1.25 \text{ and } \frac{S_2}{d} = 1.08,$$

where  $S_1$  is the longitudinal interval of the spike system;  $S_2$  is the lateral interval of the spike system;  $d$  is the spike diameter.

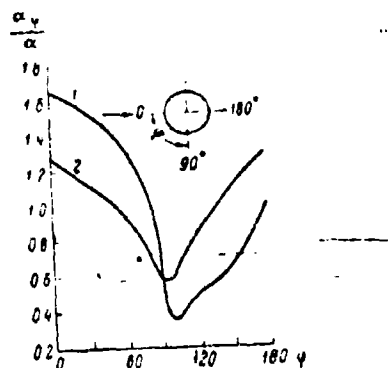


Figure 40. The dependence of spike heat transfer on air flow direction and heat removal location.

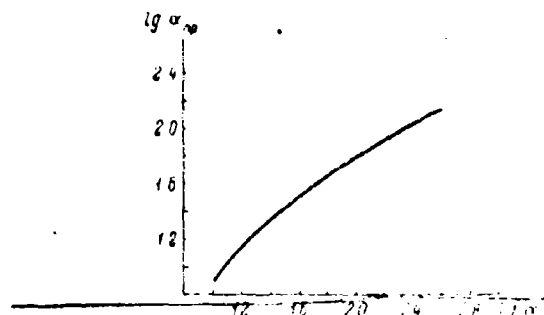


Figure 41. Dependence of the true heat transfer coefficient ( $\alpha$ ) on the reduced coefficient ( $\alpha_{red}$ ).

These conditions refer to air flow rates in which  $Re \geq 300$ .

The analytical determination of the numerical value of the coefficient of heat transfer for spicular radiator systems is a rather complex technological problem. However, for a first evaluation in the calculation of the value of this coefficient, we may use the relationship

$$\alpha_{sp} = \frac{Q}{V_s H}.$$

where  $\alpha_{red}$  is a reduced heat transfer coefficient, which takes into consideration the resistance to the passage of heat of the mass and surface of the spicular system;  $Q$  is the heat quantity passed through the radiator system from the thermopile (kCal/h);  $V_c$  is the difference between the average temperature of the spike and the temperature of the surrounding medium;  $H$  is the sum of the area of all radiator spikes,  $m^2$ .

In order to determine the true value of the heat transfer coefficient  $\alpha$ , we may employ the graph represented in Figure 41, where the dependence  $\alpha_{red} = f(\alpha)$  is shown.

We must note that the relationship for the determination of the reduced heat transfer coefficient is a rough approximation and is correct when the assumption is made that the radiator system forced flow rate corresponds to Reynolds numbers falling within the range  $Re = 10-100$ .

#### §4. A Liquid System with Natural Circulation

In some types of thermocooling devices (for example, in every day refrigerators), a comparatively large quantity of heat is released on the hot junction of the thermoelectric pile. To release this heat by means of natural convection to the surrounding air would require radiator systems with an area of several square meters. In such systems the heat transfer coefficient usually does not exceed  $3-5 \text{ kCal}/m^2 \cdot h \cdot \text{deg}$ . The creation of an effective heat coupling between the radiator plate and the heat source is an important difficulty in the utilization of such systems. Since the hot junction area of the thermoelement usually does not exceed several square centimeters, and high density heat fluxes are generated in this area, the fin-air heat transfer coefficient is reduced.

In this connection the necessity to disperse the heat flux of the hot junctions of the thermopile arose. One of the possible variations in the solution of this problem, proposed by A. N. Voronin and S. G. Platonova, consists of employing an intermediate heat-transfer agent which circulates freely in a closed system. With this method the heat transfer from the hot plates of the thermoelectric pile is accomplished with water.

The hot water exchanges places with the colder water which creates a self-circulating flow in the closed system. Such a system is equipped at the appropriate location with radiator fins from which the heat discharge to the surrounding air occurs. A device with the heat transfer utilizing natural liquid circulation is shown schematically in Figure 42.

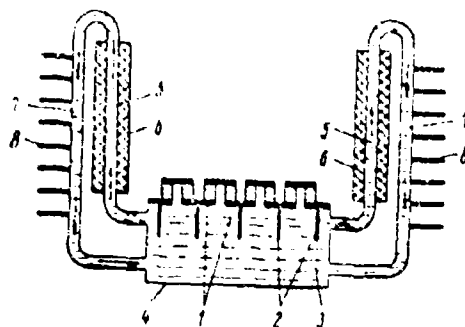


Figure 42. A diagram of a liquid heat-transfer system with natural liquid circulation.

The hot junctions of the thermoelectric battery 1 are equipped with radiator plates 2, which are immersed in water 3, which in turn is located in sealed tank 4. Hot water under the influence of heat from the radiators rises through pipes 5 which are equipped with layers of thermoinsulation 6 in order to reduce heat transfer from the surrounding air which would interfere with self-circulation. After having entered external pipes 7, the water is cooled as a result of heat-transfer with the surrounding air. Radiator plates 8 serve to intensify the heat transfer. The cool water enters 4, and the process is continuously repeated.

As a result of a decrease in the parasitic heat differentials between the hot junctions of the thermopile and the water, where the individual heat fluxes have the greatest value, it is possible to obtain radiator-water heat transfer coefficients equal to  $10^2$ - $150 \text{ kcal/m}^2 \cdot \text{h} \cdot \text{deg}$ , i.e., 20-30 times higher than with a natural convection heat exchange system.

It must be noted that from the standpoint of heat discharge, a heat transfer system with an intermediate heat-transfer agent must have the same radiator area as a system employing natural convection cooling. However, the specific heat flows from the water to the air in this case will be so insignificant that the heat exchange surface may be fabricated from the materials with relatively low heat conductivity, for example, from plastic.

A quantitative evaluation of the effectiveness of a heat-transfer system employing an intermediate heat-transfer agent consists of a hydrodynamic calculation of a closed circuit, in which water of varying

density self-circulates, and of a heat engineering calculation of the heat transfer coefficient. The hydrodynamic calculation is conducted in the following sequence.

1. The quantity of water circulating in the system is

$$G = \frac{Q_0}{t_1 - t_2}, \text{ kg/h,}$$

where  $Q_0$  is the output released at the hot junctions of the thermopile, kcal/h;  $t_1$  and  $t_2$  represent water enthalpy at the lowest and the highest temperatures, respectively, in the circuit.

2. In establishing the water circulation rate in the system, we shall determine the total transfer section of the listing pipes of the circuit:

$$f_0 = \frac{G}{3.6 \cdot 10^3 \cdot W_0 \bar{\gamma}}, \text{ m}^2,$$

where  $G$  is the quantity of the circulating water, kg;  $W_0$  is the circulation rate, m/sec;  $\bar{\gamma}$  is the water density at an average temperature in the circuit, kg/m<sup>3</sup>.

The value of  $\gamma$  may be determined from corresponding tables. The pipe transfer sections are determined, depending on the quantity of the listing pipes selected. Naturally the water circulation rate in the descending pipes will be the same.

3. The dynamic resistance of the listing pipes to the water passing through them is determined in accordance with the equation

$$\Delta P = \frac{\lambda l W^3}{2gd}, \text{ kg/m}^2,$$

where  $\lambda$  is the water-metal friction coefficient;  $l$  is the length of one branch of the pipe, m;  $\bar{\gamma}$  is the average water density, kg/m<sup>3</sup>;  $W$  is the average rate of flow of the water in the pipe, m/sec;  $d$  is the internal diameter of the pipe, m;  $g$  is the accelerated force of gravity, m/sec<sup>2</sup>.

The value of  $\lambda$  may be determined from the graph shown in Figure 43.

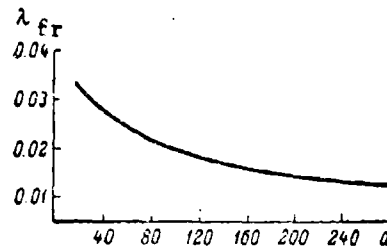


Figure 43. Dependence of the coefficient of friction ( $\lambda$ ) on pipe diameter ( $d$ ).

We may, with a satisfactory degree of accuracy, employ equations pertaining to the natural convection of liquid in a free volume for a determination of the coefficient of heat-transfer at given water circulation flow rates in the circuit. The heat-transfer coefficient from the hot junctions of the thermopile to the water may be determined in accordance with the equation

$$\alpha = \frac{0.15 \delta}{l} (Pr Gr)^{0.25}, \text{ kcal/m}^2 \cdot \text{h} \cdot \text{deg}$$

where  $\delta$  is the coefficient of heat conductivity of the water ( $\text{kcal/m}^2 \cdot \text{h} \cdot \text{deg}$ );  $l$  is the governing dimension of the heat exchange surface;  $Pr$  is the Prandtl number;  $Gr$  is the Grashof number.

The product of the Prandtl and the Grashof numbers are determined by the relationship

$$Pr Gr = \frac{g \delta \Delta t}{\nu a}.$$

here  $g$  is the accelerated force of gravity,  $\text{m/sec}^2$ ;  $\nu$  is the coefficient of the kinematic viscosity of water,  $\text{m}^2/\text{sec}$ ;  $a$  is the coefficient of the thermoconductivity of water,  $\text{m}^2/\text{h}$ ;  $\delta$  is the coefficient of volume expansion of water,  $\text{deg C}^{-1}$ ;  $\Delta t$  is the fin-water temperature difference.

The average value of the coefficient of heat-transfer for a given heat exchange surface may be determined with a sufficient degree of accuracy from the equation

$$\alpha = 2.28 \cdot 10^5 \cdot f_0 W_0 \gamma \bar{t} \frac{t - t_1}{t - t_2},$$

where  $f_0$  is the pipeline section,  $m^2$ ;  $W_0$  is the water circulation rate, m/sec;  $\gamma$  is the water density at the average temperature of the circuit,  $kg/m^3$ ;  $\bar{t}$  is the average temperature of the heat exchange surface;  $t_1$  is the temperature of the water entering the circuit;  $t_2$  is the temperature of the water leaving the circuit.

#### §5. Employment of the Latent Heat of Fusion

Substances with a high latent heat of fusion may be employed as one of the possible methods of heat elimination from the hot junctions of a thermopile in an insulated system. A choice of substances is dictated by operating conditions. These include the following: the required temperature stabilization level of the cooled object  $T$ , the value of the temperature drop  $\Delta T$ , obtained in the thermoelectric refrigerator, and also temperature  $T_0$  of the surrounding medium.

It is advantageous to select compounds with a melting point  $5-10^\circ$  higher than the temperature of the surrounding medium. In this case the volume occupied by the substance with a high heat of fusion does not require heat insulation.

The duration of the maintenance of a stable temperature in the thermostat is determined by the value of output  $W$ , which is released at the hot junctions of the thermopile, and by the quantity and the latent heat of fusion of the material employed.

If the latent heat of fusion is calculated in kilocalories per gram, then the calculation of the specific effectiveness of the material chosen must be made in accordance with quantity  $Q\rho$ , where  $\rho$  is the density in  $g/cm^3$ .

The time at which the stable temperature may be maintained can be determined with a sufficient degree of accuracy in accordance with the equation

$$t = \frac{q_2 V}{W},$$

where  $V$  is the volume occupied by the material,  $\text{cm}^3$ ;  $W$  is the heat output removed,  $\text{cal/sec}$ ;  $t$  is time,  $\text{sec}$ .

Table 4 shows the characteristics of several substances which may be employed for the purposes indicated. The stability of the temperature maintained in the thermostatically controlled volume depends essentially on the heat conductivity of the substance. In employing the latent heat of vaporization of metals (or alloys), the heat-transfer resistance of the fusion is not great, which is explained by the large value of its heat conductivity. In this case the thermocontact with the semiconductor pile is provided by the metal from which the heat receiver is constructed.

Table 4  
The Characteristics of Substances with a High Latent Heat of Fusion

Substance	Melting point, $^{\circ}\text{C}$	$q$ , $\text{cal/g}$	$\rho$ , $\text{g/cm}^3$	$q\rho$ , $\text{cal/cm}^3$	$\lambda$ , $\text{cal/cm}\cdot\text{sec}\cdot\text{deg}$
Crystallized cadmium nitrate	59.4	25.3	2.45	62.0	*
Crystallized nickel nitrate	56.7	36.4	2.05	74.6	*
Stearic acid	69.0	47.6	0.847	40.3	*
Cetyl alcohol	49.0	33.8	0.818	27.6	*
Dimethyl ether of oxalic acid (dimethyl oxalate)	49.5	42.7	1.148	49.0	*
Eladic acid	47.0	52.1	0.851	44.3	*
Urethan (ethyl carbamate)	48.7	40.9	1.11	45.0	*
Wax	63.0	42.3	0.96	40.6	0.00021
Paraffin	52.4	35.1	0.88	30.9	0.0005--0.0006
Naphthylamine	53.0	30.0	1.123	33.7	0.00036
Wood's alloy	65.5	8.4	9.7	81.05	0.0319

NOTE. The asterisks indicate that there no data available in published sources. A tentative value is  $\lambda \sim 6 \cdot 10^{-4} \text{ cal/cm}\cdot\text{sec}\cdot\text{deg}$ .

The heat conductivity of salts is significantly lower than for metals or alloys, therefore when they are employed it is necessary to take special measures in order to reduce their heat-transfer resistance to fusion. In



the opposite the temperature of the hot junctions of the thermopile increases slowly and it is not possible to stabilize the temperature within the cooled volume. This undesirable phenomenon can most simply be reduced to a minimum by extending the surface of the radiator within the heat-accepting substance.

In the ideal case the surface of radiators must represent a mechanical sponge, filled with salt in a solid state. As an example of the method of heat removal described above, a graph of the dependence of temperature within the operating chamber of a thermoelectric microrefrigerator on time is shown in Figure 44. Wood's alloy (with a volume of  $300 \text{ cm}^3$ ) was the heat-absorbing substance in this case. The temperature of the surrounding medium was  $60^\circ$ . It is apparent from the graph that the duration of the maintenance of the stable temperature exceeded 2 hours.

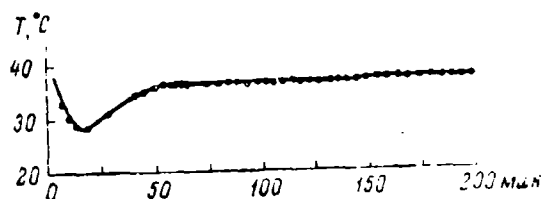


Figure 44. Temperature dependence in the operating chamber of a microrefrigerator on time for a case of heat-transfer to Wood's alloy (power released by the thermopile equals 10 w).

#### 56. Utilization of the Latent Heat of Vaporization

The latent heat of vaporization for many liquids is significant. This may be employed for the elimination of heat released on the hot junctions of thermopiles in systems with a limited period of service.

One possible design arrangement for a thermoelectric system in which heat is eliminated as the result of the latent heat of vaporization of liquid is shown in Figure 45. Here hot junctions 1 of the thermoelectric pile 2 with good thermocontact are coupled to copper corner plate 3, to which copper box 4, filled with water, is soldered. In order to increase the vaporization surface, several copper plates 5, jacketed with special tricort material 6, which possesses good wick properties, were placed in the upper cover. The lower ends of the tricort wick extend into the box and are submerged in water.

## GRAPHICS NOT REPRODUCIBLE



Figure 45. A thermopile utilizing latent heat of vaporization for heat removal.

With small dimensions and low weight (600 g) including the weight of the thermopile, the system specified, after the operating volume (50 cm<sup>3</sup>) is filled with water, eliminates 5 w of heat output released on the hot plates of the thermoelectric pile in the course of 4 hours.

Radiator fin surface temperature dependence on time is shown in Figure 46. The temperature difference between the radiator and the hot junction did not exceed 1°. The curve shown was obtained with a surrounding medium temperature of 50°.

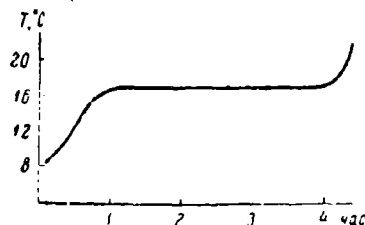


Figure 46. Fin temperature dependence on time in a device employing latent heat of vaporization.

Another construction variation for a heat-transfer system employing the latent heat of vaporization is shown in Figure 47. Here the water is poured into two vessels 1 constructed of plexiglass. The side surfaces of these vessels 2 are fabricated from copper and are soldered to corner plates 3, which support thermopile 4. In contrast to the previous design, here there is no system of radiators equipped with wicks. Vaporization of water in vessels 2 leads to a temperature reduction of the corner plates in correspondingly of the hot junctions of the thermopile. Openings 5, covered by fine mesh 6, serve to release vapor and as a filler opening for water. With a filled water volume of 100 cm<sup>3</sup> (in two vessels), the thermopile releases 5 w and may operate continuously for 5 hours. The total weight of the system (without water) is 670 g.

## GRAPHICS NOT REPRODUCIBLE

Figure 47. A second construction variation for a heat-transfer system employing the latent heat of vaporization.

We may employ the following relationships in order to obtain a quantitative evaluation of the method of heat removal as the result of the latent heat of vaporization.

The quantity of vaporized water  $G$  (kg/h) equals

$$G = \alpha F \frac{d - d_{wa}}{240},$$

where  $\alpha$  is the water-air heat transfer coefficient (kcal/m<sup>2</sup>·h·deg);  $F$  is the area of the surface of the water, m<sup>2</sup>;  $d$  is the air humidity close to the surface of the water, g/kg of dry air;  $d_{wa}$  is the humidity of the air at the temperature of the water and with full saturation, in g/kg of dry air.

The values  $d$  and  $d_{wa}$  are determined from corresponding graphs.

In a case when  $G < 0$ , the vaporization of water occurs, and when  $G > 0$ , condensation of water vapor takes place. Heat quantity  $Q$  which may be removed by the evaporated water equals

$$Q = G(595 - 0.54t_1) + \alpha F(t_2 - t_1), \text{ kCal/h}$$

here  $t_1$  is the water temperature;  $t_2$  is the air temperature.

The first element on the right side of the equation determined the quantity of vaporized water, and the second element takes into the consideration the heat exchange between the water and the surrounding medium.

The value  $Q$  in turn consists of two elements -- the output of the thermoelectric pile  $W$  (w) and the refrigerating capacity  $Q_0$  (w) of the pile, i.e.,

$$Q = (W + Q_0) 0.86, \text{ kCal/h}$$

#### 57. A Heat Transfer System Utilizing Specific Heat

One possible method of removing heat from a thermoelectric pile may be the utilization of materials with high specific heat. In this case the heat released at the hot junctions of the thermopile will be expended in increasing the temperature of the heat acceptor, which is a distinctive heat accumulator.

The heat-transfer process from the thermo-cooling device to the heat acceptor will be non-steady. In the course of time the temperature of the heat acceptor will increase, and the quantity of heat accepted by it from the thermopile will correspondingly decrease. In addition, the heat exchange of the heat acceptor with the surrounding medium will also not be constant with time.

For a first approximation in making a quantitative evaluation of the basic parameters of this type of device, it is possible to disregard the heat exchange between the heat acceptor and the surrounding medium, the change in the specific heat with temperature and the change with time of the quantity of heat transferred from the thermopile to the heat acceptor:

In this case the solution to the problem is considerably simplified and we may with sufficient accuracy determine the mass of the heat acceptor by using the following relationship:

$$M = \frac{Q_0 t}{c \Delta T},$$

where  $M$  is the mass of the heat acceptor, g;  $Q_0$  is the quantity of heat transferred from the thermopile to the heat acceptor, cal/sec;  $c$  is the specific heat of the heat-transfer material, cal/deg;  $t$  is the time, during which the system must operate, sec;  $\Delta T$  is the temperature change of the heat acceptor during time  $t$ . It must be noted that the relationship mentioned is correct when conditions are such that  $t \gg \tau$ , where  $\tau$  is a quantity which is dependent on the geometric dimensions and on several physical parameters of the heat acceptor material:

$$\tau = \frac{L^2 c \rho}{\lambda},$$

where  $\lambda$  is the heat conductivity, cal/cm·sec·deg;  $d$  is the specific heat, cal/g·deg;  $\rho$  is the density, g/cm<sup>3</sup>;  $L$  is a linear dimension, cm.

In other words, value  $\tau$  characterizes the rate of heat dispersal in the heat acceptor material.

Calculations for a heat transfer system employing the specific heat of the material are shown below as an example. We shall proceed from the following initial data:

- 1) the thermoelectric pile releases 5 w, or 1.16 cal/sec at the hot junctions;
- 2) the pile operating time is 5 minutes;
- 3) after an elapsed time of 5 minutes, the temperature of the heat acceptor must have increased by not more than 5°;
- 4) aluminum is employed as the heat acceptor material ( $c = 0.2$  cal/g·deg,  $\lambda = 0.5$  cal/cm·sec·deg,  $\rho = 2.7$  g/cm<sup>3</sup>);
- 5) the heat acceptor is fabricated in the form of a cylinder 5 cm in height.

The mass of the heat acceptor equals

$$M = \frac{1.5 \cdot 300}{0.2 \cdot 5} = 350 \text{ g.}$$

On the basis of the parameters of the material specified and the geometry of the heat acceptor, we determine the value of  $\tau$ :

$$\tau = \frac{25 \cdot 0.2 \cdot 2.7}{0.5} = 27.$$

Since the specified system operating time equals 300 seconds, the condition  $t \gg \tau$  is satisfied and the chosen mass value of the heat acceptor will be sufficient to satisfy established requirements.

#### §8. The Utilization of Solutions with a Low Cryohydrate Temperature

It is possible to suggest the utilization of water solutions of salts with a low cryohydrate temperature as one method for the removal of heat from the hot junctions of thermoelectric piles. This method permits us to obtain by simple means a significant reduction in the temperature of the hot junction, and the reduction is determined by the selection of a corresponding salt. The cryohydrate temperatures of several salt solutions are shown in Table 5. Here the cryohydrate temperature value corresponds to the formation of crystals in a eutectic mixture (ice and salt).

It is possible to offer several different solutions for the problem indicated. However, of all possible design variations, the most advantageous are systems in which heat removal is provided by the circulation of the solution itself or by the circulation of an intermediate heat transfer agent situated in close thermocontact with the cryohydrate solution.

A cooling device for the removal of heat from the hot junction of a thermopile may be constructed in the form of an independent sub-assembly, connected with the thermoelectric device by means of hoses.

In selecting a salt it is necessary to take into consideration that the solution which will be employed for cooling must have a minimal corrosive effect on the circulating system. The presence in the solution of solid residues is also undesirable, since these will significantly impair the cooling of the thermopile; in other words it is necessary to employ a salt with good solubility.

Table 5

The Basic Characteristics of Several Water Solutions of Salts

Salt	Water temp., °C	Heat of the solution kCal/g·mol	Solubility per 100 cm <sup>3</sup> at 20°, g	Cold capacity of a solution at saturation per cm <sup>3</sup> of water, of relative units
NH <sub>4</sub> NO <sub>3</sub> . . . . .	18	6.4	192	15.3
RbNO <sub>3</sub> . . . . .	21	8.7	53.3	3.4
Ba(NO <sub>3</sub> ) <sub>2</sub> . . . . .	18	9.0	9.2	0.31
NaNO <sub>3</sub> . . . . .	17	5.018	88.0	5.2
KNO <sub>3</sub> . . . . .	18	8.52	31.6	2.6
CaCl <sub>2</sub> ·2H <sub>2</sub> O . . . . .	18	4.564	74.5	2.35
NaCl . . . . .	18	3.895	37.2	2.7
NaCl·2H <sub>2</sub> O . . . . .	18	1.281	36.0	5.45
KClO <sub>3</sub> . . . . .	18	10.2	7.4	0.62
K <sub>2</sub> Cr <sub>2</sub> O <sub>7</sub> . . . . .	18	17.4	13.1	0.78
(NH <sub>4</sub> ) <sub>2</sub> SO <sub>4</sub> . . . . .	18	2.39	75.4	4.36
K <sub>3</sub> Fe(CN) <sub>6</sub> . . . . .	18	14.3	17.5	0.76
NH <sub>4</sub> HCO <sub>3</sub> . . . . .	15	9.69	21.0	1.78
(NH <sub>4</sub> ) <sub>2</sub> C <sub>2</sub> O <sub>4</sub> . . . . .	16	19.9	32.05	2.7
KHCO <sub>3</sub> . . . . .	15	5.32	31.6	1.66
NaHPO <sub>4</sub> ·12H <sub>2</sub> O . . . . .	18	22.83	7.7	1.47

The employment of salts with high solubility, with the same system volumes, permits increasing the operating cycle with one charge. One of the basic characteristics in the selection of a salt is the latent heat of solution.

A list of salts which may be employed for the indicated purpose is shown in Table 6. Not all substances in Table 5 are included in this table, since the majority of these salts have a low heat of solution. The various cyanide compounds are also not shown in the table due to their high toxicity.

Table 6

The Cryohydrate Temperatures of Salt Solutions

Salt	T, °C	Salt	T, °C
CaCl <sub>2</sub> ·6H <sub>2</sub> O	-54.9	NH <sub>4</sub> NO <sub>3</sub> . . .	-17.35
K <sub>2</sub> CO <sub>3</sub> ·H <sub>2</sub> O	-56.5	NH <sub>4</sub> Cl . . . .	-15.8
MgCl <sub>2</sub> ·12H <sub>2</sub> O	-33.6	KCl . . . . .	-11.1
NaCl·2H <sub>2</sub> O	-21.2	MnSO <sub>4</sub> ·7H <sub>2</sub> O	-10.5
(NH <sub>4</sub> ) <sub>2</sub> SO <sub>4</sub> . . .	-19.05	KNO <sub>3</sub> . . . . .	-2.9
NaNO <sub>3</sub> . . . . .	-18.5	Na <sub>2</sub> SO <sub>4</sub> ·H <sub>2</sub> O	-1.2

It is apparent from an examination of the salts shown in Table 6 that the best characteristics are possessed by ammonium nitrate ( $\text{NH}_4\text{NO}_3$ ), which possesses a relatively high heat of solution, a low cryohydrate temperature and high solubility. It should be noted that ammonium nitrate is produced in large quantities by industry and that the cost is not significant. In order to obtain an idea of the quantity of the solution required, a calculation is shown below for a case involving heat removal from a semiconductor pile which releases 15 eCal/h at the hot junctions. The calculation is made under the following conditions.

Temperature $T_1$ of the surrounding medium	20°
Required temperature $T_2$ of the hot junction	5°
Operating time $t$	6 hours
Salt employed	ammonium nitrate
Heat insulation of the solution container	peat board
Coefficient of heat conductivity $\lambda$	0.08 kCal/m·h·deg
Thickness $\delta$ of the heat insulation	$5 \cdot 10^{-2}$ m
Insulation-surrounding air heat-transfer coefficient $\alpha_1$	10 kCal/m <sup>2</sup> ·h·deg
Internal volume-insulation heat-transfer coefficient $\alpha_2$	500 kCal/m <sup>2</sup> ·h·deg

Under these conditions the derived coefficient of heat-transfer is

$$K = \frac{1}{\frac{1}{\alpha_1} + \frac{\delta}{\lambda} + \frac{1}{\alpha_2}} = 1.38 \text{ kCal/m}^2 \cdot \text{h} \cdot \text{deg}$$

The heat quantity transmitted to the vessel containing the salt from the surrounding medium is

$$Q_0 = KF\Delta T,$$

where  $F$  is the vessel surface, m<sup>2</sup>;  $\Delta T$  is the temperature drop ( $T_1 - T_2$ ).

If  $F = 1 \text{ m}^2$ , then

$$Q_0 = 1.38 \cdot 1.15 = 20.5 \text{ kCal}$$



In order to cool 15 l of the solution, the following heat quantity must be removed.

$$Q_1 = cm\Delta T = 15 \cdot 1 \cdot 15 = 225 \text{ kcal}$$

In order to remove this quantity of heat it is necessary that

$$P_1 = 2.8 \text{ kg of salt}$$

The quantity of heat which is transmitted each hour to the vessel from the semiconductor pile and as a result of heat exchange with the surrounding medium is

$$Q = Q_0 + Q_1 = 20.5 + 15 = 35.5 \text{ kcal}$$

In order to provide for the removal of this heat, with a solution temperature increase of not more than  $2^\circ$ , each hour a charge is required which equals

$$P_2 = 0.44 \text{ kg of salt}$$

Thus in the course of 6 hours, 5.4 kg. of salt is required for stable operation of the semiconductor thermopile. The calculation shown is correct for short (2 m), well insulated hoses which connect the thermopile with the vessel containing the solution. When it is necessary to move the vessel containing the solution a great distance from the thermopile, then heat exchange between the hoses and the surrounding medium must be taken into consideration.

An evaluation was made of the temperature drop on rubber-canvas hoses (2.5 m in length, at a water flow rate of 1 l/m), which were located in chamber with 100% humidity and under an environmental temperature of  $25^\circ$ . The temperature drop was  $1^\circ$ , which corresponds to a heat flux of 60 kcal/h. Thus in order to provide for the successful operation of a thermo-cooling device employing rubber-canvas hoses 5 m in length, it would be necessary to provide an additional charge each hour of 0.75 kg of salt.

To provide for a temperature reduction at the hot junction of the thermopile with the parameters previously indicated, for 6 hours of operation it is necessary to provide

$$P = P_1 + 6(P_2 + P_3) = 2.8 + 7.14 = 10 \text{ kg of ammonium nitrate.}$$

The temperature change of the ammonium nitrate solution with time for for a volume of  $400 \text{ cm}^3$  in which the heat output is  $3 \text{ kcal/h}$ , is shown in Figure 48. A charge consisting of the regular portion of salt was added each hour.

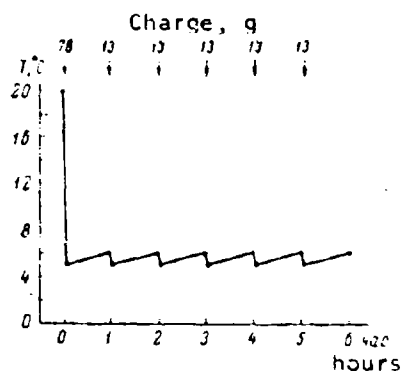


Figure 48 Temperature change of the ammonium nitrate solution with time (with a solution volume of  $400 \text{ cm}^3$ , and a released heat output of  $3 \text{ kcal/h}$ ).

## CHAPTER VIII

### Power Supplies for Thermoelectric Cooling Devices

Since the input for thermoelectric cooling devices requires a direct current at relatively high intensity at low voltage, the problems of the selection of a corresponding power supply acquires considerable significance. Depending on the specific operating conditions of a thermoelectric device, rectifiers, storage batteries, current converters and thermoelectric generators may be employed as a source of current.

#### §1. Rectifiers

Under stationary operating conditions it is most advantageous to supply a thermoelectric device from a rectifier. Notwithstanding the required direct current at high intensity, the power required by a thermoelectric cooling device from the power supply is not high and usually does not exceed several dozen watts, although usually only a few watts are required. In this connection a suitable rectifier will be small and relatively simple in design. As a rule, rectifiers for the supply of thermoelectric devices are connected in a full-wave configuration, as a result of which direct current with a 67% ripple is obtained at the output. The maximum reduction of direct-current ripple is a most important circumstance, since the presence of an alternating component will lead to the release of Joule heat at the thermopile, which reduces the cooling effect.

The dependence of the temperature drop at the thermoelement on the ripple value of the supply current is shown in Figure 49.

The achievement of the required rectified current stabilization is a rather complex problem, since in this case we must deal with high intensity currents at low voltage, which practically eliminates the usage of capacitive filters. Therefore filtering of the rectified current is, as a rule, accomplished with an inductive filter, i.e., with a choke.

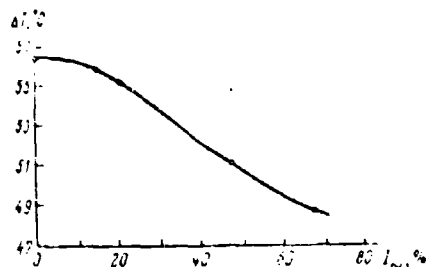


Figure 49. The dependence of the temperature drop ( $\Delta T$ ) at the thermoelement on the ripple value ( $I_{\sim}$ ) of the supply current.

Since all of the relationships shown previously which characterize the operation of a thermoelectric cooling device referred to a case of current supply with a pure direct current, we shall examine the influence of an alternating component in the current supply on the operation of the thermopile. Two phenomena will occur in supplying a thermopile with rectified current in which an alternating component is present. These include Joule heat, which is proportional to the rms value of the alternating current component, and Peltier heat absorption, which is proportional to the average value of the direct-current component of the supply.

These two values are related to each other by the so-called form factor  $F$ , which is defined as the ratio of the rms value of the alternating component  $I_{rms}$  to the average value of the direct-current component  $I_{dc}$ , i.e.,

$$F = \frac{I_{rms}}{I_{dc}}$$

It is apparent that a form factor which is not unity will reduce the thermoelectromotive force value  $\alpha$  to  $\frac{\alpha}{F}$ . In agreement with this, in all relationships which characterize the operation of the thermoelectric pile, i.e. in terms which take Joule heat into consideration we must introduce the rms current value, and in terms which define Peltier heat, we must write the average value of the direct-current component

$$I_{dc} = \frac{I_{rms}}{F}.$$

It is not difficult to show that the basic parameters of a thermoelectric pile which is supplied by a current having an alternating component will differ from these same parameters in the case of a direct-current pile supply by the value  $F$  or  $F^2$ . If we designate the parameters of a thermopile supplied by a current with an alternating component by an asterisk, then the relationship of these parameters to those of a thermopile supplied by a direct current will have the following form:

a) for a maximum temperature drop

$$\frac{\Delta T_{\max}^*}{\Delta T_{\max}} = \frac{1}{F^2};$$

b) for the current under a condition of maximum refrigerating capacity

$$\frac{I_0^*}{I_0} = \frac{1}{F};$$

c) for the current involving a condition under a maximum coefficient of performance

$$\frac{I_c^*}{I_c} = F;$$

d) for a condition of maximum refrigerating capacity

$$\frac{\epsilon_{\max}^*}{\epsilon_{\max}} = \frac{1}{F^2} \cdot \frac{1 - F^2 \frac{\Delta T}{\Delta T_{\max}}}{1 - \frac{\Delta T}{\Delta T_{\max}}}.$$

Basic parameter dependencies of a thermoelectric pile on the value of the form factor are shown graphically in Figure 50.

It is apparent from the curves shown, that for the small temperature differences which exist in a number of cases involving the use of low-current thermopiles, the influence of the form factor does not seriously affect the basic parameters. However when it is necessary to obtain maximum possible temperature differences, the form factor has a very significant influence on the operation of the thermopile.

In this connection a rectifier intended for the supply of a low-current thermopile may have a ripple of 20-26% at the output. In a case involving the supply of heavy-current thermopiles, the rectified current ripple ratio must be reduced to a minimum and may not exceed 5-7%.

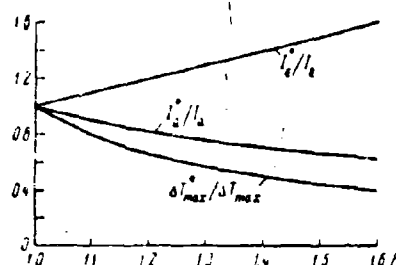


Figure 50. Optimum current values under a condition of maximum coefficient of performance ( $\epsilon$ ), under a condition of maximum refrigerating capacity ( $Q$ ) and at temperature drop ( $\Delta T_{\max}$ ) as a function of form factor ( $F$ ).

A no less important circumstance is the correct choice of rectifiers, since in order to achieve a high rectifier efficiency, the forward voltage drop across the rectifier must be comparatively small. High-current germanium diodes are considered to be the most suitable for the indicated purpose.

Domestic industry produces germanium high-current diodes in current ranges from 1 to 1,000 a and at voltages from 15 to 200 v (depending on class). The forward voltage drop for germanium rectifiers lies in the ranges from 0.16 to 0.22 v for group A and 0.5 v for group Ye. Depending on the cooling conditions involved, rectifiers are divided into types VG, which includes natural or forced air cooling and VGV, which includes water cooling. Germanium rectifiers operate at extremely high current densities, reaching 100 a/cm<sup>2</sup> whereas selenium and copper-oxide rectifiers operate at forward current densities of 0.03-0.1 a/cm<sup>2</sup>. Such operating current densities have permitted the fabrication of germanium rectifiers of small size and low weight. For example, the specific volume of a germanium rectifier equals 0.02-0.2 cm<sup>3</sup>/w, which is 50-100 times smaller than the corresponding figure for a selenium rectifier. Differences in

specific mass for germanium and selenium rectifiers are just as significant (0.02-0.2 g/w and 0.4-5 g/w, respectively). The low forward voltage drop across the rectifier, which is an important characteristic, falls within the range of 0.16 to 0.5 v, in agreement with the rectifier classification characteristic. The efficiency of a germanium rectifier approaches 98%.

In so far as the shortcomings of high-current germanium rectifiers are concerned, we must consider the low overload capability. In this connection the operating temperature of a germanium rectifier must not exceed 50°. The basic data for high-current germanium rectifiers are shown in Table 7.

Table 7  
The Basic Parameters of High-Current Germanium Rectifiers  
(GOST [All-Union State Standard] 10662-63)

Rectifier type	Nominal rectified current, a	Nominal operating voltage amplitude, b	Forward voltage drop at nominal current, v	Inverse current at the nominal inverse voltage, ma	Diode weight with radiator, g	Overall size with leads and radiator, mm	Type of cooling
D302	1	200	0.25	1	25	46 × 22 × 19	Natural air cooling
D303	3	150	0.3	1	100	46 × 24 × 24	
D304	5	100	0.3	3	170	46 × 22 × 24	
D305	10	50	0.35	3	500	46 × 22 × 24	
D305	10	50	0.35	3	500	46 × 22 × 24	
VG-10-15	10	15	0.16-0.22	10	200	77 × 43	Forced air cooling at a rate of 5 m/sec
VG-10-30	10	30	0.16-0.22	10	200	77 × 43	
VG-25-15	25	15	0.16-0.22	10	200	77 × 43	
VG-25-30	25	30	0.16-0.22	10	200	77 × 43	
VG-50-15	50	15	0.16-0.22	10	200	77 × 43	
VG-50-30	50	30	0.16-0.22	10	200	77 × 43	Water
VG-100-15	100	15	0.16-0.22	50	700	300 × 70 × 70	
VG-100-30	100	30	0.16-0.22	50	700	300 × 70 × 70	
VG-200-15	200	15	0.16-0.22	50	700	300 × 70 × 70	
VG-200-30	200	30	0.16-0.22	50	700	300 × 70 × 70	
VG-500-15	500	15	0.16-0.22	50	700	300 × 70 × 70	
VG-500-30	500	30	0.16-0.22	50	700	300 × 70 × 70	
VG-1000-15	1000	15	0.16-0.22	50	700	300 × 70 × 70	
VG-1000-30	1000	30	0.16-0.22	50	700	300 × 70 × 70	

NOTE. Values given in this table for the forward voltage and the inverse current were measured at an ambient air temperature of 20°: for rectifiers D302 and D305 average values are given which were obtained during measurement in a half-wave rectifier circuit; for rectifiers VG10 and VG50, values are given which were obtained during a measurement in a direct current circuit.

In recent years high-current silicon rectifiers have been developed and their mass production has been mastered. The basic advantage of a silicon rectifier over a germanium rectifier consists of the fact that the silicon rectifier has a higher operating temperature, extending to 200°. This circumstance permits the employment of silicon rectifiers at current densities of 300-500 a/cm<sup>2</sup>, which is 5 times higher than that for germanium rectifiers. An important shortcoming of silicon rectifiers is the fact that the forward voltage drop is almost twice as high as for germanium rectifiers; this is extremely undesirable in utilizing these rectifying devices in low voltage rectifiers used to supply thermoelectric devices. The size and weight characteristics of silicon rectifiers are better than for germanium, a fact which is linked to the small dimensions of the silicon crystal. In particular, the specific volume and the specific mass of a silicon rectifier is only 0.002 cm<sup>3</sup>/w and 0.01 g/w. However, due to the small dimensions of the silicon crystal, the overload capability of the rectifier is lower than for germanium. The basic characteristics of mass-produced silicon rectifiers are shown in Table 8. The range of operating temperatures for the rectifiers listed in the table is -50 to +125°, but the normal rectifier operating temperature is considered to be +40°. With every 10° increase in operating temperature, the value of the permissible forward current through the rectifier must be reduced by 10%.

Table 8

The Basic Parameters of High-Current Silicon Rectifiers

Rectifier type	Normal rectified current, a	Nominal operating voltage, v	Voltage drop in the forward direction, v	Type of cooling
D 214	5	100	1.0	Natural air cooling
D 214A	10	100	1.0	
D 215	5	200	1.0	
D 215A	10	200	1.0	
VK-10	10	50	0.4-0.5	Forced air cooling at a rate of 5 m/sec
VK-25	25	50	0.4-0.5	
VK-50	50	50	0.4-0.5	
VK-100	100	50	0.4-0.5	
VK-200	200	50	0.4-0.5	Water
VKD-500	500	50	0.4-0.5	
VKV-200	200	50	0.4-0.5	
VKV-350	350	50	0.4-0.5	
VKV-500	500	50	0.4-0.5	
VKV-750	750	50	0.4-0.5	
VKV-1000	1000	50	0.4-0.5	



The comparative parameters of high-current rectifiers of various types are shown in Table 9.

Table 9  
The Comparative Parameters of Various Types of Power Semiconductor Rectifiers

Parameter	Rectifier type			
	Copper-oxide	Selenium	Germanium	Silicon
Breakdown voltage, v	20-60	50-120	100-1000	200-5000
Nominal voltage (maximum value), v	5-15	25-85	15-400	50-3000
Normal forward voltage (specification), v	0.3-0.6	0.6-0.9	0.2-0.6	0.4-1.2
Nominal current density (average value), a/cm <sup>2</sup>	0.01-0.06	0.03-0.1	30-100	50-500
Maximum permissible operating junction temperature, °C	50-60	75-130	65-75	140-200
Efficiency, %	50-60	70-80	95-98	98-99
Specific volume (with cooling), cm <sup>3</sup> /w	4-20	0.7-1	0.02-0.2	0.002-0.2
Specific mass (with cooling), g/w	5-30	0.1-5	0.02-0.2	0.01-0.5
Maximum nominal power of 1 rectifier, kw	0.15	0.35	100	300

NOTE. For the parameters of domestic semiconductor power rectifiers, see also GOST 10662-63 and GOST 10765-64.

In those cases when rectifier economy is not a deciding factor, selenium washers may be employed as rectifiers. It is true that as a result of the large voltage drop, in comparison with germanium and silicon rectifiers, the efficiency of silicon rectifiers equals 70-80% in place of 95-98% for germanium rectifiers and 98-99% for silicon rectifiers. However, this circumstance is compensated for by the simplicity, accessibility and inexpensiveness of selenium rectifiers.

It must be noted that as a result of the development of germanium and silicon power rectifiers in recent years, a reduced amount of attention has been devoted to selenium rectifiers. This must be considered to be incorrect, since in a number of cases the employment of selenium rectifiers is more advantageous and has a greater economical justification than the employment of germanium or silicon rectifiers.

As an illustration we may cite an example of the employment of selenium rectifiers in the power supply of a contemporary thermoelectric refrigerator. Four selenium discs measuring 100 × 100 mm each were connected in a bridge circuit. The rectifier assembled from these washers supplied a direct current of 25 a at a voltage of 3.5 v. In this case the efficiency of the rectifier equalled 75%.

## §2. Storage Batteries

In a number of cases thermoelectric devices are employed in locations where an electrical supply net is lacking or the devices themselves are not stationary. As an example, we may cite the employment of microtomic and microscope stages, microrefrigerators for laboratory purposes and other devices under field conditions where stationary power supplies are lacking. Another group of devices, for example, thermoelectric microrefrigerators for the transportation of the sperm of farm animals, are by their very nature portable devices and, naturally, cannot be connected to a stationary source of electrical energy. In these cases it is necessary to employ an independent power supply. Since a thermoelectric cooling device requires a high current at a low voltage, storage batteries may be employed as portable power supplies.

The basic parameters of various types of storage batteries which may be employed for this purpose are shown in Tables 10, 11 and 12.

Table 10  
Acid Storage Batteries

Storage battery type	Number of elements	Nominal voltage, v	Capacity during a 10-hour discharge, 30°, ah	Discharge current during a 10-hr cycle, a	Weight, kg
3-ST-60	3	6	60	6.0	17
3-ST-70	3	6	70	7.0	19
3-ST-81	3	6	81	8.1	21
3-ST-98	3	6	98	9.8	23
3-ST-112	3	6	112	11.2	26
3-ST-126	3	6	126	12.6	30
3-ST-135	3	6	135	13.5	31
6-ST-34	6	12	34	3.4	33
6-ST-68	6	12	68	6.8	38

Table 11

## Alkaline Storage Batteries (Nickel-Cadmium)

Storage Number battery type	of elements	Nominal voltage, v	Capacity during 10-hour discharge 30°, ah	Discharge current during 8-hr cycle, h	Weight, kg
4-NKN-15	4	5.0	15	2.0	14
4-NKN-30	4	5.0	30	2.0	24
4-NKN-100	4	5.0	100	2.0	34
14-NKN-22	14	12.0	22	2.75	21
17-NKN-22	17	21.25	22	2.75	35
5-NKN-15	5	6.25	15	3.65	17
7-NKN-15	7	8.75	15	3.65	24
10-NKN-15	10	12.5	15	3.65	33.5
5-NKN-30	5	6.25	30	7.5	20
5-NKN-100	5	12.5	100	7.5	30
10-NKN-100	10	12.5	100	12.5	58.5
10-NKN-200	10	12.5	200	12.5	75

Table 12

## The Basic Characteristics of Silver-Zinc Storage Cells and Batteries

Type of storage cell or battery	Overall dimensions (length, width, height) mm	Weight with electro- lyte, g	Nominal capacity for a 10-hour discharge, ah	Specific capacity for a 10-hour discharge, ah/kg	5 min discharge current, a	Normal charging current, a
STs-0.5	24 × 12 × 17	24	0.85	65	2	1.5
STs-1.5	28 × 14 × 20	35	1.8	65	5.5	1.5
STs-3	43 × 18 × 23	95	4.5	80	35	1.5
STs-5	43 × 22 × 27	105	7.5	70	60	1.5
STs-11	24 × 41 × 100	190	11	60	120	1.5
STs-12	48 × 22 × 115	135	14	95	80	1.5
STs-15	48 × 28 × 115	245	16.5	95	100	1.5
STs-18	48 × 33 × 115	300	20	100	120	1.5
STs-25	48 × 48 × 150	500	25	100	150	1.5
STs-40	53 × 50 × 160	720	45	60	180	1.5
STs-45	53 × 50 × 165	760	50	60	200	1.5
STs-50	64 × 49 × 165	840	55	60	250	1.5
STs-70	91 × 50 × 166	1350	80	60	400	1.5
STs-95	71 × 53 × 212	1820	95	50	1200	1.5
STs-100	106 × 50 × 153	1600	100	60	600	1.5
STs-120	71 × 53 × 237	1900	130	70	650	1.5
3STs-5	96 × 45 × 77	590	7.5	70	60	4.5
5STs-5	160 × 45 × 77	1020	7.5	70	60	7.5
8STs-45	200 × 110 × 160	6480	50	60	200	12.0
15STs-45	332 × 126 × 170	10800	45	60	200	22.5

It is apparent from an examination of the storage batteries shown in the tables that the most suitable for purposes of supplying current to thermoelectric devices are the silver-zinc storage batteries, which, while possessing small dimensions and low weight, have significant capacity and can furnish high discharge currents. This is particularly applicable to the silver-zinc storage batteries, in which a parallel connection of the cells may be used to obtain an extremely high capacity and correspondingly high discharge currents. Thus, for example, storage battery 8STs-45 with series-connected cells has a capacity of 50 ah with an operating voltage of 12v; whereas with parallel-connected cells, this battery has a capacity of 360 ah, but at a voltage of 1.5 v.

In a case when a thermoelectric refrigerator in an operating condition is transported by motor vehicle, the supply may be provided from the automotive storage battery or from an additional storage battery which is recharged from the electrical supply system of the motor vehicle.

It is not without interest to note the possibility of employing a power supply for thermoelectric devices consisting of galvanic cells. Naturally, in this case a 1-time source is involved and as a result its application must be closely matched to the operating condition of the thermo-cooling device. Manganese-air-zinc cells are best employed to serve as this type of source. The parameters of several of these cells, which are mass-produced by industry, are shown in Table 13.

Table 13  
The Basic Characteristics of Several Manganese-Air-Zinc Cells

Type of cell	Initial characteristics at a temp of +20°C		Discharge conditions		Dimensions, mm			Weight, kg
	Voltage, v	Capacity, ah	Resistance to heating, ohm	Voltage at discharge, v	Length	Width	Height	
1.3-1VMTS-50	1.3	45	10	0.9	57	57	132	0.4
1.3-1VMTS-100	1.3	100	10	0.9	122	57	132	0.8
1.3-1VMTS-150	1.3	150	10	0.9	162	57	132	1.2
1.3-1VMTS-250	1.3	250	10	0.9	228	80	150	2.0
1.3-1VMTS-325	1.28	325	2	0.8	160	160	185	6.0

### 53. Current Converters

In a case when a thermo-cooling device is supplied from a storage battery, the operating time is limited by the value of the capacity of the latter. When low currents are taken from the storage battery, it will naturally operate for a longer period of time. In this connection, several types of current converters have been developed to supply high-current thermo-cooling devices from storage batteries. The converter accepts a direct current of low intensity, but at a relatively high voltage, and converts it into a high intensity current at a low voltage.

The principal design of one converter is shown in Figure 51. This device is intended to convert the energy of direct current at a voltage of 24 v into direct-current energy at a voltage of 1.5 v. The principle of operation of the converter is as follows: direct current from the initial voltage source (a storage battery) is converted by means of a generator into an alternating current which is transformed and then rectified by means of high-current rectifiers.

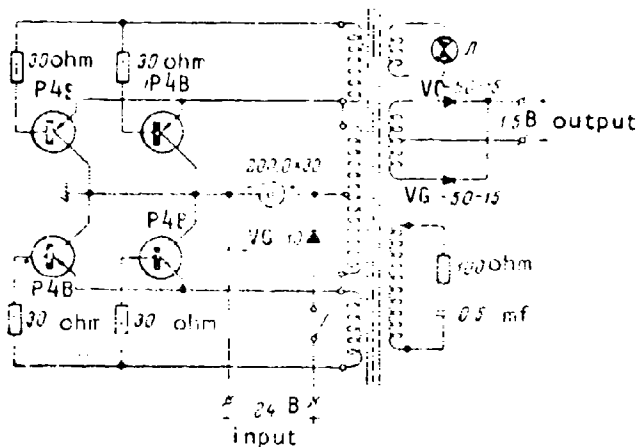


Figure 51. The principal design of a converter for direct current.

The converter is assembled according to the design of a push-pull blocking oscillator, loaded by a full-wave rectifier. The blocking oscillator employs P4B semiconductor triodes connected in pairs in each of the two branches. The rectifier design employs VG-50-15 germanium

diode power rectifiers. Germanium diode VG-10-15 is included in the input circuit in order to protect the semiconductor triodes from failure as a result of non-observance of polarity in connecting the converter to the storage battery. Current will pass through the diode only if the initial current source is correctly connected.

The blocking oscillator delivers an alternating voltage with a wave shape that is almost a square, and with a frequency of approximately 100 hz. In order to eliminate spikes on the leading edge of the voltage pulses which might lead to destruction of the triodes, and RC-circuit is employed, which is connected to a special winding of the toroidal power transformer.

The basic technical parameters of the converter are as follows.

Initial source of direct current	Storage battery, 24v
Current drawn from the initial source	3.2 v [sic]
Converter output voltage	1.5 v
Converter output current	40 a
Efficiency	70%
Direct current ripple at the converter output	60 mv
Apparatus dimensions (ht x wdth x lgth)	140 x 210 x 260 mm
Apparatus weight	6.6 kg

An overall view of the current converter is shown in Figure 52.

GRAPHICS  
NOT REPRODUCIBLE

Figure 52. An overall view of an industrial type of direct-current converter.

In conclusion we must mention the appearance recently of current converter designs employing silicon-controlled rectifiers (KUV [SCR]) or, as they are sometimes called theristors. These converters possess a number of essential advantages over triode converters; in particular, their efficiency may reach 80-85%.

#### §4. Thermoelectric Generators

Thermoelectric generators, from which, as is known, a direct current of high intensity at low voltage may be obtained, may be successfully employed to supply thermal cooling devices. A difference in temperature must be maintained between the cold and the hot junctions of a thermoelectric generator for normal operation. In this case the value of the current obtained from a generator under load is determined by the relationship

$$I = \frac{\alpha(T_1 - T_0)}{R + r},$$

where  $\alpha$  is the sum of the thermoelectromotive forces of both arms of the thermoelement;  $T_1$  is the temperature of the hot junctions of the thermoelement;  $T_0$  is the temperature of the cold junctions of the thermoelement;  $R$  is the resistance of the load connected to the thermoelectric generator;  $r$  is the internal resistance of the thermoelement.

The useful power delivered by the thermoelectric generator to the load equals

$$W = \alpha^2 (T_1 - T_0)^2 \frac{m}{r(m+1)^2},$$

where

$$m = \frac{R}{r}.$$

And finally, the efficiency of the thermoelectric generator under a condition of maximum power delivery to the load equals

$$\eta = \frac{1}{2} \cdot \frac{T_1 - T_0}{T_1 + \frac{z}{2} (T_1 - T_0)}$$

where  $z$  is a quantity which characterizes the thermoelectric properties of the materials employed.

Thus the efficiency of a thermoelectric generator is fully determined by the temperature difference at the ends of the thermoelements, by the value which determines the quality of the materials employed, and by the ratio of the load resistance to the internal resistance of the thermoelectric generator.

For semiconductor materials employed at the present time in thermoelectric generators (ZnSb + constantan),  $z = 0.5 \cdot 10^{-3} \text{ deg}^{-1}$ .

Under the actual operating conditions of thermoelectric generators, the temperature of the hot junction does not exceed  $400^\circ$ . With higher temperatures the process of diffusion of solder into the semiconductor materials is accelerated, which in the final analysis shortens the period of service of the thermoelectric generator.

With a temperature difference between the hot and cold junctions of  $300^\circ$ , the efficiency of a thermoelectric generator proves to equal 3-5%.

The design layout of a thermoelectric generator which is intended to supply thermo-cooling devices depends on the electrical parameters required, on the source of heat employed, on the system of heat removal and on a series of other initial data.

The common design coupling of a thermoelectric generator with a thermo-cooling device, illustrated in Figure 53, is of some interest. An overall view of one variation of such a device is shown in Figure 54. Here thermo-cooling device 1, for example a microrefrigerator for laboratory purposes, is in contact through hot junctions 2 of thermoelectric pile 3 with heat removal system 4, which is a hollow cylinder through which water flows after passing through nipple 5. On the opposite side, cold junctions 6 of the pile of the thermoelectric generator 7 are connected with the heat removal system. Heating element 9 is attached from the hot side of the thermogenerator pile 8. Due to the heating element, the required temperature difference at the thermoelectric generator is created. A storage battery, the common electrical supply, or any other source of electrical energy, either direct or alternating current, may be used as a source of initial voltage to supply the thermoelectric generator heater. Thus in this case the thermoelectric generator is simultaneously also a current convertor.



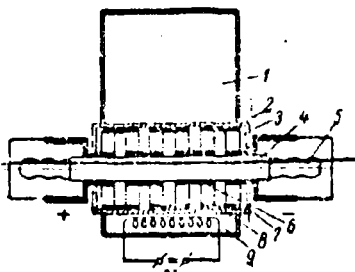


Figure 53. The diagram of a thermoelectric generator coupled with a thermoelectric refrigerator.

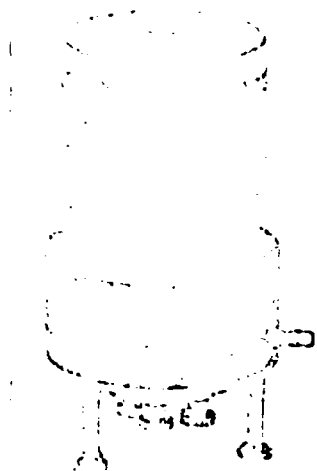


Figure 54. An overall view of a thermoelectric generator coupled with a thermoelectric refrigerator.

In the system described, the thermoelectric generator is not only a source of electrical energy which supplies the pile of the thermoelectric cooling device, it may also be employed for smooth regulation of the cooling value. In fact, if the value of the current which supplies the heater of the thermoelectric generator is varied, the temperature on

the hot junction of the pile will change; the value of the current passing through the cooling pile will change in conformity with the temperature change.

Notwithstanding the fact that devices of this type operate with a very low efficiency, their practical employment in a number of cases is quite advantageous.

In a case when the established period of service of the thermocooling device is small and can be measured in minutes, a flare with the required burning time may be employed at the heat source for the thermoelectric generator.

## CHAPTER IX

### SEVERAL PROBLEMS IN THE TECHNOLOGY OF THE MANUFACTURE OF THERMO-COOLING DEVICES

The production technology of thermo-cooling devices encompasses a number of considerations, the most important of which are described below. Technological problems in the manufacture of semiconductor materials for thermopiles are unique and will not be discussed here.

#### §1. The Manufacture of Thermoelement Arms

Semiconductor alloys possessing electron and hole conductivity ( $\text{Bi}_2\text{Te}_3 + \text{Bi}_2\text{Se}_3$  and  $\text{Bi}_2\text{Te}_3 + \text{Sb}_2\text{Te}_3$ ), or, as we shall now call them, n-type and p-type alloys, are produced by the appropriate enterprises in the form of ingots.

The first operation is the grinding of the ingot in a porcelain mortar or, for large quantities, in a ball mill, lined with rubber and equipped with steel balls. After grinding, sifting of the powder obtained is accomplished with two sieves with mesh sizes of 50 and 80. P-type and n-type alloys are ground and sifted separately, each in its own mill and with its own sieves. In order to avoid oxidation of the alloys in the powdery state, they must be preserved in glass bottles with ground glass stoppers. The quantity of alloy subject to simultaneous grinding must not exceed a 1 or 2 day requirement for these materials.

The molding of the thermoelement arms is a very important operation. The molding conditions for the p-type and n-type alloys are different. The p-type alloy is molded at a temperature of  $410^\circ$  with a pressure of  $8.5 \text{ t/cm}^2$ . The pressure must be maintained for a period of 5 minutes.

The n-type alloy must be molded at a temperature of  $435^{\circ}$ , with a pressure of  $8 \text{ t/cm}^2$ , and the pressure must be maintained for 5 minutes. Deviations from the values indicated are permissible within the following ranges: temperature,  $\pm 5^{\circ}$ , pressure  $\pm 0.5 \text{ t}$ , duration of applied pressure,  $\pm 1$  minute. The molding is accomplished on a hydraulic press, in a special split casting mold, which is shown diagrammatically in Figure 55. Heating of the casting mold to the required temperature is accomplished by electric heater 1, situated in ring 2 of the casting mold. Die 3 consists of 2 parts machined to the shape of a cone on the outside. It is placed in a corresponding conical opening in the ring. It is usually necessary to accomplish 2-sided molding of the product, and for this reason 2 punches 4 and 5 and rubber ring 6 are employed. Temperature measurement in the casting mold is accomplished by thermocouple 7.

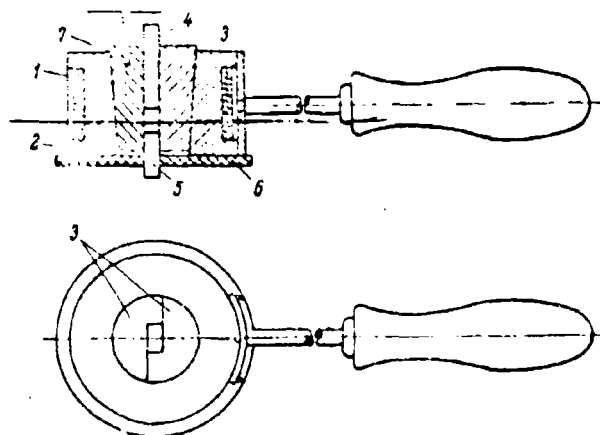


Figure 55. The design of a split casting mold for molding thermoelement arms.

The selection of an appropriate material for the die and the punches of the casting mold is an important consideration. The fact is that tellurium, which is a component part of the p-type and n-type alloys, at molding temperatures interacts with the material of the casting mold and forms pits which increase with time and which contribute to the failure of the casting mold. In addition, the material of the die and the punches must not anneal at operating temperatures and pressures.

Type 3X2B8 chrome-vanadium steel, hardened to  $R_c = 55-60$ , is a material which satisfies all requirements relatively well. However, the

possibility cannot be excluded that several types of heat resistant alloy steels may prove to be more resistant to the action of the alloy than 3X2B8 steel. We note that an attempt has been made to manufacture dies and punches for casting molds from corundum ( $Al_2O_3$ ). This material does not interact at all with the alloys, however, the manufacture of such casting molds at the present time is associated with a great deal of technical difficulty.

In 1959, A. N. Voronin and R. V. Grinberg proposed a method of cold molding of thermoelement arms. The essence of this method consisted of conducting the molding process at room temperature, and then the molded articles were subject to normal annealing in a vacuum in accordance with a special process. In so far as their electrical and thermophysical properties are concerned, the articles obtained by the cold molding methods are better than those obtained in a hot casting mold. However, the cold-molded articles possess reduced mechanical strength, which must be taken into consideration in apparatus design.

The dependence of the mechanical properties (compression strength) and the temperature drop at the thermoelement on the pressure value during the molding is shown in Figure 56.

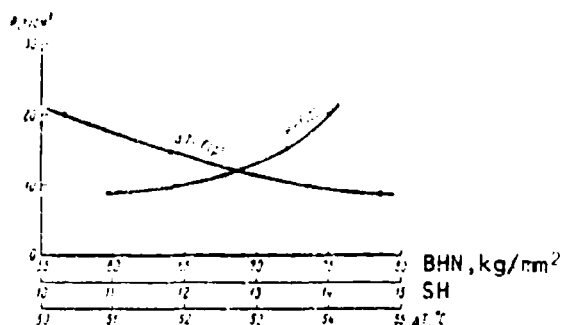


Figure 56. Temperature difference ( $\Delta T$ ) and compression strength according to Brinell (BHN) and Shore (SHN) hardness as a function of pressure (P) during the molding of thermoelement arms.

Domestic industry produces alloys for thermoelements which are accomplished through cold molding for the p-type arm and by hot molding

for the n-type arm. The basic properties of industrially-produced thermoelectric alloys are shown in Table 14.

Table 14

The Basic Parameters of Industrially-Produced Thermoelectric Alloys.

a) Марка сплава	b) Тип термоэлемента	c) Коэффициент электропроводности, Ом <sup>-1</sup> ·см <sup>-1</sup>		d) Коэффициент термоэлектромоторной силы, мВ/град	e) $\alpha^2$	f) Прессовка			g) Отпуск	
		до 750°С	до 900°С			давление, т/см <sup>2</sup>	время, мин.	температура, °С	время, ч	температура, °С
TVEKh-1	n-type	680	750	17,5	195	25,0	5	5	400	-
TVEKh-2	n-type	700	900	16,1	22,0	22,0	5	5	400	-
TVDKh-1	p-type	680	850	200	220	34,0	9	1	20	12
TDVKh-2	p-type	700	900	195	32,5	32,5	9	1	20	12

NOTE. The thermoelectric alloys listed in the table provide a temperature difference of 52-56° for a single-stage thermoelement in air under a layer of wadding at a hot junction temperature of +20°.

Key: a, Type of alloy; b, Type of conductivity; c, coefficient of electrical conductivity  $\sigma$ , ohm<sup>-1</sup>·cm<sup>-1</sup>; d, coefficient of thermoelectromotive force  $\alpha$ ,  $\mu$ V/deg; e,  $\alpha^2$ ; f, molding; g, annealing; h, pressure, t/cm<sup>2</sup>; i, time, minutes; j, temperature, °C; k, time, hours; l, temperature, °C.

After molding, the articles obtained are anisotropic. In the manufacture of thermoelement arms, sometimes briquettes of large dimensions are molded, which are then cut into pieces of the required size. In this connection it is necessary to follow the following rules: the direction of the passage of the electrical current through the thermoelement must be perpendicular to the direction of the molding. The cutting of the briquette-stock is accomplished on a special machine tool with thin abrasive vulcanite-bonded disks. The thickness of the disks employed is 0.2 mm.

Numerous experiments have been conducted in the manufacture of thermoelement arms by the casting method with directional crystallization and pulling of arms from the melt. Specimens obtained in this manner possess high thermophysical and electrical properties, but the processes of casting with direct crystallization and pulling from the melt have thus far proved to be low in productivity. After appropriate improvement and the creation of a high-output apparatus, these methods of manufacturing thermoelement arms will prove to be more effective. This is also apparent because thermoelements of this type have a higher figure of merit, which reaches a value of  $3.0 \cdot 10^{-3} \text{ deg}^{-1}$  for the p-type arm and  $2.8 \cdot 10^{-3} \text{ deg}^{-1}$

for the n-type arm. Thus for the commutated thermoelement,  $z$  proved to equal, on the average,  $2.8 \cdot 10^{-3} \text{ deg}^{-1}$ . Such thermoelements prove in one stage a temperature difference of  $63-65^\circ$  (with a hot junction temperature of  $20^\circ$ ).

## §2. The Tinning of Thermoelement Arms

The connecting together of the thermoelements, and as a part of this process, the tinning of the arms, is one of the most important processes in the technology of the manufacture of thermo-cooling devices.

As we have pointed out previously, the thermoelement figure of merit is defined by the value

$$z = \frac{\pi^2 c}{\kappa} \cdot \frac{1}{\pi p}.$$

In this equation only the specific resistance ( $\rho$ ) of the arm material is taken into consideration, and it is assumed that all the remaining resistance in the thermoelement circuit is infinitely small. In actual practice the resistance of the junction contacts between the semiconductor and the connecting plates of the cold and hot junctions must be added to the characteristic resistance of the thermoelement arms. It is not difficult to show that in this case the figure of merit of a practical thermoelement will be determined by the ratio

$$z = \frac{\pi^2}{\kappa \left( \rho + \frac{r_0}{l} \right)},$$

where  $r_0$  is the semiconductor contact resistance with the connecting plate having an area of  $1 \text{ cm}^2$ ; and  $l$  is the length of the thermoelement arm, cm.

It is apparent from the ratio shown that the contact resistance decreases the value of the thermoelement figure of merit, and thus causes the operating parameters of the device to deteriorate.

Therefore, one of the basic tasks in the technique of thermoelectric cooling is the search for methods of connecting the semiconductor with the connecting plates while maintaining sufficiently small junction resistances. Elementary calculations reveal that the value of the specific junction resistance must be  $\leq 10^{-5} \text{ ohm}\cdot\text{cm}$ . This condition

may be satisfied by direct soldering of the connecting plates to the thermoelement arms. However, as is known, the process of soldering is always accompanied by diffusion of the solder into the material of the parts joined together. While during the soldering of ordinary materials this diffusion only increases the mechanical strength of the solder joint, in the case of soldering semiconductors even minute penetration of the solder into the basic material of the semiconductor may cause a radical change in the properties of the latter. On the other hand, in order to obtain mechanical strength of the solder joint, it is necessary to permit solder diffusion into the semiconductor.

The solution to this problem lies in the search for appropriate solders, which must satisfy the following basic requirements: 1) the solder must not unite with the material of the semiconductor to form compounds which possess high ohmic resistance; 2) in penetrating the semiconductor, the solder must not change its electrical, mechanical and thermal properties; 3) the solder must have a melting point not higher than 450°; 4) in a melted state the solder must serve as a good semiconductor wetting agent; 5) at the melting point the solder must be fluid; 6) and the solder must display a small temperature difference between the points of initiation and termination of melting (a small difference between the liquidus and solidus lines); 7) the solder must possess the required mechanical strength.

It is quite clear that to select a solder which possesses all of the requirements enumerated is quite difficult. However, a solder based on bismuth has properties which are sufficiently close to those required. The composition and melting point of those solders which particularly recommend themselves in practice are shown in Table 15.

Table 15  
The Composition and Properties of Solders for Semiconductor Tinning

Solder composition (% by weight)	Melting point, °C	Semiconductor adhesion
100Bi	271	Satisfactory
99Bi + 1Sn	265	Excellent
95Bi + 5Sn	255	Good
90Bi + 10Sn	235	Good
90Bi + 20Sn	350	Excellent
80Bi + 20Sn	400	Excellent



The application of a layer of solder to the facial surfaces of the thermoelement arms is effected with an electrical soldering iron, equipped with a head of pure nickel. The employment of a nickel rather than a copper iron is dictated by the fact that copper dissolves in solder, which penetrates the semiconductor and forms tellurium compounds with the latter, which possess high resistance. The temperature of the iron must be 20-30° higher than the melting point of the solder employed. Higher soldering iron heat is not permissible.

While soldering it is necessary to employ flux in order to insure that the surface of the semiconductor is well wetted. Soldering flux for thermoelement arms must fulfill the following requirements: 1) it must have a melting point considerably lower than the melting point of the solder; 2) in a liquid state it must thoroughly wet the semiconductor surface; 3) in a liquid state it must possess neutral or weakly restoring effects; 4) it must not react with solder and with the semiconductor; 5) it must be easily removed after soldering. Pure stearic acid, which is usually employed as a flux, satisfies the properties listed when bismuth-tin solders are used.

In using bismuth-antimony solders, which have a higher melting point, it is best to employ a flux consisting of 20% sal ammoniac ( $\text{NH}_4\text{Cl}$ ) mixed with glycerin.

Experiments have been conducted in tinning arms with an ultrasonic soldering iron. These tests did not yield positive results since the semiconductor, being relatively soft, suffered surface destruction under the influence of ultrasonic cavitation, which interfered with the bond between the solder and the semiconductor.

Tests were conducted in the preliminary preparation of the semiconductor surface for soldering by means of a galvanic deposit of a thin layer of nickel or iron. The results obtained with this method reveal a lack of junction resistances at the places coated. However, the practical realization of this connection method is associated with a great deal of technical difficulty.

In tinning a semiconductor with pure bismuth or with bismuth solders, the solder layer usually must have a thickness of 0.2-0.3 mm. This is required in order to create a distinctive buffer layer which must separate the semiconductor and the connecting plate, since their coefficient of layer expansion differ greatly. If no buffer layer were present, the influence of frequent temperature shocks, generated when switching the thermopile on and off, would cause microcracks in the junction which would increase the junction resistance and correspondingly reduce the effectiveness of the thermopile.

### §3. Thermopile Connections

Thermopile connections are part of the process of connecting the separate, previously tinned thermoelement arms in the thermobattery by means of so-called connecting plates. As we have pointed out previously, depending on the chosen design connection of the apparatus, the individual thermoelements may be connected with each other in series, in parallel, or in series-parallel. These thermopile connections, just as the tinning of the thermoelement arms, are very important operations; the parameters of the completed apparatus depends on the quality of their execution. High-quality connections must satisfy the following basic requirements:

- 1) The value of the junction connecting layer must be not more than  $10^{-5}$  ohm·cm;
- 2) The connecting plates, by means of which the electrical connection between the separate arms of the thermoelement is accomplished, must be manufactured from a material which possesses high electrical conductivity (copper or aluminum);
- 3) The connecting plate junction with the semiconductor must possess sufficient mechanical strength; this requirement is dictated by the fact that in the process of thermoelement operation significant mechanical stress is generated within the element which might lead to element destruction;
- 4) The chosen method of connection must provide for extended operation of the apparatus without a change in basic electrical and thermal technical parameters as a result of connecting plate alloy diffusion into the semiconductor;
- 5) After extended storage of the thermo-cooling device, the processes of recrystallization and dispersed solidification must not occur in the connecting layer, since they might lead to a deterioration in the quality of the connections;
- 6) The selected connection method must be sufficiently perfected for production so that method execution may be achieved by workers of average qualifications.

In recent times many thermoelectric pile connection methods have been tested; however, the highest quality method proved to be that of direct soldering of the connecting plates to previously tinned thermoelement arms with low melting-point and soft solders. The composition and melting points of solders employed for thermoelectric pile connections are shown in Table 16.

Table 16  
The Composition and Melting Point of Connecting  
Solders

a) Температу- ра плавления, град. С	b) Состав сплава (вес. %)				c) Название сплава
	d) Вис- мут	e) Свинец	f) Олово	g) Кад- мий	
60	50	25	12.5	12.5	Wood's alloy
70	50	27	13	10	Lippwitz alloy
77	45.3	17.9	24.5	12.3	" "
80	45.3	25.3	20.1	9.5	" "
92	50	30	20	—	Lichtenberg's alloy
94	50	25	25	—	—
100	57.2	17.8	25	—	—
105	50	30	20	—	—
110	50.5	30.5	27	—	—
116	33.4	33.3	33.3	—	—
123	45.5	25.5	—	—	Tserobeyz <sup>1</sup>
135	58	—	42	—	—
140	35	35	30	—	Rose's alloy
144	60	—	—	40	—
150	16	36	48	—	—

Key: a, Melting point, °C; b, alloy composition  
(% by weight); c, name of the alloy; d, bismuth;  
e, lead; f, tin; g, cadmium

The wide range in melting points of connecting solders is due to the fact that in the number of specific cases, depending on the conditions of operation of a thermoelectric cooling device, the thermoelectric pile operates under various temperature conditions. In addition, in several multi-stage thermopile designs the individual stages are connected with solders of various melting points for convenience in assembly.

Basically the connection process is accomplished with the usual electrical soldering iron with a copper head, previously tinned with a thin layer of tin. The head temperature of the iron must not exceed the melting point of the solder by more than 10-20°. Otherwise an intensive diffusion occurs from the connecting solder into the solder with which the semiconductor was tinned, and as a result junction resistance is sharply increased.

<sup>1</sup>"Translated from the Russian. This is a possible trade name for a metal alloy."

Pure stearic acid is usually employed as a flux during the connection process.

Due to the fact that the process of thermopile connection is relatively time consuming, work involving the mechanization of this operation deserves attention. Thus, for example, I. L. Gerlovin developed the method of so-called simultaneous thermopile connections. The essence of this method consisted of the following: the copper connecting plates were tinned by immersion with a thin layer of connecting alloy, consisting of 70% Bi and 30% Sn, which had a melting point of  $170^{\circ}$ . The thermoelement arms were not tinned, but merely cleaned with fine emery cloth at the soldering areas. Then the thermoelement arms and the tinned plates were placed in a special device in which they were pressed against each other by means of a spring.

The soldering process was carried out strictly by means of immersing the device in stearic acid, which was heated to a temperature of  $25-30^{\circ}$  higher than the melting point of the solder with which the connecting plates had been tinned. The length of time that the device was maintained at the established temperature depended on a number of factors, but usually did not exceed 5 minutes. The quality of the connections using the method described depended on the value of the pressure pressing the connecting plates to the semiconductors. The best results were obtained with pressures from 0.75 to 1 kg/cm<sup>2</sup>.

The junction resistance in thermoelement specimens, prepared by the simultaneous connection method, was sufficiently low and was  $1.42 \cdot 10^{-5}$  ohm·cm for the p-arm and  $0.86 \cdot 10^{-5}$  ohm·cm for the n-type arm.

However it must be noted that the method of simultaneous connections thus far may be employed only in those cases when a thermoelement or a simple thermopile represents a constructively finished sub-assembly, which in a finished form is assembled in an apparatus. In the majority of cases a thermoelectric pile is an integral construction element of the device and its connection by the method described might present certain difficulties.

Quality control of the connections in an individual thermopile or a finished device is most easily accomplished by means of measuring the voltage drop on individual thermoelements. During the passage of the rated design current through a properly constructed thermoelement, the voltage drop across the element must lie in the range of 70-85 mv. The voltage drop on the p-arm must be 30-35 mv, and on the n-arm, 45-50 mv.

It must be stipulated that the indicated value of normal voltage drops on a thermoelement depends on the electrical conductivity of the

material utilized and on the thermoelement temperature. Therefore, for a more exact determination of the value of the voltage drop, we must make use of the equations presented in Part I, Chapter I. In any case, the value of the voltage drop on separate arms or thermoelements of a thermoelectric pile must not differ by more than  $\pm 5\%$ . A voltage drop which exceeds the specified limit indicates a low-quality connection. A significant increase in the voltage drop on a thermoelement indicates a defective connection as a result of thermostresses or mechanical damage. A decrease in the voltage drop below the standard amount indicates the presence of a short circuit in the pile, which is usually the result of excess solder on the semiconductor.

#### §4. Other Technological Considerations

In a number of designs of thermo-cooling devices aluminum is employed instead of copper with the aim of decreasing the weight and of replacing scarce materials. When such a substitution is made, it is necessary to take into consideration that the coefficient of heat conductivity for aluminum is 2 times higher than the coefficient for copper. In this connection type "A-0" or "A-00" aluminum must be employed as the construction material for the manufacture of heat transfer sub-assemblies and parts in thermo-cooling devices.

In employing aluminum in heat transfer systems, the necessity often arises to provide for a heat and electrical junction from aluminum to copper. This type of junction may be provided by one of the following methods:

1) by direct soldering of the copper part to the aluminum with pure tin with the application of 34-A standard flux;<sup>1</sup>

2) by electroplating (the Schoop process) aluminum in places subject to soldering with zinc, iron, nickel or other metals with subsequent soldering to the metallized layer of the copper parts with any solder;

3) by galvanically coating the aluminum with nickel with subsequent soldering of the copper parts to this layer with soft solders.

A high grade nickel coating on aluminum may be obtained in accordance with the following procedure:

---

<sup>1</sup>The composition of 34-A flux is as follows: lithium chloride 35%, potassium fluoride 12%, zinc chloride 15%, potassium chloride 38%.

1) degassing of aluminum in a bath with the composition: 25 g/l  $\text{Na}_2\text{CO}_3 \cdot 10\text{H}_2\text{O}$ , 25 g/l  $\text{Na}_3\text{PO}_4 \cdot 12\text{H}_2\text{O}$ , with a solution temperature of 60-80°, and a degassing time of 1-3 minutes;

2) a careful washing in water;

3) pickling in a 20-25% solution of  $\text{H}_2\text{SO}_4$  at a temperature of 85-90° for 2-5 minutes;

4) washing in running water;

5) the application of a zinc film in a solution of 400-500 g/l  $\text{NaOH}$ , 50-100 g/l  $\text{ZnO}$ , with a solution temperature of 20-30°, and a processing time of 0.5-1 minute;

6) washing in running water;

7) removal of zinc film in a 50% solution of  $\text{HNO}_3$ ;

8) washing in running water;

9) repetition of the application of the zinc film;

10) washing in running water;

11) nickel plating in a solution of the following composition: 95 g/l  $\text{NiSO}_4$ , 95 g/l  $\text{Na}_2\text{SO}_4$ , 18 g/l  $\text{NH}_4\text{Cl}$ , 15 g/l  $\text{H}_3\text{BO}_3$ , with an electrolyte temperature of 21-27°, and a current density of 1-4  $\text{a/dm}^2$ .

The nickel coating obtained in the manner described is exceptionally well bonded to the aluminum, which permits multi-stage soldering to it with soft solders.

When joining aluminum with other metals, it is necessary to keep in mind the electrochemical potentials of both metals. If this circumstance is not considered, the joined area, under the influence of moisture from the surrounding air, will be subject to corrosion. In order to prevent moisture penetration to the contact areas of aluminum with other metals, these areas are sealed with epoxy resin.

In order to create an electrically insulated heat junction in some devices, oxidized aluminum or oxidized copper parts are employed. Here we shall show the oxidizing processes and the formula for the baths.

### Oxidization of aluminum

Electrolyte	200 g $H_2SO_4$ , density 1.84 and 1000 g $H_2O$
Anode	Aluminum
Cathode	Lead
Voltage	8-12 v
Current density	10-20 a/dm <sup>2</sup>
Duration of the process	20-25 minutes
Electrolyte temperature	5-10°

### Oxidization of copper

Electrolyte	100 g NaOH in 1000 g $H_2O$
Anode	Copper
Cathode	Iron
Ratio of cathode area to anode area	5:1
Voltage	8-10 v
Current density	0.5 a/dm <sup>2</sup>
Duration of the process	20-30 minutes
Electrolyte temperature	80-90°

Epoxy compounds are widely employed in the technique of creating thermoelectric cooling devices. Of the large number of compounds, the most suitable proved to be a compound which polymerizes at room temperature, and a thermoreactive compound which requires heat for polymerization. The following is the formula for their preparation.

I. ED-6 epoxy resin	100% by weight
Polyethylene polyimine	14% by weight
Dibutyl phthalate	25% by weight
Polymerization temperature	room temperature
Complete polymerization time	24 hours
II. Phthalic anhydride	35% by weight
Dibutyl phthalate	15% by weight
ED-6 resin	100% by weight
Polymerization temperature	160-180°
Polymerization time	2 hours

The manufacturing process of a thermo-cooling device is associated with the carrying out of a number of technical-chemical operations.

The basic formulas are shown below.

1) Smooth etching of soft steel and nickel. One part by volume of  $H_2SO_4$  (1.84) and 5 parts by volume by water at temperature  $T = 80^\circ$ .

Vigorous washing is accomplished after the etching period.

2) Vigorous matte etching of soft steel and nickel. One part by volume of  $HNO_3$  (1.4) and 1 part by volume of  $H_2SO_4$  (1.84) at temperature  $T = 20-30^\circ$  for 5 seconds. Drying is accomplished in a thermostatic chamber after washing in running water.

3. Etching of constantan. One part by volume of  $H_2SO_4$  (1.84) and 9 parts by volume of water at temperature  $T = 60^\circ$ . Washing is accomplished in running water, and in methyl alcohol, after which drawing is accomplished in a current of warm air.

4. Etching of high-chromium steel. One part by volume of  $HCl$  (1.19) and one part by volume of water at temperature  $T = 60^\circ$ . Washing is accomplished in running water, and drying in dry air.

5. Matte etching of copper and its alloys. One part by volume of  $HNO_3$  (1.4), 2 parts by volume of  $H_2SO_4$  (1.84) and 7 parts by volume of water at temperature  $T = 70^\circ$  for a period of 1-4 minutes. Drying is accomplished after washing in warm water.

6. Bright etching of copper and its alloys. 7.5 g  $NaCl$ , 7.5 g  $NaNO_3$ , 375 ml  $HNO_3$  (1.4), 375 ml  $H_2SO_4$  (1.84) and 700 ml of water at temperature  $T = 25^\circ$  for approximately 1.5 minutes. Drying in a thermostatic chamber is accomplished after vigorous washing in water and ethyl alcohol.

7. Scouring of copper oxide ( $CuO$ ) from the surface of copper and copper junctions. The mixture is a solution of  $FeSO_4$  and a 5% solution of  $H_2SO_4$ .

8. Matte etching of tungsten. One hundred fifty g  $K_3Fe(CN)_6$ , 1,000 g  $NaOH$  and 5 l of water at temperature  $T = 70^\circ$  for a duration of 0.5 to 2 hours. Washing is accomplished in warm water, then a rapid wash in  $HCl$  (1:2), the washing in water is repeated and drying is accomplished in warm air.



9. Matte etching of molybdenum and nickel. One hundred parts by volume of  $\text{H}_2\text{SO}_4$  (1.84) and 20 parts by volume of  $\text{HNO}_3$  (1.4) at temperature  $T = 80^\circ$ .

10. Smooth etching of molybdenum, tantalum, and columbium. Nine parts by volume of KOH and 1 part by volume of  $\text{NaNO}_2$ . Fuse the salts in an iron crucible, followed by quick etching (not longer than 1 second) of the parts in this melt, rapid washing in boiling water, and washing in running water and ethyl alcohol. Drying is accomplished in warm air.

11. Smooth etching of tungsten. Etching is accomplished in fused  $\text{NaNO}_2$ ; the remainder of the process is the same as in formula 10.

12. Electrochemical degreasing and etching of all metals and alloys. A bath with the solution 6 parts by weight of NaOH, 2 parts by weight of NaCN, 2 parts by weight of  $\text{K}_2\text{CO}_3$ , 0.8 parts by weight of water glass, 100 parts by weight of water at a temperature  $T = 25^\circ$  for 1-2 minutes; the parts are on the cathode, the anodes are steel, the voltage is 6-10 v, current density 4-8 a/dm<sup>2</sup>. Drying is accomplished after careful washing.

13. Bright electrolytic etching of tungsten in molybdenum. Two hundred g NaOH, 30 g  $\text{Na}_2\text{SO}_4 \cdot 10 \text{H}_2\text{O}$  and 1 l of water. Alternating current is employed at a voltage of 20-30 v. The electrodes are of nickel. Duration of the etching is 10-20 seconds at temperature  $T = 25^\circ$ . The bath is switched to direct current at a voltage of 25-40 v; the parts are on the anode, and etching duration is 5-10 seconds. Washing is accomplished in running water, rinsing in  $\text{HCl}$  (1:1), then washing in running water, and drying in a current of warm air.

14. Bright electrochemical etching of nickel, its alloys and high-chrome steel. Five hundred g  $\text{H}_3\text{PO}_4$  (1.7), 250 g  $\text{H}_2\text{SO}_4$  (1.84) and 25 g water at temperature  $T = 25^\circ$  for a duration of 10-30 seconds. Vigorous scouring. The voltage is 15-30 v, current density ~ 400 a/dm<sup>2</sup>, the parts are on the anode, and the cathodes are steel. Drying is accomplished in a thermostatic chamber after washing in running water for 2-3 hours.

15. Bright electrochemical etching of copper and its alloys. The bath is  $\text{H}_3\text{PO}_4$  (1.7) at temperature  $T = 25^\circ$ , while etching duration is 10-30 seconds; the parts are on the anode, the cathodes are steel, the voltage is ~ 30 v, current density is 80 a/dm<sup>2</sup>. Drying is accomplished in a current of dry air after careful washing in distilled water and ethyl alcohol.

16. Electropolishing of steel, nickel, and nickel platings on aluminum alloys. The bath is 750 mL  $\text{H}_3\text{PO}_4$  (1.7), 150 mL  $\text{H}_2\text{SO}_4$  (1.84), 100 g  $\text{CrO}_3$ .

When the temperature  $T = 60-80^\circ$ , the current density for steel is 30-40  $\text{a/dm}^2$ , for nickel, 25-35  $\text{a/dm}^2$  for a duration of 1-3 minutes; for aluminum alloys, 20-30  $\text{a/dm}^2$  for a duration of 5 minutes.

17. Chemical blackening of copper. Degreasing and etching in  $\text{HNO}_3$  of copper parts suspended in a bath of the following composition: 15 g  $\text{K}_2\text{S}_2\text{O}_8$  (potassium persulfate), 50 g NaOH, 1 L of water (distilled). The solution temperature is  $60-65^\circ$ . Blackening time is 5 minutes. During the blackening process the parts are turned in the solution in order to remove air bubbles which settle on them. After blackening the parts, they are washed, dried and rubbed with a clean soft cloth.

18. Chemical blackening of brass. Degreasing and etching in  $\text{HNO}_3$  of the parts which are suspended in a bath of the following composition: 7.5 g  $\text{K}_2\text{S}_2\text{O}_8$ , 52 g NaOH, 1 L of water (distilled). The solution temperature is  $60-65^\circ$ . Blackening time is 15-20 minutes.

19. Chemical oxidization of brass to a black color. Degreasing and etching of brass parts for 15-20 minutes while they are immersed in a solution as follows: 125 g  $\text{CuCO}_3 \cdot \text{Cu}(\text{OH})_2$  (basic copper carbonate), 355 mL  $\text{NH}_4\text{OH}$  (25% solution), 1 L of water. The solution temperature is  $18-20^\circ$ .

20. Surface coating, i.e. obtaining by electrochemical means thick, non-transparent oxide films on aluminum gives the coated article an enameled appearance. This is employed as an electrically-insulating and decorative covering. The covering possesses significant thermal stability and high mechanical properties. This technique of surface coating consists of the following: polished, degreased and washed aluminum parts placed on hangers of pure aluminum and submerged in a bath of the following composition: 30 g/L  $\text{CrO}_3$ , 1-2 g/L  $\text{H}_3\text{BO}_3$ . The electrolyte temperature is  $45 \pm 3^\circ$ , the voltage is 40-80 V, and current density is 0.4-1  $\text{a/dm}^2$ . The oxidization duration is 1 hour. The part undergoing oxidization forms the anode. The cathode is a stainless steel plate. The process of surface coating is conducted in the following sequence. The articles are hung on the anode rod with no current flowing, then during the course of 5 minutes, the voltage is raised smoothly to

a value of not more than 40 v, and the bath is maintained at this voltage for 30 minutes. Under these conditions the current density must be 0.4-0.5 a/dm<sup>2</sup>. Then the voltage is increased to a value of 80 v and maintained at this value for 30 minutes. Here the current density must be 1 a/dm<sup>2</sup>. After coating of the surfaces, the parts are washed and the oxide film obtained is fixed by means of boiling in water for 30 minutes. In the case of future necessity, the film coating may be painted any color in water solutions of organic dyes.

In order to measure the temperature on the operating surface or in the chamber of the majority of thermal-cooling devices, the MKMT-16 or other types of sending units are employed. In order to provide a reliable thermocontact between the cooled or the heated surface and the microthermistor, the latter is sheathed with a silver or copper amalgam. These amalgams possess excellent heat conductivity and high mechanical properties. The single disadvantage of utilizing an amalgam is the sealed nature of the junction, as a result of which extraction of the sheathed microthermistor without damaging it is not possible. Both silver and copper amalgams are mass-produced by industry as dental material.

The following are amalgam formulas.

Silver amalgam. Three-four parts by volume of silver alloy are placed in a mortar and in the course of several minutes are ground until a fine powder is obtained. Then 1 part by volume of mercury is added and the mixture is stirred until a uniform paste-like mass is obtained. After the amalgam is obtained it is placed in a cheesecloth and excess mercury, which has not combined with the silver, is squeezed out. The thermistor to be covered is placed in a shallow opening which is filled with the amalgam and sealed over. Full hardening of the silver amalgam occurs in 6-8 hours.

Copper amalgam is prepared in the following manner. Depending on requirement, one or more plates of the amalgam are placed in a metallic spoon and heated over a low flame until drops of emerging mercury appear. After the appearance of the mercury, the plates are placed in a mortar and ground until a uniform plastic mass is obtained. The surplus mercury is pressed out in a cheesecloth. After this the amalgam is ready for use. If part of the prepared amalgam hardens, it may be returned to the plastic state by repeated heating. Complete hardening time for the copper amalgam is 2-3 hours. Copper amalgam, just as the silver, forms a connection which cannot be disassembled.

### PART III. THERMOELECTRIC COOLING IN PRACTICE

#### CHAPTER X

##### HIGH-VACUUM COLLECTORS WITH THERMOELECTRIC COOLING

###### §1. Purpose

Contemporary vacuum technology in the majority of cases deals with devices and installations in which the operating pressure reaches  $10^{-6}$ - $10^{-7}$  mm Hg. Such pressures, as a rule, are created by means of diffusion vapor-jet pumps, in which the gases subject to evacuation are diffused in a jet of vapors of the pump working fluid. Subsequently, upon condensation of the vapors, these gases are freed and are evacuated by a pre-evacuation pump. Mercury is employed as a working fluid in diffusion pumps (in mercury-vapor pumps)<sup>1</sup> or special oils with a high molecular weight ( $M = 250-550$ ) and low vapor pressure (in diffusion oil vapor pumps) may be employed. Specific types of mineral oils (naphthene types) may be employed as working fluids in oil vapor pumps, including organic oils (for example, the ethers of several organic acids), or, finally, synthetic organic oils and silicones (and polysilicones).

VM-1 vacuum oil is widely employed in the domestic vacuum industry. These oils represent heavy fractions of vaseline oil, obtained as a result of vacuum distillation.

---

<sup>1</sup>At the present time mercury vapor-jet pumps are seldom employed, and then in special areas of vacuum technology (in the evacuation of mass-spectrometers, and of mercury gas-discharge devices). Therefore, subsequent descriptions will pertain basically to oil diffusion pumps.

It has been established from the usage of high-vacuum evacuation devices that the basic factor which establishes the pressure reduction limit in an evacuated space is the vapor pressure of the working fluid utilized in the pump. Ordinary oils employed in oil vapor pumps permit the attainment of an ultimate vacuum of  $2-3 \cdot 10^{-6}$  mm Hg. Further pressure reduction is not possible due to the presence in the high-vacuum part of the system of so-called residual vapors.

The main source of residual vapors which impair the vacuum is the vapor-jet pump, from which "streams" of oil, reaching  $10^{-3}$  mg/cm<sup>2</sup>·h, are emitted. In addition, the walls of the vacuum chamber and the parts distributed within the chamber, and also products released as a result of operations accomplished within the chamber may be a source of residual vapors.

In addition to impairing the vacuum, the presence of residual oil vapors seriously impairs the operation of a number of vacuum devices. In addition, in elementary particle accelerators, the presence of oil vapors causes a diffused scattering of the beam, contaminates sources, and is also a reason for the appearance of electrical breakdowns. In precision vacuum metallurgy oil vapors contaminate the product obtained. Powerful tube-equipped oscillators in the very short wave and microwave bands, operating under a constant vacuum, fail to operate when oil vapors strike them. If even an insignificant quantity of oil vapors strikes the oxidized cathodes in electro-vacuum devices, the loss of cathode emission capability will occur. In electron-ray devices (electron-optical converters, photoelectron multipliers, receiving and transmitting television tubes, etc.), the presence of oil vapors on the light-sensitive element -- the photocathode or the mosaic -- leads to failure of the apparatus.

From the examples cited, the urgency of the problem of preventing the penetration of residual oil vapors from the diffusion pump into the space evacuated is apparent.

One of the basic methods of improving the ultimate vacuum and significantly reducing the quantity of residual vapors is the supplementary condensation of oil vapors by means of a cooled collector, which is situated between the pump and the space evacuated. It should be noted that the cooled collectors are not independent pump assemblies. While not influencing the pressure of the majority of gases in vacuum devices, they condense the vapors and maintain them on their operating surfaces.

Vapor pressure reduction on the condensation surfaces of the collector is a time function and is characterized by the rate of collector

operation, which in turn is determined by the vapor condensation rate on the cooled surfaces. The rate of vapor condensation in a cooled collector may be determined with a sufficient degree of accuracy from the equation

$$S = \frac{62}{\sqrt{M}} \left( 1 - \frac{P_1}{P_2} \right) A,$$

where  $S$  is the collector vapor condensation rate,  $l/sec$ ;  $M$  is the molecular weight of the vapors of the condensing liquid;  $P_1$  is the vapor pressure at the condensation temperature, mm Hg;  $P_2$  is the partial pressure of the condensed vapors (mm Hg) at a temperature of  $18^\circ$ ;  $A$  is the value of the effective collector condensation surface,  $cm^2$ .

It is apparent that with an increase in the temperature of the collector condensation surfaces, value  $P_1$  will approach  $P_2$  and when  $P_1 = P_2$ , the vapor condensation rate in the collector will equal zero.

At the present time freon compression machines, or so-called brine and liquid nitrogen types, are employed to cool high-vacuum collectors.

Among the shortcomings of freon collectors we must consider their relatively high temperature, and the low efficiency of the system (1-3%), which occur as a result of high heat losses, since a system consisting of a compressor and vaporizer is situated outside the collector.

The brine method of refrigeration, based on the temperature reduction phenomenon in the solution of several salts in water, has not been widely employed in vacuum technology due to insufficient cooling of the collector condensation surface ( $-19^\circ$ ) and a large number of operating inconveniences.

The use of liquid nitrogen, especially in huge vacuum installations with a large number of powerful pumps, is associated with a number of deficiencies, of which the following are basic: a large expenditure of relatively scarce liquid nitrogen, which requires the construction of special and extremely expensive cryogenic stations; the presence of a complex system of distribution of liquid nitrogen, in which large losses are unavoidable; the complexity of the control apparatus for the nitrogen level and the collectors and a number of other factors.

Experience in the use of numerous high-vacuum installations has revealed that the application of liquid nitrogen for the cooling of congealation collectors in a majority of cases is not justified.

Mass-spectrometric investigations of the quantity of condensed oil vapors as a function of temperature have revealed that practically complete condensation of residual vapors occurs at a temperature of  $-40^{\circ}$ . The mass spectrogram, shown in Figure 57, was taken with the aid of an omegatron which was installed on a type TsVL-100 oil vapor pump operating on heavy fractions of vaseline oil. Peaks showing hydrogen, water, carbon dioxide and a series of hydrocarbon peaks with mass numbers from 43 to 148, which characterize oil vapors and products of their reduction (cracking) were registered in the mass spectrogram. A louvered type of collector, the temperature of which could be changed, was placed between the omegatron and the pump. With a temperature on the collector condensation surfaces of  $-40^{\circ}$ , the intensity of the basic peaks with mass numbers 57-148 decreased 10-30 times (the shaded areas in Figure 57). It is natural that at this temperature products with low mass numbers (2-28) were not frozen out. However, the presence of insignificant quantities of  $H_2$ ,  $H_2O$  and  $CO_2$  in the residual vapors is not as dangerous as the presence of heavy hydrocarbons.

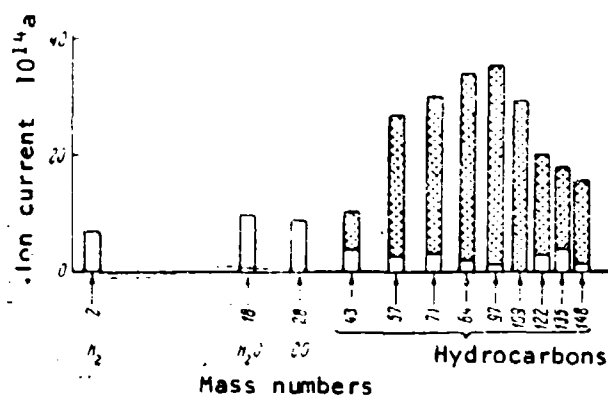


Figure 57. The mass spectrogram of residual oil vapors passing through the vacuum collector of the louvered type.

The shaded area represents an uncooled collector; the non-shaded area represents a collector cooled to  $-40^{\circ}$ .

The data presented above indicates that in the overwhelming majority of cases, cooling of the condensation collector to  $-40$ - $50^{\circ}$  completely satisfies the basic requirements for the operation of high-vacuum systems

On this basis, the high-vacuum collectors described below with thermoelectric cooling equipped with 2-stage thermoelectric piles, provide for a temperature of  $-50$  to  $-55^{\circ}$  on the condensation surfaces of the second stage.<sup>1</sup> A 3-stage thermopile provides a temperature of  $-65$  to  $-70^{\circ}$  on the condensation surfaces of the third stage. However, the complexity involved in this construction is considered to be unjustified, since the vapor condensation effect proves to be approximately the same as with a temperature of  $-50^{\circ}$ .

Oil penetration from the pump to the exhausted space may occur in two ways: either in the form of residual vapors, which did not condense in the pump cooling system, or by means of migration of oil in the liquid state along the internal surfaces of the sides of the vacuum system. If the residual vapors may be sufficiently and effectively delayed by the cooled collector, then additional devices are required in order to prevent the penetration of oil migrating along the walls to the exhausted space. Many anti-migration devices have been proposed; however, all of these merely delay the rate of oil migration, and not one of them permitted the complete elimination of this extremely undesirable phenomenon. All known anti-migration devices are based on the artificial lengthening of the oil path by means of creating extended surfaces, or pockets, on the internal sides of the vacuum system of the collector. In some cases these pockets have the same temperature as the sides, and in other cases they are artificially cooled by water or liquid nitrogen.

In the development of designs for the thermoelectric cooling of collectors, a new type of anti-migrator was proposed which was based on the utilization of a material which is not wetted by oil.

In addition to non-wettability, the anti-migrator material must possess low vapor pressure in a vacuum. These conditions are satisfied by teflon (a crystallized polymer of tetrafluoroethylene).

An anti-migrator manufactured from teflon comprises two rings 1 and 2 (Figure 58), which are tightly fitted inside the collector casing. The distance between the teflon rings is established by duralumin ring 3. Such a system, which forms a "lock", not only permits extending the surface of the teflon, but also excludes the possibility of oil vapor spray on the internal ring surface.

The development of the theory in practice of thermoelectric cooling made it possible to create in 1957, for the first time, a high-vacuum

<sup>1</sup>Both here and subsequently the temperature on the collector condensation surfaces was measured at a pressure of  $10^{-5}$  mm Hg and with a heat removal water system temperature of  $18^{\circ}\text{C}$ .



cooler with thermoelectric cooling for the MM-40A oil-vapor pump. In recent years thermoelectric coolers for all diffusion pumps produced by domestic industry have been developed.

The mass production of thermoelectric collectors began in 1960.

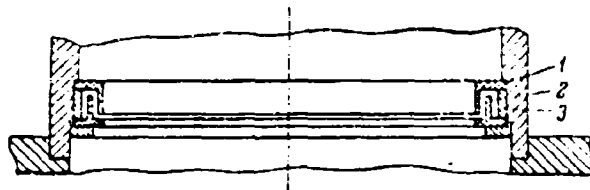


Figure 58. Diagram of an oil anti-migrator

## §2. Thermoelectric Collectors for the Unified Series of Pumps

In the period from 1957 to 1964, high-vacuum collectors with thermoelectric cooling were developed, intended for operation with oil diffusion pumps of the so-called unified series. To this series belong the pumps with outputs 100 l/sec. (H-1c); 500 l/sec. (H-5c); 2,000 l/sec. (H-2T); 5,000 l/sec. (H-5T); 8,000 l/sec. (H-8T) and 20,000 l/sec. (H-20T). A collector for the pump with an output of 40,000 l/sec. (H-40T) is now in the developmental stage.

All collectors of this series indicated have two-stage thermoelectric piles, the cold collectors of which are the condensation surfaces for the oil vapors. Heat removal from the hot junctions of the thermoelectric pile in all types of collectors is provided by a flow of water, which is delivered to the collector in series with the cooling system of the high-vacuum pump. The spatial distribution of the collector condensation surfaces forms a "louvered" system, which provides for a minimum of 2-fold impingement of oil molecules on the cooled surface. Due to this fact, the "flight" of the oil through the collector does not exceed  $10^{-5}$  mg/cm<sup>2</sup>·h. In addition, in the choice of the number, shape and relative distribution of condensation surfaces, the requirement for minimum reduction in the evacuation pump rate by the collector was also taken into consideration. Numerous tests of thermoelectric collectors have revealed that with a condensation surface temperature on the second stage of  $-50^{\circ}$ , the ultimate vacuum in the evacuated chamber is improved by 0.7-0.8 order of magnitude.

A sectional representation of the TVL-40-2 thermoelectric collector for the MM-40A pump is shown in Figure S9.

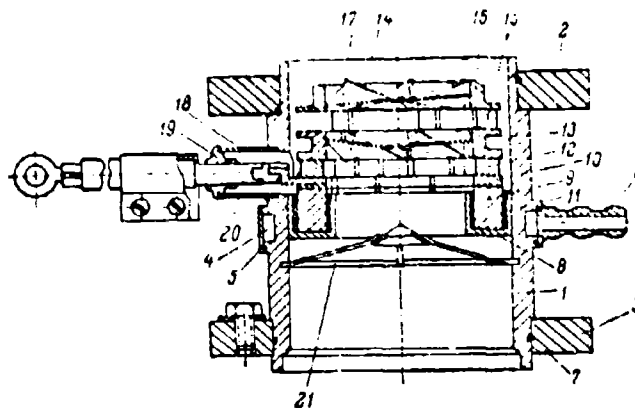


Figure S9. A section of the TVL-40-2 collector for the MM-40A pump.

The collector casing 1 with flanges 2 and 3, which serve to connect the collector to the pump and to the space being evacuated, is constructed of steel. The central part of the casing is equipped with annular channel 4, covered by ring 5, which forms the system of heat removal for the collector. Water is supplied to the cooling jacket and merges through the two nipples 6. All parts of the casing are vacuum sealed and are brazed with copper along joints 7.

Simultaneously with the copper brazing of the collector housing parts, hot copper plating of the internal surface of the casing is accomplished. This is required for subsequent soldering of copper parts to the casing and to create a protective anti-corrosion coating. Copper ring 8 is soldered with PSR-72 solder to the casing from the inside. The heat transfer system from the collector thermoelectric pile is arranged in the following manner.

The lugs 9 are manufactured from type AO or type AOC aluminum and are electrochemically coated with a thin (2-4  $\mu$ ) layer of aluminum oxide. Due to the thickness and the good heat conductivity of aluminum oxide, this layer possesses insignificant heat transfer resistance. Simultaneously this layer is a good electrical insulator. Copper plates 10, to which the thermopile will be attached, are soldered on top of the aluminum lugs with pure tin. In order to create a good thermocontact between the oxidized lugs and ring 8, the latter is packed with special alloy 11

which has a melting point of  $140^{\circ}$ . The two-stage thermoelectric pile of the collector has 6 thermoelements in the first stage which are connected in parallel with 3 thermoelements of the second stage.

The semiconductors 12 of the first stage are soldered, using a solder with a melting point of  $90^{\circ}$ , to the heat transfer elements. The cold junction collectors of the first stage are made of copper segments 13. Condensation surfaces 14 are soldered to the internal surfaces of the copper plates with PSR-72 solder.

The semiconductors 15 of the second stage are soldered with Wood's alloy to the cold junction collectors of the first stage. The condensation surfaces 17 of the second stage are soldered to the 3 segmented parts 16. The quantity of condensation surfaces in the first and second stages and their mutual spatial distribution are chosen so that the oil vapor molecule undergoes a minimum of 2-stage reflection from the cooled surfaces and, in addition, so that the collector possesses maximum conductivity. In the system of condensation surfaces selected, the vacuum resistance, offered by the collector, equals 60%. The current supply of the thermoelectric pile is provided through a vacuum sealed entrance, consisting of cover sleeve 18, which is brazed with copper to the casing, through which passes molybdenum electrode 20 in glass 19. The second side of the collector current supply is attached to the casing. Oil reflector 21 serves to prevent the penetration of oil through the central area of the collector.

An overall view of the TVL-40-2 collector is shown in Figure 60.

## GRAPHICS NOT REPRODUCIBLE

Figure 60. An overall view of  
the TVL-40-2 collector for  
the MM-40A pump.

Three thermoelectric collector design variations were developed for the TSVL-100 pump. They have received the designations TVL-100-1, TVL-100-2 and TVL-100-3, respectively. The TVL-100-1 collector has a sector-shaped system of condensation surfaces mounted on the first and second stages of the thermoelectric pile. The heat transfer system and other construction elements of the collector are similar to those of the TVL-40-2 collector, described above. The second collector construction variant, the TVL-100-2, has a dual-row louvered system of condensation surfaces and a fluid heat removal system, which is situated in the collector vacuum cavity. And, finally, the third variant, the TVL-100-3, was developed with the aim of providing the maximum reduction of the resistance to the collector evacuation rate. For this purpose, the collector casing was barrel-shaped with a large cross-section in the area of the location of the thermopile. The TVL-100-2 collector was placed in mass production.

A sectional view of this collector is shown in Figure 61. Heat transfer sub-assembly 1, manufactured of nonoxidized copper of the "MB" type, was connected with PSR-72 solder to form a vacuum tight seal with the steels collector casing. Water passes through the internal channels formed in this sub-assembly, and removes the heat from the hot junctions of the collector thermopile. Water input and output are accomplished through nipples 2. The thermoelements 3 of the first stage are soldered to the heat-transfer base through electrically insulated heat junctions 4. The second stage of thermoelements 5 are soldered to the thermoelements of the first stage. The condensation surfaces 6 and 7 of the first and second stages of the collector thermopile form a "louvered" dual-passage system, which provides for practically complete condensation of residual oil vapors with a relatively small reduction in the pump evacuation rate.

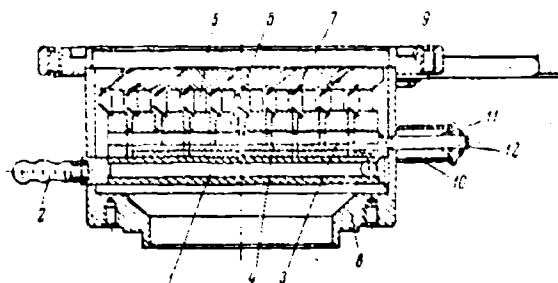


Figure 61. A section of the TVL-100-2 collector for the TSVL-100 pump.

The connection of the collector to the pump and to the exhaust space is accomplished by means of base 8 and flange 9. The current supply to the collector thermopile is connected to the casing and to a vacuum-tight current conductor, consisting of kovar sleeve 10 and kovar lead 12, which passes through glass 11 and is soldered to the sleeve. All steel, copper and kovar sub-assemblies of the collector are soldered to form vacuum-tight seals with copper and silver-copper solders in a hydrogen oven.

An overall view of the TVL-100-2 collector is shown in Figure 62.

## GRAPHICS NOT REPRODUCIBLE

Figure 62. An overall view of  
the TVL-100-2 collector for  
the TSVL-100 pump.

Tests of the collector have revealed that the minimum temperature on the condensation surfaces of the second cascade of the collector are established 55 minutes after the unit is switched on, and then the temperature reduction is not linear with respect to time. This pertains to all types of thermoelectric vacuum collectors.

The temperature reduction rate on the condensation surfaces of the second cascade of the TVL-100-2 collector is shown in Figure 63.

A section of the TVL-5s-4 collector for the N-5s pump is shown in Figure 64.

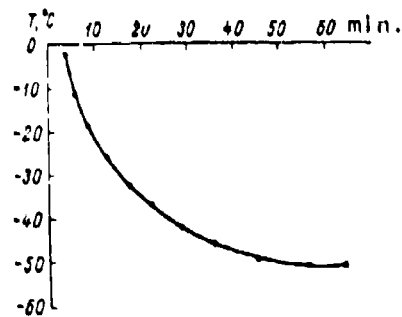


Figure 63. The temperature reduction rate on the condensation surfaces of the second cascade of the TVL-100-2 collector.

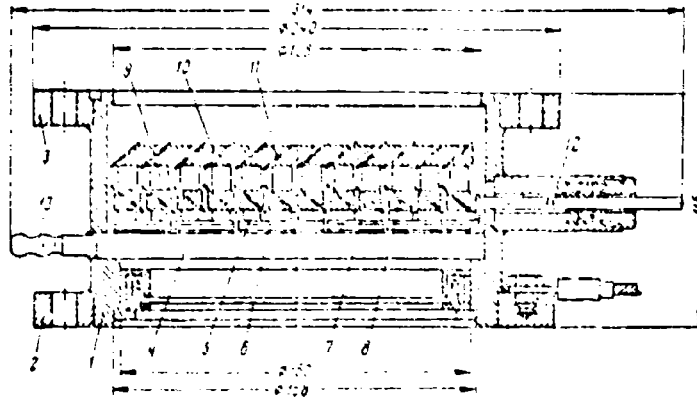


Figure 64. A section of the TVL-5s-4 collector for the N-5s pump.

Flanges 2 and 3 are welded to steel casing 1. These flanges serve as collector connections to the pump and to the evacuated space. The heat removal system is welded to the casing of the collector. This system is comprised of steel insert 4 with 2 channels for the passage of water, which removes heat from the hot junctions of the thermopile. The thermoelement 5 of the first stage are soldered with crimped heat junction 6 to the heat-transfer base. The collectors 7 of the cold junctions, the condensation surfaces 8, which are situated at an angle of  $45^\circ$  to the axis of the junctions. The condensation surfaces have a temperature of  $-26^\circ$ .

The thermoelements 9 of the second stage are soldered to the collectors of the cold junction of the first stage, and here the electrical supply of the second stage of the thermopile is accomplished in parallel with the current supply to the first stage. The thermoelement of the second stage carry the collectors 10 of the cold junctions, which are equipped with condensation surfaces 11, situated at an angle of  $90^\circ$  to the condensation surfaces of the first stage. The temperature on the condensation surfaces of the second stage, as we have indicated previously, is  $-50$  to  $-52^\circ$ .

The electrical supply to the thermoelectric pile is accomplished by means of vacuum-sealed lead 12. The second pole of the supply to the thermopile is connected to the collector casing. Water for the heat removal system is delivered through nipples 13.

An overall view of the collector is shown in Figure 65.



**GRAPHICS  
NOT REPRODUCIBLE**

Figure 65. An overall view of the  
TVL-5s-4 collector for the  
N-5s pump.

A collector for more powerful pumps (beginning with the N-2T pump) differs in construction from the collectors described. These differences include the following.

1. As a result of the significant heat load on the condensation surface of the first stage, carried by the oil vapors, an additional row of condensation surfaces was proposed, mounted directly on the heat transfer bases and having the same temperature as the water in the heat removal system. Thus this system of condensation surfaces accepted the main heat load, at the same time reducing the heat load on the thermopile.

2. The rate of "collector evacuation" is determined by the volume of the vapor condensing in the collector in one second, therefore an increase in the effective collective area was proposed, i.e., an extension of the condensation surfaces. In this case the collector casing has an increase cross-sectional area, with no change in the connecting dimensions. As a result, notwithstanding the presence of a 3-row system of condensation surfaces (a nitrogen collector has 1 row of condensation surfaces), the evacuation resistance of the thermoelectric collector proved to be less than for corresponding nitrogen collectors.

Recently separable collectors have been developed and produced for pumps (beginning with N-2T), in which the thermoelectric pile with the system of condensation surfaces may be withdrawn from the collector casing. This type of construction facilitates the disassembly of the collector for periodic cleaning out of condensed oil, since disassembly of the collector from the vacuum system is not required.

Figure 66 illustrates a section of the TVLR-2T-2 separable collector for the N-2T pump. Here the thermoelectric pile in conjunction with the electrical supply and heat removal system is an independently constructed sub-assembly, which is installed in the casing and is vacuum-sealed along the side surface of the casing flange. Collectors for the N-5T, N-8T and N-20T pumps differ from each other by the number of thermoelements in the thermopile, by electrical supply methods and overall dimensions.

Figure 67 shows a general view of the TVLR-20T-1 separable collector for the N-20T pump, which was installed on the VA-2-2 exhaust assembly for tests.

Comparative test data for thermoelectric and nitrogen collectors for ultimate vacuum and evacuation rates<sup>1</sup> are shown in Tables 17 and 18. These tests revealed that the ultimate vacuum obtained using assemblies equipped with thermoelectric coolers was not worse than that obtained with coolers equipped with liquid nitrogen cooling, and the evacuation rate of assemblies equipped with thermoelectric collectors was somewhat higher than with nitrogen collectors. A selenium rectifier (the VFA-3M, for example,) or a rectifier with high-current germanium diodes, which satisfy the required parameters, may be employed as a power supply for thermoelectric collectors.

---

<sup>1</sup>Complete collector vacuum tests were conducted by N. M. Karpenko and Ya. L. Mikhelis.



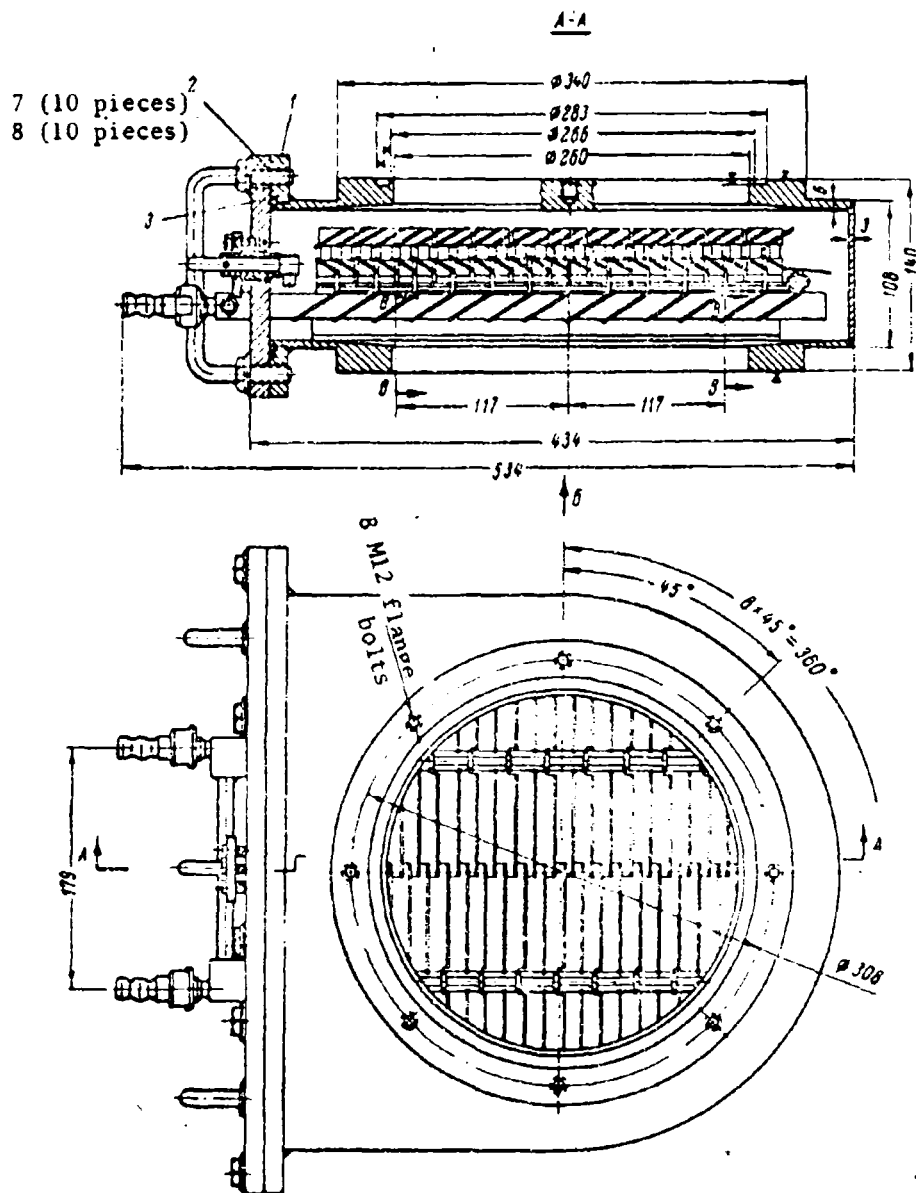


Figure 66. A section of the TVLR-2T-1 separable collector for the N-2T pump.

# GRAPHICS NOT REPRODUCIBLE

Figure 67. An overall view of the TVLR-20T-1 separable collector for the N-20T pump.

Table 17  
Ultimate Vacuum Obtained on Assemblies Equipped with  
Thermoelectric and Nitrogen Collectors

a) Тип вакуум- ного агрегата	b) Тип коллектора	c) $t_{\text{эксп}}$ , мин. время эксплуатации в вакууме, мин.	d) Давление, мм рт. ст.	
			e) с термоэлектри- ческим коллектором	f) с азотным коллектором
VA-01-1	TVL-100-2	40	$8 \cdot 10^{-7}$	$8 \cdot 10^{-7}$
VA-05-1	TVL-5s-4	60	$6 \cdot 10^{-7}$	$5 \cdot 10^{-7}$
VA-2-3	TVL-2T-1	60	$6 \cdot 10^{-7}$	$5 \cdot 10^{-7}$
VA-5-4	TVL-5T-1	70	$6 \cdot 10^{-7}$	$5 \cdot 10^{-7}$
VA-8-4	TVL-8T-1	80	$7 \cdot 10^{-7}$	$5 \cdot 10^{-7}$

Key: a, type of vacuum assembly; b, collector type;  
c, a collector operating time, minutes; d, pressure,  
mm Hg; e, with a thermoelectric collector; f, with  
a nitrogen collector.

Table 18

The Evacuation Rate for Vacuum Assemblies with Thermoelectric and Nitrogen Collectors

a) Тип агрегата	b) Тип ловушки	c) Скорость откачки, л/сек.	
		термоэлектрический ловушка	азотная ловушка
VA-01-1	TVL-100-2	50	50
VA-05-1	TVL-35-4	280	190
VA-2-3	TVL-ST-1	550	500
VA-5-4	TVL-ST-1	1300	1200
VA-8-4	TVL-ST-1	3400	2500

Key: a, assembly type; b, collector type; c, evacuation rate, l/sec; d, thermoelectric collector; e, nitrogen collector

The TSLR-1-1 thermoelectric separable pre-vacuum collector was developed in order to prevent the penetration of oil vapors from the pre-vacuum main line into the high-vacuum pump. An overall view of this collector is shown in Figure 68.

GRAPHICS  
NOT REPRODUCIBLE

Figure 68. An overall view of the type TSLR-1-1 thermoelectric collector for pre-vacuum main lines.

### 93. A Thermoelectric Collector for Mercury-Vapor Pumps

As we have pointed out previously, thermoelectric collectors intended for use with oil vapor pumps have been developed. The application of thermoelectric coolers to mercury vapor pumps in order to freeze out mercury vapors is not as effective as with oil vapor pumps. The reason for this is that the mercury molecule accommodation coefficient has a lower value than that for oil. This means that a molecule of mercury vapor, having struck the cooled condensation surface, does not reach thermoequilibrium with this surface, and, having experienced elastic diffusion, may pass through the collector. In this connection, collector designs for the purpose of freezing out residual vapors in mercury vapor pumps must have a relatively high number of condensation surfaces, the spatial distribution of which must exclude a "shoot-through" of the collector even after a 2-or 3-fold reflection. This circumstance, however, leads to a decrease in the carrying capacity of the collector.

In those cases when the carrying capacity value of the collector does not play an important role, as a result of appropriate configuration and number of condensation surfaces, it is possible to develop a thermoelectric collector which effectively freezes out mercury vapors. A second and not less important consideration, which must be taken into consideration in the design of thermoelectric collectors for mercury vapor pumps, is the exclusion of the possibility of amalgamation of the materials of the thermoelectric pile. If the thermoelements themselves are weakly exposed to the influence of mercury, then the solders and the connecting plate materials and other construction elements of the collector will be subject to amalgamation, which, naturally, leads to failure of the collector. Maximum attention was given to the requirements cited above in the design of a collector intended for use with the DRN-10 mercury pump. A section of this type of collector, which has been given the conditional designation TVL-RN-2, is shown in Figure 69.

The single-stage thermoelectric pile of the collector consists of two rows of thermoelements 1, which are soldered to the side surfaces of the steel pipe 3 through the copper collectors of the cold junctions 2 with two diametrically opposed sides. Louvers 4, which form the condensation surfaces of the collector, were connected with PNVh-33S-11 special solder, which does not interact with mercury in the hydrogen furnace, to opposite sides of the central pipe in order to provide a multi-path capability for the collector. The number and spatial distribution of the louvers provides sufficient carrying capacity for the collector due to a 6-fold passage (the mercury vapor molecule must undergo 6 collisions with the cooled surface before it passes through the collector). The hot thermoelement junctions 5 are equipped with water cooling system 6

which has combined nipples for water and electrical power connections to the collector. The thermopile assembly is constructed of separate units, electrically insulated from each other by means of an epoxy resin filler.

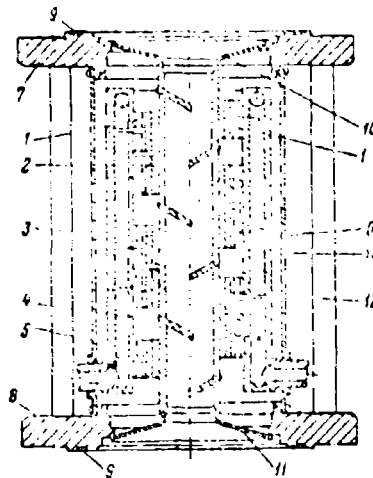


Figure 69. A section of the TVL-RN-2 collector for the DRN-10 mercury pump.

The collector is attached to the corresponding vacuum system by means of flanges 7 and 8. Sealing resin is applied to annular channels 9.

In order to reduce heat losses from the internal collector pipe to the flanges to a minimum, the pipe is attached to the flanges by means of membranes 10 and 11, which are manufactured from thin kovar or invar, i.e., from materials which possess a small heat-transfer coefficient. Steel rods 12 are placed between the flanges in order to provide the entire construction with the mechanical strength required.

External cover 13 serves to protect the thermopile of the collector from mechanical damage. All of the metallic parts of the collector which come into contact with mercury vapors during operation, are

manufactured from a material (steel), which is not subject to amalgamation, and are connected together by means of argon arc welding.

An overall view of the TVL-RN-2 collector is shown in Figure 70.



Figure 70. An overall view of the TVL-RN-2 collector for the DRN-10 mercury pump.

#### §4. Thermoelectric Collectors for Automatic Evacuation Devices

The majority of the products of the electrical-vacuum industry (radio tubes, klystrons, magnetrons, etc.), are, as a rule, evacuated by automatic devices, for which high-vacuum pumps are mounted on revolving automatic turrets. Depending on the construction of the automatic device and the types of articles to be evacuated on them, the number of pumps on a turret may be 12, 24, 36, or 48. Naturally the use on such automatic evacuation devices of collectors, cooled by periodically moving cooling agents (liquid nitrogen, or solidified carbon dioxide), or collectors, cooled by freon compressor assemblies, is completely out of the question.

In addition, it is known that oil diffusion pumps, installed on automatic turret evacuation devices, operate under extremely unfavorable conditions (a relatively high temperature of cooling water, a high ambient temperature, the periodic appearance in the pump of small portions of air from the first evacuation operations, etc.), which lead to a significant escape of oil from the pump. Thus for example, the type VO-589 pump with an output of 7 l/sec, widely employed on 36-position

automatic evacuation devices, results in an "escape" of oil in the upper flange section of  $0.685 \text{ mg/cm}^2 \cdot \text{h}$ . If we consider that the evacuation stem of radio tubes, evacuated on these automatic devices, has a transfer diameter of 3 mm and a corresponding sectional area of approximately  $0.07 \text{ cm}^2$ , then the quantity of oil passing from the pump through the evacuation stem will equal  $0.05 \text{ mg/h}$ . Since the evacuation cycle of a majority of the types of receiving and low power amplifier tubes, modulator and other types of radio tubes equals 25-30 minutes, then  $0.025 \text{ mg}$  of oil is deposited inside the tube, (!).

Since the overwhelming majority of radio tubes have oxide-coated cathodes, quite sensitive to the presence of impurities, the impingement upon them of even insignificant quantities of oil is completely inadmissible. In this connection, the TVL-7-1 thermoelectric collector was developed, intended for use with the VO-589 vapor-jet pump. Tests of the collector revealed that after its installation, the "escape" of oil amounted to  $0.07 \text{ mg/cm}^2 \cdot \text{h}$ , i.e., almost 100 times less than for the pump without the collector. The design of the collector provides for its mounting on a 36-position automatic evacuation device without any type of alterations to the latter.

Figure 71 shows a section of the TVL-7-1 collector. The thermoelectric pile consisting of two pairs of thermoelement 6 are mounted across cemented heat junctions 5 in steel casing 1, which is copper-brazed in a hydrogen furnace. For convenience in mounting the system of collectors for the cold junctions 8, which are the condensation surfaces, the pairs of thermoelements have different heights and thus different sections. Ring 10 forms a "lock" with the condensation surfaces, which prevents the direct passage of oil vapors through the collector. The electrical supply for the thermopile of the collector is provided through two vacuum-sealed current-carrying leads 9, which are insulated from the casing. The necessity for providing 2 current leads is dictated by the fact that all 36 collectors, which are mounted on the automatic machine, are electrically connected in series. Heat removal from the collector thermopile is provided by running water from the water cooling system of the vapor-jet pumps. Water connection to the collector casing is made by means of nipple 7, from which water passes through channel 2, situated under the thermoelectric pile.

Mounting of the collector on the pump is accomplished by means of a resin seal, tightened by means of sleeve nut 3. An evacuation recess is provided through resin seal 4 on the top of the collector.

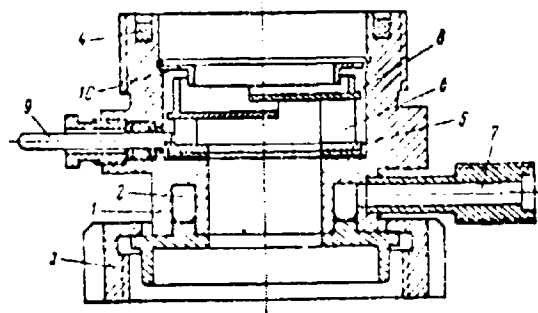


Figure 71. A section of the TVL-7-1 collector for automatic radio tube evacuation devices.

An overall view of the collector for a 36-position automatic radio tube evacuation device is shown in Figure 72.

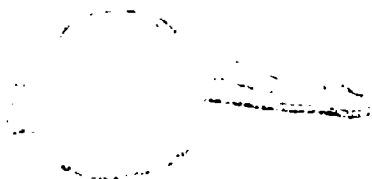


Figure 72. An overall view of the TVL-7-1 collector for automatic radio tube evacuation devices.

With a water temperature in the heat removal system of  $18^{\circ}$  and a vacuum of  $10^{-4}$  mm Hg, the temperature on the condensation surfaces of the collector was  $-37^{\circ}$ . The presence of the collector on the automatic machine reduces the pump evacuation rate by 40%. However, this may be disregarded since the basic evacuation rate resistance is provided by the evacuation socket and the tube stem.

As we have pointed out previously, the electrical supply for all the collectors mounted on the automatic machine is provided in series from



one rectifier. The rectifier chosen is a full-wave design employing the VG-10 diodes. In order to reduce rectified current ripple, the rectifier is equipped with an inductive filter ( a choke coil). The operating parameters of the rectifier are: current, 28 a; voltage 10 v; current ripple, 10%. The rectifier is mounted directly on the rotating turret of the automatic exhaust device.

The basic parameters of thermoelectric collectors are shown in Table 19.

Table 19  
The Basic Specifications of Thermoelectric Vacuum Collectors

Collector type	Pump type	Operating current, a	Vol- tage drop, v	Temperature, °C		Water flow rate, l/h	No. of thermoelements, units		Height Dia. mm	Weight, kg
				First stage	Second stage		First stage	Second stage		
TVL-7-1	VO-589	28	0.2	-37	—	40	2	—	62	1.12
TVL-40-2	MM-40A	50	4.4	-20	-52	60	5	3	80	2.1
TVL-100-2	TSVL-100	60	6.9	-20	-52	60	10	5	25	4.6
TVL-55-4	N-5	80	1.0	-20	-50	55	24	12	55	10.6
TVLR-2T-1	N-2T	115	3.6	-20	-50	120	45	24	165	25.0
TVLR-5T-1	N-5T	120	5.6	-18	-50	150	92	56	170	120
TVLR-5T-1-1	N-5T	120	9.2	-19	-60	150	110	55	220	240
TVLR-20T-1	N-20T	120	21	-20	-51	150	144	72	246	320
TFLR-1-1	—	60	1.2	-15	-62	60	12	6	120	9.3
TVL-FN-2	DRN-10	75	1.0	-24	—	60	10	—	150	5

NOTE. The temperature values on the first and second stages were obtained at a heat removal water system temperature of 18° and at a pressure of 10<sup>-5</sup> mm Hg.

## CHAPTER XI

### THERMOELECTRIC COOLERS FOR RADIANT ENERGY RECEIVERS

#### 51. Microthermostat Systems for Cooling Photoconductive Cells

Recently photoconductive cells have found ever-increasing applications in various automatic and telemechanical systems. However, the basic parameters which characterize the operation of photoconductive cells depend heavily upon temperature. A decrease in the temperature of a photoconductive cell reduces the value of inherent noise, increases the sensitivity shifts into a longer-wave portion of the spectrum.

As an example, Figure 73 shows the dependence of photocurrent ( $I_{ph}$ ), which is one of the most important parameters, on temperature for the type FS-K1 photoconductive cell, which is constructed of cadmium sulfide.

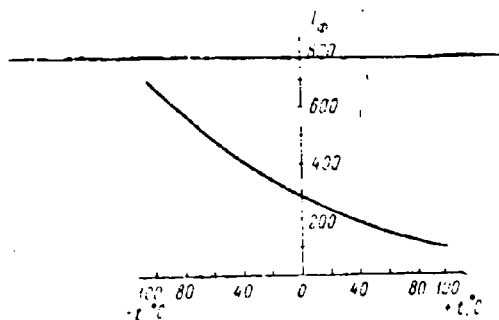


Figure 73. Photocurrent dependence on temperature for the FS-K1 photoconductive cell.

In modern equipment utilizing photoconductive cells, the temperature within the assemblies may reach 70-100°, which makes the operation of the photoconductive cells very unstable. Widely employed methods of cooling, including the use of refrigerators or cooling agents (liquid nitrogen, solid carbon dioxide) may not always be applied, by virtue of a number of operating inconveniences.

The thermoelectric method of cooling has permitted the development of systems which are small in size, and which reduce the temperature of the photoconductive cell by 100°, with respect to the temperature of the surrounding medium. In addition, these systems permit temperature stabilization of the photoconductor cell by means of an external circuit at any given level with an accuracy of  $\pm 0.1^\circ$ .

Four design versions of the systems were developed for cooling photoconductive cells, and these systems differ from each other in maximum temperature difference, a system of heat removal from the thermoelectric pile, or rail dimensions, and by a number of other parameters arising from operating requirements.

Devices of all types were made in the form of independent, structurally complete sub-assemblies, which could be placed directly in the apparatus. Figure 74 shows an axonometric section of the first version of the device.

Photoconductive cell 2 is attached to cold junction 1 of two-stage thermoelectric element 5, which is mounted on aluminum base 8. In order to insulate the hot collectors of thermoelement 7 from the base, the latter is covered with a thin (1-2  $\mu$ ) layer of aluminum oxide, which is electrochemically applied. The electrical supply for the thermoelement, and also the leads from the photoconductive cell and the microthermistor are connected through insulators 10 to octal lamp base 13, by means of which the microthermostat system is connected to the apparatus. Epoxy resin 11 provides for hermetic sealing of the glass insulators in the case. The top of the thermocouple is covered with cap 6, which is equipped with mica window 3. Epoxy resin is also used to attach the mica to the cap and the cap to the case. Temperature maintenance of the photoconductive cell at the required level is accomplished by means of an external circuit, for which microthermistor 4, which is attached to the cold junction of the thermoelectric pile, serves as the sensor.

## GRAPHICS NOT REPRODUCIBLE

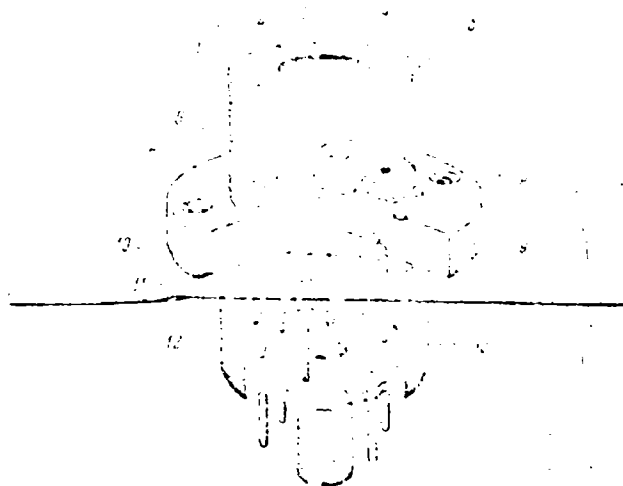


Figure 74. An axonometric section of the first version of a microthermostat system for cooling photoconductive cells.

In order to reduce heat exchange between the surrounding air and the assembly consisting of the cold collector of the thermoelement and the photoconductive cell, which is mounted on the element, the internal volume of the device is placed under a vacuum. Evacuation of the device is accomplished by means of metallic stem 12, which is "sealed off" by cold welding. Attachment of the microthermostat system to the apparatus is accomplished by means of flange 9, which provides good thermocontact and corresponding heat transfer from the thermoelement.

The basic parameters of the microthermostat system are shown below.

Maximum temperature difference (at a surrounding air temperature of 20°)	60°
Optimum current	20a
System voltage drop	0.15 v
Power requirement	3 w
Dimensions: height	60 mm
diameter	47 mm
Weight	150 g

The second design variation of the device is intended for more intensive cooling of the photoconductive cell, extending from  $-60$  to  $-65^{\circ}$ . The semiconductor pile in this design of the device consists of 3 stages, which are connected in parallel, in which the first stage consists of 3 pairs of thermoelements, the second stage consists of 2 thermoelements and the third stage is represented by 1 thermoelement. The number of thermoelements in each stage is determined by the required refrigerating capacity which must provide for the acceptance of heat released by the hot junctions of the upper stages. The hot connecting plates of the thermopile have straight-through channels for the passage of water which serves to remove heat from the thermopile.

The electrical supply is connected through 2 terminals, which are soldered to the cooling water fittings.

All elements of the thermopile are filled with a thermoreactive epoxy compound, after which the system becomes a unit-constructed finished device. The photoconductive cell is cemented to the collector of the cold junctions of the third stage of the thermopile and within 1 or 2 minutes after the connection to the thermopile acquires the temperature of the collector.

In order to reduce heat exchange from the first and second stages to the surrounding medium, the entire thermopile is covered with foam plastic.

The basic parameters of the device of this type are as follows:

Optimum current	94 a
System voltage drop	0.21 v
Power requirement	19.8 w
Heat removal	Running water
Water consumption rate	0.5 l/min
Maximum temperature difference (at a water temperature of $20^{\circ}$ )	$80^{\circ}$
Dimensions: diameter	55 mm
height	40 mm
Weight	250 g

Notwithstanding the significant difference provided by the 3-stage microrefrigerator described, its application is possible in an apparatus which may be supplied with water. In a number of cases involving the employment of photoconductive cells, these conditions cannot be satisfied. In this connection a third design version of the microrefrigerator was

developed which provides for intensive cooling of a photoconductive cell with heat removal from the hot junctions of the thermopile by means of a system of air radiators, which are cooled by forced air from a small fan. The device was intended to cool a film photoconductive cell, which was placed in a glass vacuum bulb. A temperature difference of  $100^{\circ}$  (from an ambient temperature of  $40^{\circ}$ ) was required for cooling.

The 3-stage thermoelectric pile of the device, in contrast to the thermopile employed in the version immediately preceding, where all three stages were connected in parallel with each other, has the first and second stages connected in series, and the third stage in parallel with the second. Such a method of connecting the stages permits the refrigerating capacity of the second stage to be increased when a specified operating current is supplied to the pile.

The devices constructed in the form of a radiator block, on which the thermoelectric pile is mounted. On the outside the radiator block has a cover which is equipped with a fan and a small-size, economical electric motor.

A section of this version of the device is shown in Figure 75.

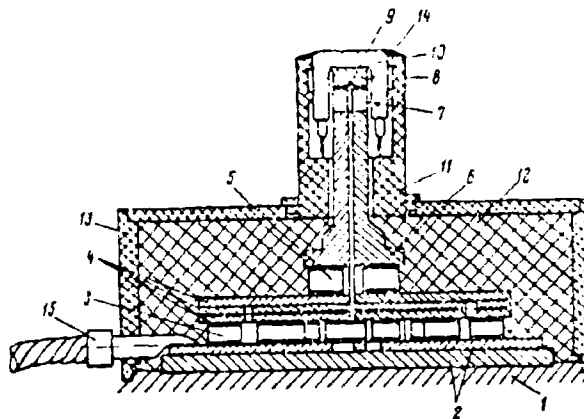


Figure 75. A section of a 3-stage cooler for photoconductive cells with series-parallel current supply to the stages.

The first stage 3 of the thermoelectric pile is mounted over special heat junctions 2 on heat transfer base 1. The thermoelements of second stage 5 are connected in parallel with the first stage through heat junctions 4. The collectors of the cold junctions of the second stage are made in the form of a curled rod 6, which is split along its diameter. Thermoelement of third stage 7, which is connected in parallel with the thermoelements of the second stage, is located on the upper part of the rod. Microthermistor 9, which is the sensor in the temperature stabilization circuit, is attached in silver amalgam in the collector of the cold junction of third stage 8. Photoconductive cell 10, which is mounted in a vacuum bulb, is located directly on the thermoelement of the third stage. Thermoinsulation 11 and 12, formed from foam plastic, serves to reduce heat flux from outside the device. The thermopile is covered on the outside with a protective case of decorative plastic 13. The photoconductive cell is attached to the cooler with epoxy compound 14. The electrical supply to the thermopile is provided by 2 flexible busbars 15. The basic parameters of this type of cooler are shown below.

Operating current	52 a
Voltage drop in the thermopile	1 v
Power requirement	52 w
Heat removal system	forced air
Maximum temperature difference (with a surrounding air temperature of 40°)	102°
Time required to establish minimum temperature	2 min
Type of electric motor used with fan	MU-010
Electric motor voltage	27 v
Power required by the electric motor	3 w
Number of revolutions of the ventilating fan	6,000 rpm
Dimensions: diameter	130 mm
height	65 mm
Weight (without the heat removal system)	250 g
Starting time	4 min

An overall view of the cooler with air heat removal is shown in Figure 76. The thermoinsulation has been removed.

The fourth microrefrigerator design variation for photoconductive cells is intended for operation in an infrared liquid analyzer.



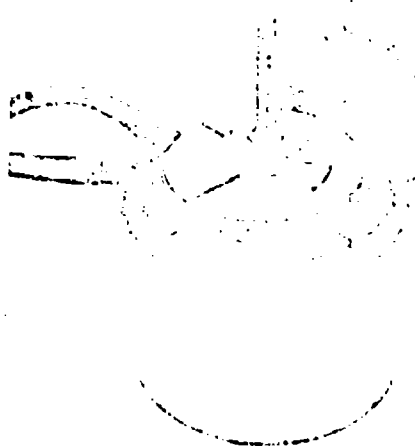


Figure 76. An overall view of a 3-stage cooler with an air heat-removal system (the thermoinsulation has been removed).

A semi-automatic device for the analysis of various liquid chemical products, with respect to their absorption of infrared radiation, is widely employed in modern chemical production. The type 1 F-1 photoconductive cell has been specially developed to serve as an infrared-radiation detector. Under operating conditions the surrounding temperature may reach a value of  $60^{\circ}$ , whereas the sensitivity of the photoconductive cell employed is at a maximum near  $0^{\circ}$ . In this connection the development of a thermoelectric cooler was required, which was small in size, economical in operation, and capable of operating in an atmosphere of corrosive substances.

Two versions of the device were developed, which differed from each other in external shape and intended for installation in different apparatuses.

A section of one of the versions of this device is shown in Figure 77. Aluminum casing 1 is equipped with a system of radiator plates 2, which provide for heat removal from the hot junctions of the thermopile by means of natural convection. Thermoelement 4 is mounted on two crimped heat junctions 3 in the casing. The collector 5 of the cold junction is made in the shape of a ring, in which photoconductive cell 6 is mounted.

The photoconductive cell is attached to thermoelement by sleeve nut 7. Inside, the thermoelement and the photoconductive cell and thermally insulated from external influences by two blocks 8 and 9 of foam plastic. Annular ring 10 is located in the upper foam plastic block. The ring contains a silica gel or alumo gel, which serves to dry the air inside the device and at the same time to exclude the formation of moisture on the photoconductive cell. The drying agent is covered on the top by fine screen 11 and by plastic ring 12. The electrical supply to the thermoelement is delivered through two current-carrying busbars 13, which are hermetically sealed in the casing. Leads 14 to the photoconductive cell and to the microthermistor, which serves as a sensor for the automatic temperature stabilization circuit, are also hermetically sealed in the casing of the device by means of special epoxy compound 15.

The basic parameters for the type of cooler described are shown below.

Operating current	25 a
Voltage drop	0.25 v
Power requirement	6.25 v
Photoconductive cell temperature (with an ambient temperature of 60°)	0°
Time required for temperature stabilization	20 min
Weight of the device	430 g
Dimensions: diameter	90 mm
height	47 mm

An overall view of this device is shown in Figure 78.

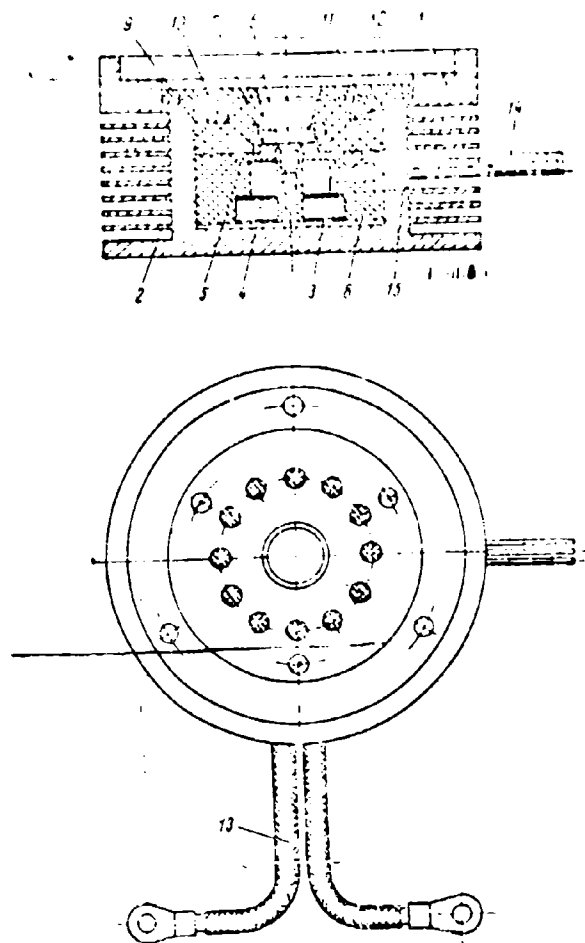


Figure 77. A section of a photoconductive cell cooler for an infrared liquid analyzer.

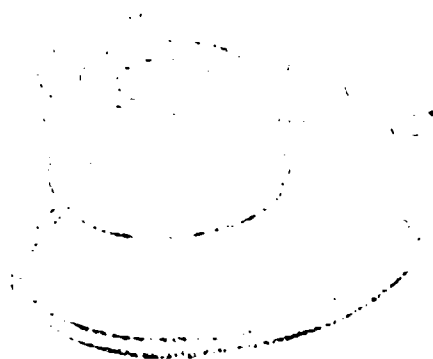


Figure 78. An overall view of a photoconductive cell cooler for an infrared liquid analyzer.

## §2. A microthermostat System for Bolometer Cooling

Bolometers, as ordinary and high-sensitivity receivers of radiant energy have found comparatively wide application. Bolometers of the semiconductor type, manufactured from oxide compounds of cobalt, manganese, and other materials, have received the most widespread usage. Notwithstanding their known merits, semiconductor bolometers have one essential shortcoming, which is a significant dependence of the output signal on temperature. This dependence is illustrated in Figure 79 for the BKM-1 bolometer, which is mass-produced by industry. It is obvious that for normal operation of this type of device, the temperature reduction and stabilization are required. A thermoelectric device was developed for this purpose. A sectional view of the device is shown in Figure 80.

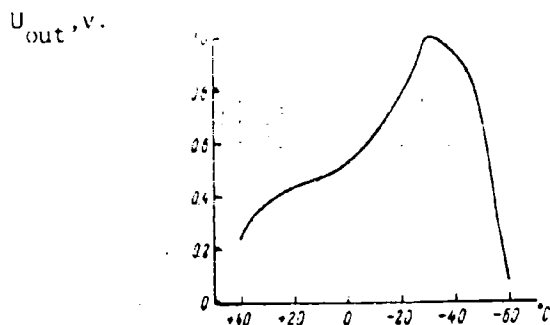


Figure 79. Dependence of the output signal of the BKM-1 bolometer on temperature.

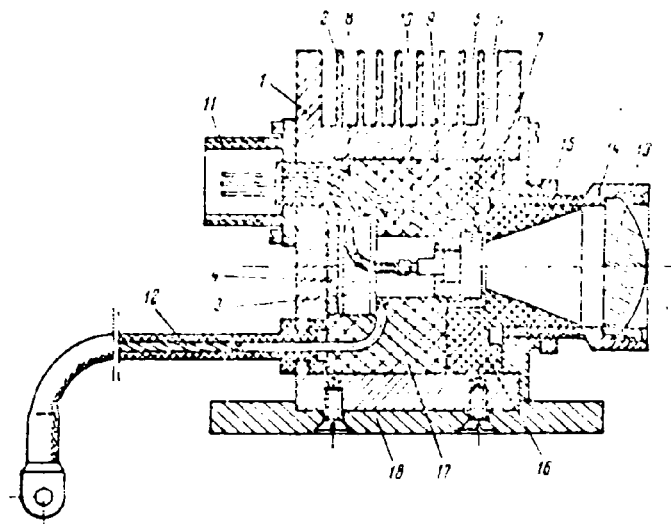


Figure 80. A section of a microrefrigerator for bolometers.

The casing 1 of the device is manufactured from type "A-0" aluminum, which is equipped with a system of radiator fins 2, by means of which convection heat removal from thermoelement 3 is accomplished. Thermoelement 3 is mounted on crimped heat junction 4, which are soldered to the casing base. Bolometer 6 is located in the collector of the cold junctions of thermoelement 5. The bolometer is attached within the collector by means of sleeve nut 7. The leads 8 to the bolometer are in special hermetically-sealed joint 11. Leads 10 of microthermistor 9, which serves as the temperature sensor of the device is connected to the same location. The electrical supply to the thermoelement is made through the 2 busbars 12 which are hermetically sealed in the casing. The flow of radiant energy striking the receiver is focused by lens 13, which is attached to tube 14. Tube positioning is accomplished by lock nut 15. Thermoinsulation of the thermoelement and the bolometer from the surrounding medium is accomplished by foam plastic 16 and 17. Base 18 serves to attach the device to another apparatus.

The following are brief technical specifications for the device.

Operating current	25 a
Voltage drop	0.1 v
Power requirement	2.5 w
Temperature difference provided by the device (with an ambient temperature of 20°)	52°

Dimensions:	diameter	70 mm
	length	75 mm
Weight		335 g

An overall view of a microthermostat system for bolometer cooling is shown in Figure 81.

**GRAPHICS  
NOT REPRODUCIBLE**

Figure 81. An overall view of a microrefrigerator for bolometers.

### 83. A Thermoelectric Cooler for Radiation Balance-Meters

Radiation balance-meters are widely employed in meteorological practice to determine the quantity of solar energy falling on the earth and also to determine the quantity of heat emitted by the surface of the earth to the surrounding air.

Basically a radiation balance-meter has an "absolutely black" receiving surface, which is usually a blackened plate of specified area. A thermocouple is attached to the reception plate, which registers the plate temperature. The temperature difference and the heating rate of the balance-meter receiver from the surface of the earth and from the sun serve as initial data for the determination of radiation balance.

In order to increase measurement accuracy, differential balance-meters are usually employed which have two receiving surfaces, one of which measures the radiation from the earth and the other measures from the sun. Sometimes balance-meters are employed with only 1 receiving surface, which is attached with a special pivoted device, which permits alternate measurements of earth and sun radiation to be made. However, the method of radiation balance measurement described results in significant errors due to the influence of moving air -- the wind -- on the receiving surface. Temperature change on the receiving surface under the influence of the wind is, in practice, very difficult to take into consideration, as a result of which the absolute reliability of measurements is low.

The influence of the wind on balance-meter indications may be significantly reduced if the temperature of the receiving surface is maintained at a level close to the temperature of the surrounding air. Naturally the application of widely-employed cooling methods for the receiving surface of small devices such as radiation-balance meters which are employed under field conditions, is not possible.

The thermoelectric method of cooling has permitted the development of a device for the purpose indicated. Due to the low weight, low power requirement and self-contained nature of the system, a thermoelectric cooler has still another inherent advantage: by means of this type of cooling the temperature on the receiving surface of the balance-meter may be established at the desired level by means of changing the value of the current supply to the cooler. When necessary the mode of operation can be changed from cooling to heating by reversing the direction of the current.

The cooler itself (Figure 82) consists of thermoelectric couple 1, the cold-junction of which is formed by plate 2. Semi-cylinders 3, which are insulated from each other, are soldered to the hot junctions of the thermoelement. The cylinders are equipped with fins 4 in order to increase the heat dispersion surface. The current supply to the thermoelement is connected to terminals 5. Attachment of the cooler to the balance-meter system is accomplished by means of special bar 6. In order to reduce parasitic heat flow to the thermoelement from the surrounding medium, the thermoelement is surrounded by a layer of thermal insulation 7, fabricated of foam plastic. The outside surface of the thermopile is protected by ring 8, which is manufactured of decorative plastic.

An overall view of a thermoelectric cooler for radiation balance-meters is shown in Figure 83.

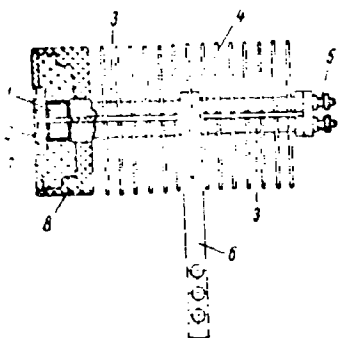


Figure 82. A section of a cooler for radiation balance-meters.



Figure 83. An overall view of a cooler for radiation balance-meters.

The basic technical data for the device are as follows.

Maximum operating current	22 a
Power requirement (at maximum current)	2.3 w
Range of temperature change	$\pm 5^\circ$
Time required for temperature stabilization (at a surrounding air temperature of $24^\circ$ and a wind speed of 5 m/sec)	30-60 sec
Dimensions: diameter	66 mm
height	133 mm
Weight	600 g

In a case when a thermoelectric cooler is utilized in fixed meteorological stations, its current supply may be provided from the alternating current network through a 4-wave rectifier, which provides the current parameters.

If there is no fixed electrical supply network in the area where the device is being used, it may be supplied from appropriate storage batteries directly or through a current convertor.

#### §4. Thermoelectric Coolers for Photomultipliers

Photomultipliers are widely employed in various devices used in electronics, atomic physics, astronomy, geology, archeology and other fields of modern science and technology.

Photomultipliers in conjunction with scintillators are employed in counting elementary particles and their use with various luminophors



permits measuring weak radiation in the wide spectrum range from the infrared to gamma-ray radiation, inclusively. Photomultipliers permit the amplification of small light signals by  $10^5$ - $10^7$  times without additional circuits, which favorably distinguishes them from vacuum photoelements.

Photomultipliers produced by industry in a majority of cases employ an antimony-cesium photocathode as the light-sensitive element. Photomultiplier threshold sensitivity is limited by the value of the dark current, which depends on:

- 1) the thermionic emission of the photocathode and the first dynodes;
- 2) the leakage currents between the anode and the other electrodes;
- 3) the secondary emission from the photocathode and the emitters when they are bombarded by residual gas ions;
- 4) the autoelectronic emission from the photocathode and the dynodes;
- 5) the fluorescence of the glass and the last dynodes.

With good gas removal in the process of manufacturing of the multiplier and with a high vacuum in the finished article, the greater part of the dark current occurs as the result of the first two causes. Therefore the most effective means of decreasing the dark current is the suppression of thermionic emission of the photocathode and the first emitters (dynodes). This is accomplished by cooling the entire device or the photocathode and the first dynodes.

It follows from published data that cooling the photomultiplier with an antimony-cesium cathode to  $0^\circ$  reduces the dark current by three times, and reducing the temperature to  $-10^\circ$  reduces the dark current by five times, and a reduction of  $-30^\circ$  reduces the dark current by 30 times. Further cooling leads to an even more significant reduction in the dark current.

Various methods are employed to cool photomultipliers (liquid air, cryogenic mixtures, forced air cooling, solid carbon dioxide, etc.). However, as the result of technical difficulties and operating inconveniences, these methods have not enjoyed a widespread application. In this connection the utilization of semiconductor thermoelectric piles presents a great deal of interest, since they permit the development of simple and small cooling devices.

Several types of these devices have been developed. Figure 84 shows a section of one of the cooling devices with the SEU-19 M photomultiplier (developed in 1956) mounted inside.

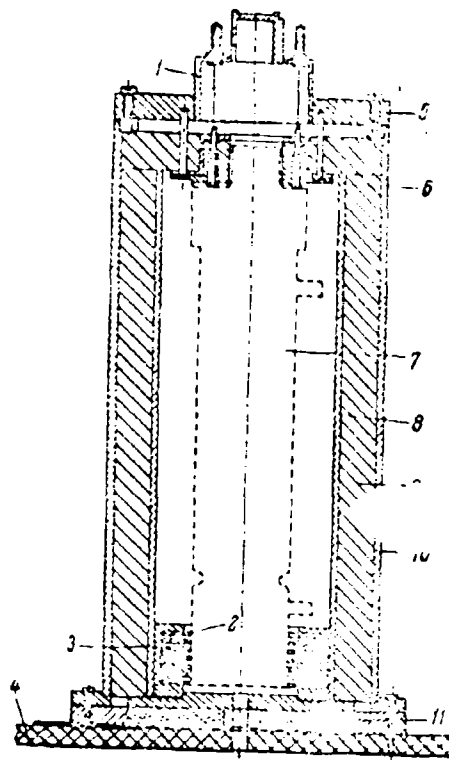


Figure 84. A section of a volumetric cooler for a photomultiplier.

The thermoelectric pile 11 consists of 80 series-connected thermoelements, which after immersion in epoxy resin form a single block. The cold junction of the thermoelectric pile are coupled to part 3, which in turn is coupled through a system of spring contacts 2 with the glass column of the photomultiplier 7 in the area adjacent to the photocathode. A layer of thermoinsulation 9, of foam plastic, is located between the external housing 10 of the device and the internal glass 8. The upper

removable cover 5 of the device has panel 6, in which the photomultiplier is placed. Socket 1 on the cover serves as a connection to the circuit. Heat from the hot junctions of the thermopile is dispersed to frame 4.

The light input to the photocathode is accomplished by means of an aperture in the thermopile. The device described is intended for operation in automatic tracking systems employed in conducting astronomical observations.

Another type of thermorefrigeration device was developed and manufactured for the purpose of cooling photomultipliers employed in scintillation analysis (with the employment of solid or liquid scintillators). Figure 85 shows a thermoelectric refrigerator used for cooling the FEU-11 photomultiplier, which is employed in a device intended for a natural  $C^{14}$  count. In this device heat removal from the hot junction of the thermopile is accomplished by running water. A place has been provided for a bulb containing a liquid scintillator in the refrigeration chamber, the details of which differ little from those shown in Figure 84.

## GRAPHICS NOT REPRODUCIBLE

Figure 85. An overall view of a refrigerator for the FEU-11 photomultiplier, which is employed in a scintillation analysis device.

In the thermoelectric refrigerators described (with a volume of  $800 \text{ cm}^3$ ), the temperature reduction obtained, with respect to room temperature, is  $30-35^\circ$ . A steady-state condition in the chamber is established in 40-50 minutes, after which the photocathode temperature is  $-10$  to  $-12^\circ$ , and the temperature in the chamber is  $5-6^\circ$  higher. It must be kept in mind that condensation of water vapors, which occurs in the cooled space, may significantly impair the operation of the photomultiplier, therefore a drying agent (silica gel, anhydron or alumo gel).

During tests of the thermoelectric refrigerators described above, it became clear that in order to achieve the same results it was not necessary to place the entire photomultiplier in the refrigeration chamber; it was sufficient to reduce the temperature of the end portion of the photomultiplier, to which the photocathode is attached.

Figure 86 shows a section of a thermoelectric refrigerator for cooling the end of the FEU-19 multiplier. The thermoelectric pile of this multiplier has two stages, and the overall temperature difference obtained is  $55^\circ$ . Heat removal from the hot junctions of the thermopile is accomplished by means of running water with a water consumption rate of approximately 50 l/h. The employment of water for the cooling system permitted a sharp reduction to be made in the dimensions and weight of the refrigerator. Heat removal from the photomultiplier is accomplished by means of an effective heat coupling of the thermopile cold junction collector with the end surface of the photomultiplier. As a result of this coupling the operating diameter of the photocathode is reduced somewhat (from 40 to 25 mm), however, in the overwhelming majority of cases such a reduction plays no significant role.

The thermoelectric pile for a refrigerator of this type has both the first and the second stages distributed in a circle, the center of which forms an aperture for the penetration of light to the multiplier photocathode.

The system of hot connecting plates of the refrigerator consists of 9 aluminum segments 6. Annular channel 1 is located inside the segments and forms a path for the water which removes heat from the hot junctions of the thermopile. Red-copper washers 2 are soldered to the aluminum at the locations where the hot connecting plates are soldered to the semiconductors of the first stage. Water is supplied to and flows through two nipples 3, which are attached to the casing with epoxy cement. The entire system of hot-connecting plates is filled with epoxy resin 4, and in a preliminary step, electrically-insulating washers 5 are placed between the segments. This assembly system for the base of the thermoelectric pile permits obtaining a single, mechanically strong sub-assembly with

the connecting plates electrically insulated from each other. The thermoelectric pile of the first stage consists of 8 thermoelements. The second stage consists of two thermoelements. An overall view of a refrigerator of this type with the SEU-19 M photomultiplier installed is shown in Figure 87.

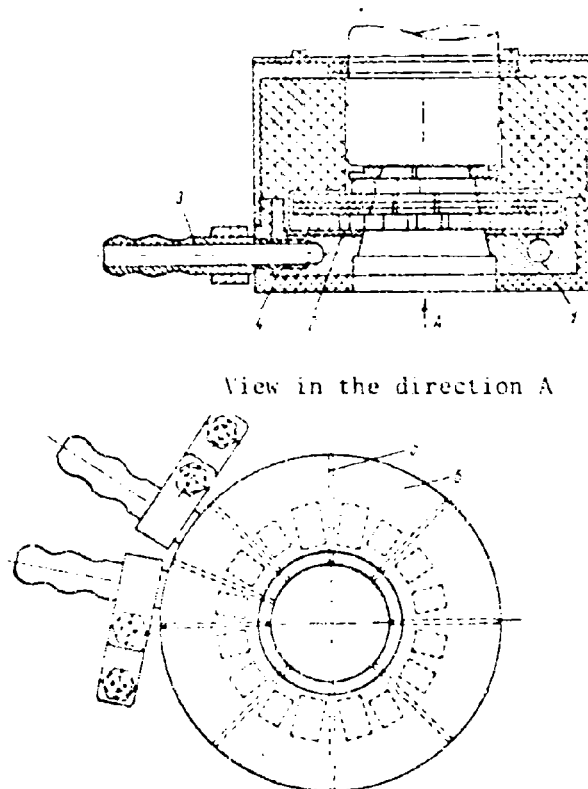


Figure 86. A section of a refrigerator with liquid heat removal for cooling the front portion of a photomultiplier.

## GRAPHICS NOT REPRODUCIBLE

Figure 87. An overall view of a refrigerator with liquid heat removal installed on a photomultiplier.

In connection with the success achieved in the technology of the manufacture of thermoelectric cooling devices, in 1959 a new design variation of the device for the cooling of the photomultipliers was developed. The designer of the device provided for the cooling of the glass bulb, to which the photocathode is applied, just as in the previous version with liquid heat removal. The distinguishing characteristic of this design is the possibility of providing for liquid of force air heat removal from the hot junctions of the thermopile. The two-stage thermoelectric pile employs series feeding of the first and second stages. A high second-stage refrigerating capacity is obtained by this method, with a correspondingly high temperature difference, obtained for the device as a whole, of 60-65°.

The thermopile is connected through electrically-insulated junctions which possess low thermal resistance, and is soldered to an aluminum block which is equipped with a system of radiator plates for air heat removal and with a channel for the passage of water during liquid heat elimination. In order to provide for a maximum reduction in the sides of the device and to reduce its weight, the surface of the radiator plates is cooled with a small fan, mounted in a fitting attached to the cover of the device. Due to the application of forced air cooling, the surface of the radiator plates was successfully reduced by 7 times, with respect to the area required with natural convection heat removal.

The thermocoupling between the end portion of the photomultiplier and the cold junction collector of the thermopile second stage is

provided by means of a resin washer 0.2 mm in thickness, which is cemented to the collector. This coupling method excludes poor thermal contact of the end of the photomultiplier envelope with the cold thermopile junctions. The device is equipped with thermal insulation, fabricated from foam plastic, in order to reduce the heat load on the thermopile from the surrounding medium. Electrical system connections to the thermopile are accomplished through current leads, and the water connection in the case of liquid heat removal is provided through nipples.

An overall view of the thermoelectric refrigerator with a combined air-liquid heat elimination system is shown in Figure 88, with the SEU-19 photomultiplier installed. Tests of the refrigerator have revealed that with a surrounding air temperature of 20°, the temperature in the center of the photocathode was reduced to -37° after 10 minutes of operation with the air heat removal system.

GRAPHICS  
NOT REPRODUCIBLE

Figure 88. An overall view of the photomultiplier refrigerator with a combined air-liquid heat elimination system.

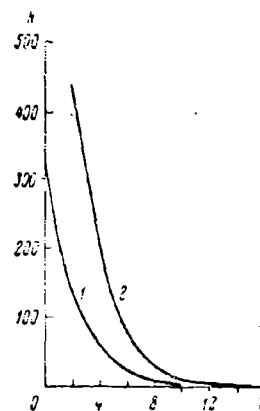


Figure 89. The noise characteristics of the SEU-19 photomultiplier with and without a refrigerator.

N, Scaler reading, 6/4;  
V, Discriminator signal level, v.

The noise characteristics of the SEU-19 photomultiplier with the refrigerator (curve 1) and without the refrigerator (curve 2) are shown in Figure 89.

The basic technical parameters of thermoelectric refrigerators for photomultiplier cooling are shown in Table 20.

Table 20.  
Basic Data for Thermoelectric Devices for Photomultiplier Cooling

a) Type of device	b) Minimum photocathode temperature, °C	c) Operating current, A	d) Operating voltage, V	e) Power requirement, W	f) Dimensions, mm			g) Water consumption, l/h	h) Height, mm	i) Diameter, mm	j) Weight, g	k) Fan motor
With natural convection heat elimination (with cooling of the entire photomultiplier)	-15	10-13	30	—	280	110	5000					
With liquid heat elimination (with cooling of the entire photomultiplier)	-20	10-13	30	50	300	110	3500					
With liquid heat elimination (with photocathode cooling)	-40	8-10	0.8	30-5	50	60	50	250				
With air-liquid heat elimination (with photocathode cooling)	-50 to -40	6-10	1.5-2	27-40	100	95	114	2000				

Key: a, Type of device; b, minimum photocathode temperature, °C; c, operating current, A; d, operating voltage, V; e, power requirement, W; f, water consumption, l/h; g, dimensions, mm; h, height; i, diameter; j, weight, g; k, for the fan motor.

Experiments conducted with the cooled FEU-19 M photomultiplier have revealed that in individual cases cooling of the photocathode did not lead to the expected reduction in the value of the dark current. This is explained by the fact that the dark current of the photomultiplier is caused not only by photocathode thermionic emission, but also by discharge phenomena in the residual gas and, which is most important, by  $K^{40}$  radio activity, contained in the glass from which the multiplier envelope is constructed, and from the mica on which the dynodes are mounted.



Thus the successful application of cooling, in particular, with thermoelectric refrigerators, for the reduction of the dark current is closely associated with photomultiplier production technology. In the case where the dark current is caused only by photocathode thermionic emission, the employment of thermoelectric refrigerators is quite effective.

## CHAPTER XII. Thermoelectric Cooling Devices for Medicine

### §1. A Thermoelectric Cataract Cryoextractor

Cataracts -- clouding of the crystalline lens of the eye -- are one of the most frequent reasons of complete loss of sight among elderly persons. Various types of cataracts are encountered among patients and other adult groups, including congenital cataracts in children.

The first mention of this disease was in Assyrian treatises dated in the third century B.C. Since that time scientists of our World have searched for the most logical method of removing the dull cataract disc situated over the pupil and interfering with the penetration of light into the eye. The ancient oculists studied various mechanical methods of pushing the clouded crystalline lens from the pupil. This method received the name of "scale removal". However in a short time the crystalline lens resumed its initial state and the patient was again deprived of sight.

In 1752 the French physician Daviel succeeded for the first time in extracting a cloudy crystalline lens from the eye with thin pincers through a corneal incision. In the course of the next 200 years the operation of extracting cataracts underwent a number of refinements, both in the development of modern instruments, as well as in the development of operational techniques. At the present time the only method of curing cataracts is the surgical removal of the clouded crystalline lens with subsequent compensation of its optical properties by spectacles.

Notwithstanding such widespread application, the cataract extraction operation still has many weak areas, the elimination of which has been the subject of a great deal of work by both Soviet and foreign authors.

In contemporary ophthalmologic practice there are four methods of crystalline lens extraction:

- 1) mechanical seizure of the crystalline lens by means of special pincers or suction devices with subsequent withdrawal of the lens through an operational incision in the cornea,
- 2) extrusion of the crystalline lens through an operational incision;
- 3) a combination of the methods of extraction and extrusion;
- 4) the employment of special chemical substances which destroy the ciliary fibers supporting the crystalline lens in the eye.

Mechanical methods of seizure and removal of the crystalline lens do not guarantee successful execution of the operation, since the point of application of the instrument is the crystalline lens capsule, which has insignificant thickness and strength. Until recent times the removal of the cloudy crystalline lens in the capsule has presented significant technical difficulties and has been achieved only by ophthalmologists of high qualifications. In this connection the intercapsular extraction operation is often replaced by the extracapsular extraction operation, i.e., removal of the crystalline lens in parts. However in this connection part of the crystalline lens capsule remains (the posterior membrane), and sometimes the cataract mass as well, which serves as a substratum for the formation of a film -- the secondary cataract.

The crystalline lens extrusion method is associated with the danger of prolapse of the vitreous body, which leads to complete loss of the eye.

Chemical action on the ciliary fibers which support the crystalline lens in the eye only partially facilitates removal of the crystalline lens, however chemical substances employed for this purpose also act on the surrounding tissues of the eye and this leads to numerous complications.

Statistical data available in eye clinics of the Soviet Union reveal that with the utilization of the methods of cataract extraction described above, only 30-40% of the patients successfully endure this operation, and 60-70% of the patients suffer post-operative complications which require additional hospitalization and treatment.

In 1961 the Polish ophthalmologist Krvavich proposed a new method of cataract extraction -- cryoextraction. Basically this method consists of the following.

A massive metallic "pencil" with a bead on the end -- the cryoextractor -- is submerged in a mixture of solid carbon dioxide and methyl alcohol. The long narrow tip of the instrument, which is cooled to a temperature of  $-78^{\circ}$ , is introduced into the incision until it contacts the crystalline lens. The crystalline lens freezes to the cryoextractor and is then withdrawn from the eye. However, Krvavich's instrument had a number of serious shortcomings, which limited its widespread application, among these shortcomings, the following must be considered.

1. Uneven temperatures on the edges of the cryoextractor. At the moment of withdrawal from the cooling mixture, the temperature of the instrument is too low, and then rises rapidly as the result of heat flow from the surrounding air and from the eye tissues. As a result, the moment of achievement of optimum temperature is often missed.

2. In case the cryoextractor contacts the cornea, the iris or other eye tissues, these parts freeze, which leads to serious post-operative complications.

3. The relative scarcity and expense of solid carbon dioxide and difficulties associated with transportation limit the use of Krvavich's method to the eye clinics of large cities.

In 1963 a device was developed intended for the intercapsular extraction of cataracts, based on the cryoextraction method, but without the shortcomings of Krvavich's device.

The phenomenon of thermoelectric cooling was employed in the device proposed. This permitted obtaining the required temperature on the operating part of the device, which could be maintained at the required level for an unlimited period of time. Whenever necessary a switch on the control panel of the device permits raising of the temperature of the cooled end to  $20^{\circ}$ .

The thermoelectric cataract cryoextractor is a refrigerator made in the form of a miniature handle, with a cooling semiconductor thermoelement in the end. Screwed to the thermoelement in the operating tip in the form of a cone with an off-set extended point. The electrical supply to the thermoelement is provided from a special small rectifier which is equipped with automatic and interlock elements which prevent improper operation of the device.

Heat removal from the thermoelement is accomplished by means of running water from the water supply which passes to the cryoextractor through two rubber hoses, in which the current-carrying bushings are

also located. Efficient construction of the cryoextractor, the control panel and the current supply system make the apparatus compact, convenient and free from failures in operation. The method of employment of the thermoelectric cataract cryoextractor consists of contacting the crystalline lens, which has been exposed during the course of the operation, with the tip, which is cooled to a temperature of  $-30$  to  $-35^{\circ}$ . In 2 or 3 seconds the crystalline is firmly frozen to the tip and is easily withdrawn from the eye. The freezing zone encompasses not only the crystalline lens capsule, but partially penetrates the lens, which prevents rupture of the capsule and complications associated with this.

Experimental versions of the thermoelectric cataract cryoextractors were made in the Semiconductor Institute of the Academy of Sciences of the USSR and were forwarded for clinical tests to a number of leading eye clinics of the Soviet Union. According to official records of the clinics and to operating surgeons, the application of the thermoelectric cataract cryoextractor significantly simplifies the technique of inter-capsular cataract extraction. Due to the utilization of this device the extraction of cataracts is no longer the lot of only a few chosen ophthalmologists but can be accomplished by surgeons of average qualifications.<sup>1</sup>

Operations performed on a large number of patients revealed practically no post-operative complications, and the sight of all the patients was returned.

The cryoextractor itself (Figure 90) consists of duralumin casing 8, which has two red-copper polycylinders 6 and 7 in the front part, which are insulated from each other and from the casing. The cylinders form the base on which the thermoelectric element is mounted. Electrical insulation of the polycylinders from the casing of the device is accomplished by means of epoxy resin. In order to remove the heat released at the thermoelement, the base parts have internal channels connected to two red-copper pipes 9, through which the cooling water flows. The thermoelement which consists of two semiconductors 4 and 5, which have n-type and p-type conductivity, are soldered to the heat transfer base. Operating tip 1, which is constructed of chrome-plated copper and which has the shape of an elongated cone with an off-set point, is screwed to the collector of the cold junction of thermoelement 2.

---

<sup>1</sup>At the Leipzig International Fair in 1966 the thermoelectric cataract cryoextractor was awarded a large gold medal.

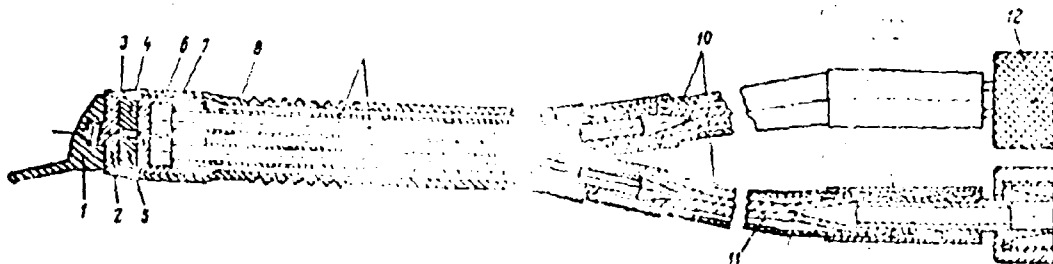
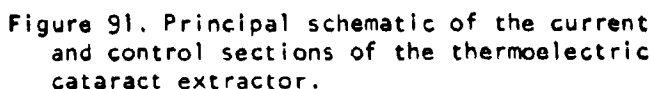


Figure 90. A section of a thermoelectric cataract cryoextractor.

The device uses a combined current-supply system, which provides for easy manipulation of the handle of the cryoextractor during the operation. This system consists of two rubber hoses 10,  $7 \times 5$  mm in diameter, and 1300 mm long. Inside the hoses are current busbars 11, which are 2.5 mm in diameter, which connects the electrical supply to the thermoelement. The busbars are constructed of flexible 100-copper cable in teflon insulation. Thus the current conductors are constantly immersed in water, as a result of which, notwithstanding the high current passing through the cables, their section has been made relatively small. Water connection to the device is accomplished by means of combined coupling 12.

In order to seal the device hermetically, which is required for sterilization during preparation for an operation, the thermoelement is covered by protective cap 3 of lactic plexiglass and is sealed hermetically with epoxy resin. Operational control of the cryoextractor is concentrated in one control section, in which the thermoelement current supply rectifier and also the automatic and interlock elements are mounted. The principal electrical diagram of the control section is shown in Figure 91.

The rectifier which supplies the thermoelement is of the full-wave type and consists of power transformer  $T_r$ , two germanium diodes  $D_1$  and  $D_2$  (type VG-50-15) and filter choke Ch. The rectified voltage output at the choke has a ripple of 5-7%, which does not effect thermoelement operation. The primary winding of the power transformer is designed for connection of the device to a 220/127 v network through voltage selector switch  $S_1$ .



Hydraulic relay  $K_2$ , placed to interrupt the input circuit, excludes the possibility of turning on the device without the preliminary delivery of water. The signal lamps  $L_1$ ,  $L_2$  and  $L_3$ , which are installed on the front panel of the control section, indicate that the device is switched on and whether the device is being operated in the "cooling" or "heating" mode. The signal lamps are switched into the circuit by relay  $K_3$ , which protects the lamps from overvoltage caused by the heavy current at the moment of switching polarity of the current. Resistor  $R_1$  serves to exclude the application of voltage to the cryoextractor in an emergency condition, if a breakdown occurs between the primary and secondary windings of the power transformer.

The temperature of the operating tip in the thermoelectric cataract cryoextractor depends on the temperature of the water in the heat removal system. But even with a water temperature of 20° (during the summer for Southern regions of the country), the temperature at the tip is equal to -21°, which is quite sufficient for normal operation of the device.

The basic specifications of the cataract cryoextractor are shown below.

Operating current	90 a
Operating voltage	1.7 v
Power requirement	153 w
Input power requirement	260 w
Temperature at the operating tip of the device (with a water temperature in the heat removal system of 15°)	-25 to -30°
Time to establish cooling mode	2 min
Time required to heat tip to 20°	20-25 sec
Water flow rate in the heat removal system	40 l/h
Weight of the handle of the cryoextractor	65 g
Handle dimensions: diameter	16 mm
height	105 mm
Weight of the control section	18 kg
Control section dimensions	280 × 220 × 185 mm
Continuous operating time	unlimited
Operating life	5 years
Storage life	5 years

An overall view of the thermoelectric cataract cryoextractor with the control section is shown in Figure 92.

## §2. A Device for Thermal Stimulation of the Skin -- a Thermod<sup>1</sup>

In practical physiological investigations cooling or heating of a limited area of the skin is often required. Various skin thermal devices are usually employed for this purpose.

The application of thermal stimulation with the aid of "thermal packs" and other devices employed for this purpose, i.e., thermods, filled with water or ice do not provide the exact measure of thermal stimulation and require further modernization. In addition, temperature reduction in these devices by means of various cooling agents (water, ice, solid carbon dioxide, etc.) do not satisfy practical requirements due to the impossibility of providing for a rapid temperature change, which in a number of cases is definitely indicated.

<sup>1</sup>"No exact equivalent of this term can be found. It is possibly a generic term for devices used in the therapeutic application of heat or cold.--Tr."



## GRAPHICS NOT REPRODUCIBLE

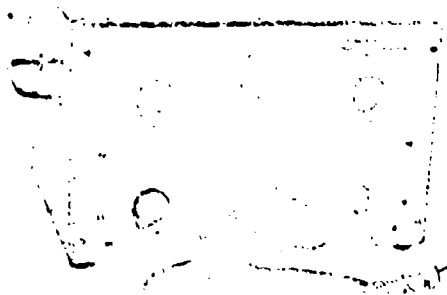


Figure 92. An overall view of the thermoelectric cataract cryoextractor with the power supply and control section.

The thermod design represents a thermoelectric device, which does not possess the shortcomings indicated. With insignificant size and weight (450 g), it permits an exact measure of thermal stimulation and when required can be switched from a cooling to a heating mode in a short period of time. The temperature of the operating part of the thermod may be changed from  $-35$  to  $+50^{\circ}$ . For convenience the device is made in the form of a handle (Figure 93). Cooling or heating of the operating portion 1 of the device is accomplished by thermoelectric couple 2 and 3, which consist of one high-current thermoelement. Heat removal from the thermopile is accomplished by means of running water, which enters the device through two rubber hoses 4. Current conductors 5, which deliver current to the thermoelement, pass inside the water hoses and are immersed in water during operation. Such an electrical and water system supply to the device permits a significant reduction to be made in the section of the current-carrying conductors, which in turn permitted the development of the flexible, conveniently manipulated device. The water connection and also the electrical supply are accomplished through nipples 6 and terminals 7.

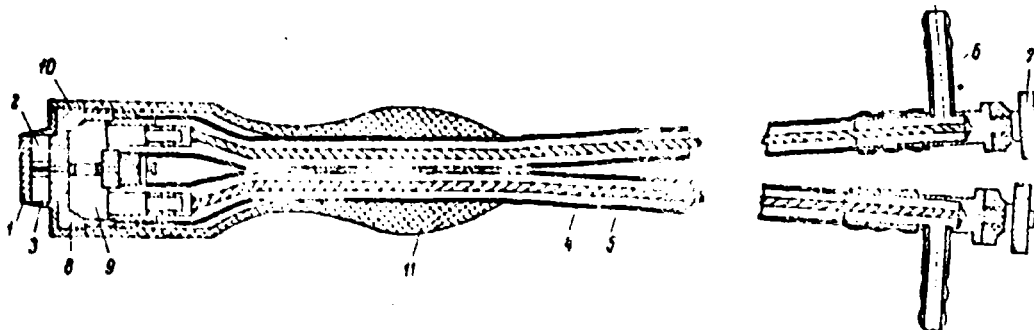


Figure 93. A section of a thermoelectric device for thermal skin stimulation  
-- a thermod.

A high-sensitivity semiconductor thermocouple provides continuous measurement of the temperature of the operating surface of the device. The thermocouple arms consist of tellurium and an n-type ternary alloy, employed for the negative arms of the thermoelements. The ends of the thermocouple used for measurement are extended from the device with the electrical and water supply system hoses. The hot connecting plates 8 of the thermoelement with channel 9 for the passage of water are manufactured of copper and immersed in epoxy resin tin. The housing 11 is manufactured of ebonite.

The electrical control circuit of the device (Figure 94) is sufficiently simple and reliable to permit the device to be used by average medical personnel which have no specialized training.

Maintenance of the required temperature of the device both in the cooling as well as in the heating mode is accomplished by changing the value of resistance  $RT$ , which is switched into the arm of a bridge circuit. Subsequent temperature stabilization is accomplished automatically by the measuring thermocouple  $MT$ , which is switched into the same bridge circuit. A change in the value of resistance  $RT$  leads to bridge unbalance. A constant voltage originating in the bridge diagonal is applied to vibrator converter  $VC$ , where the unbalance signal is converted to an alternating current, which after amplification is applied to relay  $K_2$  the contacts of the relay close and turn on the rectifier, which supplies current to thermoelement  $TE$ . The temperature on the operating surface of the device begins to change (cools or heats), which leads to the appearance of a voltage on the measurement on the thermocouple, which in turn decreases bridge unbalance.

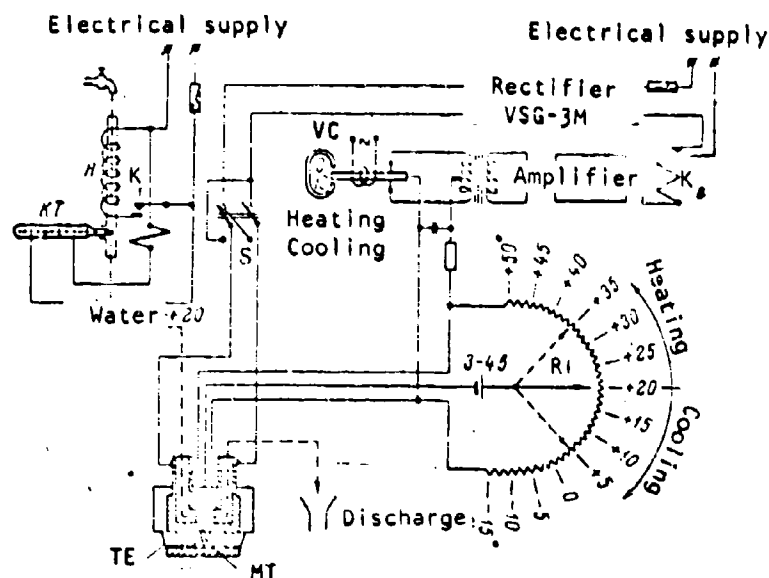


Figure 94. The electrical circuit of the supply and central sections of the thermod.

At the moment when the temperature on the operating portion of the thermod reaches the value set on scale RT, the bridge is balanced and signal delivery to the amplifier ceases. When there is no signal at the amplifier input, relay  $K_2$  switches the rectifier off. Thus the circuit

shown permits automatic temperature maintenance of the operating part of the thermod at any previously set level with an accuracy of  $\pm 0.1^\circ$ .

The temperature stability of the water employed for heat removal has a significant influence on the accuracy of temperature maintenance. Temperature stabilization of the water entering the device is accomplished by means of the contacts of thermometer KT, which through relay  $K_1$  connect or disconnect the electrical supply to electrical heater H.

Test of the device revealed its high operating qualities. It provides a constant measure of thermostimulation in the possibility of rapid change (in 1 or 2 minutes) from the cooling to the heating mode, which permits the device to be employed in experiments with frequent alternations in thermostimulation. An overall view of the thermoelectric device for thermostimulation is shown in Figure 95.

## GRAPHICS NOT REPRODUCIBLE



Figure 95. An overall view of the device for  
thermostimulation -- the thermomod.

### §3. A Microrefrigerator for the Treatment of Skin Diseases

Some skin diseases may be successfully treated by means of local cooling. If the temperature of the affected portion of the skin is reduced by 8-10° below body temperature, a number of substances required by the cooled skin segment is reduced, as the result of which recovery occurs in a short period of time.

Depending on the type of disease and the general condition of the patient, the cold application time on the affected skin segment may extend from several weeks to several months. Naturally a cooling device for the purpose indicated must have insignificant weight and dimensions, must be fully automatic, must not hamper the patient, and must permit operation during non-stationary treatment conditions.

The design of a microrefrigerator intended for the purpose indicated is shown in Figure 96. The single-stage thermoelectric pile of the device contains 12 thermoelements 1. The hot junctions of the thermoelements, through electrically insulating connecting plates 2, are soldered to the heat removal system 3, which is constructed of aluminum in order to reduce the weight. The system of radiator plates 4 serves to remove heat from the thermopile by means of natural convection to the surrounding air. The collector 6 of the cold junctions, which is the operating surface of the device, is soldered to the cold junctions of the thermopile through electrically insulating plates 5. Ring 7 of decorative plastic protects the thermopile from external mechanical disturbances and gives the device a finished appearance. The power supply is connected to the microrefrigerator by means of two terminals 8.

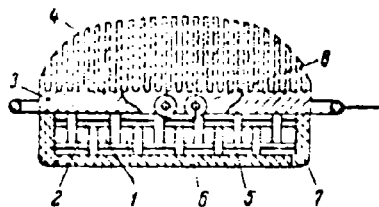


Figure 96. A section of a microrefrigerator for the treatment of skin diseases.

Special straps serve to attach the device over the affected skin area of the arm or leg. In cases when a temperature reduction on another part of the body is required, the design of the device is somewhat different. This difference mainly pertains to the system of heat transfer to the thermopile and the method of attaching the device to the body. One possible design variation in the heat transfer system may be a system of two flexible copper or aluminum strips, which are attached by means of a bandage to a nearby healthy area of the skin. In this case heat transfer from the thermopile will be accomplished directly to the body, which has a relatively constant temperature.

The electrical parameters of the power supply for the thermoelectric pile microrefrigerator are chosen so that the required refrigerating capacity is obtained with a minimum of current requirement. In addition, the method of supplying electrical energy to the device must agree with existing independent power supplies. Silver-zinc storage batteries, which have small dimensions and are low in weight, possess high capacity and may be used as power supplies. Since the treatment process of the skin diseases with local cooling may continue for an extended period of time, it is necessary to have two storage batteries, each of which may be recharged alternately.

Naturally, the device described may be supplied also from fixed power supplies, i.e., rectifiers, and only temporarily switched to a storage battery supply.

Figure 97 shows an overall view of the device (the design version for arm treatments).

## GRAPHICS NOT REPRODUCIBLE



Figure 97. An overall view of a refrigerating device for the treatment of skin diseases.

The following are the basic technical characteristics of the device.

Operating current	3 a
Operating voltage	0.4 v
Power requirement	1.2 w
Size of the operating surface: diameter	50 mm
Dimensions: diameter	80 mm
height	47 mm
Weight of the device	360 g
Weight of the device with the storage battery	1180 g

#### §4. Microtomic Stages with Thermoelectric Cooling

The method of microtomy is widely employed in histologic, patho-anatomical and cytologic practice in order to obtain extremely thin sections of biological tissue. In order to obtain a high-quality section, the tissue must be cooled in advance; the degree of cooling is determined by the type of the tissue under investigation.

In widely employed freezing microtomes, cooling of the tissue block is accomplished by means of throttling liquid carbon dioxide. In this connection the microtome stage must be connected with a carbon dioxide tank. This method of cooling the tissue before microtomy has a number of essential shortcomings; the basic ones are described below:

- 1) the impossibility of controlling the amount of cooling, which in a number of cases leads to overcooling and tissue destruction;
- 2) the relative scarcity and high cost of liquid carbon dioxide, which limits the application of tissue microtomy in rayon and country clinics, in the practice of forensic medicine and under field conditions;
- 3) the high rate of consumption of carbon dioxide (one tank is sufficient for 4-6 hours of operation);
- 4) difficulties involved in the transportation of carbon dioxide tanks (one tank weighs approximately 100 kg).

The development of thermoelectric cooling technology has permitted the creation of several designs for freezing microtome stages, free from the shortcomings listed above.

The first design version of a thermoelectric microtome stage is shown in Figure 98. Thermoelectric pile 1 consists of four thermoelements, mounted on the hot-connecting copper plate 2. The configuration and geometry of these plates are chosen in agreement with the connection system and the requirement for maximum heat transfer from them to the radiator. The upper connecting plates 3 of the thermopile form the operating surface of the stage, on which the block of tissue which is subject to cooling is placed. The system of hot and cold connecting plates, with the semiconductors, is filled with epoxy resin. The thermoelectric pile is cemented to the base 4 of the stage, which is manufactured of aluminum and equipped with a system of air radiators 5.

GRAPHICS  
NOT REPRODUCIBLE

Figure 98. A microtome stage with natural convection heat removal.

The base of the stage is coated by electrochemical means with a thin aluminum oxide layer, which provides good thermocontact between the thermopile and the stage and is also an electrical insulator which excludes contact between the hot connecting plates of the thermopile.

The measurement of parasitic temperature differences on the electrically insulated aluminum oxide layer revealed that at heat flows appropriate to operating conditions of the thermopile, they did not exceed 2-3°. The electrical supply to the thermopile stage is accomplished by means of two current conductors 6, which are connected to the connecting plates of the thermopile and to the terminal block 7. The total area of the radiator plates of the stage is 500 cm<sup>2</sup>.

With natural convection heat exchange with the surrounding air, a radiator of this area may provide a temperature on the hot junctions of the thermopile of 25° (with a surrounding air temperature of 20°). With a temperature difference developed by the thermopile of 30°, the operating surface of the stage may be provided with a temperature of -5°. However at higher surrounding air temperatures, the stage is not provided with the required operating temperature.

In this connection another microtome stage design was developed with thermoelectric cooling, equipped with a combined air-liquid system of heat removal. This design differs from the design described above in that a  $\Pi$ -shaped channel for the passage of water was made in the aluminum plate of the stage base. Water input and output is accomplished through two nipples. In this case, when the surrounding air temperature does not exceed 20°, heat removal from the stage is accomplished by means of air radiators. When the temperature of the surrounding air exceeds 20°, which occurs in Southern areas of the country, a water supply must be connected to the stage.

In the microtome stage designs described, the operating surface, which is formed by the cold connecting plates of the thermopile, equalled 240 mm<sup>2</sup>, which completely satisfies the requirements of histologic and cytologic practice. However, sections of a large area are often required in patho-anatomical investigations. For these purposes a microtome stage was designed with a cooled operating surface of 1600 mm<sup>2</sup> (40 × 40 mm).

In this design (Figure 99), the thermoelectric pile consists of five thermoelements 1; heat removal from these is accomplished by means of running water. Water input and output is accomplished through nipples 2. The hot connecting plates 3 of the thermopile are constructed of brass and have internal channels for the passage of water. Cold-connecting plates 4 form the operating surface of the stage. Pin 5, which passes through base 6, serves to attach the stage to the microtome. The



thermopile is mounted on the base. All elements of the stage are filled with epoxy resin 7. The electrical supply to the stage is accomplished by means of two terminals 8, which are attached to the cooling water nipples.

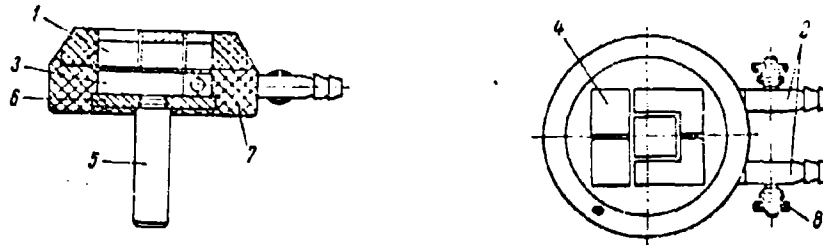


Figure 99. A section of a large-area microtome stage with liquid heat removal.

All of these microtome stage design variations with thermoelectric cooling have mounting areas compatible with microtomes produced by industry. As a result, a stage can be installed on a microtome in 1-2 minutes.

Regulation of the degree of cooling of a block of tissue placed on the microtome stage is accomplished within wide limits by changing the value of the current fed to the stage. During stage tests, sections of brain tissue 4-6  $\mu$  in thickness were obtained in 1-3 minutes.

Figure 100 represents a thermoelectric microtome stage with liquid heat removal, installed on a microtome.

The basic technical characteristics for the stages described are shown in Table 21.

#### §5. A Cooler for Plastic Surgery

In the conduct of plastic surgical operations, especially in the area of the face, cases involving the atrophy of a block of transplanted tissue often occur. The reason for this is an insufficient quantity of blood to supply the transplanted tissue from the patients organism. As a rule, in the conduct of plastic surgical operations in the area of the face, intermediate adaptation of the transplanted block of tissue is accomplished in the shoulder area of the arm.

## GRAPHICS NOT REPRODUCIBLE

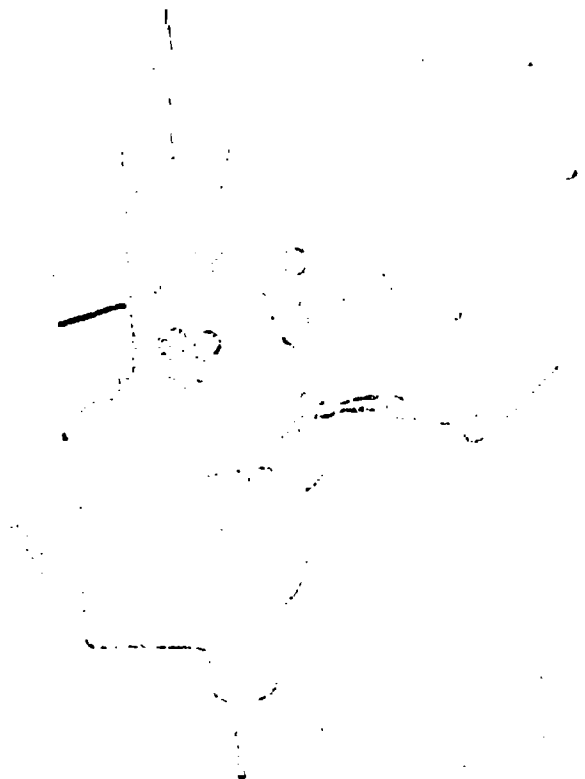


Figure 100. An Industrially-produced version of a microtome stage, installed on a microtome. The rectifier which supplies the stage is shown in the background.

In order to prevent atrophy of the transplanted block of tissue, it is necessary to reduce the tissue requirement for nourishing substances (blood). This is accomplished by cooling the block to a temperature of 15-25°, i.e., by 20-15° lower than normal body temperature. When we consider that the cold effect must continue uninterruptedly for an extended period of time (from several weeks to several months), it becomes apparent that the employment of earlier known methods of cooling and, in particular, periodically acting cold producing agents are not suitable for the purpose indicated. In addition, it is extremely desirable that the patient not be confined to his bed for the duration of the treatment, but have the capability of independent movement.

Table 21  
Basic Data for Microtome Stages with Thermoelectric Cooling

Parameter	Type of Stage		
	With air heat removal	With air- liquid heat removal	With liquid heat removal
Operating area, mm <sup>2</sup>	240	240	2600
Maximum cooling	-7 to -5°	-10 to -5°	-20°
Optimum current, a	12	12	50
Optimum voltage, v	0.3	0.3	0.4
Power requirement, w	3.6	3.6	12
Time required to establish minimum temperature, min	3	3	2
Water consumption, l/min	—	0.5	0.5
Dimensions, mm	110×72×84	15×72×84	⊙=70, h=22
Weight, g	650	580	340

A miniature thermoelectric refrigerator which has been designed for the purpose described satisfies all of the conditions listed above. Small in size and of insignificant weight, the refrigerator may be employed directly on the face of the patient while not causing him any particular discomfort. The cooling surfaces are formed of sheet lead, which permits them to be easily shaped to fit most conveniently the block of transplanted tissue subject to cooling.

The current supply of the refrigerator is accomplished by means of a special rectifier, which is connected with the refrigerator by means of a long combined current and water supply conductor. Such a connection system of the refrigerator with the power supply and the heat removal water system does not tie the patient down, but provides him with sufficient freedom of movement. Regulation of the degree of cooling is provided by changing the value of the refrigerator supply current. When necessary, sustaining or changing the temperature of the refrigerator may be accomplished in accordance with any established schedule; for this purpose a simple programming device must be connected to the input of the rectifier.

A section of the thermoelectric refrigerator for plastic surgical operations is shown in Figure 101.

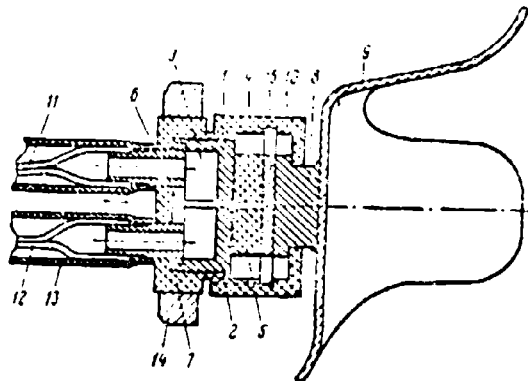


Figure 101. Section of a Refrigerator for plastic surgery.

Two red-copper polycylinders 1 and 2, which have channels 3 for water, form the base of the device. Two semiconductors 4 and 5 are soldered to the base. The polycylinders are insulated from each other by textolite washer 6 and are filled in with white decorative epoxy resin 7. As a result, a single, structurally finished sub-assembly is formed. Red-copper disc 15, 22 mm in diameter, which is the collector of the cold junction, is connected above the thermoelement. To make the device as universal in application as possible, the cooling surfaces sub-assembly is replaceable, and, as has been pointed out above, is made of lead. Thermal contact between the cold junction of the thermoelement and the cooling surfaces sub-assembly is accomplished by means of tight pressure on the latter through the use of plastic sleeve and nut 10 of part 8. Lead surfaces 9 are soldered to part 8. The electrical supply to the thermoelement is accomplished through two current-carrying busbars 11 and 12, which are enclosed in rubber hose 13, through which water flows simultaneously in order to remove heat from the hot junctions of the thermoelement. Duralumin ring 14 serves to attach the refrigerator to the patient by means of straps or bandages.

Specifications of the refrigerator are shown below.

Operating current (at which cooling of a block of tissue from 10 to 15° is achieved)	40 a
Voltage drop	0.05 v
Direct current power requirement of the refrigerator	2 w

Power requirement from the alternating 100 w current supply	
Length of the hoses connecting the device with the power supply	up to 2 m
Refrigerator weight with cooling-surfaces	200 g
Device dimensions (without the cooling-surface sub-assembly): diameter	40 mm
height	25 mm

An overall view of the refrigerator is shown in Figure 102.

~~GRAPHICS~~  
~~NOT REPRODUCIBLE~~

Figure 102. An overall view of a refrigerator  
for plastic surgery.

## CHAPTER XIII. Thermoelectric Devices for Radioelectronics

### §1. A Microthermostated Device for Radioelectronic Devices

Contemporary radioelectronic equipment employs a number of elements, in which operational stability depends to a large extent on temperature. These elements include germanium crystal diodes and triodes, frequency stabilization crystals, photoconductive cells, several special high-stability resistors, capacitors, etc.

In agreement with contemporary operating requirements established for these devices, the external temperature may change within the range of  $-60$  to  $+60^{\circ}$ . In addition, the requirement to develop compact radioelectronic apparatus leads to a quite significant increase in the temperature inside separate sections, which occasionally reaches  $100^{\circ}$  and higher.

The widespread application of radioelectronic devices in contemporary technology demands maximum reliability under various operating conditions.

The elements listed above, under the influence of such significant temperature differences, begin to display operational instability, which in the final analysis leads to failure of the entire apparatus. To a great extent this pertains to germanium diodes and triodes which have temperatures exceeding  $40-50^{\circ}$  begin to display unstable operation.

The usual methods of temperature reduction include the use of compressor or absorption refrigerating machines, the application of cooling mixtures (liquid nitrogen, solid carbon dioxide, ice,) may not be employed for the purpose indicated due to a number of operating inconveniences. Thus, for example, the application of refrigerating machines operating on the compressor or the absorption principle is

advantageous only for temperature reduction in comparatively large spaces involving the release within these spaces of heat output calculated in dozens or hundreds of watts. In this case the refrigerator operates with a high coefficient of performance. During operations with a refrigerator with a refrigerating capacity of less than 20 w, its coefficient of performance falls to 10-20%.

In addition to purely heat engineering considerations, the employment of refrigerators for temperature reduction in small spaces is not advantageous for the reason that even the most compact machine occupies a relatively large space, has a weight of not less than 30 kg, and requires a significant expenditure of electrical energy to supply it. The application of various cooling methods for the purposes indicated requires periodic refilling, which is not permissible under operating conditions. The thermoelectric method of cooling permits reducing temperatures in a small volume with a device of insignificant dimensions and weight. When required the temperature provided by a thermoelectric cooling device may be stabilized at the required with a great degree of accuracy, by means of a special circuit. Thus, for example, a thermoelectric microthermostat system sustains the temperature of the articles inside the system at a level of  $30 \pm 0.1^\circ$  with an external temperature change of  $-50$  to  $+70^\circ$ .

Thermoelectric cooling devices operate most effectively when low heat outputs are released within the cooled volume. Practical designs of thermostat systems are capable of providing the calculated temperature difference with heat loads not exceeding 5-10 w. When large heat loads are released in the cooled volume, the cooling effectiveness is reduced.

Depending on specific conditions, applicable thermoelectric microrefrigerators may be produced in various design versions. Shown below is a description of the design of one type of thermoelectric microrefrigerator, intended for the reduction of the operating temperature of germanium triodes and for crystal frequency stabilization.

The operating volume of the refrigerator (Figure 103) is an aluminum sleeve 1, which is in good thermocontact with cold junctions 2 of the thermoelectric pile. In order to exclude electrical contact between the cylinder and the pile, the end surface of the aluminum shell is coated by electrochemical means with a thin aluminum oxide layer, which provides good heat conductivity and high resistance.

In order to reduce heat flow from outside, shell 1 is protected by a layer of thermoinsulation consisting of foam plastic 3. External shell 4 surrounds the microrefrigerator on the outside. In order to connect articles into the circuit which are located inside the thermostat system, feed-through glass insulators 6 are situated on removable cover 5.

Heat removal from the hot sides of the thermopile is accomplished through aluminum plate 7, which is coated with aluminum oxide on one side. During construction of the thermostat system, the plate is tightly pressed to the frame of the device. The thermoelectric pile of the thermostat system consists of 18 series-connected thermoelements, which are filled with epoxy resin and form a single sub-assembly.

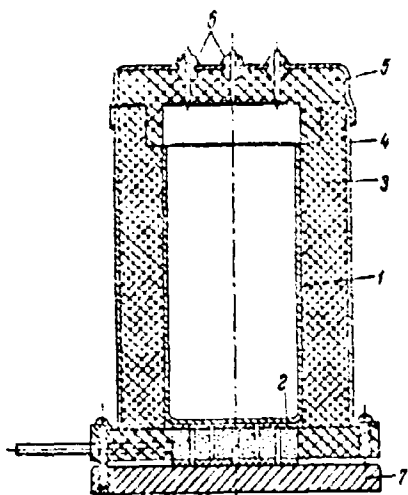


Figure 103. A section of a microthermostat system for radioelectronic devices.

The basic parameters of the microthermostat system described are as follows:

Supply current	8 a
Voltage	1.2 v
Maximum temperature difference:	
at an ambient temperature of 20°	30°
at an ambient temperature of 50°	40°
Dimensions: height	120 mm
diameter	65 mm
useful volume	75 cm <sup>3</sup>
Weight	390 g



Figure 104 shows an overall view of the microthermostat system described.

## GRAPHICS NOT REPRODUCIBLE

Figure 104. An overall view of a microthermostat system for radioelectronic devices.

In the design formulation shown, microthermostat systems with a useful volume from 25 to 300 cm<sup>3</sup> were developed. As we have pointed out previously, the refrigerating capacity of thermoelectric microrefrigerators is not great. In this connection a combination of devices must be accomplished in such a manner that only the element requiring thermostatic control be placed within the microthermostat system. The heat output of the device must not exceed the indicated value.

In a number of cases it is necessary not only to reduce the temperature of part of a radioelectronic device but also to stabilize it at a required level. This problem may be resolved by various methods,

based on the application of 1) liquid thermoregulators, 2) contact thermometers, 3) bimetallic thermoregulators, 4) thermocouples and thermistor electronic regulators.

The first three temperature stabilization methods cannot be recommended for thermoelectric cooling devices due to insufficient sensitivity with respect to the large dimensions and significant inertia of the sensors. Thus, for example, the accuracy of the temperature maintained by a bi-metallic sensor equals  $3-5^\circ$ , which in a number of cases is insufficient.

The fourth method is the most widely employed one for the purpose indicated, in which low-inertia thermocouples or thermistors are used as sensors. This method, in conjunction with a comparatively simple electronic circuit, permits maintaining the temperature in a thermostatically controlled volume with an accuracy of  $\pm 0.1^\circ$  and above. One possible electronic temperature regulation circuit is shown in Figure 105. The temperature sensors are two microthermistors, which are connected in a bridge circuit; the unbalance signal is amplified by a sub-miniature tube amplifier and is applied to a relay which changes the direction of the current supply to the thermoelectric pile, and thereby switches it from the cooling to the heating mode. The overall dimensions of such an electronic temperature stabilizer are  $100 \times 100 \times 50$  mm.

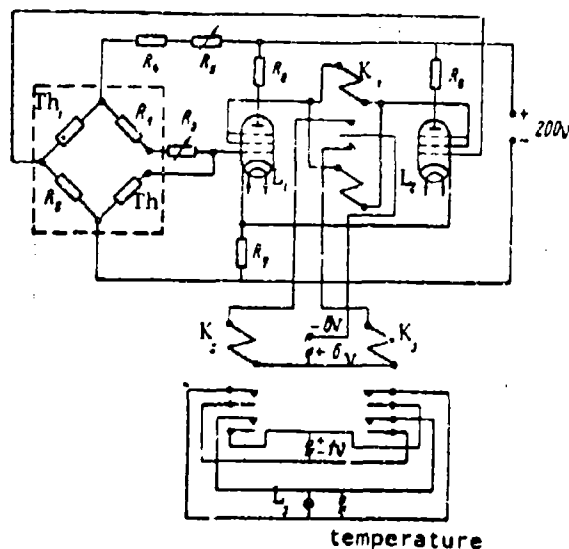


Figure 105. The principal circuit of an electronic temperature stabilizer.

The electronic stabilizer constructed in accordance with the circuit shown maintains the temperature in the operating volume of the thermoelectric microrefrigerator with an accuracy of  $0.1^{\circ}$ . A further reduction in the size and weight of the stabilizer is possible by replacing the electron tubes with semiconductor triodes and by using a magnetic amplifier.

## §2. A Thermoelectric Ultrathermostat System

Temperature stabilization with a high degree of accuracy is often required in contemporary radioelectronics, and also in laboratory practice. The parameters of existing ultrathermostat-system designs do not always satisfy practical requirements. Thus, for example, the most widely employed gepler ultrathermostat has the following shortcomings: the electric motor creates interference and vibration in the device; the water employed as a heat-transfer agent causes corrosion of the internal parts of the thermostat system; and the contact thermometer does not provide the required operational reliability. All these factors reduce the operational capability of the device.

The electronic ultrathermostat system with thermoelectric cooling is free from the defects listed above. The lack of moving parts and of corrosion caused by the liquid, the smoothness and continuity of regulation in junction with a high degree of temperature stabilization provides for high operating qualities of the device which permits it to be used in the most demanding radioelectronic devices for a temperature stabilization of Weston reference cells, where separate design elements and sub-assemblies, and also in laboratory investigations.

The electronic ultrathermostat system maintains a constant temperature ( $20 \pm 0.01^{\circ}$ ) in a 6-liter volume with an environmental temperature of 10 to  $30^{\circ}$ .

A stable temperature is established in the thermostat system chamber containing no thermostatically controlled bodies in the course of not more than 10 minutes. If two normal Weston cells are placed in the chamber, a stable temperature is established in the chamber in two hours. The thermoelectric ultrathermostat system is supplied from the alternating current network of 220 v with a power consumption of 100 w.

The operating principle of the ultrathermostat system.

The electronic ultrathermostat system, which is shown in block diagram in Figure 106, is a closed system of automatic temperature regulation. It consists of regulating objects (the thermostat), the sensitive element and the electron regulator. The electron regulator consists of an amplifier

with a vibrator power pack at the input and an action element (a power amplifier).

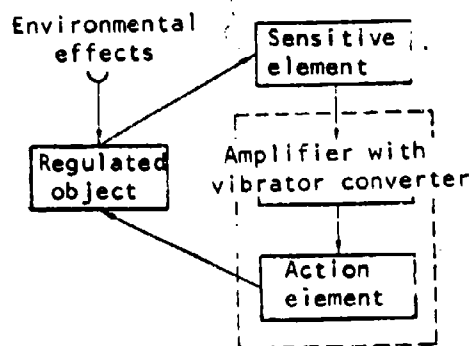


Figure 106. A block diagram of a thermoelectric ultrathermostat system.

A bridge is employed as a sensitive element to sense the temperature change in the thermostat system chamber. The bridge is formed of two MMT-1 thermoresistors connected in series in opposite arms of the bridge, and two manganin resistors which are connected in the two remaining arms of the bridge. The series connection of the thermoresistors is for the purpose of reducing the power dissipated on each resistor to a value below the permissible limit (0.01 w with a power limit of 0.05 w).

The bridge is supplied from a battery consisting of 61-KSU-3 cells with a total voltage of 9v, and is balanced at a temperature of 21°. Bridge unbalance occurs when the temperature changes in the thermostat system chamber. The unbalance signal is applied to the input of the amplifier and after conversion by the VUS.3 vibrator converter into an alternating current signal with a frequency of 50 Hz is amplified by the first two stages of the amplifier, which is equipped with 6 Zh 8 tubes. The amplified alternating voltage is detected at the second contact of the vibrator converter. The dc amplifier is equipped with 6 N 9C electron tubes in a cathode compensated circuit. The signal obtained at the output of the amplifier is applied to the power amplifier (which is a cathode-coupled stage equipped with 6 P 3 C electron tubes) which feeds the preheater of the thermostat system chamber. The phase of the control signal is such that the system continuously balances the bridge unbalance signal. Indicator kicks of the galvanometers of the measuring circuits

which are observed when thermostats operating on the principle of positional regulation are employed, are eliminated due to continuous regulation in this device.

Cooling of the operating chamber is required for normal operation of the thermostat system. In the ultrathermostat system described, thermoelectric cooling is employed which eliminates the inconveniences associated with the use of temporarily effective cooling agents. The semiconductor thermopile is supplied from a separate non-regulated rectifier, situated in the electronic regulator section, with an output of 3 v and an operating current of 4 a. The temperature within the cold chamber is reduced 12° below the temperature of the surrounding medium. The maximum permissible current through the thermopile is 8 a. Heat removal from the hot junctions of the thermopile is accomplished with a system of air radiators which are distributed in a fan-shaped manner around the lower part of the thermostat system.

#### Construction of the ultrathermostat system.

Construction of the ultrathermostat system has been accomplished in the form of two separate sections: the thermostat system and the electronic regulator, which are interconnected by a cable with plug-in socket connections.

The thermostat system section consists of two parts: the refrigerator and the thermostat system chamber. The thermoelectrical part of the device is a thermally-insulated cylindrical chamber with a volume of 22 liters. The thermoelectric pile, consisting of 72 series-connected thermoelements, is mounted on a textolite ring in the lower part of the chamber. The hot junctions of the thermopile are equipped with a system of radiators which provide for sufficient heat removal to the surrounding air. The refrigerator chamber is thermally insulated with foam plastic with a thickness of 50 mm.

The cold junctions of the thermoelement are equipped with a system of red-copper plates, which are distributed vertically along the entire inner side surface of the operating chamber, which facilitates adequate heat transfer between the thermopile and the air inside the chamber. An aperture is provided in the top of the chamber, which is covered by a plug of foam plastic, for the entry of the wires from the thermostatically cooled objects and the sensors of the temperature stabilization control circuit. The thermosensitive element -- the bridge with the thermoresistors -- are situated close to the sides of the chamber. A three-section preheater winding is situated on the outside surface of the thermostat system chamber. The output of the preheater may vary up to 15 w, which in conjunction with continuous chamber cooling permits temperature stabilization without changing the sensor adjustment.

The electronic regulator is constructed as a separate section. The following are situated in this section. A regulated source of anode voltage of 250 v, with a current of 5 ma; a non-regulated power amplifier power supply with a voltage of 350 v and a current of 100 ma; a non-regulated thermopile power supply with a voltage of 3 v and a current of 4 a; and the battery supply for the thermosensitive bridge.

The temperature measurement circuit.

Figure 107 shows a schematic of the temperature measurement section within the thermostat system chamber. Within the chamber are located the standard Weston III cell of the NE class, a copper resistance thermometer TS and reference coil OKS-2. The resistance thermometer, reference coil and the KNS-6 resistance box are connected in series in the battery circuit with a voltage of 1.5 v.

Temperature change within the chamber is measured by the indirect method, by measuring with the PPTN-1 potentiometer the change in voltage on the resistance thermometer, with a constant voltage on the reference coil. When the measurement is initiated, the voltage on the resistance thermometer and the reference coil is established at 18 mv. During subsequent measurements, the voltage on the reference coil is controlled by the PPTN-1 potentiometer with an error of 0.0001 mv.

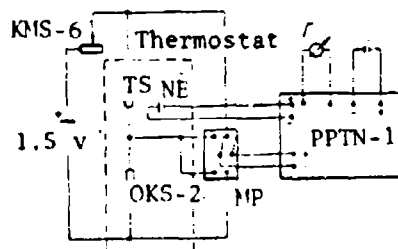


Figure 107. A schematic of the temperature measuring section of the ultrathermostat system.

The F-16 photo-compensated amplifier with a sensitivity of 2  $\mu$ v on the scale is used as an indicator. When required, this voltage is adjusted by means of the KNS-6 resistance box. The connection of the PPTN-1 potentiometer with the OKS-2 reference coil and resistance thermometer TS is accomplished by means of oil switch MP.

With a constant voltage on the reference coil, the voltage change on the resistance thermometer is accomplished mainly by a temperature change in the thermostat system chamber. The temperature change with respect to the voltage change on the resistance thermometer is defined by the equation

$$\Delta T = K \Delta V_{TS},$$

where  $\Delta T$  is the temperature change within the chamber;  $K$  is a proportional coefficient, equal to 15 in the case examined;  $\Delta V_{TS}$  is the voltage change on the resistance thermometer.

A graph of temperature change with time in the operating chamber, plotted on the basis of experimental data, is shown in Figure 108.

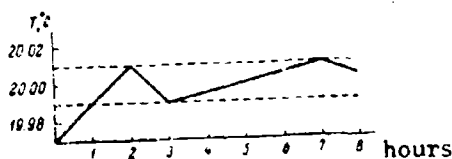


Figure 108. Temperature change with time in the operating chamber of a thermoelectric ultrathermostat system.

### §3. A Thermoelectric Cooler for a Parametric Amplifier

The noise coefficient of a parametric amplifier is defined by the so-called noise temperature of the diode employed in the amplifier and the resonator system noise. The noise temperature of the resonator, as a rule, does not exceed 10% of the total amplifier noise level. Thus the basic source of noise in a parametric amplifier is the diode.

Figure 109 shows the dependence of the effective noise temperature ( $T_{N,EFF}$ ) of a parametric amplifier on temperature ( $t$ ). Curve 1 pertains to a diode manufactured of germanium with an impurity concentration of  $10^{19}$ ; curve 2 pertains to a diode of silicon with an impurity concentration of  $10^{20}$ . From the curve shown it is obvious that the noise temperature may be reduced by reducing the diode temperature. The operating condition.

of parametric amplifiers, as a rule, do not permit the employment for diode cooling of compressor refrigeration machines or periodically acting cold-producing agents (liquid nitrogen, or solid carbon dioxide). In this connection a model of a thermoelectric cooler was developed which provides for diode cooling in a typical parametric system resonator to  $-53^{\circ}$ .

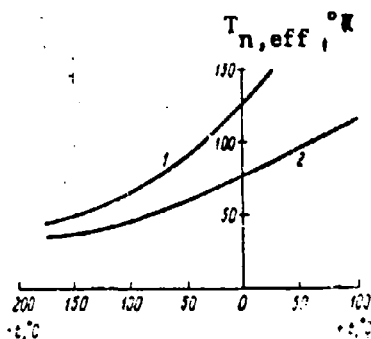


Figure 109. The dependence of the effective noise temperature ( $T_{n,eff}$ ) of a parametric amplifier on diode temperature ( $t$ ).

A section of a thermoelectric refrigerator installed on the wave guide channel of a parametric amplifier resonator is shown in Figure 110. The thermoelectric pile which consists of two stages 1 and 2, is soldered through ceramic heat junctions 3 to the heat transfer base, which is installed at the bottom of housing 4. Heat removal from the thermopile in a device of this construction is accomplished by means of running water, which delivered through nipples 5 and flows through channels 6. The cold junction collector of the thermoelement of second stage 7 has a calibrated recess in the upper part, in which diode 8, which is subject to cooling, is placed. The upper lead of the diode is connected through a special clamping cap with thin conductor 9, which is soldered to feed-through insulator 10. Electrical contacts between the diode and the resonator wave guide 11 is accomplished through two thin washers 12 and 13. These washers retard heat flow from the cooled diode to the side of the wave guide. Diode temperature is measured by MKMT-16 microthermistor 14, which is placed in silver amalgam in the collector of the cold junctions of the thermopile second stage. The



leads of the thermistor, for subsequent circuit connection, are attached to terminal block 15, which is fastened to the housing. The thermopile current supply is accomplished from a source of direct current, which is connected through current-carrying busbars 16.

Thermoinsulation of the thermopile and the diode in the wave guide is accomplished by foam plastic 17. The refrigerator itself is attached to the wave guide channel of the resonator by means of two bolts 18. Replacement of the diode is accomplished by removing the refrigerator from the wave guide.

The basic parameters of the thermoelectric refrigerator described are listed below.

Operating current	60 a
Thermopile voltage drop	0.5 v
Direct current power requirement	30 w
Diode temperature (with a heat removal water system temperature of 18° and an environmental temperature of +20°)	-50°
Temperature difference provided by the device	68°
Refrigerator dimensions (not including the resonator)	50 × 66 × 46 mm
Refrigerator weight excluding the resonator	725 g
Water consumption rate in the heat removal system	60 l/h

An overall view of the thermoelectric refrigerator for a parametric amplifier is shown in Figure 111.

#### §4. A Thermoprobe

In the production of transistors and in laboratory practice it is necessary to have a method of quickly determining the nature of the conductivity of an ingot of a silicon or germanium, as well as determining the boundaries of various conductivity areas along the ingot. A system of hot probing is usually employed for a similar rapid method of determining the sign of the conductivity; many devices have been constructed on this principle.

The essence of this method consists of the following: a metallic point, or a probe, heated to a temperature of 40-50° is applied to the test material in the area required. A millivolt meter, connected between the probe and the specimen being tested, shows the direction of the thermoelectromotive force generated in the circuit, which will be proportional to the value of the temperature difference between the hot probe and the ingot, and the polarity of the thermoelectromotive force

will depend on the nature of the conductivity of the object being investigated. Along with simplicity in convenience in measurement, the hot probing method has one significant shortcoming. When the temperature of the probe is close to the temperature of the onset of self-conductance in the semiconductor, this method gives false indications and proves to be unsuitable.

In this connection, the necessity arose to create a temperature difference between the probe and the ingot not by increasing the probe, but by decreasing it. The thermoelectric method of cooling permitted this problem to be solved successfully, and facilitated the development of a device required by industry.

This device (Figure 112) consists of thermocouple 7 and 8; code collector 10 of the thermocouple with the point at the end forms the probe with a base area of  $6 \text{ mm}^2$ . The outside of the thermocouple and the cold collector is covered with a protective cap 9 of decorative plastic. Heat removal from the hot junctions of thermocouple 5 is accomplished by means of radiator system 4, with natural convection heat removal.

The electrical supply to the thermoelement is delivered through the radiator system, which is divided into two parts, A and B, which are electrically insulated from each other. Current conducting busbars 1 and 2 are connected to the appropriate parts of the radiator system. Coupling rings 3 and 6 serve as rigid couplings for the two parts of the radiator system. The cold collector, which is the probe, has an electrical lead for connection to the measuring device. Two minutes after the device is switched on a temperature of  $-17^\circ$  is established at the tip of the probe, with an operating current of 20 a. The voltage drop on the device is 0.07 v. Thus the power required by the device from the power supply equals 1.4 w.

The sides of the device (the diameter of the upper part is 40 mm, and the height is 161 mm) and its weight (470 g) permits it to be utilized for an extended period of time without any kind of stress.

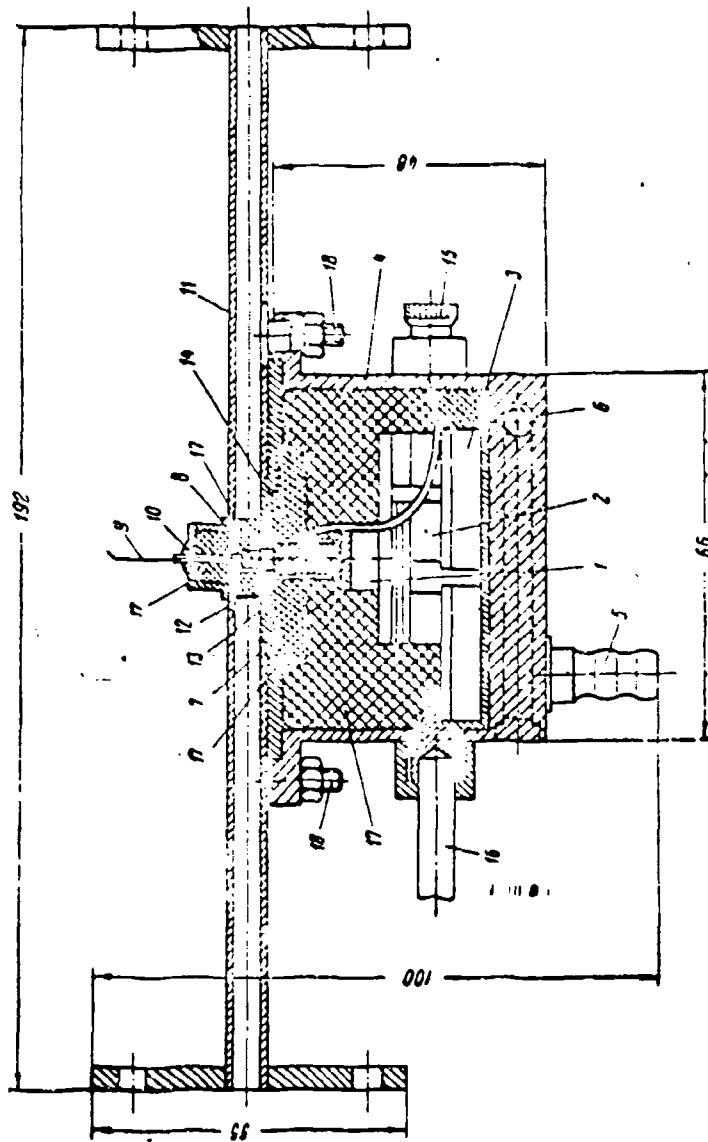


Figure 110. A Thermoelectric refrigerator for a parametric amplifier.

**GRAPHICS  
NOT REPRODUCIBLE**

Figure 111. An overall view of a thermoelectric refrigerator for a parametric amplifier, installed on the wave guide channel.

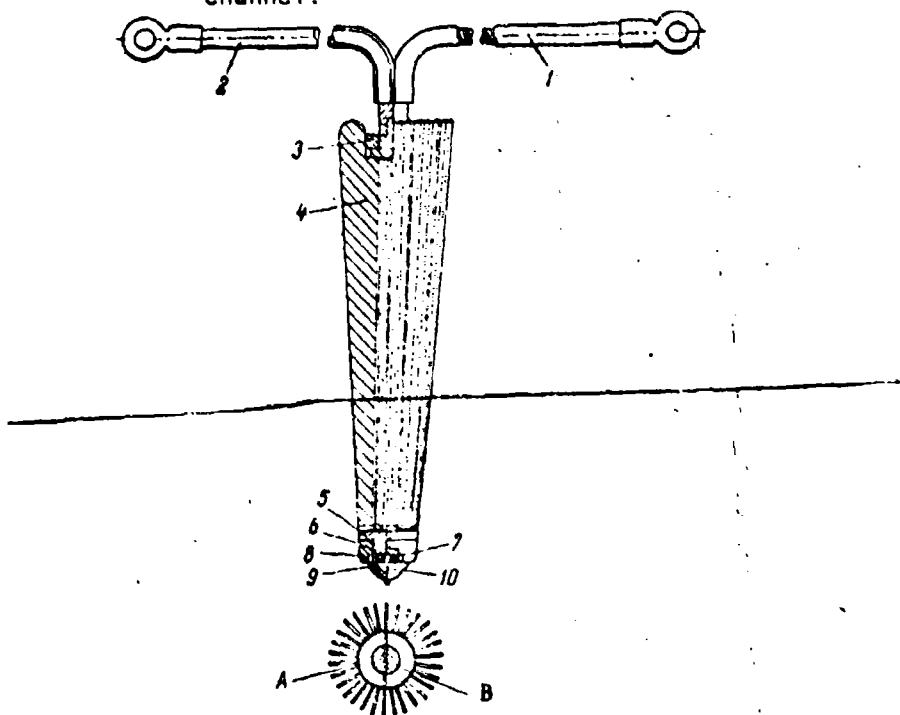


Figure 112. A section of a thermoprobe.

## CHAPTER XIV. General Purpose Thermoelectric Refrigerators

### §1. Microrefrigerators for Laboratory Purposes

In various types of laboratory investigations the necessity often arises to examine the behavior of a model or the progress of a process in a wide range of temperatures. In a case when the temperature range which interests the investigator extends into the area below room temperature, the conduct of these experiments is associated with a great deal of difficulty. This difficulty is caused by the fact that all existing methods of temperature reduction do not permit the establishment, with simple methods of smooth temperature regulation within the operating range. By virtue of this circumstance, in practice it is necessary to develop complex and large thermoregulating devices, which, however, do not always satisfy established requirements.

The thermoelectric method of cooling and heating has permitted the development of microrefrigerators, which are free from the shortcomings listed above. By changing the value of the supply current to the thermoelectric pile, the temperature in the operating chamber of the device can be changed with any degree of accuracy and rate of change. Whenever required, a transition from the cooling mode to the heating mode and the reverse can be accomplished by reversing the direction of the current supply of the microrefrigerator.

Three design versions of microrefrigerators for laboratory purposes have been developed. The first version of the microrefrigerator (Figure 113) is equipped with a single-stage thermoelectric pile 6, which consists of five thermoelements. The cold junctions of the thermopile are coupled with good thermal contact with aluminum disk 5, to which the operating chamber 1 is soldered, which is constructed of aluminum.

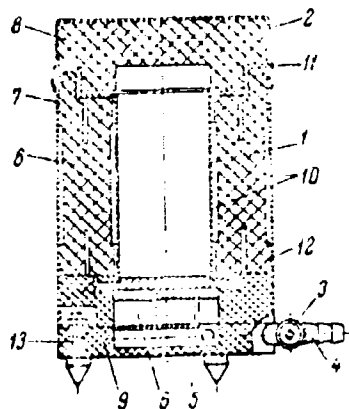


Figure 113. A section of a microrefrigerator for laboratory purposes. The first design version is shown.

In order to exclude electrical contact between the connecting plates of the thermoelectric pile and the bottom of the operating chamber, the latter is electrochemically coated with a thin (0.5-1.5  $\mu$ ) layer of aluminum oxide. This layer displays insignificant heat transfer resistance and at the same time provides good electrical insulating properties.

Heat removal from the thermoelectric pile is accomplished by running water, which flows in channels provided directly within the hot connecting plates of the thermopile. Water input and output for the device is accomplished by means of two nipples 4. The electrical supply to the device is through terminals 3, which are soldered to the water supply nipples. The system of hot connecting plates is filled in with thermoreactive epoxy compound 9, thus forming a rigid, structurally finished sub-assembly. The outside of the operating chamber of the device is protected by a layer of thermal insulation 8, constructed of foam plastic. In order to reduce heat losses through the side section of the thermal insulation, narrow recesses 10 have been cut into the insulation. Aluminum cylinder 7 forms the external housing of the device. Thermally-insulated cover 2 provides access to the operating chamber.

Protective ring 11, of decorative plastic, is located at the area where the cover joins the chamber. Resin ring 12 provides constant thermal contact between the operating chamber base and the thermopile.

The external cover is attached to the thermopile by means of shaped screws 13, which also serve as the legs of the device.

As we have pointed out previously, the value of the maximum temperature difference provided by a thermoelectric cooling device depends on the heat load on the thermopile, which in turn is determined by the heat released by the objects subject to cooling, by parasitic heat flows from outside through the layer of thermal insulation, and by the heat conductivity of the thermoelement arms.

The technical parameters of the microrefrigerator described are shown below, and a general view is presented in Figure 114.

Chamber volume	75 cm <sup>3</sup>
Minimum operating chamber temperature (with a water system heat removal temperature of 15°)	-30°
Maximum operating chamber temperature	+50°
Operating current in the maximum cooling mode	45 a
Operating current in the maximum heating mode	10 a
Power requirement, cooling mode	18 w
Time required to establish minimum temperature in the operating chamber, filled with glycerin	25 min
Water consumption rate	0.2 l/min
Dimensions: diameter	85 mm
height	130 mm
Weight	540 g

**GRAPHICS  
NOT REPRODUCIBLE**

Figure 114. An overall view of the first version of a microrefrigerator for laboratory purposes.

The second design version of a microrefrigerator for laboratory purposes provides for lower temperatures in the operating chamber of the device. This is achieved by utilizing a two-stage thermoelectric pile in place of the single-stage pile employed in the first version of the device. In order to provide sufficient refrigerating capacity in the second stage, the current is supplied in series with the first stage. In addition, the thickness of the thermal insulation of the operating chamber of the device has been increased.

A section of this type of microrefrigerator is shown in Figure 115. The two-stage thermoelectric pile with series-fed stages 1 consists, in the first stage, of ten thermoelements; there are two thermoelements in the second stage. Operating chamber 3 is soldered to the cold collectors of the second stage of the thermopile through the electrically insulated ceramic heat junctions. This arrangement provides for a minimum heat transfer resistance. The hot junctions of the first stage of the thermopile, which are again connected through ceramic heat junctions, are soldered to collector 4 of the hot junctions, which in turn is soldered to the heat removal system 5. Heat removal from the thermopile is accomplished by running water, which is supplied to the device through two nipples 6.

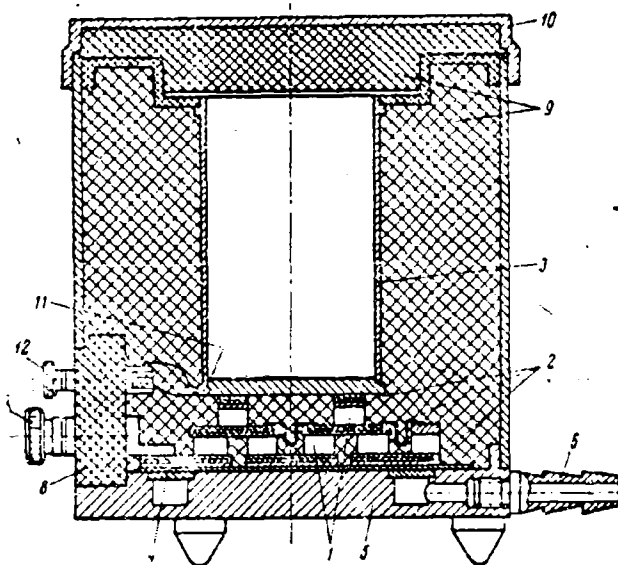


Figure 115. A section of a microrefrigerator for laboratory purposes. The second design version is illustrated.



The electrical supply to the device is connected through two terminals 7, installed on electrically insulated panel 8. The operating chamber of the device is protected by a layer of thermal insulation 9, formed of foam plastic. Cover 10 provides access to the operating chamber. Microthermistor 11, mounted in the operating chamber with amalgam, serves to measure the temperature in the operating chamber of the device. The leads of thermistor 12 are extended to the insulated panel.

The thermoelectric pile of the microrefrigerator described possesses a comparatively high refrigerating capacity, which is illustrated in Figure 116. This graph shows an experimental curve of the change in the temperature difference provided by the refrigerator as a function of the heat released in the operating chamber of the device.

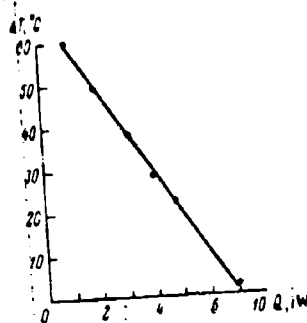


Figure 116. The temperature difference provided by the second design version of a microrefrigerator for laboratory purposes as a function of the value of the heat released in the operating chamber.

An overall view of the device is shown in Figure 117.

The third version of the thermoelectric refrigerator for laboratory purposes is a single, structurally finished device, which contains, in addition to the refrigerator itself, the rectifier, the temperature measurement circuit, and also automatic and control elements which provide for reliable operation.

## GRAPHICS NOT REPRODUCIBLE

Figure 117. An overall view of the second design version of the microrefrigerator for laboratory purposes.

The basic parameters of this type of microrefrigerator are as follows.

Optimum current	50 a
Voltage drop	1.64 v
Power requirement	82 w
Minimum operating chamber temperature (with a water system heat removal temperature of 18°)	-53°
Maximum operating chamber temperature	55°
Operating chamber volume	125 cm <sup>3</sup>
Dimensions: diameter	120 mm
height	160 mm
Weight	2.4 kg

The electrical circuit of the microrefrigerator is shown in Figure 118.

The two-stage thermoelectric pile Th of the refrigerator is supplied from a full-wave rectifier, consisting of power transformer Tr and VG-50-15 germanium rectifiers (D<sub>1</sub> and D<sub>2</sub>). Filter choke Ch serves to smooth out rectified-current ripple to a value of 5-7%. Switch S<sub>1</sub> serves to transfer the thermopile from the cooling to the heating mode. In this case the thermopile receives current reversed in polarity, from half of the

secondary winding of the power transformer, rectified by VG-10-15 diode  $D_3$ . Resistor  $R_1$  serves to limit the flow of heating current. Temperature measurement in the microrefrigerator is accomplished by means of microthermistor  $R_2$ , which is attached in silver amalgam to the side of the cylinder which forms the operating chamber of the device.

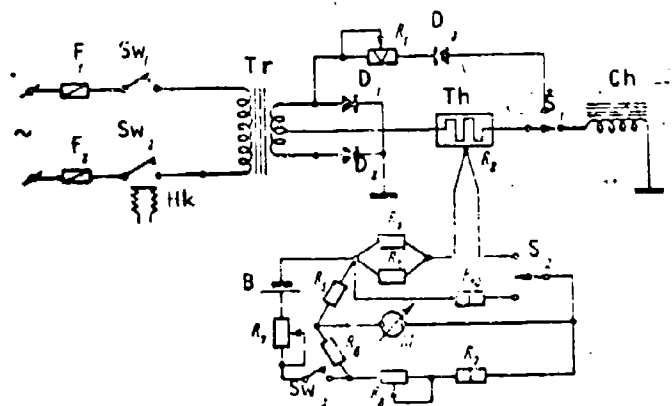


Figure 118. The electrical circuit of the third version of the microrefrigerator for laboratory purposes.

The temperature measurement circuit consists of a bridge; the arms of the bridge are made up of resistors  $R_3$ ,  $R_4$ ,  $R_5$ ,  $R_6$ ,  $R_8$  and  $R_9$ . Resistor  $R_2$ , which is connected in the measurement arm of the bridge, is a microthermistor. The current supply to the bridge flows from battery B, which is connected to the bridge by switch  $Sw_3$ . The value of the voltage required to supply the bridge is established by resistor  $R_7$ . Switch  $S_2$  serves to calibrate the bridge, and this is accomplished by means of resistor  $R_8$ . The M-24 microammeter is employed as measuring device M and is connected in the diagonal of the bridge. The scale of the meter is graduated in degrees centigrade. The current supply to the device is from the 127/220 v network through fuses  $F_1$  and  $F_2$ . Switch  $Sw_1$  serves to switch on the voltage supply. Hydraulic relay Hk- $Sw_2$  is connected in the water supply circuit from the hot junctions of the thermopile in order to break the circuit to the microrefrigerator if there is no water in the heat removal system.

Brief technical characteristics for the microrefrigerator are shown below.

Optimum current in the cooling mode	50 a
Voltage drop in the cooling mode	1.64 v
Power requirement in the cooling mode	82 w
Minimum operating chamber temperature (with a water system heat removal temperature of 15°)	-50°
Optimum current in the heating mode	6 a
Voltage drop in the heating mode	0.2 v
Power requirement in the heating mode	1.2 w
Maximum temperature in the heating mode	50°
Operating chamber volume	75 cm <sup>3</sup>
Dimensions:	250 × 250 × 160 mm
Weight	5 kg

An overall view of the third design version of the microrefrigerator is shown in Figure 119.

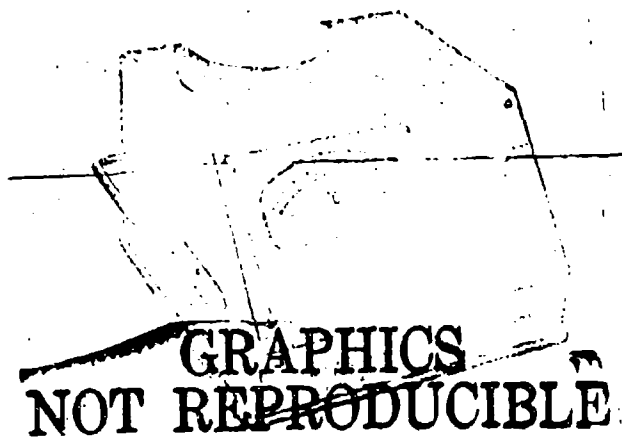


Figure 119. An overall view of the third design version of the microrefrigerator for laboratory purposes.

## 52. Experimental Thermoelectric Microchambers

Thermochambers are used in a number of branches of engineering for checking the efficiency of articles within a range of operating temperatures. Temperature reduction in these chambers is accomplished by means of compressor refrigerating machines, and heating is accomplished by electrical heaters. According to existing standards, experimental chambers must provide a temperature range of  $-60$  to  $+60^{\circ}$ . The use of compressor thermochambers in practice is associated with a number of inconveniences, based on the following factors: relatively large energy requirements, significant size and weight and extended period of time to reach operating levels, and a number of other factors. A particularly important shortcoming is the large volume of the operating chamber, calculated in hundreds and thousands of liters. Very often, however, the volume of articles subject to investigation may amount to several cubic centimeters. In addition, it is often necessary to carry out thermal tests with the simultaneous application on a device undergoing tests of vibrational and accelerating loads. It is not possible to carry out such tests in thermochambers cooled by freon compressors. With these considerations in mind, two design versions of low-volume experimental thermoelectric chambers were developed.

The first version of the chamber was constructed in the form of a rectangular parallel piped, the sides and the bottom of which form a two-stage thermopile with a series current supply. Heat removal from the hot junctions of the thermopile is accomplished by means of running water, which passes through channels located in the duraluminum panels on which the thermopiles are mounted. The channels for water are situated in such a manner that after assembly of the device, they form a single series-connected water system. As we have pointed out previously (Part II, Chapter VI, §6), such a system of distribution of the thermopiles reduces to a significant extent parasitic heat flow to the chamber from the outside. It is the circumstance which excludes the application of external thermal insulation. All five thermopiles are connected in series by a system of special connectors. The total number of thermoelements and the method of their connection provides for a sufficiently high chamber refrigerating capacity. The space between the connecting plates of the second stage of the thermopile forms the operating chamber of the device. The side walls of the operating chamber are formed by the individual connecting plates of the second stage of the thermopiles, and the bottom of the operating chamber consists of the continuous metal plate, soldered to the collectors of the cold junctions of the second stages of the lower thermopile.

For a maximum reduction in mechanical stresses, generated in the lower thermopile, this plate is manufactured of a material with a low

thermal distribution coefficient (invar). In order to reduce heat transfer between the first and second stages of the thermopiles, foam plastic thermoinsulation is placed between them. Access to the operating chamber of the device is accomplished through a removable upper cover, which is equipped with a layer of foam plastic thermal insulation. In order to conduct dynamic tests of articles located within the chamber, twelve conductors are connected to the operating chamber through a special plug and socket connection. Busbars carrying the electrical supply to the chamber thermopiles, and also nipples for the delivery and the output of water for the heat removal system are brought out to the side wall of the device.

Brief technical characteristics of the experimental chamber are shown below.

Operating current in the cooling mode	45 a
Voltage drop in the cooling mode	11 v
Power requirement in the cooling mode	495 w
Minimum operating volume temperature (with a heat removal water system temperature of 20°)	-40°
Operating current in the heating mode, to a temperature of 40°	16 a
Voltage drop in the heating mode	3.5 v
Power requirement in the heating mode	56 w
Time required to establish cooling mode	2.5 hours
Time required to establish heating mode	1.5 hours
Water consumption rate in the heat removal system	75 l/h
Operating chamber volume	1008 cm <sup>3</sup>
Operating chamber dimensions	160 × 90 × 70 mm
Dimensions	255 × 174 × 175 mm
Weight	13.1 kg
Operating range of microchamber static overloads	up to 50 g

An overall view of the first design version of the thermoelectric experimental chamber is shown in Figure 120.

A second version of the thermoelectric experimental chamber is in the form of a single device with a rectifier in an automatic temperature control circuit.

Two-stage thermopiles, with a series current supply to the stages, are soldered to all four sides and to the bottom of the operating chamber of the device, which is constructed of copper, 2 mm in thickness. This distribution of thermopiles permits creating a system with comparatively high refrigerating capacity. All five thermopiles are connected in series. The liquid heat removal systems for the individual piles are also

connected in series. In contrast to the first version of the thermo-chamber, where heating and cooling were accomplished by reversing the direction of the current supply to the thermopile, in the second version the heating function is accomplished by a special electrical heater, which is located on the operating chamber of the device.



## GRAPHICS NOT REPRODUCIBLE

Figure 120. An overall view of the first version of the experimental thermoelectric microchamber.

A block diagram of the electrical part of the device is shown in Figure 121. The current for the thermoelectric piles and for all automatic control and regulation elements is supplied from a rectifier. The thermopile supply is a full-wave rectifier with 6 D-243 A diodes as rectifiers, connected with three diodes in each arm. A platinum resistance thermometer is the temperature sensor for the automatic temperature assembly section, which in turn changes the value of the current supplying the heater and, therefore, the temperature in the chamber, through the amplifier and the control section. The temperature indicator, which is located on the front panel of the device, signals the fact that a specified temperature has been established in the operating chamber of the device.

Setting of the value of the temperature is accomplished by means of two controls on the front panel; one of these establishes tens of degrees, and the other, degree units. Accuracy of the sustained temperature is accomplished automatically within the device. Access to the

operating chamber of the device is accomplished through a hinged, thermally-insulated cover, through which leads may be introduced in order to test articles located within the chamber.

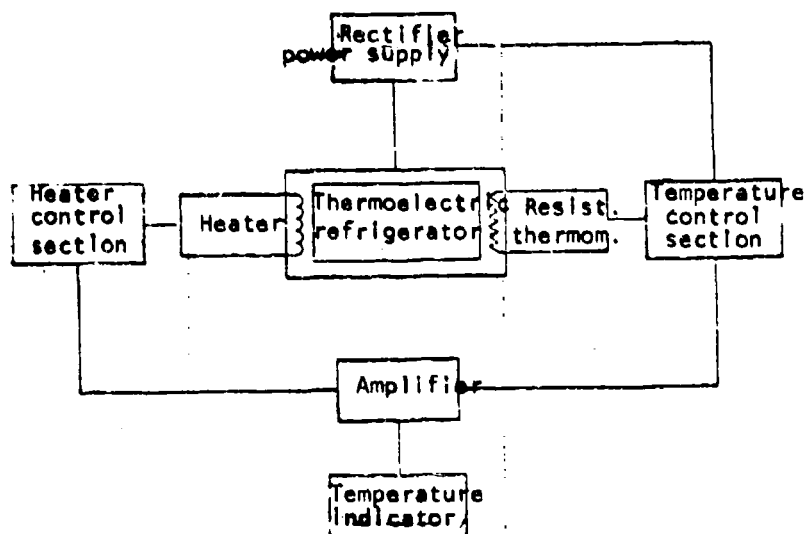


Figure 121. The electrical circuit of the second version of the automatic experimental thermoelectric chamber.

Brief characteristics for this type of thermochamber are listed below.

Operating current	47 a
Voltage drop	5 v
Thermopile power requirement	235 w
Minimum operating chamber temperature (with a water system heat removal temperature of 15°)	-55°
Maximum operating chamber temperature	+60°
Temperature maintenance accuracy	±0.2°
Operating chamber volume of the device	612 cm <sup>3</sup>
Operating chamber dimensions	125 × 70 × 70 mm
Power required from the power network	375 w
Water consumption rate in the heat removal system	75 l/h
Dimensions	400 × 375 × 210 mm
Weight	24 kg



An overall view of the automatic experimental thermochamber is shown in Figure 122.

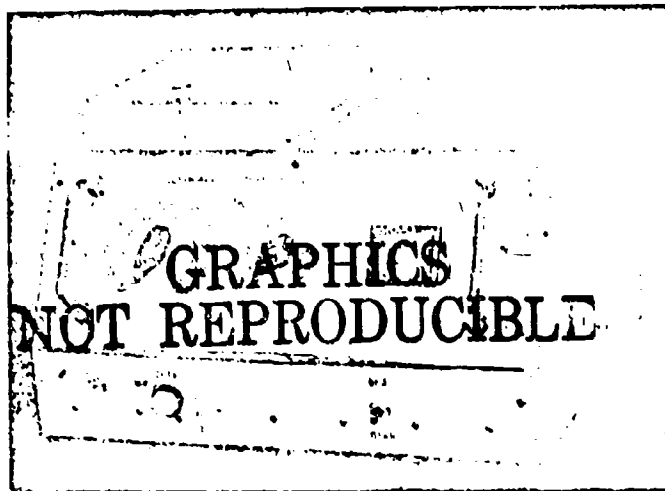


Figure 122. An overall view of the automatic thermoelectric chamber.

### 93. Thermoelectric Condensation Hygrometers

The necessity often arises in industrial and laboratory practice to determine the quantity of moisture in the air or in various gases. Many devices have been proposed for humidity measurements; among these, psychrometers, hair hygrometers and hygrometers based on measurement of the dew point have been the most widely employed. The measurement of humidity with a psychrometer is possible only for positive temperatures, and hair hygrometers possess insignificant accuracy and their measurements reliability is low. The use of hygrometers based on the establishment of the temperature of the formation of condensate, or the dew point, satisfy requirements. Devices of this type are called condensation hygrometers.

Knowing the temperature of the dew point, it is possible to calculate the absolute moisture content in a gas under investigation. The possibility of automating the process of measurement, i.e., of developing a continuously operating device is an unquestionable virtue of condensation

hygrometers. Cooling of the condensation surfaces in condensation hygrometers is accomplished by means of various cryostatic mixtures, solid carbon dioxide, liquid nitrogen, or by means of throttling compressed gas.

These methods of cooling possess a number of shortcomings, including the necessity of periodically renewing the cold producing agent, which sharply decreases the operating capabilities of the device.

The use of the thermoelectric method of cooling the condensation surface has permitted the development of several types of structurally simple hygrometers which are operationally reliable.

#### A visual hygrometer.

The most structurally simple hygrometer is one in which the moment of the deposit of dew is established visually by misting of the operating surface of the device. In concept, this device is the hygrometer of Lembricht, but in place of ether, thermoelectric means are used to cool the condensation surface of the device. The hygrometer is a self-contained device which requires only a connection to an appropriate rectifier. The basic construction elements of the hygrometer (Figure 123) include thermoelement 1, the cold junction of which is soldered to copper disk 2 which is the condensation surface. For a more exact determination of the moment of the appearance of dew on the condensation surface, the latter is surrounded by a polished ebonite ring 3, which is encircled by comparison control surface 4.

The thermoelement and the condensation assembly are covered with a layer of foam plastic thermal insulation 5. The hot junction of the thermoelement is soldered to collector 7, which is equipped with a system of radiator plates 6. Measurement of the temperature at which the dew appears is accomplished with an alcohol thermometer which is located in channel 8. The head of the device is mounted in metallic housing 9 and is installed on column 10. The thermoelectric pair of the hygrometer permits reducing of the temperature of the condensation surface by  $30^{\circ}$ , relative to the temperature of the surrounding air. At an operating current of 20 a, the power required by the element equals 2 w.

The overall dimensions of the hygrometer are as follows: the diameter is 60 mm, the height is 250 mm. The weight of the device is 1.5 kg.

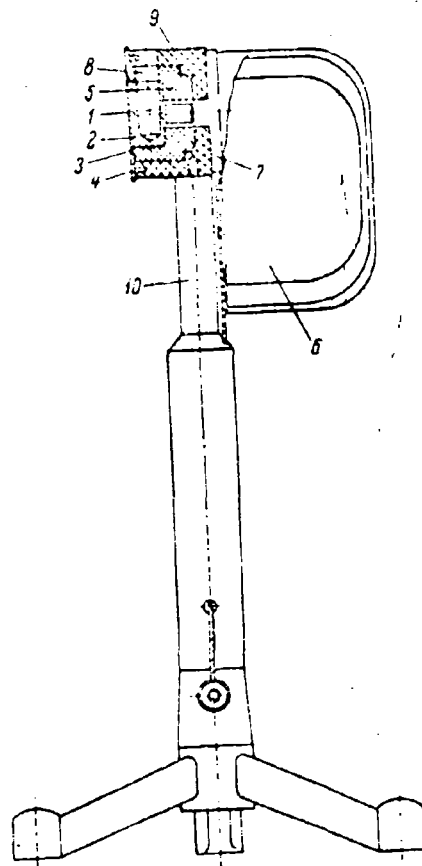


Figure 123. A section of a visual hygrometer.

A periodically acting hygrometer.

In a hygrometer of this type, for which the block diagram is shown in Figure 124, the dew point is established by a change in the condensation surface of a glass which is cooled by a thermocouple. The hygrometer has the following basic sub-assemblies: a cooling system, a dew indicator, an electrometric bridge, a two-stage magnetic amplifier, a rectifier to supply the bridge, a microthermistor for temperature measurement, and a fan with a starting mechanism for drawing in the gas tested.

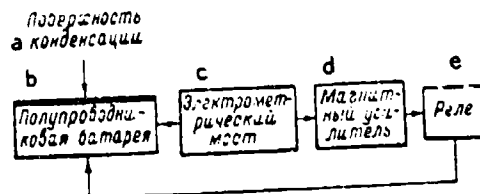


Figure 124. The block diagram of a periodically-acting hygrometer.

Key: a, Condensation surface; b, Semiconductor pile; c, Electrometric bridge; d, Magnetic amplifier; e, relay.

The cooling system consists of a thermocouple and a radiator for heat removal from the hot junctions of the thermoelement to the surrounding air. In order to reduce the temperature difference between the hot junction of the thermoelement and the surrounding air, the radiator area was increased somewhat in comparison with theoretical calculations, and amounts to 1,000 cm<sup>2</sup>. This provides a reduction of 2-3° in the parasitic temperature drop between the radiator and the surrounding medium. Under fixed conditions, and with an optimum supply current of 10 a and a surrounding air temperature of 20°, a temperature of -11° is obtained on the cold junction after 50-60 seconds. In drawing-in gas under investigation, the heat load on the cold junction increases and the maximum temperature difference obtained decreases. At a selected air flow rate of 3 m/sec, a temperature of -10° was established on the cold junction.

A glass (width 2 mm, length 5 mm, thickness 0.2 mm), serves as the dew indicator. A platinum coating<sup>1</sup> is applied to the glass by means of cathod sputtering which has a gap with a width of 10-30 μ. Electrodes for connection of the platinum with the electrical circuit of the hygrometer are soldered with Wood's alloy to silver contacts which are applied by braising. The glass with its applied coatings is attached with an epoxy cement to the cold junction of the thermoelement. The semiconductor pile and the condensation surface are protected with a

<sup>1</sup>Platinum was chosen after it became clear that a coating of silver, copper, palladium and a number of other metals were destroyed during the operating process. This was apparently associated with the low mechanical strength of the bond between these coatings and the glass under the influence on these coatings of capillary forces of condensed moisture.

heat insulating cover to provide thermal insulation from the surrounding medium. The gas tested is drawn in through a special nipple.

The hygrometer is supplied from the 220 v network. The operating principle of the electrical circuit of the device is as follows: as a result of the appearance of dew, the balance of the electrometric bridge changes, and a signal of 30-40  $\mu$  a is applied to the magnetic amplifier; the unbalance signal, amplified to 24 ma, opens relay RKS, which interrupts the circuit to the thermoelement and vaporization of the condensed moisture occurs. When the dew disappears, the relay switches on the thermoelement and the process is repeated. The temperature at which the dew appears is measured by a thermistor MT-54, which is mounted directly under the cooled glass. The temperature of the surrounding medium is measured by another thermistor, which is placed in the flow of the gas undergoing investigation. The circuit permits balancing the electrometric bridge before beginning measurements, and also permits establishing the required voltage for the thermistors.

It must be noted that the sensitivity of the device changes, depending on the width of the gap in the layer of platinum applied to the glass. It was revealed that with a distance between the electrodes of 10 $\mu$  (with a gap resistance of 1-1.5 megohms), the device establishes the appearance of dew several seconds earlier than can be established with a microscope ( $\times$  119). It was established that the hygrometer sensitivity is basically established by the response time of the relay in the amplifier, therefore the employment of films with very small gaps in a given construction is not advantageous. One measurement cycle (condensation -- vaporization) requires 20-30 seconds.

Tests of the device have revealed that the dew point temperature is determined with an accuracy of  $\pm 1\%$ , and the measurement spread does not exceed  $0.5^\circ$ . The hygrometer permits measuring the humidity of gases with a dewpoint temperature from  $+20$  to  $-10^\circ$ . Measurement of the humidity of drier gases is limited due to the fact that in this connection moisture condensation occurs in the form of a solid phase and the surface conductivity of the glass changes by an amount insufficient to obtain the required signal.

An overall view of a periodically acting hygrometer is shown in Figure 125.

## GRAPHICS NOT REPRODUCIBLE

Figure 125. An overall view of a periodically acting hygrometer.

A continuously operating hygrometer.

An automatic continuously operating hygrometer is based on a change in the reflectivity of a mirror upon the appearance of dew.

In 1958 an industrial version of a thermoelectric automatic condensation hygrometer featuring continuous operation was developed, which permitted measuring the temperature of the dewpoint of air or of any industrial gases from  $+50$  to  $-50^{\circ}$ . The principal block diagram of the hygrometer is shown in Figure 126. Mirror 1 is placed on the cold junction of the thermoelectric pile. A jet of gas, the humidity of which must be determined, is blown over the mirror in the process of measurement. The mirror is illuminated by a beam of light from illuminator 2, which is supplied from source 3. The light which is reflected from the mirror falls on the FC-K photoconductive cell 4. The electronic control circuit is adjusted in such a manner that when the quantity of light which falls on the photoconductive cell changes, which occurs when dew appears on the mirror, photocurrent amplifier 5 delivers the signal to the

The temperature at which dew appears on the mirror is established by microthermistor 10, which delivers a signal to the regulating device and to the recorder. After the temperature of the appearance of the dew is established, the regulating device delivers a signal to the reverse current circuit 8, which supplies the thermopile from rectifier 9. The thermopile is switched from the cooling to the heating mode; dew, which has condensed on the mirror, is vaporized, after which the reversing circuit delivers a forward current to the thermopile and the entire process is repeated. The hygrometer is capable of automatically measuring the humidity with a rate of 30 cycles per hour.

The thermoelements 2 and 9 of the first stage consisting of 5 couples are soldered to the heat removal system, which consists of 6 brass bars 11, which are electrically insulated from each other. Channels for the passage of water are located within the bars. Water is delivered to the thermopile through nipple 1. The heat removal system is filled with epoxy resin 10, and as a result of the system forms a single,

structurally finished sub-assembly. One thermoelement 4 of the second stage is soldered to the dual-connecting plates 6 and 8, which are attached with epoxy cement. The metallic mirror is subsequently soldered to the collector of the cold junctions 5 of the second stage. In order to reduce parasitic heat flows, the thermoelements are covered with a layer of foam plastic 3 and are protected with plexiglass cap 7. The electrical supply to the thermopile is accomplished through two current-carrying busbars, which are attached to the nipples of the cooling water supply. The thermoelectric pile described possesses significant refrigerating capacity as a result of the series connection of the first and second stages. This is achieved by means of the selection of an appropriate design for the connecting plates, and for the number and geometry of the semiconductors and a number of other factors. An overall view of the thermoelectric hygrometer is shown in Figure 128.

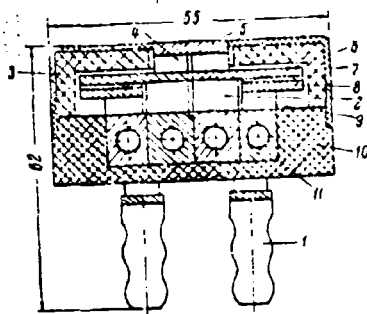


Figure 127. A section of a thermopile for a continuously operating hygrometer.

GRAPHICS  
NOT REPRODUCIBLE

Figure 128. An overall view of the hygrometer for continuous operation (the power supply and regulation section is not shown).

The basic specifications for the continuously operating hygrometer are shown below.

Operating current in the maximum cooling mode	60 a
Thermopile voltage drop	0.4 v
Thermopile water consumption rate	50 l/h
Size of the condensation surface (mirror)	10 × 15 mm
Dimensions of the basic sub-assembly of the device (excluding the power supply and the automatic regulating circuit):	
height	275 mm
diameter	180 mm
Weight of the basic sub-assembly of the device	11 kg



In 1964 still another version of the condensation hygrometer for continuous operation was developed, utilizing thermoelectric cooling of the condensation surface.<sup>1</sup>

The DDN-1 automatic photoelectronic humidity indicator, which is mass-produced by industry, was selected as the basis for this device. In the DDN-1 device, cooling of the condensation surface, which is the mirror, is accomplished by means of throttling compressed air. The moment of the appearance of dew is established by measuring the reflectivity of the mirror with a special photoelectronic circuit. The mirror temperature is measured by a platinum resistance thermometer. The use of the DDN-1 device is associated with a number of inconveniences, including the necessity to have available a source of high-pressure air (up to 250 atm) to cool the condensation surface. At the same time the basic sub-assemblies of the device, which include the photoelectronic capacitors and the temperature gauge possess sufficiently high accuracy and reliability in operation. Therefore, a thermoelectric cooler was developed for the DDN-1 device. Structurally, the thermoelectric cooler was made in such a way that with minimum alterations it could replace the cooler of the DDN-1 device.

The thermoelectric cooler was assembled with a three-stage thermopile with series current supply to all stages. There are 15 thermoelements in the first stage of the thermopile, three in the second, and one in the third. Heat removal from the hot junctions of the thermopile is accomplished by running water. A full-wave rectifier equipped with VG-50-15 diodes serves as the power supply for the thermopile.

A filter choke is used to smooth the rectified current ripple. The thermoelectric cooler and the rectifier power supply are mounted on the frame of the DDN-1 device in place of several sub-assemblies and parts which cooled the device by means of throttling compressed air. A chromium mirror is soldered to the collector of the cold junction of the third stage thermoelement. A change in the reflectivity of the mirror signals the appearance of dew. Since the device is intended for continuous operation, after each cooling cycle it is necessary to clean the moisture from the mirror. This is accomplished by heating the mirror to a temperature of 30-40°.

Heating of the mirror could be accomplished by means of reversing the polarity of the current to the thermopile, but this would lead to undesirable temperature fluctuations of the entire pile. Therefore the collector of the cold junction of the third stage thermoelement was wound

---

1 In addition to members of the APAN SSSR [Institute of Semiconductors of the Academy of Sciences of USSR], A. S. Kucherov participated in the development of this device.

with a heater, which is switched on automatically when it is necessary to vaporize moisture which has condensed on the mirror. Here the thermopile is not turned off, but a positive temperature on the mirror is achieved due to the fact that the output of the heater predominates over the refrigerating capacity of the thermopile third stage. A platinum resistance thermometer is wound on the collector of the cold junction of the third stage thermoclement. The thermometer is the sensor for the automatic dewpoint measurement circuit. When the gas being investigated flows over the mirror at a rate of 3 m/sec., the mirror temperature may be reduced to  $-70^{\circ}$ .

Some data characterizing the thermoelectric cooler for the DDN-1 device are shown below.

Operating current	42 a
Voltage drop	1.5 v
Power requirement	63 w
Minimum condensation surface temperature (with a water system heat removal temperature of $+18^{\circ}$ )	$-70^{\circ}$
Temperature difference provided by the thermopile	$88^{\circ}$
Water consumption rate in the heat removal system	50 l/h
Diameter of the condensation surface (mirror)	20 mm
Thermopile dimensions	120 × 55 × 60 mm
weight	1.3 kg

#### 54. A device for Thermometer Calibration

Mercury and alcohol thermometers, before being released from the manufacturer for use, must undergo a calibration operation, which consists of a comparison of the indications with the indications of a standard thermometer. The calibration operation is also carried out in meteorological organizations during periodic checking of the thermometers in use.

Although this checking presents no difficulty in the range of temperatures above room temperature, the establishment of temperatures from room temperature to temperatures below  $0^{\circ}$  is associated with a certain amount of difficulty. In these cases a number of cooling agents are employed, which have specific, so-called cryostatic temperature points. The thermometer undergoing tests and the standard thermometer are placed in an appropriate mixture, and on the basis of their indications the temperature error at one or more points on the scale is determined.

However, the method described is associated with a number of shortcomings, including discreteness of comparison temperature points. If the capillary tubes of the thermometers were of exactly the same diameter along their entire length, the method of extrapolation from point to

point would result in the temperature values along the entire scale of the thermometer. But due to a number of technical causes, the capillary tube diameter is not constant, and as a result the thermometer scale will not be completely uniform. The comparison of thermometers at specific temperature points will not give true temperature indications in the interval between these points.

Thus a pressing need arose for a smooth temperature change within the medium in which the calibration is being conducted. The use of refrigerators for this purpose is associated with difficulties in establishing smooth regulation. In this connection a special thermoelectric device (Figure 129) was developed which permits changing the temperature both in the positive and in the negative ranges. The value and accuracy of the temperature change is established by the value of the current supply to the device.

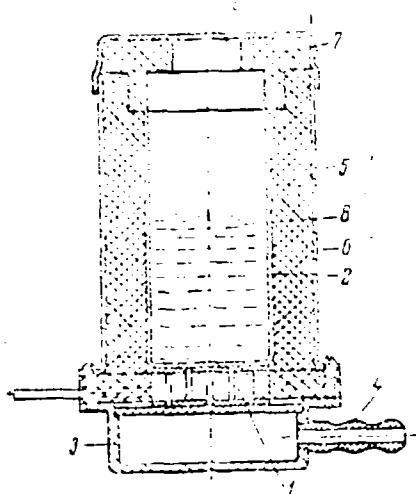


Figure 129. A section of a device for thermometer calibration.

The cold side of the thermoelectric pile 1 of this device is in good thermal contact with internal shell 2, which forms the operating chamber of the device. Heat removal from the hot junctions of the thermopile is accomplished by means of cooling system 3. Water is connected to the device through nipple 4, and flows through the cooling system. The exterior surface of the interior shell is surrounded by a layer of foam

plastic thermal insulation 5. External cover 6 is equipped with a removable top with thermal insulation 7. For best heat transfer inside the operating chamber of the device, the latter is filled with a mixture of alcohol and water 8. Both the thermometer undergoing calibration and the standard thermometer are introduced into the internal volume of the thermostat system through an aperture in top 9. A smooth temperature change within the thermostat system is accomplished by means of changing the value of the current supply to the system. When it is necessary to perform calibration operations in the temperature range above room temperature, the direction of the current supply to the pile is reversed and the operating liquid is replaced with oil.

The thermostat system is characterized by the following operating parameters.

Maximum temperature reduction in the cooling mode (with a water system heat removal temperature of 15°)	40°
Maximum current supply	25 a
Direct current power requirement	20 w
Internal volume	75 cm <sup>3</sup>
Maximum positive temperature	50°
Dimensions: diameter	65 mm
height	120 mm
Weight	450 g

A second version of the thermoelectric device for thermometer calibrations (Figure 130) was developed subsequently. This device differs from the first version only in the structural configuration of the water system of heat removal from the thermopile. In the second version of the device, water passes through channels formed directly within the hot connecting plates of the thermopile. As a result, parasitic temperature differences between the water and the hot thermopile junctions are reduced to a minimum and the maximum temperature difference furnished by the device was raised to 45°.

#### 55. Thermoelectric Null-thermostat Systems

Differential metallic thermocouples are usually employed in industrial and laboratory practice in order to measure the temperature. As is known, a differential thermocouple has a so-called control junction, which must be maintained at a constant temperature. For convenience in reading the values of the temperature measured, the control junctions are usually placed in melting ice, which has a temperature of 0°.

In a number of cases the employment of melting ice is associated with specific operating inconveniences, especially during thermocouple utilization in remote-controlled systems. In this connection two design versions of thermoelectric null-thermostat systems, which furnish an automatically maintained temperature of  $0^{\circ}$  were developed.

In the first type of null-thermostat system, automatic temperature maintenance inside the operating chamber of the device is accomplished by means of a special two-position regulating circuit. The temperature sensor is a small mercury relay.

A section of this type of null-thermostat system is shown in Figure 131. Thermoelectric pile 5 consists of four thermoelements. Section 2, which is subject to thermostatically-controlled cooling, is soldered to these cold junctions of the thermoelements through dual connecting plates 9. The hot-junction side of the pile thermoelements are soldered through dual connecting plates 10 to heat transfer base 7, which is equipped with a system of radiator plates 6. This system provides for heat removal from the thermopile to the surrounding air. The control junctions of thermocouple 3 and temperature sensor 4 are installed within thermostatically-controlled block 2, which is manufactured of copper. In order to reduce heat flow to the thermostatically-controlled section from the surrounding medium, the section is protected by a layer of thermal insulation 8. The device is inclosed within metallic shell 1, which is equipped with a cover. Mounted on the cover is a block with the extended control leads for the thermocouple.

## GRAPHICS NOT REPRODUCIBLE

Figure 130. An overall view of the second version of the thermometer calibration device.

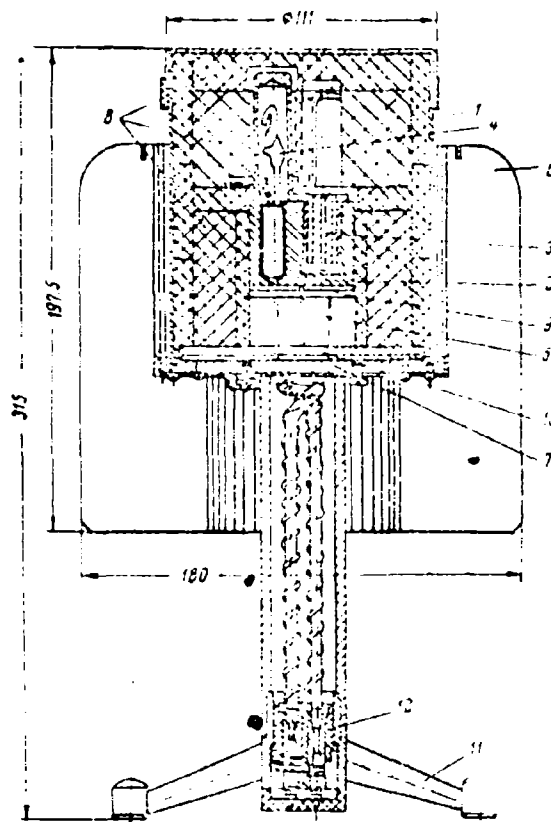


Figure 131. A section of a null-thermostat system.

The device is mounted on special stand 11, which is equipped with terminal block 12 through which the rectifier is connected to the thermostat system. The supply rectifier for the thermoelectric pile of the thermostat system is a full-wave circuit (Figure 132). Power transformer  $Tr_1$  may be connected to a line input of 127/220 v. Power germanium diodes  $D_1$  and  $D_2$  are employed as rectifiers. Filter choke Ch serves to smooth ripple of the direct current delivered to the thermopile. The automatic temperature stabilization circuit includes transformer  $Tr_2$ , rectifier  $D_3$ , electrolytic filter capacitor C, two relays  $K_1$  and  $K_2$ ,

which on command from the temperature sensor connect the current supply to the thermopile. Signal lamp LC and LH serves as indicators to show the thermopile mode of operation, "heating" or "cooling".

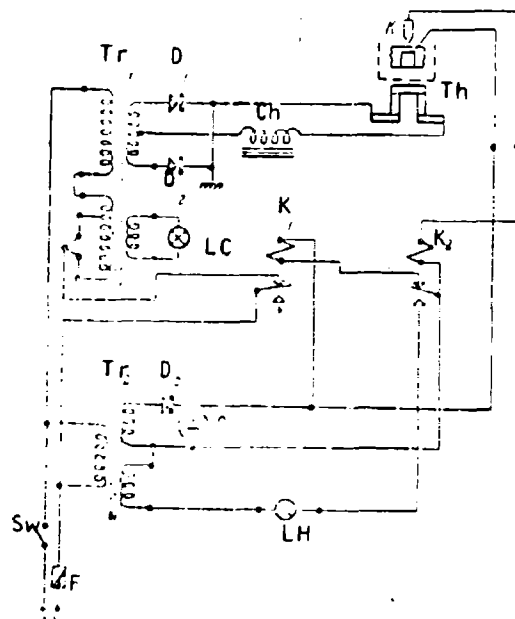


Figure 132. The electrical power supply and regulation circuits of the null-thermostat system.

The basic specifications of the null-thermostat system are shown below.

Operating current in the cooling mode	16 a
Thermopile voltage drop in the cooling mode	0.4 v
Operating temperature on the thermostatically controlled section (with an ambient temperature of 30°)	$0 \pm 0.015^\circ$
Dimensions: diameter	180 mm
height	315 mm
Thermostat system weight	3.5 kg

Dimensions of the power supply and regulation section:

height	150 mm
width	150 mm
length	300 mm
Power supply and regulation section weight	6.8 kg

An overall view of the null-thermostat system with the power supply and regulation section is shown in Figure 133.

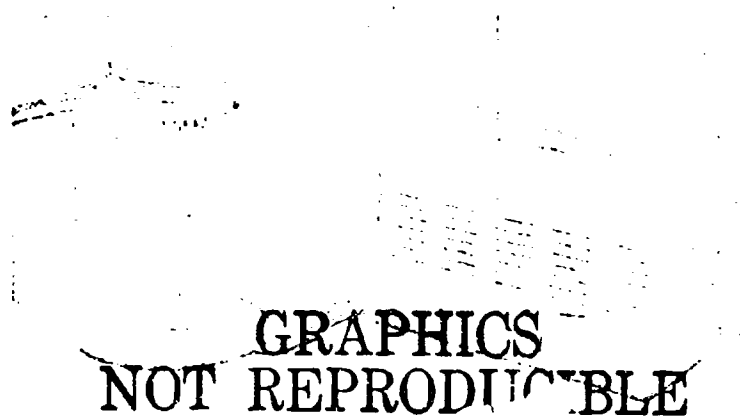


Figure 133. An overall view of the null-thermostat system with the power supply and regulation section.

In meteorological practice, and also in conducting a number of laboratory investigations, the necessity often arises to maintain a temperature of  $0^{\circ}$  with a great degree of accuracy. For this reason a precision thermoelectric null-thermostat system, which maintains a temperature of  $0^{\circ}$  with an accuracy of  $\pm 0.01^{\circ}$ , was developed. Automatic temperature maintenance at the  $0^{\circ}$  level in this device is based on a change in the volume of water when it freezes. This change in volume is registered by a highly-sensitive contact relay, which is part of a control circuit similar to that shown in Figure 132.

A section of the precision null-thermostat system is shown in Figure 134. The hot junction side of a thermoelectric pile consisting of 8 series-connected thermoelements 4 is soldered to the heat removal system. The water and the electrical supply to the thermopile are furnished through nipple 5. Copper cylinder 3 is soldered to the cold



junctions of the thermopile through electrically-insulated connecting plates. The entire internal volume of the cylinder is filled with distilled water. The control junctions of thermocouple 1, with which are subject to thermostatically-controlled cooling, are introduced into the cylinder through special feeling device 2. Bellows 6 are hermetically attached to the upper surface of shell 3. Relay contacts 7, which are connected to the control circuit of the devices, are located inside the bellows.

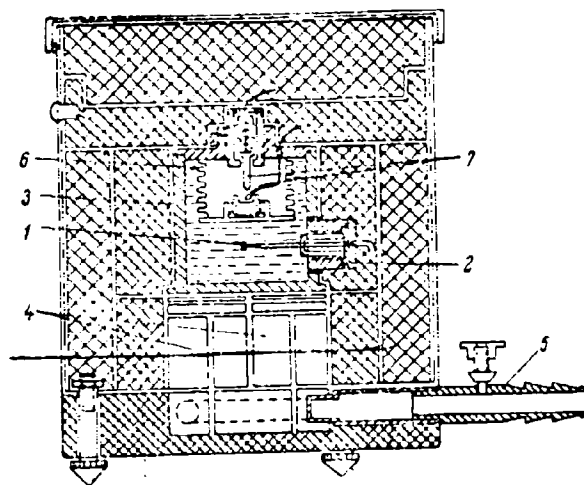


Figure 134. A section of a precision null-thermostat system.

During operation of the thermopile, water located in the cylinder is cooled and upon attaining a temperature of  $0^{\circ}$  begins to freeze near the walls of the cylinder. When the ice forms, its greater volume creates pressure on the water which remains unfrozen, which transmits this pressure to the bellows. The bellows are compressed and close the contacts of the relay. The signal from the relay is applied to the control circuit and the latter interrupts the current to the thermopile. While the thermopile is disconnected, environmental heat flow and heat flow along the arms of the thermoelements cause partial melting of the ice on the cylinder walls, which leads to a volume reduction and correspondingly to a reduction in pressure on the bellows. The bellows open the relay contacts, and the control circuit switches on the circuit to the thermopile. In this manner, a specific quantity of ice is continuously maintained inside the cylinder. The quantity of ice is determined by the position

of the relay contacts in the bellows. With a uniform state inside the cylinder, the ice-water within is maintained at a temperature of  $0^{\circ}$ . In order to reduce parasitic heat flow from outside the operating volume of the device, the top and side are thermally insulated with a layer of foam plastic.

The basic specifications of the device are as follows.

Operating current	16 a
Voltage drop on the device	0.7 v
Operating chamber temperature	$0 \pm 0.001^{\circ}$
Water system heat removal temperature	$20-30^{\circ}$
Surrounding air temperature	$0-40^{\circ}$
Heat removal water system temperature	0.5 l/min
Dimensions: diameter	100 mm
height	120 mm
Weight	1.1 kg

#### §6. Microscope Stages with Regulated Temperatures

In conducting microscopic investigations it is often required to trace the progress of a flow process for the behavior of a biological subject under various temperature conditions. Existing designs for instruments intended for these purposes permit, as a rule, the establishment of a temperature above room temperature. Investigations at temperatures below room temperature are, in practice, difficult to achieve due to the complexity of the apparatus employed for these purposes, although the low-temperature range is of paramount interest in some cases. Four design versions of microscope stages were developed for the purposes indicated.

Figure 135 shows a thermoelectric microscope stage intended for the investigation of objects in transmitted light in the temperature range from  $-7$  to  $+60^{\circ}$ . Four thermoelectric couples 3, which form the thermoelectric pile in the shape of a closed tetragon, are mounted on five segmented plates 5, which form the base of the stage. Straight-through aperture 6 is located in the middle of the pile for the passage of light from the microscope light source. When the stages operating in the cooling regime, the lower segmented plates are the hot radiators, which dissipate heat from the thermoelectric couple to the frame of the microscope and to the surrounding air. The slide and the cover glass, which contain the object under investigation, are placed on cold-connecting plates 2, which lie in the same plane. The cooling effect from the upper cold-connecting plates of the thermoelements is transmitted through the slide to the object investigated. In order to provide the stage with the required mechanical strength, all the parts are cemented with epoxy resin 4. The current supply to the stage is accomplished through two

terminals 1, which are connected to the two corresponding lower connecting plates. The power required by the stage from the direct current source equals 2 w at a current of 14 a.

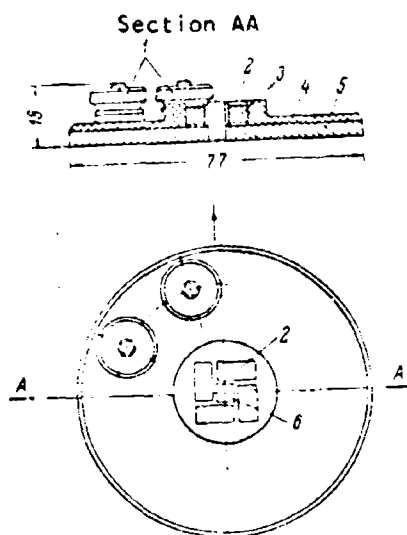


Figure 135. A transmitted-light microscope stage with self-cooling.

The overall dimensions of the stage are: height 10 mm, diameter 70 mm. The weight is 160 g. An overall view of the stage is shown in Figure 136.

**GRAPHICS  
NOT REPRODUCIBLE**

Figure 136. An overall view of the microscope stage with self-cooling.

In a number of cases it is required to conduct microscopic investigations with more intensive cooling of the objects investigated. A microscope stage which furnishes a temperature reduction of the object placed on it down to  $-25^{\circ}$  is shown in Figure 137.

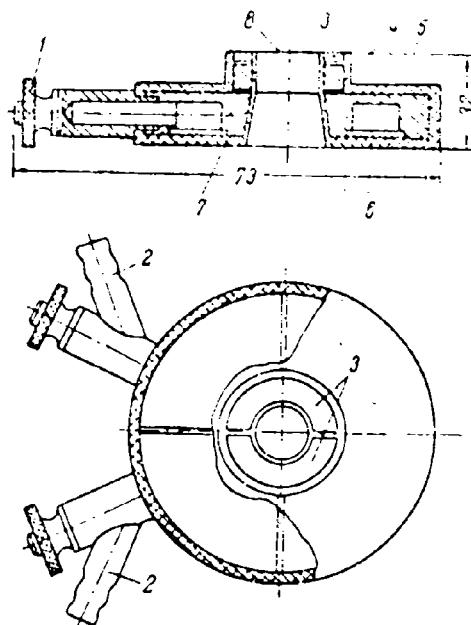


Figure 137. A transmitted-light microscope stage with liquid heat removal.

In contrast to the stage described above in which heat removal from the hot junctions of the thermoelements was accomplished by convection to the surrounding medium and to the frame of the microscope, the design of this stage provides for water cooling of the hot junctions of the thermoelements. Channels 6, through which the cooling water passes, are placed directly in the hot connecting plates 7, which form the base of the stage. Two thermoelements 4 are mounted on three plates. The cold junctions of the thermoelements are connected by two semi-circular connecting plates 3, which are equipped with straight-through aperture 8 in the middle for transmitted light from the microscope light source. The slide with the object under investigation is placed on the upper connecting plates.

The current supply is delivered through terminals 1, which are also equipped with nipples 2 for water input and output. The individual

elements of the stage are mechanically attached with epoxy resin 5. At a current of 20 a, the required power equals 3 w. The water consumption rate is 250 cm<sup>3</sup>/min. Stage dimensions are diameter 50 mm, height 15 mm. The weight is 110 g.

An overall view of a stage of this type is shown in Figure 138.

## GRAPHICS NOT REPRODUCIBLE

Figure 138. An overall view of  
a transmitted-light microscope  
stage with liquid heat removal.

In 1964 a second design version of a microscope stage for transmitted light with liquid heat removal was developed. In contrast to the first version, in this device the operating height was reduced by more than two times, i.e., the height between the plane of the object investigated and the base of the stage. This permits conducting investigations at greater magnifications than with the first version. In addition, the design of the stage permits sealing the area of the location of the slide and the cooled object, which excludes misting of the latter. A microthermistor is installed on the cold junction in order to measure the temperature. Figure 139 shows a section of this version of the stage.

Base 1, which is formed of copper, consists of two polycylinders 2 and 3, which are insulated from each other. Semiconductors 4, which form the thermoelement, are mounted in a recess in the base. In order to provide mechanical strength for this structure, each arm of the thermoelement consists of two parallel-connected semiconductors. Collector 5 of the cold junctions is a chromed copper disk with an aperture, on which slide 6 is placed which contains the object under investigation. Heat removal from the hot junctions of the thermoelement is accomplished by running water, which flows through annular channel 7, formed within the base. The water input and output are accomplished through two nipples 8. Current supply to the stage is accomplished through terminals 9, which are installed on two sides of the base. The MKMT-16 microthermistor 10, the leads of which are connected to two screws 11, measures the temperature of the cold junction collector.

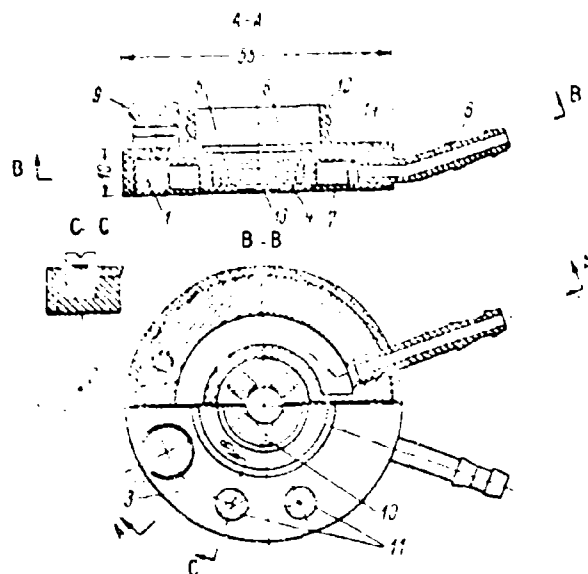


Figure 139. A section of the third version of the transmitted-light microscope stages with liquid heat removal.

Special aluminum cylinder 12, which is housed in a thin resin tube, serves to seal the internal volume of the stage in order to prevent misting of the slide. The other end of the tube is covered by the objective tube of the microscope. The lower end of the aperture in the stage is also sealed by glass 13. In order to provide the structure with mechanical stability, the stage parts are filled with white-decorative epoxy resin 14.

An overall view of this type of stage is shown in Figure 140.

The basic stage data are shown below.

Operating current	20 a
Voltage drop	0.1 v
Power requirement	2 w
Operating temperature range provided by the stage (at a water system heat removal temperature of 18°)	-25 to +50°
Water consumption rate in the heat removal system	15 l/h

Dimensions: diameter  
                  height  
Stage operating height  
Weight

60 mm  
16 mm  
12 mm  
150 g

## GRAPHICS NOT REPRODUCIBLE

Figure 140. An overall view of the third version of the transmitted-light microscope stage.

Figure 141 shows a fourth design version of a thermoelectric microscope stage, which provides for operation in reflected light.

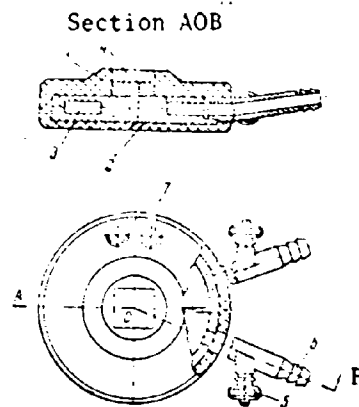


Figure 141. A section of the microscope stage for reflected-light observation.

In this stage thermoelements 1 are mounted on hot-connecting plates 2 which have an annular channel 3 for the passage of cooling water; upper plate 4, which forms the operating surface of the stage is connected to the cold-junctions of the thermoelement. The current supply is provided through terminals 5, soldered to two nipples 6, which are the connections for water input and output. The leads of the copper-constantan thermocouple are extended to two connecting screws 7. The thermocouple serves to control the temperature of the operating stage. The basic parameters of the stage of this type are shown below.

Maximum temperature difference (at a water temperature of 18°)	40°
Operating current which provides the maximum temperature difference	45 a
Power requirement	3 w
Dimensions: height	18 mm
diameter	55 mm
Weight	134 g

An overall view of the reflected-light microscope stage is shown in Figure 142.

**GRAPHICS  
NOT REPRODUCIBLE**

Figure 142. An overall view of the microscope stage for observations in reflected light.



## CHAPTER XV. Thermoelectric Conditioners and Domestic Refrigerators

In 1949 the Academician A. F. Ioffe suggested for the first time the utilization of the thermoelectric cooling effect for purposes of heating and cooling the air in official and domestic areas. For example, if a thermoelectric pile is located in the walls of a building so that the hot junction radiators are located within the room, and the cold junction radiators are located on the "street", then the cold radiators of the thermopile will absorb heat from the cold "street" air, while cooling it still further, and the hot junction radiators of the thermopile will release this heat inside the room. In this manner the thermoelectric pile provides a transfer of heat from a low-temperature medium to a higher-temperature medium, i.e., it fulfills the role of a heat pump.

The reversibility of a thermoelectric pile, i.e., the possibility of transferring the pile from the heating to the cooling regime by simply reversing the direction of the direct current permits utilization of the pile for cooling a room as well, at the expense of heating the "street" air. The system described of utilizing a thermopile for heating and cooling, i.e., air-conditioning in rooms, provides for the use of air as an operating medium. However in a number of cases water, which flows through the heat removal circuit, is the operating medium.

Thermoelectric conditions may operate with a thermodynamic efficiency of more than 100%. This means that if, for example, 100 watts of electrical power delivered to the thermopile, we obtain in the room 200-300 w. (!). Naturally, there is no violation of thermodynamic laws here, since 100 watts of energy have entered the room, released in the thermopile in the form of Joule heat and Peltier heat, and the remaining 100-200 watts of heat are transferred from the "street". This supplementary heat again returns to the "street" as a result of imperfect thermal insulation in the building walls.

In thermoelectric instrument construction technology, the work increasingly involves the development of thermoelectric conditioners of diverse types for both official and domestic purposes.

#### §1. Conditioners for Official Purposes

Transportation workers display the greatest interest in thermoelectric air-conditioners. In fact, air-conditioners employed in maritime, railroad, air and automobile transportation facilities are primarily intended for the establishment of comfortable conditions for the passengers and service personnel. A number of specific requirements have been established for air-conditioners, which are determined by operational conditions. In particular, these requirements include: quiet operation, long service life, resistance to vibrational and shock loads, operational capability while tilted or while rolling to a significant extent, minimum time to establish normal operation, simplicity and reliability in construction and a number of other factors. Air-conditioners based on the thermoelectric effect with semiconductors fully satisfy all these conditions.

During the period from 1961 to 1965, a number of organizations in the Soviet Union carried on developmental work involving thermoelectric air-conditioners for the passenger cabins of ships, for railway compartments and for other purposes. The basic parameters of these conditioners are shown in Table 22.

Table 22  
The Basic Parameters of Domestically-Manufactured Thermoelectric Air-conditioners

Conditioner type	Refrigerating capacity, kcal/h	Heat removal system	Purpose
TLZ-25	150	air-air	Universal
KR-04	350	" "	Air-conditioning in railway car compartments.
KR-1	1000	" "	Temperature stabilization in radioelectronic equipment.
--	1600	" "	Air-conditioning in railway car compartments.
KR-2	2000	" "	Temperature stabilization of radioelectronic equipment.
KR-3	3000	" "	Temperature stabilization of radioelectronic equipment.

continued on next page

Table 22 continued...

Conditioner type	Refrigerating capacity, kCal/h	Heat removal system	Purpose
KS-6	6000	Water-air	Air-conditioning in ship passenger cabins.
KS-9	8000	" "	
AGT-1	4000	Water-water	Intensive hypothermia during surgical operations.

NOTE. The conditioners listed in the table were developed at the SKB [Special Design Office] of semiconductor instruments of the Ministry of Instrument Manufacturing, Automation Methods and Control Systems of the USSR, at the Power Engineering Institute of the Academy of Sciences of the Latvian SFR, and at the Odessa Technological Institute of the Food and Refrigeration Industries.

The operational effectiveness, design, weight and overall size characteristics of thermoelectric air-conditioners depend to a large extent on the system of heat removal from the hot junctions of the thermopile. Conditioners intended for use by the sea and river fleets have, as a rule, a liquid heat removal system. Here fresh water (condensate) or sea water is employed as an operating liquid.

A diagram of a conditioner with liquid heat removal is shown in Figure 143.

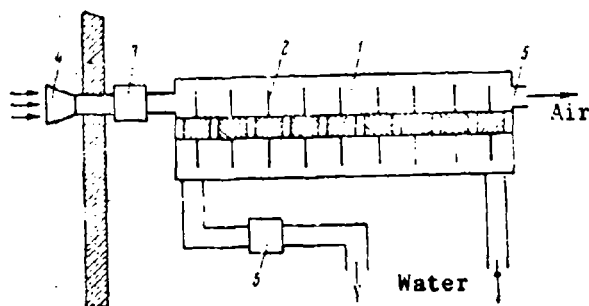


Figure 143. A diagram of the construction of a thermoelectric air-conditioner using the air-water system.

A system of heat exchange (radiator) plates 2 extends from the side of the cold junctions of thermopile 1. Air is forced through the radiator system by means of fan 3. The air intake from the outside is accomplished through opening 4, and the exhaust of cooled or warmed air is accomplished through opening 5. The hot junctions of the thermopile have an extended system of heat removal, which is submerged in running water. The water is transferred by pump 6. In constructions using a liquid heat removal system, it is necessary to take into consideration the possibility of water electrolysis (in particular, with sea water) under the influence of the voltage applied to the thermopile. In this connection, the sides of the hot junctions of the individual thermoelements must be electrically insulated from the cooling liquid (see Part II, Chapter VI, §3).

Ship air-conditioners, developed in the USSR, have refrigerating capacities from 400 to 17,000 kCal/h. Abroad, in particular, in the USA and in Japan, a great deal of attention has been devoted to the development of thermoelectric air-conditioners for submarines. This interest is completely understandable, since a contemporary submarine operates for long periods of time autonomously both on the surface and under water, which requires the establishment of normal living and working conditions for the crew. The use of compressor conditioners in submarines is extremely undesirable, for they create noise, cease operating during rolling and tilting and most importantly, employ freon as a transfer agent. The leakage of freone into the atmosphere of a submarine (under emergency conditions) is completely inadmissible. According to foreign press data, the employment of thermoelectric air-conditioners in submarines is quite important and promising.

Thermoelectric conditioners with air heat removal from the hot junctions of the thermopile are intended for use in railway transportation facilities to establish comfortable conditions in railway car compartments, to reduce the temperature in the operators cab of a traveling crane in "hot shops", in tractor cabins, in buses and in light motor vehicles, i.e., in all cases requiring the establishment of normal temperature conditions for individuals.

A diagram of a thermoelectric conditioner with air heat removal is shown in Figure 144.

A radiator system is installed on the sides of the cold and hot junctions of thermopile 1. Air is forced over the radiator systems by fans 2 and 3. The external air which passes through the radiator system of the hot side of thermopile 4 is exhausted to the outside. Air in the cold circuit is forced through the radiator system of the cold junctions of the thermopile by fan 3 and enters the operating area.

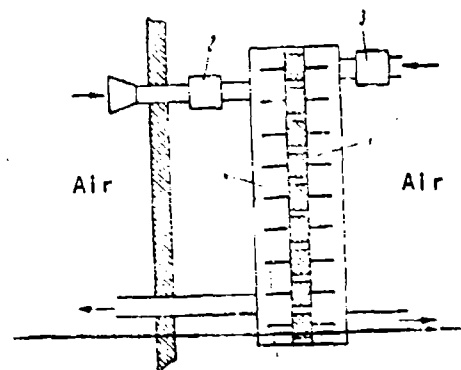


Figure 144. The construction of a thermoelectric conditioner which employs the air-air system.

Comprehensive testing of one type of thermoelectric conditioner with a refrigerating capacity of 350 kCal/h, intended to provide comfortable conditions in a railway car compartment, was accomplished at the Power Engineering Institute of the Academy of Sciences of the Latvian SSR. Two independent fans forced air at a temperature of 25° through the radiator system of the cold and hot junctions of the thermopile with flow rates of 150 and 225 kg/h, respectively. The basic operating parameters of the conditioner were determined for the cooling and heating modes as a function of the value of the supply current to the thermopile.

It is apparent from an examination of the curves shown in Figures 145 and 146 that in the cooling mode, the maximum refrigerating capacity  $Q_0$  attains the value 370 kCal/h with a current of 220 a. Here  $\Delta T = 17^\circ$ , and the coefficient of performance  $\epsilon = 0.5$ . In the heating mode, with the same current of 220 a, heat output  $Q_0^1$  attains a value of 1,040 kCal/h, with a temperature difference of  $\Delta T^1 = 29^\circ$  and the coefficient of performance  $\mu = 1.6$ .

Thus it may be concluded that even now the utilization of thermoelectric air-conditioners in railway transportation facilities on several routes in the central area of the country is technically advantageous and economically justified but notwithstanding the fact that the coefficient of performance of a thermoelectric conditioner is somewhat lower than that for compressor conditioners. However, the high coefficient of performance of a thermoelectric conditioner in the heating mode makes it significantly more economical than the method of electrical heating usually employed.

Preliminary calculations reveal that the thermoelectric conditioner, in so far as the total energy requirement is concerned (in both operating modes), will be 20-30% more economical than a system of electrical heating and refrigeration.

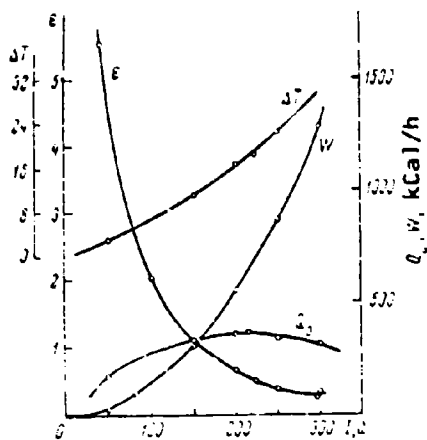


Figure 145. Air-conditioner load characteristics for an air-air system in the cooling mode.

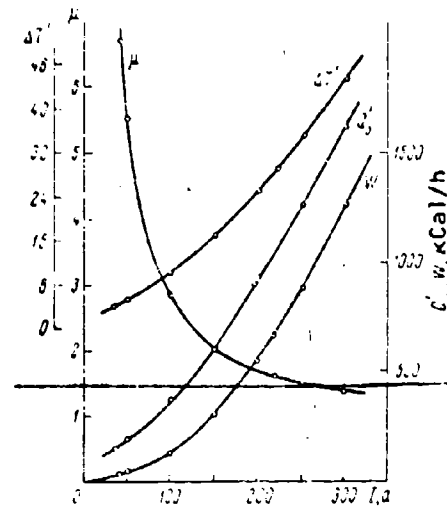


Figure 146. Air-conditioner load characteristics for an air-air system in the heating mode.

Tests of a thermoelectric conditioner with liquid heat removal from the thermopile hot junctions were conducted at the Odessa Technical Institute of the Food and Refrigeration Industry. The conditioner, which was developed at this institute, was designed to provide comfortable conditions in the passenger cabins of sea and river vessels. The results of conditioner tests in the cooling mode are shown in Figure 147. The temperature difference ( $\Delta T$ ), coefficient of performance ( $\epsilon$ ), and the refrigerating capacity ( $Q$ ) as functions of the value of the current supply ( $I$ ) to the thermopile are shown. All curves were obtained with a water temperature in the heat removal system of  $25^\circ$  and air input temperature to the conditioner of  $30^\circ$ . With a current of 150 a and a refrigerating capacity of approximately 1,000 w, the temperature difference between the input and the output air flow of the conditioner was  $\Delta T = 10.6^\circ$ , with a coefficient of performance of  $\epsilon = 2.1$ .

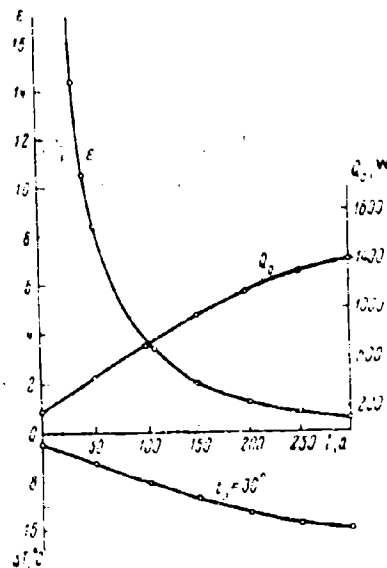


Figure 147. Air-conditioner load characteristics for an air-liquid system in the cooling mode.

It is apparent from a comparison of the test results shown above that thermoelectric conditioners for official purposes which operate on the water-air system are more effective than conditioners which operate on the air-air system.

## §2. Conditioners for Domestic Purposes

As we have pointed out previously, the thermoelectric heat pump is capable of warming a room at the expense of cooling the "street" or of reducing the temperature of a room at the expense of heating the "street". The transition from the "heating" to the "cooling" mode is accomplished simply by switching the polarity of the direct current to the thermopile. This creates very tempting possibilities for the development of thermoelectric heating-cooling assemblies for domestic needs. The basic research and experimental-design work in the development of thermoelectric heating-cooling assemblies for living areas was concentrated within the Semiconductor Heat-Pump Laboratory (LPTN), where under the direction of S. M. Lukomskiy, several types of devices designed to provide heating for living quarters in the winter and cooling for these quarters in the summer were developed. Heating-cooling assemblies of various refrigerating

capacities from 250 to 3,000 kcal/h and employing water or air as the operating medium were developed.

Figure 148 shows an assembly with a refrigerating capacity of 200 kcal/h, developed at the LPTN and manufactured at the "Santekhnika" factory. This assembly is intended to provide normal year-round temperature in small living quarters. The thermoelectric pile consists of five sections of 10 thermoelements each. Thus the refrigerating capacity of one section equals approximately 40 kcal/h. The cold and hot junctions of the thermoelements are equipped with a system of radiator plates enclosed in two housings which form the cold and hot channels for the air, which is forced through them by two independent fans. In the heating mode the coefficient of performance of the assembly was 2.5. The cost of the electrical energy required from the line by the thermoelectric heating-cooling assembly with a refrigerating capacity of 200 kcal/h is equal to only 0.67 kopeks, i.e., equal to the cost of the energy obtained from GRES [State Area Power Plant]. Here it is necessary to consider that in contrast to TETs [Heating and Power Plant], which provides only area heating, the thermoelectric assemblies also make it possible to cool these areas in the summer. With a temperature difference of 10° between the input and output of a heating-cooling assembly, the use of thermoelectric assemblies is already considered to be economically advantageous for practically all areas of the USSR. In fact, when assemblies are employed which operate on the air-air system with an ambient temperature of 30°, the temperature in the living quarters will be maintained at a level of 20°.

**GRAPHICS  
NOT REPRODUCIBLE**

Figure 148. An overall view of a thermoelectric conditioner for living quarters with a refrigerating capacity 200 kcal/h.



In utilizing assemblies employing liquid, a temperature of 25° as an operating medium (a higher water supply temperature is practically non-existent at any point in the Soviet Union), the temperature in the living quarters may be maintained at a level of 15°. The examples cited of operational tests of thermoelectric heating-cooling assemblies indicate that these assemblies are already competitive with the usual methods of heating living quarters.

### §3. High-Capacity Domestic Refrigerators

As is known, ordinary refrigerators are articles of a mass demand and are produced by industry in large quantities. At the present time compressor refrigerating assemblies or absorption devices are usually employed in ordinary refrigerators.

Compressor refrigerators are the most widely employed type. However they possess a number of defects, which include the following:

- 1) a limited period of service, which is associated with the presence in the compressor of moving parts, subject to wear, and the use of volatile refrigerants, such as freon, which produce corrosion;

- 2) the relative complexity of the manufacture of the compressor assembly, which leads to its high cost;

- 3) the significant size and dimensions of the compressor, which make it necessary to increase the size of the refrigerator cabinet.

The basic shortcoming of refrigerators employing the absorption principle is lack of economy due to large electrical energy requirements.

The concept of developing a thermoelectric domestic refrigerator arose at the very beginning of the development of thermoelectric cooling technology. The first work in this field goes back to 1951. Several models of thermoelectric refrigerators with water and air heat removal from the hot junctions of the thermoelectric piles were developed in recent years at the Semiconductor Institute of the Academy of Sciences of the USSR. The problem of heat removal in thermoelectric domestic refrigerators acquires special importance in connection with the fact that large quantities of heat are released on the hot junctions of the thermopile, which must be effectively removed. The heat removal system using running water has not been widely employed due to a number of operating conveniences, which are associated with the necessity for providing continuous water delivery to the refrigerator.

In 1955 and 1956 experimental models of thermoelectric refrigerators were developed with air heat removal to a system of radiators. However, notwithstanding a number of incontrovertible advantages, these refrigerators were not widely employed due to the insignificant volume of the operating chamber (40 liters).

On the basis of experience gained in previous developments, in 1957 a high-volume thermoelectric refrigerator was developed which employed air radiators to remove heat from the thermopile. This refrigerator, in operational and heat-engineering properties, already approached the level of contemporary refrigerators of the absorption type.

An analysis of the operation of a number of foreign and locally-produced compressor and absorption domestic refrigerators, conducted by V. A. Nayer, revealed that with an operating chamber of volume of less than 40 liters, thermoelectric refrigerators employing semiconductor materials, having  $\nu = 1.8 \cdot 10^{-3} \text{ deg}^{-1}$ , possess a higher coefficient of performance than compressor refrigerators. With operating chamber volumes up to 100 liters, thermoelectric refrigerators, economically speaking, may surpass refrigerators of the absorption type, but lag behind compressor refrigerators (Figure 149).

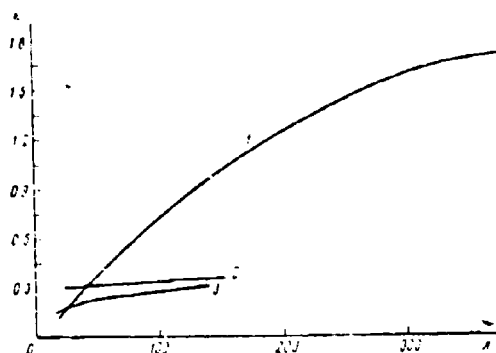


Figure 149. Dependence of the coefficient of performance on operating chamber volume for various types of domestic refrigerators: compressors (1), semiconductor (2), absorption (3).

However, structural simplicity, the lack of moving parts, and the practically unlimited period of service resulting from a lack of substances causing corrosion, it has an insignificant cost during mass-production

make the thermoelectric refrigerator a serious competitor for refrigerators of the absorption and compressor types. With an improvement in the figure of merit of semiconductor substances, more economical models will certainly be developed, which in the final analysis will displace all other types of domestic refrigerators. In this connection the clarification of problems in design and in manufacturing technology, and also the problem of obtaining full operational data for thermoelectric refrigerators are quite pressing and appropriate.

A model 1957 thermoelectric refrigerator was developed on the basis of a standard cabinet of the "Sku" refrigerator, in which the thickness of the thermoinsulation was increased to 100 mm. Mipora was used as the insulating material. Due to the increased thermal insulation, the internal volume of the refrigerator chamber proved to be 91 liters.

The internal chamber of the refrigerator was divided by a horizontal partition into two parts; the upper and the lower (Figure 150). The temperature in the upper chamber was reduced to  $3-5^{\circ}$ , which is quite sufficient for the preservation for such products as meat, wine, mild, fruit, etc. In the lower chamber, the temperature reduction was  $-4$  to  $-6^{\circ}$ , which provides for the storage of meat, sausage and other meat products. In order to reduce heat losses during opening of the refrigerator door, the lower chamber was equipped with an additional door, which is open to secure access to this chamber.

The structural configuration of the air radiators required the placement of the thermoelements in the lower part of the refrigerator cabinet, and the radiators had to be placed along the entire rear wall of the refrigerator. Since natural convection air transfer in the internal chamber of the refrigerator was not significant, temperature equalization between the lower and upper chambers was to a certain extent determined by the heat conductivity of aluminum, which was the construction material for the internal chamber.

Earlier designs for thermoelectric domestic refrigerators employing air for heat removal were equipped with thermopiles consisting of several hundred thermoelements which required a great expenditure in scarce semiconductor materials for their manufacture. The thermoelectric piles of these refrigerators were made in the form of a single unit, in which the failure of even one thermoelement necessitated a complete overhaul of the entire pile.

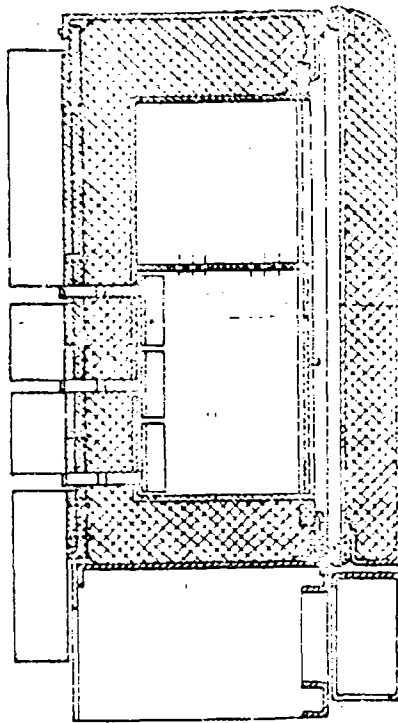


Figure 150. A section of a model 1957 thermoelectric domestic refrigerator.

In the refrigerator described, the required refrigerating capacities provided by a total of 45 thermoelements. The thermoelement (Figure 151) are constructed in the form of separate sub-assemblies, consisting of semiconductor alloys of n- and p-type conductivity 1 and 2, copper heat conductors 3, hot radiators 4 and cold radiators 5. An individual refrigerating element possesses a refrigerating capacity of approximately 0.4 kCal/h. The design of the thermoelement completely eliminates parasitic heat losses between the cold and hot radiators, which is accomplished by direct soldering of all junctions in the areas a-d. This thermoelement construction permits checking the quality and replacing individual elements independently of the remainder, which is quite important during checking of the thermoelectric pile in the process of assembly and during possible repairs under operating conditions. During refrigerator assembly the individual thermoelements are installed in

appropriate recesses which are located on the rear wall of the chamber, to which the fan-shaped air radiators have been previously attached. Soldering of the thermoelements to the hot and cold radiator fins is accomplished with special solders having low melting points.

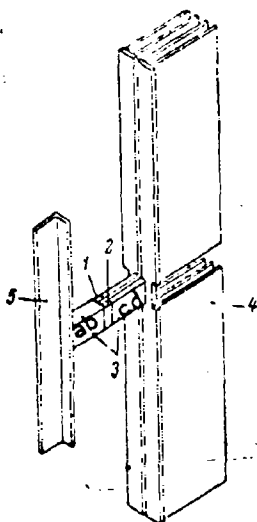


Figure 151. The thermoelement junction of a model 1957 domestic refrigerator.

The electrical supply for the refrigerator is obtained from a rectifier which is mounted in the lower part of the refrigerator cabinet. The optimum current value which corresponds to the maximum refrigerating capacity is 25 a; the voltage drop on the thermoelectric pile is 3.3 v. The rectifier consists of two VG-50-15 germanium diodes, connected in a full-wave circuit.

Germanium diodes require air cooling, which is provided by natural air convection in the rectifier section. With a rectifier efficiency of 80-85%, the electrical energy required by the refrigerator from the alternating current line is 90-100 w. Figure 152 shows an overall view of the refrigerator.

## GRAPHICS NOT REPRODUCIBLE

Figure 152. An overall view of the  
model 1957 domestic refrigerator.

In 1959-1961 I. V. Zorin, V. P. Rybal'chenko and A. G. Shcherbina developed three types of thermoelectric domestic refrigerators under the names "iceberg-1", "iceberg-2" and "iceberg-3". These refrigerators have operating chambers from 90 ("iceberg-1") to 125 liters ("iceberg-3"). Heat removal from the thermoelectric piles in all three types is accomplished by a system of air radiators, distributed along the rear wall of the refrigerator cabinet. In contrast to the model 1957 refrigerator described, the "iceberg" air radiator system has an area of  $5 \text{ m}^2$  instead of  $6 \text{ m}^2$ . As a result of the more closely spaced distribution of radiator fins and a reduction in the thickness of the fin from 2 to 1 mm, the dimensions of the radiator system were significantly reduced. The radiator system of the model 1957 refrigerator was distributed along the entire rear wall of the refrigerator cabinet, whereas the "iceberg" refrigerator radiators occupy only one fourth of the area of the rear wall. In order to improve heat transfer between the fins and the surrounding air the radiator system is enclosed on the sides with a special foam plastic ventilator housing. The presence of the housing creates an additional convectional air flow along the fins, as a result of which the radiator temperature is further reduced by  $3-4^\circ$ .

Due to the more efficient system of heat removal, the thermoelectric pile was successfully placed in the upper part of the refrigerator operating chamber, which resulted in a more even temperature distribution in the operating volume. Thermoelements of smaller size were used in the "iceberg" refrigerators, as a result of which the consumption of semiconductor materials was reduced to 200 g for the entire thermopile.

The voltage supply for the thermopiles of the "iceberg" refrigerators is 3.3 v at a current of 26 a. The rectifier for the thermoelectric pile supply is a full-wave circuit employing VG-50-15 germanium diodes. A filter choke, mounted in the rectifier section, serves to smooth rectified current ripple. In all types of "iceberg" refrigerators the rectifier is situated in the lower part of the refrigerator cabinet. With a rectifier efficiency of 80%, the power required by the refrigerator from the alternating current line is 103 w.

In critical analyzing widely-accepted requirements which are applicable to domestic refrigerators of any type, the author came to the following conclusions.

1. The temperature conditions which must be established in the operating chamber of a refrigerator are established in agreement with the assertion that a refrigerator is intended for the storage of products. Based on this, it was established that for the storage of meat, fresh fish, dressed poultry, caviar and smoked foods, a temperature range of  $-2$  to  $0^{\circ}$  is required. The storage temperature for butter, boiled butter, rendered fat, sour cream and cottage cheese is established at  $0-4^{\circ}$ . Fruit and vegetables must be stored at a temperature of  $3-7^{\circ}$ . The values of the temperatures indicated do not cause any doubt, however, domestic refrigerators are usually employed not for extended product storage but for their temporary preservation. In fact, in the overwhelming majority of cases a given food product will remain in the refrigerator for one or two days. In rare cases this may amount to two or three days. With such short periods of preservation, meat products, for example, may be quite safely stored not at a temperature of  $-2$  to  $0^{\circ}$ , but at a temperature of  $+3-5^{\circ}$ . The same considerations apply to the temperature range for the storage of other products, which may be raised to a range of  $+8-+10^{\circ}$ . It must be noted that practically all industrially-produced refrigerators, both compressor and absorption types, freeze the products to a certain extent, which causes a deterioration in their taste and nutritious properties.

2. The "freezing compartment" of any refrigerator, where the temperature range is from  $-11$  to  $-9.5^{\circ}$ , is practically never used.

If we agree with the conclusions reached above, we may examine the requirements established for thermoelectric domestic refrigerators from a new point of view. A temperature range of  $+3$  to  $+5^{\circ}$  in the lower 100-liter chamber and  $+6$  to  $+8^{\circ}$  in the upper part of the chamber may be obtained in a refrigerator in which the thermopile requires direct current at a power of 30-35 w. In considering the efficiency of the rectifier, the refrigerator will require 50-55 w from the line. This type of thermoelectric refrigerator is twice as economical as the absorption type of refrigerator "Leningrad" and in so far as the energy requirement is concerned, is on a level with the majority of compressor refrigerators. If we take into consideration that all of the advantages of thermoelectric refrigerators listed above remain in force (structural simplicity, long service life, quiet operation, insignificant cost, etc.), the incontrovertible merit of these refrigerators are apparent even with the existing figure of merit for semiconductor substances. In time, and in proportion to an increase in the value  $z$  of thermoelectric materials, semiconductor refrigerators will continue to leave behind domestic refrigerators of all other types.

In order to check the considerations outlined above, at the end of 1965 at the Semiconductor Institute of the Academy of Sciences of the USSR, a refrigerator was developed based on the establishment in the operating chamber of the temperature conditions mentioned above. The cabinet from the "Dnepr" refrigerator was used as a base. The internal chamber, with a volume of 100 liters, was constructed of aluminum, 1.5 mm in thickness. The thickness of the mipora insulation layer was 80 mm. The refrigerator thermoelectric pile consisted of 15 thermoelements installed in one row in the lower part of the refrigerator chamber. The design of the thermoelements did not differ from the design described above and employed in the model 1957 refrigerator. The rectifier for the thermopile supply was a full-wave circuit with VG-10-15 power rectifiers in the arms. Filtering of the rectified current was accomplished with a filter choke. The refrigerator rectifier was located in the lower part of the cabinet in the area previously occupied by the compressor assembly. Heat removal from the hot junctions of the thermopile was accomplished with a system of radiators located on the rear wall of the cabinet. A system of cold radiator plates, directly soldered to the heat conductors of the thermoelements was located inside the operating chamber. The series connection of the thermoelements is accomplished directly by the system of radiator plates from the hot side of the thermopile. In order to improve heat transfer from these surrounding medium, the radiator system of the hot junctions was enclosed in a housing of decorative plastic, which developed an advantageous air flow along the plates. The radiator plates were constructed of copper, 1.5 mm in thickness, which led to the practical elimination of a parasitic temperature difference along the fins. The distance between the fins



was 10 mm, and fins length and width was 450 and 50 mm, respectively. Notwithstanding these relatively small dimensions, the fin temperature exceeded the temperature of the surrounding air by only 5°.

Basic data for the refrigerator is shown below.

Operating current	24 a
Voltage drop on the thermopile	1.35 v
Direct current power requirement	32.4 w
Power requirement from the line	56 w
Operating chamber volume	100 liters
Chamber temperature along the vertical axis	
(with a surrounding air temperature of +18°):	
at a distance of 100 mm from the bottom of the chamber	+3.5°
in the middle of the chamber	+5°
at a distance of 100 mm from the top of the chamber	+8°
Power consumption per liter of cooled volume	0.56 w
Area of the "cold" radiators	0.15 m <sup>2</sup>
Operating time	10 hours
Consumption of semiconductor materials	0.23 kg

It is apparent from the parameters cited that the thermoelectric refrigerator with a "softened" temperature range in its basic parameter, power consumption per liter of operating chamber volume, surpasses not only absorption refrigerators of the "Leningrad" and "Gzoapparat" types, but also many compressor refrigerators, approaching in this parameter the "ZIL" refrigerator (0.42 w/liter).

At the present time this refrigerator is in experimental use.

#### §4. A low-Volume Domestic Refrigerator

In 1960 A. N. Voronin and E. N. Shero developed the thermoelectric domestic refrigerator "Fontan" with a low-volume chamber, equal to 20 liters. The temperature required in the chamber is provided by thermoelectric pile, consisting of a total of 8 thermoelements. Heat removal from the thermoelectric pile is accomplished by running water cooled as a result of the latent heat of vaporization.

The principal design of the water system of heat removal for the "Fontan" refrigerator is shown in Figure 153. Water is poured into vessel 1. Pump 2, which is equipped with a small, economical electric motor 3, pumps water through water jacket 4, to which the hot junctions of the

thermoelectric pile 5 are soldered. After it leaves the jacket, the water enters fountain device 6. Small streams of water 7 create a cooling effect as a result of partial water evaporation. The cooled water flows to vessel 1 and is again delivered to the thermopile. The UV-1 air humidifier, which is mass-produced by industry, is employed as the fountain device in the refrigerator. The cold junctions of the thermopile are soldered through electrically-insulated connecting plates to the side of the metallic chamber, which forms the operating volume of the refrigerator.

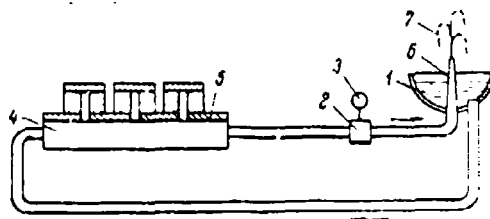


Figure 153. Heat removal diagram for the "Fontan" refrigerator.

The "Fontan" refrigerator is manufactured in the form of a cabinet, finished in an expensive type of wood. The cabinet is equipped with two sections: a refrigerator section and a small section for the storage of dishes or products which do not require cooling. In the process of operation the refrigerator loses part of the water due to evaporation, and the loss equals approximately 0.5 liters per day. For normal refrigerator operation, two glasses of water must be poured into the fountain device each day. The current supply to the thermoelectric pile is delivered by a rectifier, arranged in a full-wave circuit with VG-10 germanium diodes as rectifiers. A filter choke, mounted in the rectifier section, serves to smooth out the rectified current ripple. The rectifier is located on the rear section of the refrigerator.

It must be noted that the "Fontan" refrigerator requires a total of only 30 w from the line, which makes it quite economical. Figure 154 shows an overall view of the refrigerator.

The following are the basic technical data of the "Fontan" refrigerator.

Operating current	20 a
Thermopile voltage drop	0.5 v

Semiconductor substance consumption for the thermopile	30 g
Number of thermoelements in the thermopile	8 units
Power required from the line	30 w
Pump motor power	4 w
Operating chamber volume	20 liters
Dimensions: height	800 mm
width	750 mm
depth	500 mm

## GRAPHICS NOT REPRODUCIBLE

Figure 154. An overall view of the "Fontan" refrigerator.

Still another design version of the thermoelectric domestic refrigerator with an operating volume of 20 liters was developed in 1964 in the SKB of the Semiconductor Institute of the Academy of Sciences of the USSR in conjunction with a number of other organizations. The design of this refrigerator permits installing it on a table or attaching it to the wall. The refrigerator housing was manufactured of plastic. Heat removal from the hot junctions of thermopile, just as in the "Fontan" type of refrigerator, is accomplished through the latent heat or vaporization of water. However, in this case the water does not gush from a fountain, but is sprayed on the hot radiator plates by a special device within the refrigerator housing.

The consumption of power required from the line for 1 liter of refrigerator useful operating volume was equal to 1.35 w; semiconductor material consumption for the thermopile was 55 g.

An overall view of the table-mounted version of the "Fontan" refrigerator in a plastic housing is shown in Figure 155.

# GRAPHICS NOT REPRODUCIBLE

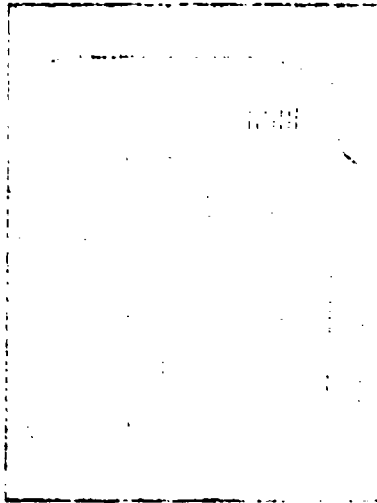


Figure 155. An overall view of the  
second version of the "Fontan"  
refrigerator.

## CHAPTER XVI. Devices for Various Purposes

### §1. Refrigerators for Stock-Raising

In stock-raising practice, the method of artificial insemination of animals, which permits accelerating by many times the process of obtaining thoroughbred offspring, is well known. However the successful mass application of this method comes up against one essential difficulty, connected with the fact sperm obtained from the producer preserves its capacity for fertilization for the relatively short time. Under existing conditions the sperm must preserve all its qualities for a rather long period of time. It has been established that when sperm is maintained at a reduced temperature, it does not lose its qualities even during storage for several years. Thus, for example, while at a temperature of 0° sperm may be preserved for several days, at a temperature of -78° may be preserved for three years.

Thus the problem of developing small thermostatically-controlled refrigerators for the transportation and storage of sperm was very important. While under fixed storage conditions this problem may be solved by means of utilizing refrigerators, during the transportation of sperm directly to the point of artificial insemination. The utilization of compressor or absorption refrigerator assemblies is not possible. The use of cooling methods involving ice, solid carbon dioxide or other periodically acting refrigerants is also not possible by virtue of operational inconveniences (relative scarcity, as a necessity for periodic refilling, etc.).

In this connection a pressing need arose to develop a low-volume, easily transported refrigerator. Several models of microrefrigerators were developed on the basis of the thermoelectric cooling method intended

were developed on the basis of the thermoelectric cooling method intended for the inter-rayon transportation and storage of cattle sperm.

In the first types of refrigerators the operating chamber volume was 80 cm<sup>3</sup>, which permitted placing 10 vials of semen in the chamber. Since in thermoelectric cooling devices it is quite essential to provide effective heat removal from the hot side of the thermopile, three design versions of the refrigerators were developed in which heat removal was accomplished by means of a system of radiators with natural air convection, with heat removal by forced air, and with water.

The first design version of the refrigerator (Figure 156) had operating chamber 1 in the form of a red-copper shell with a diameter of 36 mm and a height of 72 mm. The front part of the operating chamber was coupled with good thermal contact to the cold junctions of thermoelectric pile 2 through a thin (10  $\mu$ ) polyethylene film. The thermoelectric pile consisting of 18 thermoelements with dimensions of 5  $\times$  5  $\times$  10 mm, was filled with epoxy resin, thus forming a single, structurally-complete sub-assembly.

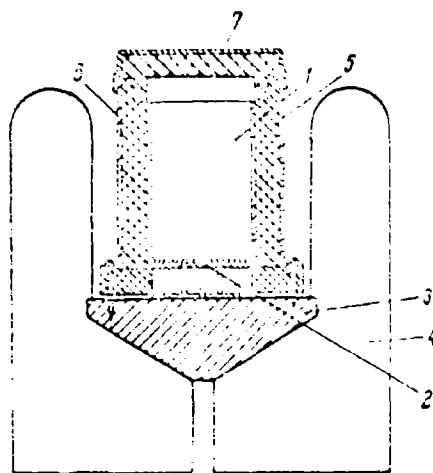


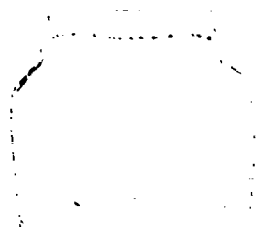
Figure 156. A section of a refrigerator with natural heat removal for stock raising.

At the location of the coupling between the thermopile and the collector, the latter was coated by electrochemical means with a thin (1-2 m) of aluminum oxide in order to exclude electrical contact. Heat

removal from the collector of the hot junctions was accomplished by a radiator system 4, consisting of 12 fins, which were also formed of aluminum.

The operating volume of the refrigerator surrounded by a layer of foam plastic thermal insulation 5, and is protected on the outside by metallic housing 6. The top of the chamber is equipped with cover 7. The refrigerator is equipped with a handle for convenience in transportation.

The electrical supply to the refrigerator is accomplished with a silver-zinc storage battery. An external view of the refrigerator of this type is shown in Figure 157.



## GRAPHICS NOT REPRODUCIBLE

Figure 157. An overall view of a refrigerator for cattle-raising, designed for natural heat removal.

The basic data for the refrigerator with natural heat removal to a system of air radiators are shown below.

The useful operating chamber volume	80 cm <sup>3</sup>
Maximum temperature reduction (with an ambient temperature of 20°)	to -2°
Thermopile voltage drop	1.2 v
Thermopile supply current	8 a
Power requirement	9.6 w
Radiator plate area	1400 cm <sup>2</sup>
Dimensions: diameter	165 mm
height	160 mm
Weight	1300 g

One of the shortcomings of the thermoelectric refrigerator with natural heat removal is the small temperature difference between the surrounding air and the operating volume. With an ambient temperature exceeding 20°, which often occurs in practice, this type of refrigerator cannot provide a temperature below 0 in the operating chamber.

The second construction version of the thermoelectric refrigerator (Figure 158) is based on forced air cooling of radiator system 1, by means of small fan 2, which is mounted in the refrigerator housing. The presence of more effective heat removal and a system of 24 radiator plates with a total area of 3,000 cm<sup>2</sup> permitted improving the heat-engineering characteristics of the refrigerator and increased the temperature difference between the environment and the internal volume. While in the refrigerator with natural heat removal from the radiator system the temperature difference was 20-22°, and the forced air system the temperature difference was raised to 28-30°. This means that the required internal refrigerator temperature of 0.2° may be provided when the external temperature reaches 28-30°, which makes it possible to employ this type of refrigerator in Southern areas. When the fan is switched off, the refrigerator provides a temperature difference of 6-8° less.

The electrical parameters of the current supply for the thermoelectric pile of this type of refrigerator are the same as those for the refrigerator with natural heat removal. However, a supplemental source of voltage is required in order to supply the fan. A 12 v dry battery was used (the current required by the fan is 0.25 a). The total weight of the refrigerator (less the power supplies) is 2300 g. The external dimensions are height 300 mm, and diameter 150 mm.

Figure 159 shows an overall view of the refrigerator with forced air cooling of the radiators.



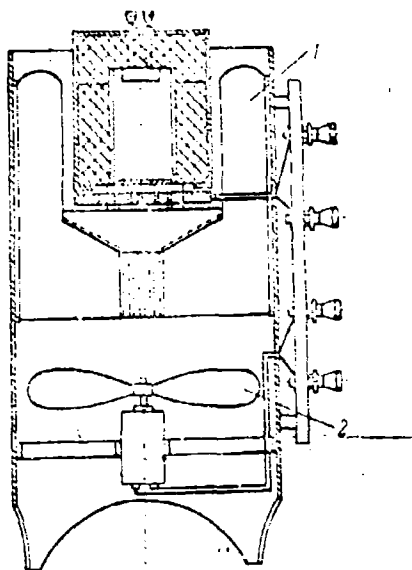


Figure 158. A section of a refrigerator for stock-raising, equipped with forced air heat removal.

GRAPHICS  
NOT REPRODUCIBLE

Figure 159. An overall view of the refrigerator for stock-raising, equipped with forced air heat removal.

The problem of providing an uninterrupted source of current to the thermoelectric pile of a refrigerator during the course of its operation is a significant one. In the refrigerator designs described, the type STs-45 storage battery may be used as a power supply. The storage battery consists of 8 cells, connected in parallel. The total capacity of the storage battery is 360 a/h; this is sufficient for continuous refrigerator operation for a period of 40-45 hours.

In a case when the refrigerator is being transported by motor vehicle, the storage battery which supplies the refrigerator may be connected to the recharging circuit of the vehicle, which permits supplying the refrigerator for a longer period of time.

A thermoelectric refrigerator was developed in the Agricultural Physics Institute of the Academy with an operating chamber volume of 500 cm<sup>3</sup>, intended for the transportation of the sperm of farm animals. In this refrigerator design (Figure 160), heat removal from the hot junctions of the thermopile is accomplished by water, which is located in tank 1, with a capacity of 20 liters. Filling of the tank and water discharge from the tank is accomplished through apertures 2 and 3.

The thermoelectric pile 4 of the refrigerator is installed between metallic shell 5, which forms the operating volume, and radiator 6. The radiator is screwed into the support ring of the water tank and is sealed by resin washer 7. In order to improve the heat transfer between the water and the radiator, the latter is equipped with a system of fin 8, which extends its surface. Temperature sensor 9 is attached to the volume chamber for automatic temperature maintenance within the operating chamber. Thermal insulation for the chamber is provided by a layer of foam plastic 10. Removable cover 11 is located on the top of the refrigerator.

The electrical circuit for the current supply to the thermopile and for automatic temperature regulation is shown in Figure 161. The voltage to supply thermopile TB is delivered from motor-vehicle 12-volt storage battery  $E_1$  through voltage-dropping resistor  $R_1$  and relay  $K_1$ . Fuse F is connected in series with the supply circuit to the thermopile. When the context of bi-metallic relay TK closed, which occurs when the temperature in the operating chamber is higher than the specified temperature, voltage from the power supply is applied to intermediate relay  $K_2$ , which turns on power relay  $K_1$ . Then the contacts of the power relay close and current is supplied to thermopile TB.

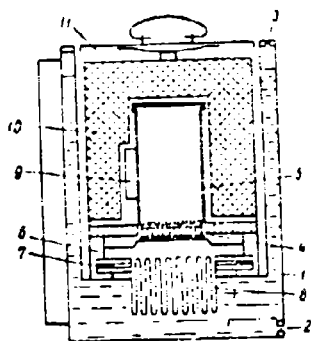


Figure 160. A section of a refrigerator for stock-raising, equipped with a water system of heat removal.

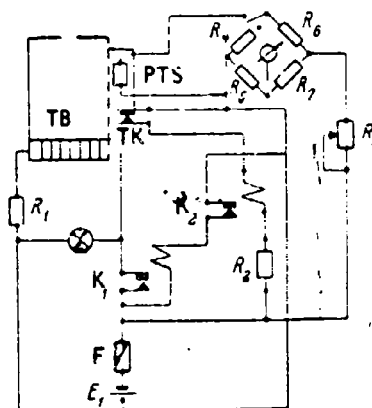


Figure 161. The electrical circuit of the power supply and automatic regulator of the refrigerator for stock-raising with a water system of heat removal.

When the temperature in the operating volume drops below the specified value, the bi-metallic relay opens, relays  $K_2$  and  $K_1$  open and the thermopile is disconnected from the power supply. Temperature measurement in the operating volume is accomplished by means of an unbalanced bridge which includes thermistor PTS in one of the arms. A microammeter is connected in the bridge diagonal as a temperature indicator. The microammeter scale is graduated in temperature values within the range  $-5$  to  $+10^\circ$ . Variable resistance  $R_3$  regulates the voltage applied to the bridge. Here control resistor  $R_4$  is switched into the circuit in place of thermistor PTS.

The results of refrigerator tests have been plotted in the graphs shown in Figure 162 where curves 1 and 2 show the relationship of the temperature drop between the operating volume and the water in the tank at a current through the thermopile of 8 a (1) and 6 a (2). Curves 3 and 4 show increased water temperatures in the tank with currents of 8 and 6 a, respectively.

From the graph shown it is apparent that a temperature difference of  $17^\circ$ , which corresponds to an operating volume temperature of  $0^\circ$ , is attained in 11 minutes with a current of 8 a and in 17 minutes with a current of 6 a. With this time difference in attaining the specified temperature is not significant, however, water heating in a current of 6 a occurs more slowly; as a result, a pile current of 6 a was chosen.

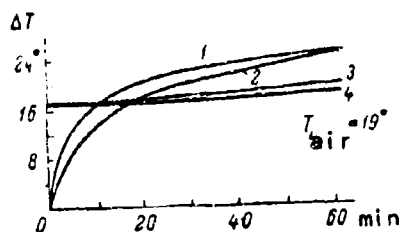


Figure 162. Temperature reduction with time in the refrigerator operating chamber.

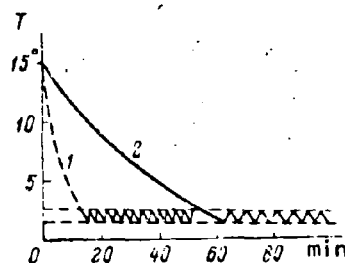


Figure 163. The temperature reduction rate in an empty operating volume (1) and in a volume filled with  $200 \text{ cm}^3$  of brine (2).

Figure 163 shows the temperature reduction in the operating volume with time for a case involving empty volume 1 and a volume filled with  $200 \text{ cm}^3$  of brine, 2. From this drawing it is apparent that the temperature

inside the operating volume is maintained by the stabilization circuit at a level of 1.5-2.5°. As a result of an increase in the thermal inertia of the filled operating volume, the temperature regulation period increases.

Figure 164 shows the temperature reduction rate for a filled operating volume 1 and empty volume 2. In this case the temperature regulator was switched off. Curve 3 shows the value of water heating in the tank with extended refrigerator operation. An analysis of these curves shows that without changing the water in the tank, the refrigerator may provide the required temperature in the operating volume for a period of 8 hours.

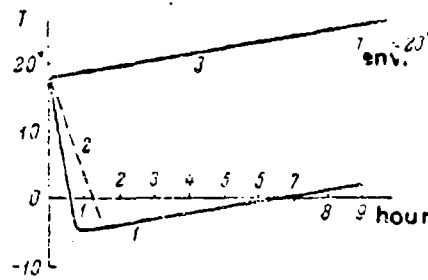


Figure 164. The temperature reduction rate in a water-filled and empty volume of the refrigerator when the temperature regulator is switched off.

The following are the basic specifications for the refrigerator described.

Operating current	6 a
Voltage drop on the device	12 v
Power requirement	84 w
Operating chamber volume	500 cm <sup>3</sup>
Chamber operating temperature (with a water temperature of 15-20° and an air temperature of 40°)	-2 to +3°
Tank water volume	20 liters
Dimensions	270 × 430 × 300 mm
Weight	25 kg

## 52. A Thermostat System for the Coke-Oven Gas Industry

In the production of hot gases by the method of coking coal, the quantity of naphthalene in the gas must be controlled. Ordinarily chemical analysis methods are employed for this purpose. However the chemical reagents employed must be maintained at a temperature of 0 to -5°. The utilization of compressor machines for periodically refrigerants is not possible because of operating conditions.

The thermoelectric method of cooling has permitted the developed of a compact, independent device which requires no special service by personnel and which fully satisfies the operating requirements of gas plants. The thermostat assembly is made in the shape of a cylindrical vessel (Figure 165) divided into three parts. The rectifier which supplies the thermopile and the temperature stabilization circuit are located in lower part A. The thermoelectric pile and the operating chamber are located in the middle part B, and the electric motor for the agitator is located in upper part C.

The single-stage thermoelectric pile 1, consisting of 16 thermo-elements, is soldered through electrically-insulated connecting plates to hollow cylinder 2. The water which removes the heat from the hot junctions of the thermopile passes through cylinder 2. The operating chamber 3 of the device is soldered to the cold junctions of the thermopile also through electrically-insulated connecting plates. In order to reduce the temperature gradient along the height of the operating chamber, the latter is manufactured of metal, which has high-heat conductivity. Temperature stabilization in the device is accomplished by means of a special circuit. Small temperature relay 4 serves as the sensor for this circuit, and is located inside the operating chamber. Three vials of Drechsel 5 which are being cooled, are placed in three cells in partition 6. Rubber hoses which deliver and remove the gas analyzed from the Drechsel vials pass through special channels formed in the thermal insulation of the device in the area of the cover fastening. Thermal insulation of the device is provided by a layer of foam plastic 7.

In order to reduce the cooling time of the reagents placed within a device, the operating chamber is filled with a mixture of water and alcohol which has a freezing point of approximately -10°. Auger agitator 8, which is rotated by small electric motor 9, serves to equalize the temperature inside the operating chamber. Access to the operating chamber is provided by cover 10, which is provided with a system of ventilation apertures to cool the agitator motor.

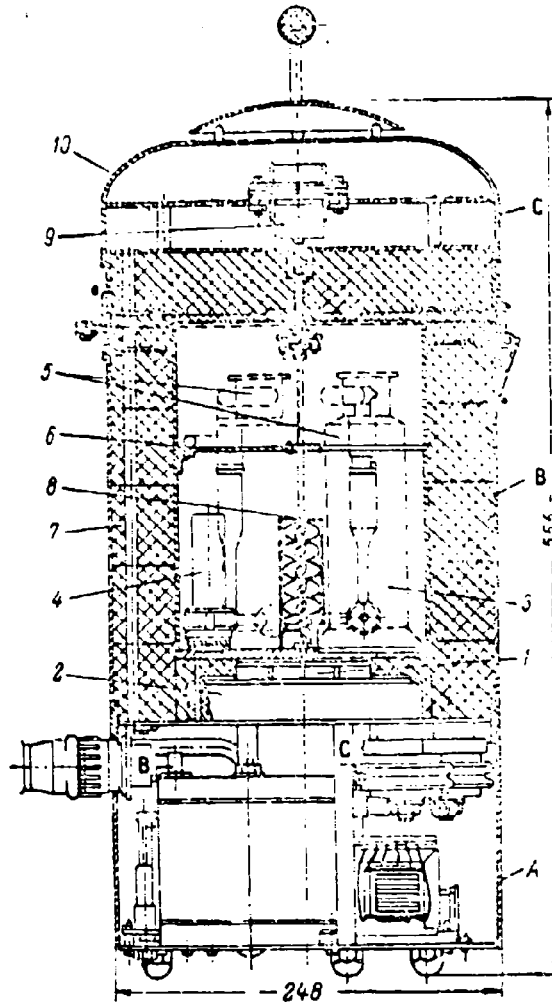


Figure 165. A section of a thermostat assembly for the coke-oven gas industry.

As we have pointed out earlier the rectifier which supplies the thermopile and the temperature regulation circuit for the operating chamber are located in the lower part of the device. The electrical circuit for these sub-assemblies of the thermostat system is shown in Figure 166. Power transformer  $Tr_1$  reduced the line voltage to a value required to supply the thermoelectric pile. Connected in series with the primary winding of the power transformer are fuse F and hydraulic relay HK, which prevent the application of voltage to the thermopile when there is no water in the heat removal system.

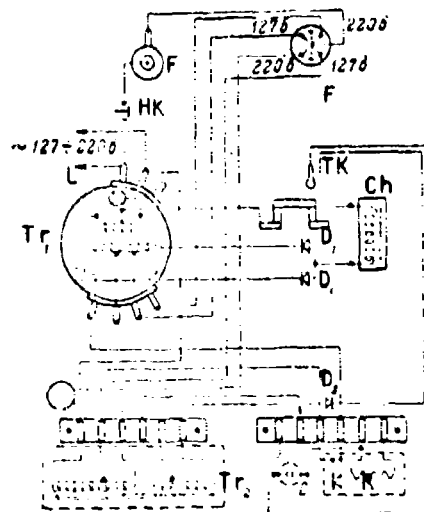


Figure 166. The electrical circuit for the power supply and the regulator of a thermostat system for the coke-oven gas industry.

Two heavy-duty VG-50-15 germanium diodes  $D_1$  are connected in a full-wave rectifier circuit in the secondary circuit of the power transformer. Filter choke Ch serves to reduce rectified current ripple.

The temperature stabilization circuit and the supply circuit for the agitator motor consists of a transformer  $Tr_2$ , type DGTs-27 diode  $D_2$ , filter capacitor C, type RMTsG operating relay K, temperature relay TK and signal lamp L. The temperature stabilization circuit operates in the following manner: when the device is switched on line voltage is applied only to transformer  $Tr_2$ . The secondary voltage of this transformer through normally closed temperature relay contacts is applied to the operating relay, which applies voltage to transformer  $Tr_1$ . When the required temperature has been attained in the operating chamber of the device the temperature relay is disconnected, the operating relay is de-energized and the power transformer which supplies the thermopile is switched off. Signal lamp L burns during operation of the thermopile and is extinguished when the thermopile is disconnected.

In order to prevent the germanium power diodes from overheating they are mounted on the steel, water-cooled base which removes heat from the thermopile. The thermostat assembly may be supplied from the alternating current line with a voltage of 127/220 v, which is connected to the device with a plug-in socket assembly.

Figure 167 shows an overall view of the thermostat system.



GRAPHICS  
NOT REPRODUCIBLE

Figure 167. An overall view of a thermostat system for the coke-oven gas industry.

The basic specifications of the thermostat system for the coke-oven gas industry are shown below.

Operating current of the thermoelectric pile	60 a
Required power from the line	150 w
Operating chamber volume	3.75 liters
Operating chamber dimensions: diameter	160 mm
height	210 mm
Operating chamber temperature	$0 \pm 0.2^\circ$
Temperature stabilization accuracy	$\pm 0.1^\circ$
Water system heat removal temperature	$1-25^\circ$
Water consumption rate	100 l/h



Electrical agitator type	SD-60
Agitator rpm	60 rpm
Duration of continuous device operation	unlimited
Dimensions: height	555 mm
diameter	248 mm
Weight	20 kg

### 53. A Refrigerator with a Detachable Thermopile

A basic shortcoming of thermoelectric refrigerators is the necessity for continuous operation of the thermopile. As soon as the current to the thermopile is switched off the temperature in the cooled volume begins to rise rapidly as the result of heat flux through the arms of the thermoelements. At the same time in the practical employment of several thermoelectric devices it is not possible to provide a continuous current to the thermopile. In particular, the fulfillment of this condition is quite desirable in refrigerators intended for the transportation of the sperm of farm animals.

In this connection a thermoelectric refrigerator satisfying the requirement stated above was developed at the Agricultural Physics Institute of the Academy of Agricultural Sciences named for V. I. Lenin.

A section of the refrigerator is shown in Figure 168. Thermoelectric pile 1 consists of 16 thermoelements 2, and the hot junctions of the thermoelements are coupled through thin organic film 3 with heat removal system 4, made in the shape of a row of radially distributed radiator plates 5, ventilated by small fan 6. The cold junctions of the thermoelements are coupled through electrically-insulated film 7 to cold junction collector 8, which is a hollow cylinder constructed of a material with good heat conductivity. Such a system, which is a structurally complete sub-assembly, is placed on ordinary vacuum bottle 9 having a volume of 2 liters. The cold collector is submerged in the liquid located in the vacuum bottle. In a case when a certain article is to be cooled, for example the sperm of farm animals, it is placed in hermetically sealed vial or container 10, and lower to the bottom of the vacuum bottle. When the liquid has attained the required temperature the thermoelectric device is disconnected from the vacuum bottle and the latter is closed with a thermally-insulated cap. A temperature increase in the liquid inside the vacuum bottle in this case will be determined by heat flux from outside, which will be minimum with good vacuum-bottle evacuation, and by the quantity of liquid in the bottle.

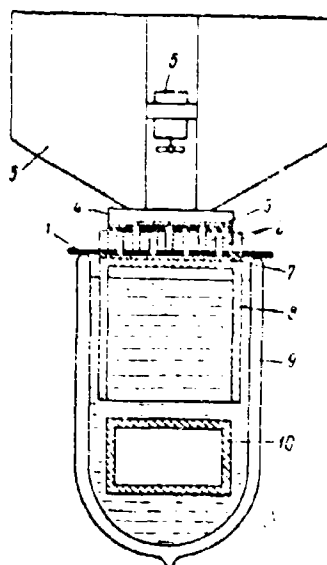


Figure 168. A schematic section of a refrigerator with a detachable thermopile.

Thus the thermoelectric cooler is structurally independent of the cooled object and is employed only during the time of liquid cooling.

The graph of Figure 169 shows a dependence of the temperature reduction of 2 liters of water, placed in the vacuum bottle, on time. During transportation of the refrigerator by motor vehicle the thermopile may be supplied from the vehicle battery. Under fixed conditions is the air radiator in the thermopile heat removal system may be replaced by a radiator utilizing running water.

The basic technical parameters of the cooler are as follows.

Operating current	6 a
Voltage drop on the thermopile	1.66 v
Power requirement	10 w
Fan motor voltage supply	12 v
Dimensions: diameter	220 mm
height	290 mm

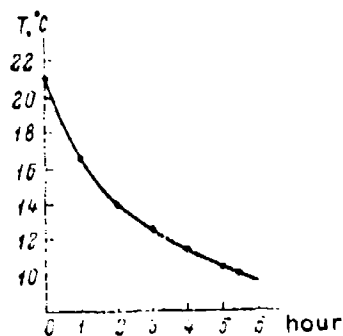


Figure 169.

#### 54. A Thermoelectric Temperature Stabilizer for Photographic Solutions

In the conduct of motion-picture operations, it is necessary to provide constant temperatures for the photographic solutions employed. The fulfillment of this requirement even under fixed operational conditions is associated with certain difficulties. Under conditions involving mobile or field operations, which occur during expeditions, the temperature stabilization of photographic solutions presents an even more complex problem. Thus, for example, in contemporary developing devices thermostatically-controlled photographic solutions are maintained at a temperature of approximately 18° with running water. However in Southern areas of the country during the summer water temperature may reach 25° or higher. Under these conditions the normal process of film development and fixing deteriorates.

A thermoelectric stabilizer permits automatically maintaining the temperature of photographic solutions in developing tanks at a specified level with a change in temperature of the running water within wide limits.

Basically the thermoelectric stabilizer is a reflux heat exchanger, in which a thermoelectric pile (Figure 170) is located between channels which can carry the photographic solution in running water. It consists of two series-connected sections 1 and 2, each of which consists of 76 thermoelements. The thermoelectric pile is soldered through

electrically-insulated connecting plates 3 to hot heat-exchanger 4 to which running water is supplied through nipple 5. Metallic spiral 6 is placed in the hot heat-exchanger in order to improve heat-exchange between the water and the thermopile. Two cold heat-exchangers 8, to which the photographic solution flows through nipple 9, are soldered to the cold junctions of the thermopile through electrically-insulated connecting plates 7.

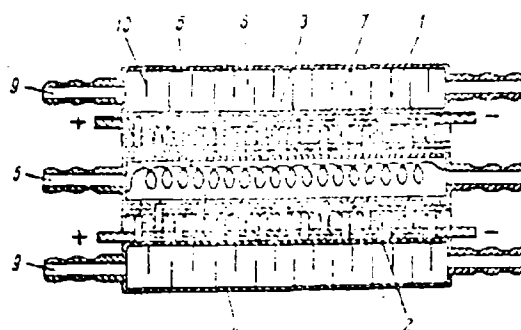


Figure 170. Diagram of a heat-exchange device of a thermoelectric temperature stabilizer for photographic solutions.

Heat-exchangers for photographic solutions are copper boxes equipped with a system of fins 10 in order to improve heat-exchange from the photographic solution. The internal surfaces of the cold heat-exchangers are silver-plated in order to prevent corrosion due to the influence of the photographic solutions. Both cold heat-exchangers consist of 4 series-connected sections, each of which has 4 channels which are connected in parallel. Such a system provides for good heat-transfer of the photographic solutions with the thermoelectric pile. With an insignificant loss in the pressure of the photographic solution passing through the device.

Solders with various melting points are used in the manufacture of the device, which provides for convenience and efficiency in assembly. The electrical circuit of the power supply and the control for the thermoelectric temperature stabilizer for photographic solutions provides for concurrent supply to both thermopiles, which are connected in series. In this case the temperature of the photographic solutions passing through the cold heat-exchangers will be identical.

The basic technical data of the device are shown.

Operating current	75 a
Thermopile voltage drop (two sections)	13.6 v
Power requirement (direct current)	1020 w
Thermopile coefficient of performance	73.5%
Thermopile refrigerating capacity	240 kCal/h
Thermopile heat output	465 kCal/h
Initial photographic solution temperature (maximum)	30°
Photographic solution operating temperature	18°
Rate of flow of running water to the thermopile	350 l/h
Quantity of photographic solution passing through the device	460 l/h
Dimensions	380 × 280 × 620 mm

A full-wave rectifier consisting of a power transformer and two power germanium diodes is employed to supply the thermopile. A filter choke serves to reduce ripple in the rectified voltage. The primary circuit of the rectifier is supplied from the 220 v alternating current line. A switch is provided in order to deliver current of reversed polarity to the thermopile, as a result of which the pile is switched from the cooling to the heating mode. Temperature stabilization of the photographic solution is accomplished automatically by means of a temperature sensor, placed in the solution, by an intermediate relay and a magnetic starter which connects or disconnects the supply to the thermopile when the photographic solution temperature deviates from the specified value. A hydraulic relay prevents application of voltage to the thermopile when water is not present in the hot heat-exchanger. The relay and other automatic regulation elements are situated in the automatic control section.

In a case when operating conditions dictate that the temperature of the photographic solution in the cold heat-exchangers must be at different temperatures, a different supply system is employed which provides for individual current supply to the thermopiles. This circuit is then two independent supply and regulation circuits, which are similar to the one described.

##### §5. Thermoelectric Devices for the Determination of the Pour Points of Petroleum Products

One of the basic parameters which characterize the operating properties of petroleum products, and of diesel fuel in particular, is the pour point. Contemporary industrial methods of determining the pour point are based on a determination of the attenuation of an ultrasonic pulse, generated in the petroleum product undergoing investigation. Sharp

ultrasonic attenuation indicates the onset of the petroleum-product pour point.

The practical operations involved in this method are the following. A special cell is filled with a portion of the petroleum product. An ultrasonic pulse from the ultrasonic generator is created in the cell. In the pauses between the delivery of the square pulses measurement of the square pulse value is reflected from the opposite side of the cell is accomplished. The temperature of the cell and the petroleum product is linearly reduced and is continuously measured by a low-inertial electrical thermometer. When the reflected ultrasonic pulse undergoes attenuation, which indicates congealing of the petroleum product, the electric thermometer establishes the internal temperature of the cell. Then the cell must be heated to a temperature of approximately  $10^{\circ}$ . The petroleum product which is drained off, the cell is filled with another portion of petroleum products, and the measurement cycle is repeated.

It should be added to the above that the entire cycle of measurement, emptying, and refilling of the cell with a new portion of petroleum product must be accomplished automatically.

The fact that a thermopile can operate in both the heating and the cooling mode permitted developing a device which satisfies all of these operating requirements. A section of a thermoelectric device for the determination of the pour point of petroleum products is shown in Figure 171.

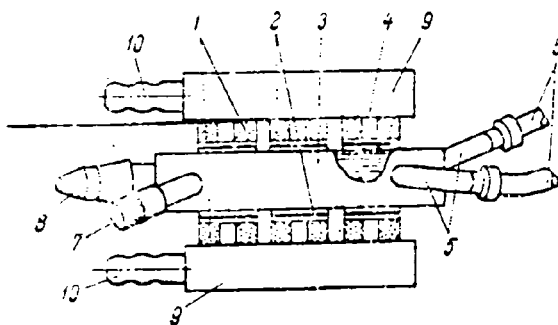


Figure 171. A section of a device for the determination of the pour point of petroleum products.

The cold junction side of two single-stage thermoelectric piles 1, which consist of 5 thermoelements each, are soldered through electrically-insulated connecting plates 2 to the opposite sides of cell 3. In order to improve heat transfer from the cell to the petroleum product 4, within the cell, the latter is manufactured of copper, which has high heat conductivity. The petroleum product under investigation enters and leaves the cell through two nipples 5. In order to reduce parasitic heat flux to the cell along the nipples, the latter are equipped with rings 6 of plastic, which possess low heat conductivity, and form heat bridges. The leads to the sensor electric thermometer are brought from the cell through plexiglass nipple 7. The sensor is a thermistor by means of which petroleum-product temperature change is measured. Piezoelectric oscillator 8, which is attached to the wall of the cell, creates the ultrasonic pulses and simultaneously receives the reflected pulses from the opposite wall of the chamber.

The hot side of the thermoelements is soldered to collectors 9, through which water passes to remove heat from the thermopile. Intake and output of water is accomplished through nipples 10. The collectors of the hot junctions are filled with epoxy resin to furnish the thermopiles with the required mechanical strength. The external surface of the cell is covered with a layer of foam plastic in order to reduce heat flux from the outside.

A block diagram of the power supply and the automatic regulation section is shown in Figure 172. The current supply to the thermopile is provided by a full-wave rectifier, in which heavy-duty germanium diodes are used as rectifiers.

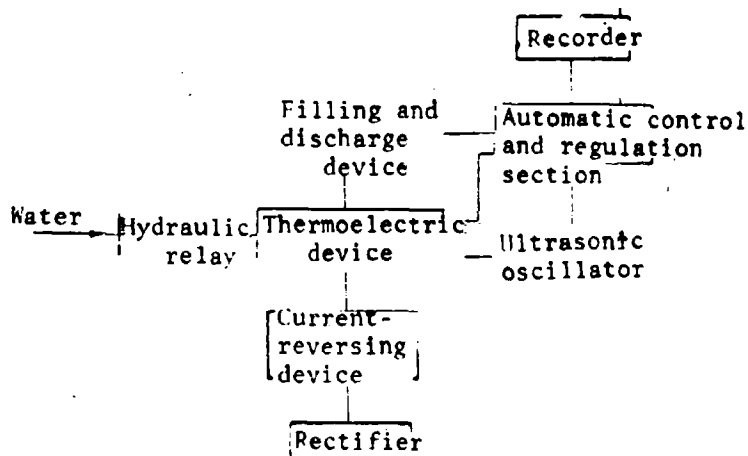


Figure 172. The block diagram of a device to determine the pour point of petroleum products.

The reflected ultrasonic pulse is applied to the automatic control section. Upon the initiation of reflected pulse attenuation, the automatic control section establishes a temperature of the petroleum product and turns on the reversing device which switches the polarity of the supply current, changing the thermopile from the cooling to the heating mode. The petroleum product is heated in the cell, and after a specified period of time the discharge device is automatically switched on which frees the cell and refills it again with a new portion of petroleum product. A forward-polarity current is then applied to the thermopile and the process of measurement is repeated. A hydraulic relay prevents current delivery to the thermopile when there is no water in the system. A recording device is included in the automatic control section which records the measurement results.

An overall view of this device is shown in Figure 173.

## GRAPHICS NOT REPRODUCIBLE

Figure 173. An overall view of the device for the determination of the pour point of petroleum products (first version).

The basic technical characteristics for this device are shown below.



Operating current in the cooling mode	34 a
Voltage drop on the thermopile in the cooling mode	0.87 v
Power requirement in the cooling mode	29.6 w
Minimum operating chamber temperature (with a water temperature of 18°)	-25°
Maximum temperature drop provided by the device	43°
Time required to establish minimum temperature in the cell	10 min
Operating current in the heating mode	4 a
Time required to heat the petroleum products to a temperature of 10°	12 min
Water consumption rate	100 l/h
Operating chamber volume	33 cm <sup>3</sup>
Dimensions	92 × 75 × 78 mm
Weight	1168 g

Tests of the thermoelectric device for the determination for the petroleum-product pour points at a number of petroleum-processing plants have revealed its high operating qualities. Nevertheless the necessity arose to develop a device operating on the same principle, but providing for lower petroleum-product pour points. Two two-stage thermopiles with series-fed stages were used in this device. There were ten thermoelements in the first stage of each half of the thermopile and there were two elements in the second stage. The cell for the petroleum products investigated were soldered between the thermopiles. Heating of the cell to the liquification point of the petroleum product is accomplished by means of a special electrical heater attached to the cell assembly.

In order to satisfy requirements that the device be explosion-proof, all pipes pertaining to the cell are manufactured of tekstolite with a wall thickness of 5 mm. In order to provide for maximum reduction in the heat flux to the cell along the pipes, the latter are of considerable length. Hermetic feeling of the device with the aim of providing an explosion-proof assembly is accomplished by direct soldering and sealing of the seams with epoxy resin. A thermopile assembly on crimped heat junctions and the use of V-shaped connecting plates, which reduce mechanical stress in the thermopile, have permitted the establishment of an extended operational cycle in the device in the heating-cooling modes under conditions prevailing in petroleum-processing plants.

The basic technical characteristics of the device are shown below.

Optimum current in the maximum cooling regime	50 a
Voltage drop at optimum current in the cooling mode	2.27 v
Power requirement in the cooling mode	114 w
Minimum cell temperature (with a water system heat removal temperature of 30°)	-42°

Maximum temperature difference provided by the device	72°
Time required to establish maximum cooling	60 min
Operating current in the heating mode	10 a
Voltage drop in the heating mode	1.3 v
Time required to establish a temperature of 10°	4 min
Cell volume	33 cm <sup>3</sup>
Heat removal system water consumption rate	80 l/h
Dimensions: diameter	228 mm
height	310 mm
Weight (without explosion protection)	3.7 kg
Thermopile-housing insulation resistance	more than 10 megohms

An overall view of the assembled device, withdrawn from its explosion proof housing, is shown in Figure 174.

## GRAPHICS NOT REPRODUCIBLE

Figure 174. An overall view of a device to determine the pour point of petroleum products (second version).

In 1964 a new method of determining the pour point of petroleum products was proposed by S. S. Palley. In agreement with this method the

temperature of the pour point of the petroleum products investigated is determined by means of the cyclic action of pressure on the cooled product on the one side of the cell, with establishment of the moment of loss of reaction to this pressure on the other side of the cell. Control of the pressure change is accomplished by means of a micromanometer. This method of determining the pour point is significantly simpler and more reliable than the method of ultrasonic sounding.

In 1965 two thermoelectric devices were developed for the determination of the pour point of petroleum products according to S. S. Palley's method. One of the devices was intended for the determination of the pour point of several types of oils. Structurally it was assembled on a two-stage thermopile with series current supply similar to the system described above. The copper cell, made of plexiglass, was mechanically attached to the collector of the cold junctions of the second stage of the thermopile. The heat-removing water system was fabricated within the flange of the device by which connection to the explosion-proof housing was accomplished.

The technical characteristics of the device for the determination of the pour point of oils are shown below.

#### Cooling Mode

Operating current	56 a
Voltage drop	1.26 v
Power requirement	70.6 w
Maximum cooling temperature (with a heat removal water system temperature of +30°)	-44.6°
Time required to obtain minimum temperature	30 min
Temperature drop provided by the device	74.6°

#### Heating Mode

Operating current	10 a
Voltage drop	0.76 v
Power requirement	7 w
Time required to achieve a temperature of +5°	4 min
Cell volume	2 cm <sup>3</sup>
Water consumption rate in the heat removal system	80 l/h
Dimensions: diameter	150 mm
height	80 mm
Weight	5.75 kg

An overall view of the device for the determination of the pour point of oils, with a layer of thermal insulation, is shown in Figure 175. The explosion-proof housing has been removed.

## GRAPHICS NOT REPRODUCIBLE

Figure 175. An overall view of a cooler, including the heat removal system, for the determination of the pour point of oils.

Still another type of thermoelectric device for petroleum products with a low pour point was developed in 1965. The pressure-change method was selected as the basis for the determination of the moment the pour point had been reached. In this device two three-stage thermopiles with series-current supply of all stages were used to provide a temperature in the cell within the limits  $-60$  to  $-70^{\circ}$ . The first stage of the thermopile consists of 15 thermoelements, and the second of 3 thermoelements; the third stage is formed by one thermoelement. The cell is tightly mounted between the three stages of the two thermopiles. The cold-connecting plates of the third stages of the thermopile are insulated from the cell by means of a ceramic heat junction in order to prevent the current supplying the pile from passing to the cell. In order to preserve reliable thermal contact between the thermopile and the cell, the collectors of the cold junctions of the third stages are constructed of lead. The device has been designed with consideration for the requirements of explosion-proof construction. Extensive tests of the device in cyclic operation in the cooling and heating modes have revealed its high operating qualities and reliability. It must be noted that a stable temperature difference of  $92^{\circ}$  has been produced in this device, which is assembled from molded thermoelements of mass-produced thermoelectric alloys.

Below are listed the basic technical parameters of the three-stage refrigerator for the determination of petroleum-products pour points.

Operating current in the cooling mode	42 a
Voltage drop in the cooling mode	3.7 v
Power requirement in the cooling mode	155.4 w
Heat removal water system temperature	+30°
Minimum temperature in a cell filled with petroleum products	-62°
Time required to attain temperature	20 min
Operating current in the heating mode, to +10°	7 a
Voltage drop in the heating mode	0.4 v
Power requirement in the heating mode	2.8 w
Time required to heat the cell to +10°	5 min
Cell volume	2 cm <sup>3</sup>
Insulation resistance of the thermopile versus the housing	10 megohms
Water consumption rate in the heat removal system	80 l/h
Dimensions of the device (without the thermal insulation and the explosion-proof housing):	
diameter	135 mm
height	160 mm
Weight	5.8 kg

An overall view of the three-stage for the determination of petroleum-product pour points is shown in Figure 176, with the thermal insulation removed.

#### 56. A Thermoelectric Milk Cooler

Fresh milk contains bactericidal substances which suppose the development of contaminating microorganisms. However, the bactericidal substances in fresh milk are active for only a short period of time. The effective action time of the bactericidal substances is significantly increased if the milk temperature is reduced. Thus, for example, at a temperature of 18-20°, fresh-first grade milk becomes second grade in 3-4 hours, but at a temperature of 7-8°, the milk preserves first-grade properties for a period of three days.

At the present time the following methods of cooling fresh milk are employed on dairy farms:

- 1) in basins containing running water or water which has been previously cooled with ice;

2) in two-section sprayer coolers, in which cooling in the first section is accomplished by means of running water, and the second section by employing brine, which is cooled with a special refrigeration device.

## GRAPHICS NOT REPRODUCIBLE

Figure 176. An overall view of a thermoelectric device for the determination of petroleum-product pour points (third-version).

The first method of cooling mild milk is connected with the requirement for the procurement and storage of ice, and the second method requires special technical servicing of the refrigerator installation and a relatively long period of time to achieve the required brine temperature.

The successful development of thermoelectric cooling techniques made it possible to develop a thermoelectric refrigerator which possesses a number of essential advantages over known method of cooling fresh milk. The thermoelectric pile of the refrigerator consists of 50 series-connected sections. Each section (Figure 177) consists of 25 thermoelements 1, mounted between two metallic panels 2 and 3, which are the collectors of the hot and cold junctions of the thermoelements. The hot 4 and cold 5 connecting plates of the thermoelements are cemented through a thin layer of electrical insulation to the panels. The thermoelements are soldered to the connecting plates with low melting-point alloys, forming

a series-connected pile. The thermopile sub-assemblies constructed in this manner are attached with thin rubber washers 6 to heat removal system 7, which is a duraluminum plate, having a number of spiral-formed channels 8, through which water passes while removing heat from the hot junctions of the thermoelements. The outside connecting plates of the thermopile are connected to rods 9, by means of which the individual sections are connected in series with each other. Such a thermoelectric section design makes it easy to assemble the device and when required to provide replacements if the device fails.

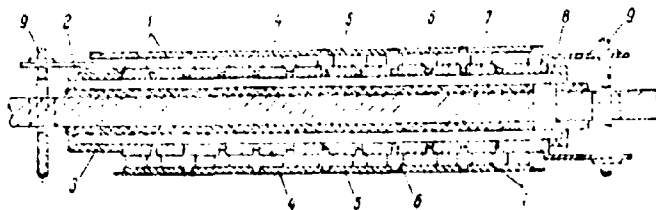


Figure 177. One section of the thermopile of a milk cooler.

The water cooling system of the device (Figure 178) has two nipples 1 and 2, through which water input and output are accomplished. Manometer 3 serves to control water pressure at the input of the refrigerator, and thermometers 4 and 5 are to measure the water temperature at the input and output of the device. The milk subject to cooling passes through nipple 6 to slot-shaped funnel 7, where it falls to cooler 8, and flows in a thin laminar layer downward, washing the cold collectors of the thermopile. The cooled milk is gathered in collector 9 and passes through nipple 10 to be placed in the appropriate receptacles. Due to the fact that the milk which is subject to cooling moves from the top downward, and the water which removes the heat from the thermopile moves upward, a reflux system is obtained, the result of which is to improve the effectiveness and power characteristics of the refrigerator.

A method of furnishing the electrical supply to the thermoelectric pile of the refrigerator is chosen in such a way that succeeding sections of the thermopile have potential differences less than the potential at which electrolysis of the milk occurs.

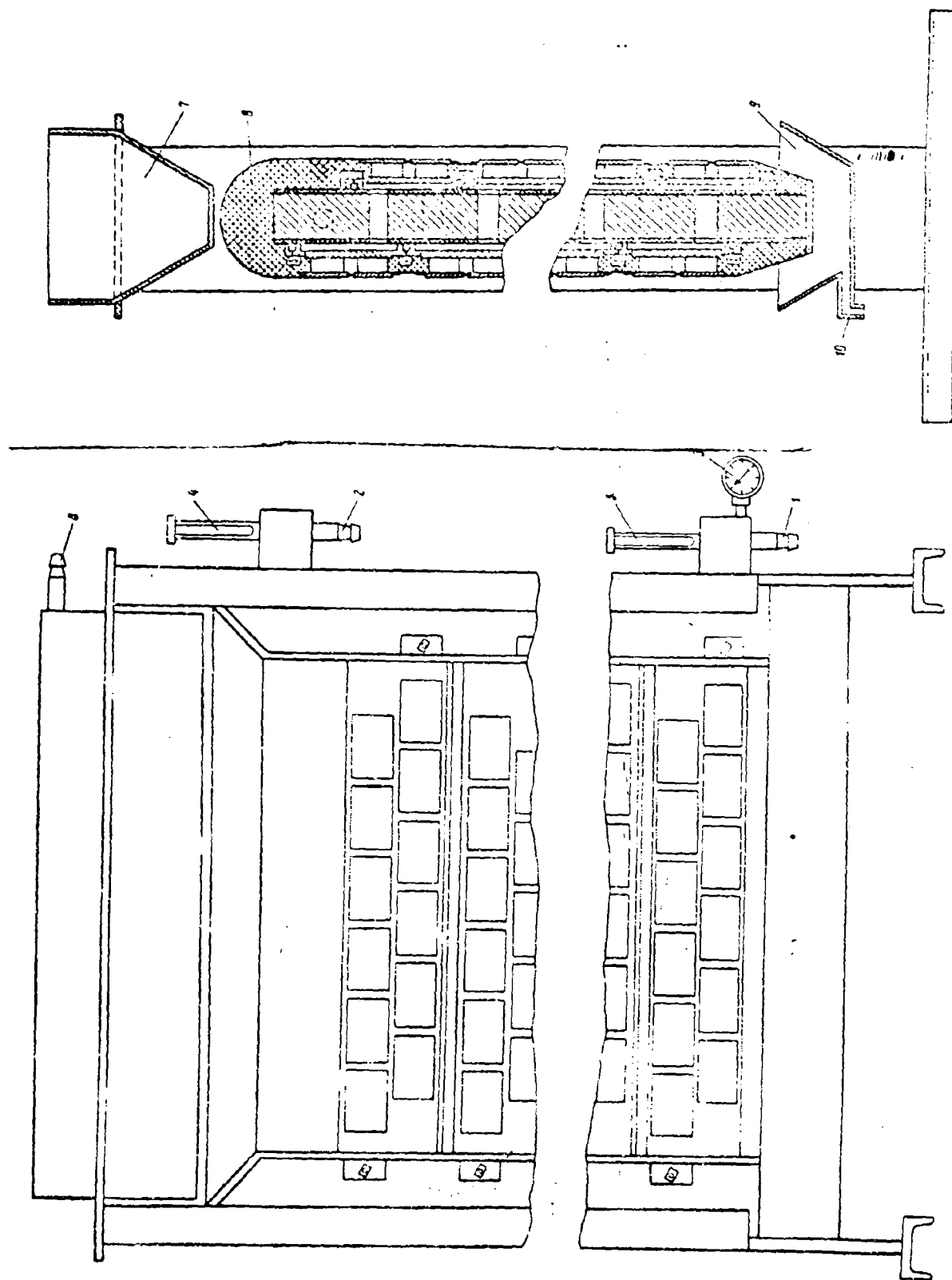


Figure 178. A schematic section of a milk cooler.



The results of refrigerator tests which are shown in Table 73 reveal that with an increase in milk output passing through the refrigerator, the refrigerating capacity and the coefficient of performance of the thermoelectric pile increased, but the temperature of the milk at the output of the device increases.

TABLE 23

The Results of Tests on the Thermoelectric Milk Cooler

a) Выход молока, л/час	b) Температура молока, °C		e) Температура воды, °C		h) Холодо- произво- димость аппарата, ккал/час	i) Потреб- ляемая мощность, вт	j) Коэф- фициент произво- дства
	c) Вход	d) Выход	f) Вход	g) Выход			
60	18.0	5.1	15.0	21.3	760	780	1.13
	18.0	5.2	15.3	24.4	800	780	1.19
	18.0	4.3	15.2	24.5	825	780	1.23
100	17.8	8.0	15.6	26.1	980	840	1.36
	17.8	7.7	15.0	26.0	1010	840	1.40
	18.0	7.5	15.8	27.0	1050	840	1.46
120	17.8	8.6	15.1	27.3	1140	870	1.52
	17.8	9.1	15.0	27.3	1080	870	1.46
	17.8	9.3	15.2	27.6	1090	870	1.46

Key: a, milk output, l/h; b, milk temperature, °C;  
c, input; d, output; e, water temperature, °C;  
f, input; g, output; h, refrigerating capacity of  
the assembly, kCal/h; i, power requirement, w;  
j, coefficient of performance.

The following are the basic technical parameters for the refrigerator.

Operating current	30 a
Voltage drop	30 v
Power requirement (direct current)	900 w
Nominal refrigerating capacity	800 kCal/h
Coefficient of performance in the nominal operational mode	1.18
Consumption of semiconductor materials for the thermopile	4.8 kg
Cooling water rate of consumption	450 l/h
Dimensions:	1170 × 260 × 200 mm
Weight (less the power supply)	45 kg

At the Agricultural Physics Institute, where the refrigerator described was developed, work continues in the development of more efficient designs for thermoelectric refrigerators for dairy farms. In particular, it has been suggested to employ a heavier-duty thermoelectric pile, which reduces the consumption of semiconductor materials for the refrigerator by two times while maintaining the same power requirement. The height of the refrigerator is also significantly reduced with an improvement in the basic heat-engineering parameters of the device.

#### §7. A Thermoelectric Drinking-Water Cooler

In the summer a railway coach, steamship, or aircraft passenger wishes to satisfy his thirst with cool water. Since all transportation facilities usually carry a limited amount of drinking water, in the course of time the latter becomes warm and unpleasant. This especially pertains to railway passenger transportation, where in the summertime the drinking water in a coach can reach a temperature of  $35^{\circ}$ . In addition, the drinking water on transportation facilities must be boiled. Railway coaches and ships carry special devices to boil unprocessed water for this purpose. Obviously, before the boiled water is used it must be cooled. In agreement with established standards, the temperature of drinking water must not exceed  $15^{\circ}$ . The OVK-380 compressor water cooler is usually employed in passenger cars of the USSR railroads. This installation is not free from the defects which characterize compressor-type cooling devices. In addition, the OVK-380 installation (and others of a similar type) are intended for operation in railway transportation facilities. The use of these in ships is practically impossible, since they do not function normally when displaced from a horizontal position, which unavoidably occurs when a ship is rolling.

In 1962 at the experimental-research and design era (EIKB), under the direction of A. L. Vaynar, an experimental model of a thermoelectric drinking-water cooler was developed for passenger railroad cars. This device, which has received the designation VO-2, consists of a sectionalized thermoelectric pile, the cold junctions of which are equipped with fins and are submerged in a space filled with the boiled water, which is to be cooled. The radiator system of the hot junctions of the thermopile are enclosed in a special housing, through which the general water supply for the car flows. Hot water which has been processed by the boiler is cooled in an intermediate heat exchanger through which water from the central water system flows, and the cooled water then flows to the operating chamber.

Structurally the VO-2 water cooler is made in the shape of a cabinet, which contains the cool water tank, the rectifier to supply the thermopile, a system of automatic regulation of the operating mode and an interlock, and

primary heat exchanger. Control over the operational mode of the device is accomplished by a remote panel located in the train conductors service compartment. Tests of the thermoelectric drinking-water cooler were conducted in a passenger car which was being used during the summer on central-Asian railroads of the USSR. The results of the tests revealed the high operational qualities of the thermoelectric cooler and its incontrovertible advantages over the OVK-380 compressor cooler.

The comparative parameters of these two types of coolers for drinking water are shown in Table 24.

TABLE 24

The Comparative Parameters of the Thermoelectric (VO-2) and the Compressor (OVK-380) Drinking-Water Coolers

Parameter	VO-2	OVK-380
Cooled water output, l/h	7	5
Preparation time, hours	1.5	3
Power requirement from the electrical source, w	200	600
Weight, kg	32	80.5
Dimensions, mm	350x350x1000	520x450x805

Work is being conducted in the EIKB to modernize the water cooler; in particular, this includes a reduction in the weight and the dimensions of the device, and also changing the system of heat removal from the hot junctions of the thermopile from water to a forced air system. Naturally, in maritime usage only the liquid system of heat removal will be used.

## BIBLIOGRAPHY

### Chapter I

1. Ioffe, A. F., *Energeticheskiye Primeneniya Termobatarey iz Poluprovodnikov* [Energy Applications of Semiconductor Thermopiles], AN SSSR Press, Moscow-Leningrad, 1951.
2. Ioffe, A. F., *Poluprovodnikovyye Termoelementy* [Semiconductor Thermoelements], AN SSSR Press, Moscow-Leningrad, 1960.
3. Ioffe, A. F., B. Ya. Moyzhes and L. S. Stil'bans, "Concerning Power Applications of Thermoelements," *FTT*, Vol. 2, No. 11, 1960.
4. Kolenko, Ye. A. and L. S. Stil'bans, *Poluprovodniki v Nauke i Tekhnike* [Semiconductors in Science and Technology], Vol. II, AN SSSR Press, Moscow-Leningrad, 1957.
5. Korenblit, I. L., "On the Problem of the Efficiency of Semiconductor Thermoelements," *Nauchn. Zap. Chernovitsk. Univ.*, Vol. 12, 1955.
6. Gross, E. T. B., "Efficiency of Thermoelectric Devices," *Amer. J. Phys.*, Vol. 29, No. 11, p. 729, 1961.
7. Guzzi, L. and H. J. V. Tyrvell, "The Maintenance of Controlled Temperature Differences Using a Thermoelectric Heat Pump," *J. Scient. Instrum.*, Vol. 41, No. 7, p. 468, 1964.
8. Holtan, H., P. Masur and S. R. de Groot, "On the Theory of Thermocouples and Thermocells," *Physica*, Vol. 19, No. 12, p. 1109, 1953.
9. Littman, H. and B. Davidson, "Theoretical Bound on the Thermoelectric Figure of Merit from Irreversible Thermodynamics," *J. Appl. Phys.*, Vol. 32, No. 2, p. 217, 1961.
10. Navarro, Martinez Jesus, "The Fundamentals of Thermoelectric Refrigeration," *Rev. Cienc. Apl.*, Vol. 17, No. 2, p. 126, 1963.
11. Sherman, B., R. R. Heikes and R. W. Ure, "Calculation of Efficiency of Thermoelectric Devices," *J. Appl. Phys.*, Vol. 31, No. 1, pp. 1-16, 1960.
12. Sherman, B., R. R. Heikes and R. W. Ure, *Calculation of Efficiency of Thermoelectric Devices. Thermoelectric Materials and Devices*, Ed. by I. B. Cadoff and E. Miller, Reinhold Publishers, N. Y., 1960.

## Chapter II

1. Ayrapetyants, S. V. and B. A. Yefimova, "The Thermoelectric Properties and the Nature of the Bond in a  $\text{Bi}_2\text{Te}_3$  --  $\text{Sb}_2\text{Te}_3$  System," *ZhTF*, Vol. 28, No. 8, 1958.
2. Ayrapetyants, S. V., B. A. Yefimova, T. S. Stavitskaya, L. S. Stil'bans and L. M. Sysoyeva, "Concerning Electron and Hole Mobility in Solid Solutions Obtained on the Basis of Lead Telluride and Bismuth," *ZhTF*, Vol. 27, No. 9, 1957.
3. Vasenin, S. I., "Thermoelectric Properties of a Bismuth-Tellurium Alloy System," *ZhTF*, Vol. 25, No. 3, 1955.
4. Vasenin, F. I., "The Thermoelectric Properties of an Antimony-Tellurium Alloy System," *ZhTF*, Vol. 25, No. 7, 1955.
5. Vlasova, R. M. and L. S. Stil'bans, "An Investigation of the Thermoelectric Properties of Bismuth Telluride," *ZhTF*, Vol. 25, No. 4, 1955.
6. Gordyakova, G. N., G. V. Kokosh and S. S. Sinani, "A Study of the Thermoelectric Properties of  $\text{Bi}_2\text{Te}_3$  --  $\text{Bi}_2\text{Se}_3$  Solid Solutions," *ZhTF*, Vol. 28, No. 1, 1958.
7. Kokosh, G. V. and S. S. Sinani, *Vliyaniye Primesey na Termoelektricheskiye Svoystva Tverdogo Rastvora  $\text{Sb}_2\text{Te}_3$  --  $\text{Bi}_2\text{Te}_3$*  [The Influence of Impurities on the Thermoelectric Properties of an  $\text{Sb}_2\text{Te}_3$  --  $\text{Bi}_2\text{Te}_3$  Solid Solution]. *FTT*, Vol. 1, AN SSSR Press, Moscow-Leningrad, 1959.
8. Kokosh, G. V. and S. S. Sinani, "The Thermoelectric Properties of Alloys of the  $\text{Sb}_2\text{Te}_3$  --  $\text{Bi}_2\text{Te}_3$  Pseudobinary System," *FTT*, Vol. 2, 1960.
9. "Materials for Thermoelectric Piles," *Priroda*, Vol. 4, No. 119, 1965.
10. Sinani, S. S. and G. N. Gordyakova, "Solid Solutions of  $\text{Bi}_2\text{Te}_3$  --  $\text{Bi}_2\text{Se}_3$  As a Material for Thermoelements," *ZhTF*, Vol. 26, No. 10, 1956.
11. Ainsworth, L., "Single-Crystal Bismuth Telluride," *Proc. Phys. Soc.*, Vol. 69B, No. 6, p. 606, 1956.

12. Benel, H., "The Thermoelectric Properties of Antimony Telluride and the Solid Solutions  $\text{Sb}_2\text{Te}_3$  --  $\text{Bi}_2\text{Te}_3$ ," *C. r. Acad. Sci.*, Vol. 247, No. 5, p. 584, 1958.
13. Bolling, G. F., "Some Thermal Data for  $\text{Bi}_2\text{Te}_3$ ," *J. Chem. Phys.*, Vol. 33, No. 1, p. 305, 1960.
14. Cluley, H. J. and P. M. Proffitt, "The Analysis of Bismuth Telluride and Related Thermoelectric Materials," *Analyst*, Vol. 85, No. 1016, p. 815, 1960.
15. Drabble, J. R. and C. H. Goodman, "Chemical Bonding in Bismuth Telluride," *J. Phys. Chem. Solids*, Vol. 5, 1958.
16. Goldsmid, H. J., "The Thermal Conductivity of Bismuth Telluride," *Proc. Phys. Soc.*, Vol. 69B, No. 2, p. 203, 1956.
17. Goldsmid, H. J., "The Thermal Conductivity of Bismuth Telluride. Report of the Meeting on Semiconductors at Rugby," *Phys. Soc.*, No. 127, London, 1956.
18. Goldsmid, H. J., "The Electrical Conductivity and Thermoelectric Power of Bismuth Telluride," *Proc. Phys. Soc.*, Vol. 71, No. 4, p. 633, 1958.
19. Goldsmid, H. J., "Effects of Impurities in Bismuth," *Proceedings of the International Conference on Semiconductor Physics, Prague, Czechoslovakia, Academy of Sciences*, No. 1015, 1960.
20. Goldsmid, H. J., "Recent Studies of Bismuth Telluride and Its Alloys," *J. Appl. Phys.*, Vol. 32, No. 10, Suppl., p. 2198, 1961.
21. Harman, T. C., M. J. Logan, B. Paris and E. H. Lougher, "Preparation and Thermoelectric Properties of  $\text{Bi}_2\text{Te}_3$  and All Alloys with  $\text{Bi}_2\text{Se}_3$ ," *Fall Meeting of the Electrochemical Society A*, September, 1958.
22. Hashimoto, K., "Electrical Properties of Bismuth Selenide  $\text{Bi}_2\text{Se}_3$ . Thermoelectric Power and Thermal Conductivity," *Mem. Fac. Sci. Kyushu University*, Vol. B2, No. 5, p. 187, 1958.
23. Jain, A. L., "Temperature Dependence of the Electrical Properties of Bismuth-Antimony Alloys," *Phys. Rev.*, Vol. 114, No. 6, p. 1, 1959.

24. MacPhee, C. A. A., "The Development of Thermoelectric Materials for Refrigeration," *Canadian Electrical Engineering*, Vol. 5, No. 2, p. 36, 1961.
25. Meyers, W. C. and R. T. Bate, "Thermoelectric Properties of  $\text{Bi}_2\text{Te}_3$  --  $\text{Bi}_2\text{Se}_3$ ," *Bull. Amer. Phys. Soc.*, Vol. 4, No. 7, p. 409, 1959.
26. Miller, G. R., Che Yu Li and C. W. Spencer, "Properties of  $\text{Bi}_2\text{Te}_3$  --  $\text{Bi}_2\text{Se}_3$  Alloys," *J. Appl. Phys.*, Vol. 34, No. 5, p. 1398, 1963.
27. Protopopescu, M. and N. Petrescu, "Aliaje Semiconductoare pe Baza de Telur Pentru Frigidere Termoelectrice. Studii si Cercetări Metalurgie," *Acad. RPR*, Vol. 2, No. 1, p. 33, 1962.
28. Protopopescu, M., St. Zămircă and N. Petrescu, "Determinarea Caracteristicilor Frigoelementelor din Aliaje Semiconductoare cu Bază de Telur. Studii si Cercetări Metalurgie," *Acad. RPR*, Vol. 8, No. 3, p. 255, 1963.
29. Rodot, H. and M. G. Weill, "Temperature Variation of the Thermoelectric Properties of Solid Solutions  $\text{Bi}_2\text{Te}_3/\text{Sb}_2\text{Te}_3$ ," *J. Phys. et Radium*, Vol. 21, No. 5, p. 502, 1960.
30. Roland, W., "Theory of Materials for Thermoelectric and Thermomagnetic Devices," *Proceedings of the IEEE*, Vol. 51, No. 5, p. 699, 1963.
31. Smirous, K. and L. Stourač, "Firm Solutions of  $\text{Bi}_2\text{Te}_3$  and  $\text{Sb}_2\text{Te}_3$  As p-Conducting Materials for Semiconductor Thermoelements," *Z. Naturforsch.*, Vol. 14a, No. 9, p. 848, 1959.
32. Sreedhar, A. K., N. H. Godhwani, R. K. Purohit and W. N. Borle, "Development of Semiconductor Materials for Thermoelectric Cooling," *J. Inst. Telecommun. Engrs.*, Vol. 10, No. 6, p. 207-211, 1964.
33. Stourač, L., "Influence of Aging on Change in Electrical Properties of Semiconducting Systems of  $\text{Bi}_2\text{Te}_3$  --  $\text{Bi}_2\text{Se}_3$ ," *Czechosl. J. Phys.*, Vol. 9, No. 6, p. 717, 1959.
34. "Thermoelectric Material Is Alloy of Bismuth Telluride," *Electron. Design*, Vol. 9, No. 18, p. 25, 1961.

35. Wolfe, R. and I. H. Wernick, "Thermoelectric Devices and Material," *Bell Lab. Res.*, Vol. 40, No. 6, p. 190, 1962.
36. Wright, D. A., "Some Physical Properties of Bismuth Telluride. Semiconductors and Phosphors," *Proc. Internat. Colloquium 1956, Garmisch Partenkirchen*, Interscience Publishers, New York, p. 477, 1958.

#### Chapter III

1. Burshteyn, A. I., *Finicheskiye Osnovy Rascheta Poluprovodnikovykh Termoelektricheskikh Ustroystv* [The Physical Bases of the Design of Semiconductor Thermoelement Devices], Fizmatgiz. Press, Moscow, 1962.
2. Kolenko, Ye. A. and L. S. Stil'bans, *Poluprovodniki v Nauke i Tekhnike* [Semiconductors in Science and Industry], Vol. 2, Chapter 17, AN SSSR Press, Moscow-Leningrad, 1958.
3. Moyzhes, B. Ya., "The Influence of the Temperature Dependence of the Parameters of Materials on the Effectiveness of Thermoelectric Generators and Refrigerators," *FTT*, Vol. II, No. 4, 1960.
4. Stavitskaya, T. S. and L. S. Stil'bans, "On the Influence of Degeneration on Thermoelement Effectiveness," *ZhTF*, Vol. 28, No. 3, 1958.
5. Stil'bans, L. S., "On the Selection of the Ratio of the Sections of Semiconductor Thermoelement Arms," *ZhTF*, Vol. 28, No. 2, 1958.

#### Chapter IV

1. Bean, T. E., "Thermoelectric Cooling," *Industrial Electronics*, Vol. 1, No. 2, p. 110, 1962.
2. Blatt, F. T., "On the Possibility of Thermoelectric Refrigeration at Very Low Temperatures," *Phil. Mag.*, Vol. 7, No. 76, p. 715, 1962.
3. Blatt, F. T., *Peltier Cooling Below 4°K. High Magnetic Fields*, John Wiley and Sons Inc., London and Technological Press, Cambridge, Massachusetts, p. 518, 1962.



4. Cuff, K. F., R. B. Horst, J. L. Weaver, S. K. Hawkins, C. F. Kooi and G. M. Enslow, "The Thermomagnetic Figure of Merit in Ettinghausen Cooling in Bi -- Sb Alloys," *Appl. Phys. Lett.*, Vol. 2, No. 8, p. 145, 1963.
5. Delves, R. T., "The Prospects for Ettinghausen and Peltier Cooling at Low Temperatures," *Brit. J. Appl. Phys.*, Vol. 13, No. 9, p. 440, 1962.
6. Fritl, M. E., P. W. Haselden and H. I. Goldsmid, "Thermomagnetic Effects in Bismuth-Antimony Alloys," *Rept. Internat. Conf. Phys. Semiconductors*, Exeter, 1962; *London Inst. Phys. and Phys. Soc.*, No. 777, 1962.
7. Goldsmid, H. J., "Thermoelectric and Thermomagnetic Cooling," *Industrial Electronics*, Vol. 1, No. 8, p. 441, 1963.
8. Goldsmid, H. J., "Thermoelectric and Thermomagnetic Cooling," *Industrial Electronics*, Vol. 1, No. 9, 1963.
9. Goldsmid, H. J., *Thermoelectric Refrigeration*, Plenum Press, New York, 1964.
10. Goldsmid, H. J. and D. E. Lacklison, "The Thermomagnetic Figure of Merit of Reheated Pyrolytic Graphite at Liquid Helium Temperature," *Brit. J. Appl. Phys.*, Vol. 16, No. 573, 1965.
11. Griffith, M. V., "Thermoelectric Refrigeration," *Advancement Sci.*, Vol. 18, No. 72, p. 135, 1961.
12. Harman, T. C. and J. M. Honig, "Theory of Galvano-thermomagnetic Energy Conversion Devices for Refrigerators and Heat Pumps," *J. Appl. Phys.*, Vol. 33, No. 3188, 1962.
13. Kooi, C. F., R. B. Horst, K. F. Cuff and S. R. Hawkins, "Theory of the Longitudinally Isothermal Ettinghausen Cooler," *J. Appl. Phys.*, Vol. 34, No. 6, p. 1735, 1963.
14. Koxodziejczak, J., L. Sosnowski and Zawadzkiw, "A Theory of Thermoelectric and Thermomagnetic Effects," *Rept. Internat. Conf. Semiconductors*, Exeter, 1962, *London Inst. Phys. and Phys. Soc.*, No. 94, 1962.
15. "New Cooler Uses Thermomagnetic Effects," *Electronics*, Vol. 36, No. 84, 1963.

16. O'Brien, B. J. and C. S. Wallace, "Ettinghausen Effect and Thermomagnetic Cooling," *J. Appl. Phys.*, Vol. 29, No. 7, p. 1010, 1958.
17. Smith, G. E. and R. Wolfe, "The Thermoelectric Properties of Bismuth-Antimony Alloys," *J. Appl. Phys.*, Vol. 33, No. 841, 1961.
18. "Theory of the Ettinghausen Cooler," *J. Appl. Phys.*, Vol. 33, No. 5, p. 1800, 1962.
19. "Thermoelectric Materials in Magnetic Fields," *Radio and Electron. Compon.*, Vol. 3, No. 6, p. 507, 1963.
20. Varda, B., D. Reich and J. Madigan, "Thermoelectric and Thermomagnetic Heat Pumps," *J. Appl. Phys.*, Vol. 34, No. 12, p. 3430, 1963.
21. Wolfe, R. and G. Smith, "Semimetals As Thermoelectric Materials," *Semicond. Prod.*, Vol. 6, No. 4, 1963.
22. Wolfe, R., G. E. Smith and S. E. Hansco, "Negative Thermoelectric Figure of Merit in a Magnetic Field," *Appl. Phys. Letters*, Vol. 2, No. 8, p. 157, 1963.
23. Wright, D. A., "Ettinghausen Cooling in Pyrolytic Graphite," *Brit. J. Appl. Phys.*, Vol. 14, No. 329, 1963.

#### Chapter V

1. Burshteyn, A. I., "Concerning a Regenerative Design for Thermoelectric Cooling," *FTT*, Vol. 2, No. 7, 1960.
2. Burshteyn, A. I., *Fizicheskiye Osnovy Rascheta Poluprovodnikovyykh Termoelektricheskikh Ustroystv* [The Physical Bases of the Design of Semiconductor Thermoelement Devices], Fizmatgiz. Press, Moscow, 1962.
3. Vikhorev, G. A. and V. A. Naer, "The Influence of Heat Transfer on the Characteristics of Semiconductor Thermopiles for Refrigerators and Heat Pumps," *FTT*, Vol. 1, No. 6, 1959.
4. Kurylev, Ye. S., "Concerning Operating Conditions of Semiconductor Cooling Devices," *Kholodil'n. Tekhn.*, No. 2, 1963.

5. Naer, V. A., "The Calculation of Transient Conditions for Semiconductor Refrigerators and Heaters," *Khолодильн. Tekhn.*, Vol. 1, 1962.
6. Naer, V. A. and S. A. Rozhentsova, "On the Design of Liquid-Flow Semiconductor Coolers and Heaters," *Inzh.-Fiz. Zhurn.*, Vol. 5, No. 11, 1962.
7. Naer, V. A. and S. A. Rozhentsova, "On the Design of Semiconductor Thermopiles for Refrigerators," *ETP*, Vol. 3, No. 4, 1961.
8. Stil'bans, L. S., "On the Selection of the Ratio of Sections of Semiconductor Thermoelement Arms," *ZhTF*, Vol. 28, No. 2, 1958.
9. Stil'bans, L. S. and N. A. Fedorovich, "On the Operation of Cooling Thermoelements Under Nonstationary Conditions," *ZhTF*, Vol. 28, No. 3, 1958.
10. Cherpakov, P. V., "Concerning the Heat Inertia of Thermoelements," *Inzh.-Fiz. Zhurn.*, Vol. 5, No. 9, 1962.
11. Shcherbina, A. G., "The Design of Thermopiles in a Nonstationary State," *Termoelektricheskiye Svoystva Poluprovodnikov* [The Thermoelectric Properties of Semiconductors], AN SSSR Press, Moscow-Leningrad, 1963.
12. Alfonso, N., *Transient and Steady-State Theory of Semiconductor Thermoelectric Cooling Cells*, thesis, Carnegie Institute of Technology, Pittsburgh, 1959.
13. Dörr, W., "The Frigistor Diagram," *Electron. Rundschau*, Vol. 14, No. 4, p. 156, 1961.
14. Gray, P. E., *The Dynamic Behavior of Thermoelectric Devices*, New York, 1960.
15. Grosby, C. R., M. H. Norwood and B. R. West, "The Effects of Heat Transfer on Optimum Peltier Heat-Pumping," *Amer. Soc. Mech. HT-11*, p. 7, 1962.
16. Heinicke, J. B., "The Design and Performance of a Thermoelectric Refrigerator," *American Society of Refrigeration Engineers Annual Meeting*, New Orleans, December 1958.

17. Jepson, R. M. and G. G. Messick, "Designing Low-Current Thermoelectric Coolers," *Electronics*, Vol. 34, No. 16, p. 58, 1961.
18. Kaye, J. and I. T. Saldi, *Quantitative Design of a Thermoelectric Cooler Direct Conversion of Heat to Electricity*, Massachusetts Institute of Technology, New York, Vol. 21, pp. 1-14, 1960.
19. Pritchard, W. Maurice, "The Coefficient of Performance of Thermoelectric Cooling Devices," *Proceedings of the IEEE*, Vol. 52, No. 4, p. 442, 1964.
20. Vought, R. H., *Design Calculations for Peltier Cooling. Thermoelectric Materials and Devices*, Ed. by I.B. Cadoff and E. Miller, Reinhold Publishers, p. 250, 1960.
21. Watanabe, A., "Unified Performance Calculations in Thermoelectric Cooling," *J. Appl. Phys.*, Vol. 33, No. 1, p. 130, 1962.
22. Watson, P. C., "Graphical Methods of Solving Thermoelectric-Pump Problems," *Electro-Technol.*, Vol. 71, No. 6, p. 74, 1963.
23. Zito, Ralph, Jr., "Dynamic Behavior of a Thermoelectric-Heat Pump," *Electro-Technol.*, Vol. 71, No. 2, p. 64, 1963.

#### Chapter VI

1. Kolenko, Ye. A., "A Method of Removing Mechanical Stress in a Thermopile," *Soviet Patent No. 13125*, No. 10, 1964.
2. Kolenko, Ye. A., *Belgian Patent No. 646,558*, 1964.
3. Kolenko, Ye. A., *French Patent No. 1,390,732*, 1964.
4. Yamono Masaru, Komatsu Sakanti, "The Thermoelectric Element," *Japanese Patent No. 5779*, 1962.
5. Clingman, W. H., "New Concepts in Thermoelectric Device Design," *Proceedings of the IRE*, Vol. 49, No. 7, p. 1155, 1961.
6. Clingman, W. H., "New Concepts in Thermoelectric Devices Design," *IRE Intern. Conv. Rec.*, Vol. 9, No. 6, p. 174, 1961.
7. Neuartige, "New Semiconductor Cooling Elements," *Techn. Rundschau*, Vol. 53, No. 20, p. 7, 1961.

8. Neuartige, "New Semiconductor Cooling Elements," *Electrotechn. und Maschinenbau*, Vol. 78, No. 14, p. 460, 1961.
9. "A New Thermoelement with an Outer Diameter of 0.34 mm," *Arch. techn. Messen.*, 309, R140, 1961.
10. "New Thermorefrigerator Elements with the Peltier Effect," *R. C. Composante Electron.*, No. 46, p. 7, 1963.
11. Rice, Warren, Flam Eric, "Design Data for Semiconductor Thermoelectric Devices," *Electro-Technol.*, Vol. 71, No. 3, p. 132, 1963.
12. Swanson, B. W., "Refrigerator Heat-Leak for Sandwiched Thermoelectric Elements," *Westinghouse Research Reports 8-0529-R27*, 1964.
13. "Thermoelectric Modules Work on Low Current," *Electronics*, Vol. 37, No. 22, p. 146, 1964.
14. "A Very Small Thermoelectric Device," *Elettronica*, Vol. 10, No. 4, p. 183, 1964.

#### Chapter VII

1. Anufriyev, V. M. and G. S. Belitskiy, *Teploperedacha i Aerodinamicheskoye Soprotivleniye Trubchatykh Poverkhnostey v Poperechnom Potoke* [Heat Transfer and Aerodynamic Resistance of Tubular Surfaces in a Transverse Flow], Energoizdat. Press, Moscow, 1948.
2. Gukhman, A. A., *Fizicheskiye Osnovy Teploperedachi* [The Physical Bases of Heat Transfer], Energoizdat. Press, Moscow, 1934.
3. Dul'nev, G. N., *Teploobmen v Radioelektronnykh Ustroystvakh* [Heat Transfer in Radioelectronic Devices], Gosenergoizdat. Press, Moscow-Leningrad, 1963.
4. Dul'nev, G. N. and N. N. Tariovskiy, "Heat Transfer from Radiators Under Natural Convection Conditions," *Inzh.-Fiz. Zhurn.*, No. 2, AN BSSR, 1960.
5. Kolenko, Ye. A., A. G. Shcherbina and V. G. Yur'yev, "A Method of Heat Removal from Semiconductor Cooling Devices," *ZhTF*, Vol. 28, No. 11, 1958.

6. *Konvektivnyy i Luchisty Teploobmen* [Convection and Radiant Heat Transfer], AN SSSR Press, Moscow-Leningrad, 1960.
7. Kondrat'yev, G. M., *Regulyarnyy Teplovoy Rezhim* [A Regulated Thermal Condition], GTTI, Leningrad-Moscow, 1954.
8. Kondrat'yev, G. M., *Teplovyye Izmereniya* [Thermal Measurements], Mashgiz. Press, Moscow, 1957.
9. Kutateladze, S. S. and V. M. Barshanskiy, *Spravochnik po Teploperedache* [Heat Transfer Reference Book], Gosenergoizdat. Press, Moscow, 1958.
10. Keys, V. M., *Igolchatyye Poverkhnosti dlya Teploobmena* [Spike Surfaces for Heat Transfer] (translated from the English), TsKTI Press, Moscow, 1956.
11. Mak-Adams, V., *Teploperedacha* [Heat Transfer], ONTI Press, Leningrad-Moscow, 1936.
12. Mikheyev, M. A., *Osnovy Teplootdachi* [The Fundamentals of Heat Transfer], Gosenergoizdat. Press, Moscow, 1956.
13. Petukhov, B. S., *Opytnoye Izucheniye Protsessov Teplootdachi* [An Experimental Study of Heat Transfer Processes], Gosenergoizdat. Press, Moscow, 1952.
14. Ramadan, A. M., *Intensifikatsiya Teplootdachi v Ustroystvakh Termoelektricheskogo Okhlazhdeniya* [Heat Transfer Intensification in Thermoelectric Cooling Devices], author's dissertation, Len. Tekhnol. Inst. Kholod. Promyshl., 1963.
15. Tulin, S. N., "Heat Transfer and Resistance in a Group of Pipes with Longitudinal Finning," *Teploenergetika*, No. 3, 1958.
16. Jacoby, J. N., "Long-Pin Approach to Dissipator Design," *Electronics*, Vol. 37, No. 24, 1964.
17. Katz, A., "Cooling High-Power Equipment by Forced Air Convection," *Electronics*, Vol. 37, No. 25, 1964.

## Chapter VIII

1. *Akkumulyatory, Elementy i Batarei* [Storage Batteries, Elements and Batteries], a handbook of state standards, Standartgiz. Press, Moscow, 1965.
2. Botoslovskiy, A. S., *Silovyye Poluprovodnikovyye Vypryamiteli* [Semiconductor Power Rectifiers], Voenizdat. Press, Moscow, 1965.
3. Voronin, A. N., *Poluprovodnikovyye Termoelektrogeneratory* [Semiconductor Thermoelectric Generators], Len. Doma Nauchno-Tekhn. Propagandy, 1957.
4. Devonisskiy, V. Yu., *Vypryamiteli na Germaniyevykh Diodakh* [Germanium Diode Rectifiers], Voenizdat. Press, Moscow, 1965.
5. Zhuravlev, A. A. and K. B. Mayzel', *Preobrazovateli Postoyannogo Toka na Transistorakh* [A Transistorized Direct Current Converter], Energiya Press, Moscow-Leningrad, 1964.
6. Zakharov, Yu. K., *Preobrazovateli Napryazheniya na Poluprovodnikovyykh Triodakh* [Semiconductor Triode Voltage Transformers], Voenizdat. Press, Moscow, 1964.
7. Iosel'son, G. L. and A. S. Dzyuba, "A Thermal Regulator for Semiconductor Theroelement Systems," *Izmerit. Tekhn.*, Vol. 5, No. 23, 1962.
8. *Kremniyevyye Upravlyayemye Ventili-Tiristory* [Silicon-Controlled Rectifiers-Theristors], a technical handbook (translated from the English), Energiya Press, Moscow-Leningrad, 1964.
9. Kulikov, I. G., *Akkumulyatory* [Storage Batteries], Oborongiz. Press, Moscow, 1958.
10. Naer, V. A. and V. A. Semenyuk, "The Influence of Current Ripple on the Characteristics of the Semiconductor Thermoelements of Heating and Cooling Devices," *Energetika*, Vol. 6, No. 31, 1963.
11. Orlov, V. A., *Malogabaritnyye Istochniki Toka* [Miniaturized Power Supplies], Voennoye Izdatel'stvo Min. Oborony SSSR, Moscow, 1965.
12. *Poluprovodnikovyye Vypryamiteli* [Semiconductor Rectifiers], a handbook of materials, TsBTI NII EP, Moscow, 1959.

13. Pomazonov, I. N. and E. L. Tikhomirov, "A Semiconductor Heat Pump on the Principle of the Combined Utilization of Thermoelectric Effects," *Izv. Len. Elektrotekh. Inst.*, No. 51, 1963.
14. *Izobrazovatel'nyye Ustroystva v Elektroenergetike* [Converters in Electrical Power Engineering], a handbook of articles, Nauka Press, Moscow, 1964.
15. Selektor, Ya. Z., *Germaniyevyye Vypryamiteli* [Germanium Rectifiers], TsBTI, Moscow, 1958.
16. *Selenovyye Vypryamiteli (Osnovnyye Tekhnicheskiye Dannyye)* [Selenium Rectifiers (Basic Technical Specifications)], TsBTI, Moscow, 1958.
17. *Silovaya Poluprovodnikovaya Tekhnika* [Power Semiconductor Engineering], a handbook, VNIIE, Moscow, 1965.
18. Yuditskiy, S. B., *Germanovyye i Kremniyevyye Silovyye Poluprovodnikovyye Vypryamiteli* [Germanium and Silicon Power Semiconductor Rectifiers], TsBTI NII EP, Moscow, 1958.
19. Corey, P. D. and A. L. Wellford, "A Controlled Rectifier Static Inverter for Intermittent Aircraft Duty," *IEEE Fall General Meeting*, CP60-130b, 1960.
20. Krieser, T. P., "Thermoelectricity Power Supply and Control," *IEEE International Convention Records*, Vol. 11, No. 3, 1963.

#### Chapter IX

1. Alatyrtsev, G. A. and Yu. N. Malevskiy, "The Connection of Thermoelements on the Base Pb -- Te and Bi<sub>2</sub>Te<sub>3</sub> -- Sb<sub>2</sub>Te<sub>3</sub>," *Teplo-energetika* [Thermal Engineering], third edition, AN SSSR Press, Moscow, 1961.
2. Angerer, Ye., *Laboratornaya Tekhnika* [Laboratory Technology], ONTI, Moscow-Leningrad, 1934.
3. Arkhangel'skiy, B. A., *Plasticheskiye Massy* [Plastics], Sudipromgiz. Press, Moscow-Leningrad, 1961.
4. Voronin, A. N. and R. Z. Grinberg, "A Method of Obtaining Briquettes for the Arms of a Thermoelement with Subsequent Thermal



Processing from  $\text{Bi}_2\text{Te}_3$  --  $\text{Sb}_2\text{Te}_3$  and  $\text{Bi}_2\text{Te}_3$  --  $\text{Bi}_2\text{Se}_3$  Alloys," *Termoelektricheskiye Svoystva Poluprovodnikov* [The Thermoelectric Properties of Semiconductors], Nauka Press, Moscow-Leningrad, 1963.

5. Voronin, A. N., R. Z. Grinberg and A. N. Savel'yeva, "The Prevention of 'Aging' in the Negative Arms of a Thermoelement," *Termoelektricheskiye Svoystva Poluprovodnikov* [The Thermoelectric Properties of Semiconductors], Nauka Press, Moscow-Leningrad, 1963.
6. Goncharenko, K. S., *Kratkiy Spravochnik Gal'vanotekhnika* [A Short Handbook in Galvanic Engineering], Mashgiz. Press, Moscow, 1955.
7. Drinberg, A. Ya., A. V. Gurevich and Ye. S. Tikhomirov, *Tekhnologiya Nemetallicheskikh Pokrytiy* [The Technology of Nonmetallic Coatings], Goskhimizdat. Press, Leningrad, 1957.
8. Ivanov, A. A., *Elektrovakuumnaya Tekhnologiya* [Electro-Vacuum Technology], Gosenergoizdat. Press, Moscow-Leningrad, 1944.
9. Kolenko, Ye. A., A. G. Tauber and A. G. Shcherbina, "A Method of Coupling the Stages in a Multi-stage Thermoelectric Pile," *Russian Patent No. 123,215. Byull. Izobr., Vol. 20*, 1959.
10. Kolenko, Ye. A. and A. G. Shcherbina, *British Patent No. 849,976*, 1959; *No. 878,481*, 1960; *No. 909,750*, 1960.
11. Kolenko, Ye. A. and A. G. Shcherbina, *USA Patents No. 3,097,425*, 1963; *No. 3,045,341*, 1960.
12. Kolenko, Ye. A. and A. G. Shcherbina, *Federal Republic of Germany Patent No. 1,152,002*, 1961.
13. Kolenko, Ye. A. and A. G. Shcherbina, *Indian Patents No. 76,574*, *No. 79,151*, *No. 76,576*, 1961.
14. Kolenko, Ye. A. and A. G. Shcherbina, *Belgian Patents No. 602,815*, *No. 609,922*, *No. 601,176*, *No. 602,813*, 1961.
15. Kolenko, Ye. A. and A. G. Shcherbina, *Egyptian Patents No. 3422*, *No. 4204*, *No. 3588*, 1961.
16. Kolenko, Ye. A. and A. G. Shcherbina, *Mexican Patent No. 64162*, 1961.

17. Kolenko, Ye. A. and A. G. Shcherbina, *French Patents* No. 1,322,472, 1962; No. 1,304,572, 1961; No. 1,389,705, 1962.
18. Kolenko, Ye. A. and A. G. Shcherbina, *Canadian Patents* No. 660,196, 1963; No. 667,082, 1963; No. 668,333, 1963.
19. Kolenko, Ye. A. and A. G. Shcherbina, *Italian Patent* No. 653,701, 1963; No. 680,850, 1961; No. 658,803, 1963; No. 645,457, 1961.
20. Kolenko, Ye. A. and A. G. Shcherbina, *Argentine Patents* No. 150,110, 1962; No. 729,262, 1962; No. 732,350, 1963.
21. Kolenko, Ye. A. and V. G. Yur'yev, "The Vacuum Properties of Epoxy Resin," *ZhTF*, Vol. 28, No. 10, 1958.
22. Finogenov, A. D., "The Galvanic Method of Connecting Thermo-elements," *Termoelektricheskiye Svoystva Poluprovodnikov* [Thermoelectric Properties of Semiconductors], Nauka Press, Moscow-Leningrad, 1963.
23. Espe, V. and M. Knol', *Tekhnologiya Elektrovakuumnykh Materialov* [The Technology of Electro-Vacuum Materials], Oborongiz. Press, Moscow, 1939.
24. Yampol'skiy, A. M., *Gal'vanotekhnika* [Galvanic Engineering], Mashgiz. Press, Moscow, 1952.
25. Beverly, Vincent Haba, "Method and Materials for Obtaining Low-Resistance Bonds to Bismuth Telluride (RCA)," *USA Patent* No. 3,017,033, 1963.
26. Hänlein, W., "The Technological Problems in the Use of the Peltier Effect," *Kältetechnik*, Vol. 12, No. 5, p. 137, 1960.
27. Heaten, A. G., "Thermoelectrical Engineering," *Proceedings of the IEEE*, Vol. 109, No. 45, p. 223, 1962.

#### Chapter X

1. Kolenko, Ye. A., "A High-Vacuum Collector with Thermoelectric Cooling," *PTE*, Vol. 3, 1957.
2. Kolenko, Ye. A., *British Patent* No. 901,890, 1959.

3. Kolenko, Ye. A., *Indian Patent No. 26740*, 1961.
4. Kolenko, Ye. A., *Belgian Patent No. 804,949*, 1961.
5. Kolenko, Ye. A., *Egyptian Patent No. 4276*, 1961.
6. Kolenko, Ye. A., *Italian Patent No. 647,731*, 1961.
7. Kolenko, Ye. A., *Argentine Patent No. 130,502*, 1962.
8. Kolenko, Ye. A., *French Patent No. 1,290,025*, 1962.
9. Kolenko, Ye. A., *USA Patent No. 3,102,290*, 1963.
10. Kolenko, Ye. A., A. G. Tauber, V. G. Yur'yev and A. G. Shcherbina,  
*Termoelektricheskaya Vyshevakuummaya Lavashka dlya Nasosa N-5*  
[A Thermoelectric High-Vacuum Collector for the N-5 Pump], *FTT*,  
AN SSSR Press, Moscow-Leningrad, 1959.
11. Kolenko, Ye. A., A. G. Tauber, V. G. Yur'yev and A. G. Shcherbina,  
*Termoelektricheskaya Vyshevakuummaya Lavashka dlya Nasosa*  
*TsVL-100* [A Thermoelectric High-Vacuum Collector for the  
TsVL-100 Pump], a handbook of TsNIIEIN, subject 31, No. P-60-11/1,  
1960.
12. Jean, R. and R. Liot, "Drawbacks in the Peltier Effect," *Vide*,  
Vol. 17, No. 98, p. 186, 1962.
13. Poslawski, R. P., "Thermoelectric Cooling Improved Baffles for  
Vacuum Pumps and Systems," *Canadian Electrical Engineering*,  
Vol. 5, No. 2, 1961.
14. Poslawski, R. P., "Developing a Thermoelectric Baffle," *Electron.*  
*Ind.*, Vol. 21, No. 5, p. 106, 1962.
15. Reich, G. von, H. G. Nöller, "Partial Pressure Analyses of the End  
Pressure of Oil Diffusion Pumps with an Omegatron," *Zangew.*  
*Phys.*, Vol. 12, 1957.
16. "Thermoelectric Vacuum Baffles Semiconductor Elements,"  
*Electronics*, Vol. 33, No. 51, p. 110, 1960.

## Chapter XI

1. Kolenko, Ye. A., Kh. V. Protopopov, D. G. Fleyshman and V. G. Yur'yev, "Thermoelectric Photomultiplier Cooling," *PTE*, Vol. 3, p. 140, 1959.
2. Mount, T. E. and I. K. Hughes, "Peltier Cooler Operates on Low Current," *Electronic Design*, Vol. 9, No. 4, p. 10, 1961.
3. "Peltier Cooling Advanced," *Missiles and Rockets*, Vol. 8, No. 7, p. 23, 1960.
4. Robertson, J., "The Designs Minute TE Heat Pump," *Electron. News*, Vol. 7, No. 310, p. 53, 1962.
5. Standon, Sidney, "Thermopile Held Advancing IR Detection Capabilities," *Electron. News*, Vol. 8, No. 391, 1963.

## Chapter XII

1. Ivanov, A. M., Ye. A. Kolenko and U. Kh. Poltinnikov, "A Thermoelectric Cataract Cryoextractor," *Soviet Patent No. 156,659*, *Izv. Akad. Nauk SSSR*, No. 10, 1964.
2. Kolenko, Ye. A., "A Microtome Stage with Thermoelectric Cooling," *Med. Promyshl. SSSR*, Vol. 3, 1959.
3. Kolenko, Ye. A., A. A. Isaakyan and A. G. Shcherbina, "A Thermoelectric Device for Temperature Stimulation of the Skin," *Fiziol. Zhurn.*, Vol. 65, No. 11, 1959.
4. Kolenko, Ye. A. and I. Kh. Poltinnikov, "Intercapsular Extraction of Cataracts with a Semiconductor Device," *Oftal'molog. Zhurn.*, Vol. 8, 1964.
5. Price, D. L. and I. Levin, "New Biological Warm Stage," *Amer. J. Trop. Med. and Hyg.*, Vol. 10, No. 5, p. 755, 1961.

## Chapter XIII

1. Valitov, R. A. and A. I. Aleksandrov, "A Thermostat Employing Semiconductors," *Izmerit. Tekhn.*, Vol. 1, 1957.

2. Iordapishvili, Ye. K. and L. G. Tkulich, "A Semiconductor Thermostat for Automatic Generators," *EHTE*, Vol. 27, No. 6, 1959.
3. Kolenko, Ye. A., V. A. Kurilov, A. E. Tauber and A. G. Shcherbina, *Elektronnyy Ul'tratermostat* [An Electronic Ultrathermostat System], handbook of TsNITEIN, No. 4, 1958.
4. Beaubien, D. J., "A Thermoelectric Chamber Stabilizes p-c Boards," *Electronics*, Vol. 35, No. 33, 64, 66, 68, 1962.
5. Fay, L. E., "Thermoelectric Junction Cools Transistors for Temperature Testing," *Electron. Design*, Vol. 8, No. 23, 1961.
6. Fortier, I. R. and C. S. Thompson, *Cooling Transistors with Thermoelectric Elements. Tunnel-Diode and Semiconductor Circuits*, McGraw-Hill Book Company, Inc., New York-Toronto-London, p. 276, 1963.
7. Goldsmid, H. Hilbourne, "Transistor Operation Aided by Thermoelectric Refrigeration," *Brit. Commun. Electronics*, Vol. 7, No. 26, 1961.
8. Jeanes, R. V. and K. E. C. Pitt, "Thermoelectrically Cooled Probe for the Determination of Semiconductor Type," *J. Scient. Instrum.*, Vol. 38, No. 1, p. 33, 1961.
9. Lautz, G., "Thermoelectric Temperature Stabilization of an Electrical Circuit Element," *ETZ*, Vol. A80, No. 21, p. 741, 1959.
10. Little, E. P., "Cooling of Avionic Equipment bby Thermoelectric Methods," *IEEE Trans. Aerospace*, Vol. 2, No. 2, p. 702, 1964.
11. Nagata Minoru, Abe Zenemon, "Thermoelectric Elements for Circuit Cooling," *Electronics*, Vol. 34, No. 41, p. 54, 1961.
12. Nagata Minoru, Abe Zenemon, *Thermoelectric Elements for Circuit Cooling. Tunnel-Diode and Semiconductor Circuits*, New York, Toronto, London, 1964.
13. Stubstad, W. R., "The Application of Thermoelectric Spot Cooling to Electronic Equipment," *IRE Trans.*, PEP-5, No. 4, p. 22, 1961.
14. "Thermoelectric Cooler Module Application Consideration," *Electromech. Design*, Vol. 8, No. 3, p. 54, 1964.

15. "Thermoelectric Cooling Improves Noise Figure," *Electronics*, Vol. 33, No. 44, p. 86, 1960.
16. Uenahara, M. and R. Wolfe, "Parametric Amplifier with Thermoelectric Refrigeration," *IRE Trans.*, Vol. ED-8, No. 6, p. 521, 1961.

#### Chapter XIV

1. Voronin, A. N., E. A. Sher and A. G. Shcherbina, "A Precision Semiconductor Null-Thermostat," *ETP*, No. 4, 1961.
2. Voronin, A. N., A. G. Shcherbina and V. N. Rybal'chenko, *Poluprovodnikovyye Gidrometry* [A Semiconductor Hygrometer], TSNIIEIN, No. 11, 1961.
3. Gol'tsman, M. I., *Osnovy Metodiki Aerofizicheskikh Izmereniy* [Fundamental Methods of Aerophysical Measurements], GIFML, Moscow, 1950.
4. Czyuba, A. S. and P. B. Kantor, "A Semiconductor Thermostat System for Checking Thermometers," *Izvesti. Tekhn.*, No. 1, 1959.
5. Kmito, A. A. and A. A. Ledonovich, "A Laboratory Condensation Hygrometer," *Kanadskaya Labor.*, No. 4, 1960.
6. Kolenko, Ye. A., *British Patent No. 864,472*, 1959.
7. Kolenko, Ye. A., *Federal Republic of Germany Patent No. 1,144,741*, 1961.
8. Kolenko, Ye. A., *Indian Patent No. 76,078*, 1961.
9. Kolenko, Ye. A., *Belgian Patent No. 696,948*, 1961.
10. Kolenko, Ye. A., *Egyptian Patent No. 4333*, 1961.
11. Kolenko, Ye. A., *Italian Patent No. 646,413*, 1961.
12. Kolenko, Ye. A., *Argentina Patent No. 134,003*, 1963.
13. Kolenko, Ye. A., *Canadian Patent No. 673,748*, 1964.
14. Kolenko, Ye. A. and A. G. Shcherbina, *British Patent No. 838,410*, 1960.

15. Kolenko, Ye. A. and A. G. Shcherbina, *French Patent No. 1,786,522*, 1961.
16. Kolenko, Ye. A. and A. G. Shcherbina, *Indian Patent No. 26,526*, 1961.
17. Kolenko, Ye. A. and A. G. Shcherbina, *Belgian Patent No. 606,814*, 1961.
18. Kolenko, Ye. A. and A. G. Shcherbina, *Egyptian Patent No. 4400*, 1961.
19. Kolenko, Ye. A. and A. G. Shcherbina, *Italian Patent No. 646,023*, 1961.
20. Kolenko, Ye. A. and V. G. Yur'yev, "A Hygrometer with Thermoelectric Cooling," *ITE*, No. 4, 1959.
21. Kolenko, Ye. A., "New Thermal Cooling Devices," *Termoelektricheskiye Svoystva Poluprovodnikov* [Thermoelectric Properties of Semiconductors], AN SSSR Press, Moscow-Leningrad, 1963.
22. Kolenko, Ye. A., "A Semiconductor Thermostat System for Laboratory Purposes," *Radio i Svyaz*, Vol. 10, 1963.
23. Kolenko, Ye. A., "A Thermoelectric Condensation Hygrometer," *Zavodskaya Labor.*, No. 9, 1965.
24. Kolomoiets, P. V., L. S. Stil'bans and N. T. Fateyev, "Measuring Air Humidity by Means of Semiconductor Thermocouples," *SHTF*, Vol. 24, No. 3, 1956.
25. Fateyev, N. P., "A New Automatic Condensation Hygrometer," *Tr. Gl. Geofiz. Observ.*, No. 83, 1958.
26. Fateyev, N. P., "A Stationary Dew Point Hygrometer," *Tr. Gl. Geofiz. Observ.*, No. 103, 1960.
27. Khasimoto Akira and Tsunako Masao Khitati Kendi and Kabusiki Kaysya, "A Thermoelectric Refrigerator with a Device for Controlling The Temperature," *Japanese Patent No. 6840 No. 13691*, 1961.
28. Crowley, I. C. W., "A Cooled Microscope Stage Using Semiconductor Thermoelectric Cooling," *J. Scient. Instrum.*, Vol. 40, No. 6, p. 330, 1963.

29. Gerthsen, P., J. A. A. Gilsing and M. Til, "An Automatic Dew Point Device with Peltier Cooling," *Philips Techn. Rundschau*, Vol. 27, No. 7, p. 211, 1959/60.
30. Landay, I., "Thermoelectric Thermostat," *Rev., Scient. Instr.*, Vol. 33, No. 9, p. 1004, 1962.
31. Ramert, Bohumil, "A Small Thermoelectric Thermostat," *Sdelovaci Techn.*, Vol. 11, No. 7, p. 269, 1963.

#### Chapter XV

1. Voronin, A. N., S. G. Platonova, Ye. G. Pokornyy and E. M. Sher, "A Thermoelectric Domestic Refrigerator with a Capacity of 20 Liters," *Termoelektricheskiye Svoystva Poluprovodnikov* [Thermoelectric Properties of Semiconductors], AN SSSR Press, Moscow-Leningrad, 1963.
2. Kolenko, Ye. A. and A. G. Shcherbina, "A Thermoelectric Domestic Refrigerator," *Len. Promysh.*, Vol. 1, No. 57, 1958.
3. Lukomskiy, S. M., "The Application of Semiconductors for the Heating and Cooling of Living Quarters," *Zhishishehn. Stroit.*, No. 10, 1959.
4. *Energosnabzheniye i Konditsionirovaniye Vozdukha na Transporte* [Power and Air Conditioning for Transport], conference materials, Zinatne Press, Riga, 1965.
5. Anderson, J. R., "Thermoelectric Air Conditioner for Submarines," *RCA Rev.*, Vol. 22, No. 2, p. 292, 1961.
6. Elfving, T. M., "The Construction and Operation of an Air-Cooled Thermoelectric Refrigerator," *Kältetechnik*, Vol. 14, No. 3, p. 76, 1962.
7. Hudelson, G. D., "Thermoelectric Air Conditioning of Totally Enclosed Environments," *Electrical Engineering*, Vol. 79, No. 6, p. 460, 1960.
8. Ott, L. H., "Electronic Cooling and Heating," *Radio Electronics*, Vol. 33, No. 1, p. 26, 1962.



9. Sickert, R. G., "A Thermoelectric Refrigerating System for Submarines," *Electrical Engineering*, Vol. 79, No. 5, p. 364, 1960.
10. "Thermoelectric Air Conditioning System for Submarines," *Progress Reports of Bureau of Ships from Research and Development Division*, Carrier Corporation, New York.

#### Chapter XVI

1. Bardeyeva, S. P., I. A. Ioffe, M. A. Kaganov and A. F. Chudnovskiy, "Semiconductor Devices for Cooling Milk," *Mekhaniz. i Elektrifik. Sots. Sel'sk. Khoz.*, No. 5, 1961.
2. Bardeyeva, S. P., I. A. Ioffe, M. A. Kaganov and A. F. Chudnovskiy, "A Semiconductor Cooler for Liquid Flows," *Handbook of TSNITEIN*, No. 11, 1962.
3. Kaganov, M. A., "Semiconductor Devices for the Cooling of Milk," *Vestn. S.-Kh. Nauki*, No. 3, 1961.
4. Kaganov, M. A., I. S. Lisker, I. G. Mushkin and A. F. Chudnovskiy, "A Semiconductor Thermostat System for the Storage and Transportation of the Sperm of Farm Animals," *Byull. Nauchno-tekhn. Inform. po Agrofizike*, No. 4, 1958; No. 5-6, 1959.
5. Kolenko, Ye. A., "New Thermocooling Devices," *Termoelektricheskiye Svoystva Poluprovodnikov* [Thermoelectric Properties of Semiconductors], AN SSSR Press, Moscow-Leningrad, 1963.
6. Kolenko, Ye. A., G. R. Brekht, V. R. Paradenko and P. G. Ivanov, "An Automatic Device with Cyclic Operation for the Determination of the Solidification Point of Fuels," *Soviet Patent No. 161865. Byull. Izobr.*, No. 22, 1962.
7. Kolenko, Ye. A. and M. A. Kaganov, E. G. Mushkin and A. F. Chudnovskiy, "A Semiconductor Refrigerator for Stock Raising," *Byull. Nauchno-tekhn. Inform. po Agrofizike*, No. 4, 1958.
8. Kolenko, Ye. A., E. G. Mushkin, A. G. Tauber and A. G. Shcherbina, "A Miniature Thermoelectric Refrigerator for Stock Raising," *Soviet Patent No. 122,077. Byull. Izobr.*, No. 16, 1959.
9. Kolenko, Ye. A., A. G. Tauber and A. G. Shcherbina, "A Thermoelectric Device for the Measurement of Liquid Heat Content," *Soviet Patent No. 122,900. Byull. Izobr.*, No. 19, 1959.

10. Lisker, I. S. and A. F. Chudnovskiy, "An Adiabatic Semiconductor Refrigerating Thermostat System," *Byull. Nauchno-tekhn. Inform. po Agrofizike*, No. 7, 1960.
11. Martynovskiy, V. A. and V. A. Naer, "Semiconductor Water Cooler," *Kholodil'n. Tekhn.*, No. 4, 1960.
12. Martynovskiy, V. A. and V. A. Naer, "An Evaporation Device," *Kholodil'n. Tekhn.*, No. 4, 1960.
13. Naer, V. A., "A Study of an Evaporating Device," *FTT*, No. 8, 1959.
14. Naer, V. A. and S. A. Rozhentsova, "A Semiconductor Liquid Cooler," *Kholodil'n. Tekhn.*, No. 1, 1963.
15. Pomazanov, I. N. and P. L. Tikhomirov, "Thermoelectric Cooling As a Result of Heat from Low-Potential Sources," *Termoelektricheskiye Svoystva Poluprovodnikov* [Thermoelectric Properties of Semiconductors], AN SSSR Press, Moscow-Leningrad, 1963.
16. Chudnovskiy, A. F., S. P. Bardeyeva, I. A. Ioffe and M. A. Kaganov, "A Counter-Flow Cooler for Liquid Flows," *TsNITEIN*, No. 3, 1961.
17. Chudnovskiy, A. F., M. A. Kaganov, Ye. A. Kolenko and I. G. Mushkin, "A Refrigerating Thermostat System for the Storage of Biological Objects," *Byull. Nauchno-tekhn. Inform. po Agrofizike*, No. 6, 1959.
18. Yamakov, I. V., "Semiconductor Thermoelement Devices," *Mashino-stroyeniye*, Vol. 11, No. 12, 1962.
19. Kelly, J. C. R., "Thermoelectric Applications to Industrial Problems," *IRE Trans. Ind. El.*, Vol. 9, No. 1, p. 61, 1962.
20. Krieser, Thomas P., "Thermoelectricity. Power Supply and Control," *IEEE Internat. Convent. Rec.*, Vol. 11, No. 3, p. 37, 1963.
21. "Contemporary Instrumentation. 'Frigitrons' and Their Application," *R. R. Nature Sci. Progr.*, No. 3341, p. 387, 1963.
22. Makow, D. M., "Portable Thermoelectric Pump Controls Heating or Cooling of Single Component," *Canadian Electronics Engineering*, Vol. 7, No. 8, p. 26, 1963.

23. Masuda Sadayoshi and Murakami Yukio, "Thermoelectric Cooling Element As Thermal Conductivity Meter," *Bull. J. SME*, Vol. 6, No. 22, p. 251, 1963.
24. Morioka, G., "Thermoelectric Cooling and Its Applied Products," *Radio and TV*, Vol. 5, No. 6, p. 24, 1962.
25. Müller, Heinz, "Construction and Operational Requirements of Peltier Installations in Cooling Equipment," *Siemens-Z.*, Vol. 37, No. 5, p. 383, 1963.
26. Rezek, Gerard, "Thermal Design and Analog Representation of a Thermoelectric Refrigerator," *IEEE Internat. Convent. Rec.*, Vol. 11, No. 6, p. 188, 1963.
27. Röhme, Bernhard, "Cooling Elements in Reference to the Peltier Effect on a Semiconductor Basis," *Electronic*, Vol. 11, No. 8, p. 225, 1962.
28. "Thermoelectric Modules Cooling Heating," *Proceedings of the IRE*, Vol. 49, No. 11, 1961.

#### Literature on the General Problems of Thermoelectric Cooling

1. Goldsmid, G., *Primeneniye Termoelektricheskova* [The Application of Thermoelectricity], Fizmatgiz. Press, Moscow, 1963.
2. Zhuze, V. P. and Ye. I. Gusenkova, *Bibliografiya po Termoelektricheskstvu (Termoelektrogeneratory i Okhlazhdayushchiye Ustroystva)* [A Bibliography in Thermoelectricity (Thermoelectric Generators in Cooling Devices)], AN SSSR Press, Moscow-Leningrad, 1963.
3. Ioffe, A. F., *Poluprovodniki v Sovremennoy Fizike* [Semiconductors in Contemporary Physics], AN SSSR Press, Moscow, 1955.
4. Ioffe, A. F., *Fizika Poluprovodnikov* [The Physics of Semiconductors], AN SSSR Press, Moscow-Leningrad, 1957.
5. Ioffe, A. F., L. S. Stil'bans, Ye. K. Iordanishvili and T. S. Stavitskaya, *Termoelektricheskoye Okhlazhdeniye* [Thermoelectric Cooling], AN SSSR Press, Moscow-Leningrad, 1956.
6. Kolenko, Ye. A. and A. R. Regel', "Thermoelectric Cooling and Its Practical Application," *Vestnik AN SSSR*, No. 5, 1964.

7. Zhuze, V. P. (editor), *Nauchnaya Literatura po Poluprovodnikam. Bibliografiya (1920-1956)* [Study Materials for Semiconductors. A Bibliography (1920-1956)], AN SSSR Press, Moscow-Leningrad, 1955.
8. Sominskiy, M. S., "The Development of Thermoelectric Electronics," *Vestnik AN SSSR*, No. 5, 1962.
9. *Termoelektricheskiye Materialy i Preobrazovateli* [Thermoelectric Materials and Converters], Mir Press, Moscow, 1964.
10. "Application of 'Frigitrons'," *Mesures et Controle Industr.*, Vol. 28, No. 309, 1963.
11. Bean, J. E., "Applications of Thermoelectric Cooling," *Industrial Electronics*, Vol. 1, No. 3, p. 132, 1962.
12. Bean, J. E., "Thermoelectric Cooling," *Industrial Electronics*, Vol. 1, No. 2, p. 110, 1962.
13. Beer, A. C., "Physics of Thermoelectricity," *Progr. Astronaut. and Rocketry*, London, Vol. 3, No. 4, p. 3, 1961.
14. Birkholz, V., "Progress in the Development of the Semiconductor Thermoelement," *Halbleiterprobleme*, No. 6, Vol. 206, 1961.
15. Blatt, F. J., "On the Possibility of Thermoelectric Refrigeration at Very Low Temperatures," *Phil. Mag.*, Vol. 7, No. 76, p. 715, 1962.
16. Bohme, B., "Cooling Elements in Reference to the Peltier Effect on a Semiconductor Basis," *Electronic*, Vol. 11, No. 8, p. 225, 1962.
17. Burnett, T. B., H. O. Lorch and J. E. Thompson, "Some Problems in the Development of a Commercial Thermoelectric Refrigerator," *Brit. J. Appl. Phys.*, Vol. 12, No. 11, p. 595, 1961.
18. Clingman, W. H., "New Concepts in Thermoelectric Devices Design," *IRE Intern. Conv. Rec.*, Vol. 9, No. 6, p. 174, 1961; *Proceedings of the IRE*, Vol. 49, No. 7, p. 1155, 1961.
19. "The Frigistor -- a New Semiconductor in Cooling Technology," *Sonenelektronen*, Vol. 7, No. 22, 1961.
20. "Design Details Outlined for Thermoelectric Unit," *Electron. Design*, Vol. 9, No. 3, p. 6, 1961.

21. Eichhorn, R. L., "A Review of Thermoelectric Refrigeration," *Proceedings of the IEEE*, Vol. 51, No. 5, p. 721, 1963.
22. Elfving, T. M., "Study of Design Problems and Mode of Operation for Thermoelectric Refrigerators," *ASHRAE Journal*, Vol. 5, No. 10, p. 69, 1963.
23. Frant, E. W., R. S. Lackey and H. A. Wagner, "Thermoelectric Spot Cooling Applications," *IRE Wisconsin Convention Records*, Vol. 3, No. 6, p. 136, 1959.
24. Gasser, F. W., "Thermoelectric Cooling -- a New Use for Semiconductors," *Schweiz. Techn. Z.*, Vol. 58, No. 36, p. 733, 1961.
25. Goltsmid, H. J., *Thermoelectric Refrigeration*, Plenum Press, New York, 1964.
26. Griffith, M. V., "Thermoelectric Refrigeration," *Advancements Sci.*, Vol. 18, No. 72, p. 135, 1961.
27. Guennoc, "'Frigatrons'," *Toute Electron*, Vol. 30, No. 278, p. 292, 1963.
28. "The Semiconductor As an 'Ice Machine'," *Funkschau*, Vol. 34, No. 5, p. 106, 1962.
29. Hänlein, W., "Semiconductor Cooling Elements," *Bull. Schweiz. Electrotechn. Vereins*, Vol. 55, No. 4, p. 142, 1964.
30. Heaton, A. G., "Thermoelectric Cooling Material Characteristics and Applications," *Proceedings of the Institute of Electrical Engineers*, Vol. 110, No. 7, p. 1277, 1963.
31. Horvay, I. B., "Thermoelectric Transients," *IEEE Trans. Applic. and Ind.*, Vol. 66, No. 111, 1963.
32. Kluth, H., "Possibilities in Thermoelectric Cooling," *Industriekurier Techn. und Forsch.*, Vol. 15, No. 17, p. 269, 1962.
33. Lautz, Günter, "Thermoelectric Effects and the Possibilities of Their Practical Application," *Math.-Phys. Semesterber.*, Vol. 10, No. 1, p. 14, 1963.
34. Marioka, G., "Thermoelectric Cooling and Its Applied Products," *Radio and TV*, Vol. 5, No. 6, p. 24, 1962.

35. Mclean, I., "Solid-State Cooling System Impractical, AF Study Shows," *Electron. News*, Vol. 9, No. 447, p. 58, 1964.
36. Ott, L. H., "Electronic Cooling and Heating," *Radio Electronics*, Vol. 33, No. 1, p. 26, 1962.
37. Parrot, J. E. and A. W. Penn, "Applications of the Peltier Effect," *AEI Engineering*, Vol. 2, No. 4, p. 202, 1962.
38. Penrod, E. B., "The Bases of Thermoelectric Cold Production," *Kaltetechn.*, Vol. 15, No. 8, p. 219, 1963.
39. Poset, Zdeněk, "Thermoelectric Cooling," *Sdělovací Tehn.*, Vol. 12, No. 7, 1964.
40. Re, Robert K., "Semiconductor Cooling Devices Survey," *Military Industr. Syst. Design*, Vol. 7, No. 4, p. 20, 1963.
41. Robert, L., "Proportional Temperature Controller for Thermoelectric Coolers," *Rev. Scient. Instrum.*, Vol. 34, No. 11, p. 1277, 1963.
42. Robert, L., "The Outlook for Thermoelectric Devices," *Electron. Industr.*, Vol. 22, No. 6, pp. D6-D9, 1963.
43. Robertson, J. T. S., "The Design of a Miniature TE Heat Pump," *Electron. News*, Vol. 7, No. 310, p. 53, 1962.
44. Romaine, O., "Thermoelectric Cooling Space," *Aeronaut.*, Vol. 38, No. 2, 1962; *Research and Development Technician's Handbook*, f15-f19, 1962-1963.
45. Sagel, K., "Bases and Problems of Thermoelectric Cold Production," *VDI Zs.*, Vol. 104, No. 7, 1962.
46. Heikes, R. R. and R. W. Ure (editors), *Thermoelectricity Science and Engineering*, Interscience Publishers, 1961.
47. Wright, T. A., "New Ways in Thermoelectricity," *Brit. J. Appl. Phys.*, Vol. 15, No. 3, 1964.
48. Zecher, W., "Peltier Cooling," *Philips Techn. Rundschau*, Vol. 8, No. 205, 1965.

UNCLASSIFIED

Security Classification

## DOCUMENT CONTROL DATA - R &amp; D

(Security classification of title, body of abstract and indexing annotation must be entered when the source report is classified)

1. ORIGINATING ACTIVITY (Corporate author) Foreign Science and Technology Center US Army Materiel Command Department of the Army		2a. REPORT SECURITY CLASSIFICATION <b>UNCLASSIFIED</b>	
		2b. GROUP	
3. REPORT TITLE  THERMOELECTRIC COOLING DEVICES			
4. DESCRIPTIVE NOTES (Type of report and inclusive dates) • Translation			
5. AUTHOR(S) (First name, middle initial, last name)  Ye. A. Kolenko			
6. REPORT DATE 26 June 69	7a. TOTAL NO. OF PAGES 338	7b. NO. OF REFS N/A	
8a. CONTRACT OR GRANT NO.		8b. ORIGINATOR'S REPORT NUMBER(S)	
9. PROJECT NO.  9223628 2301		FSTC-HT-23- 435-68	
10. AMSEL-WI-MF		11. OTHER REPORT NO(S) (Any other numbers that may be assigned this report) ACSI Control Number J-6003	
12. DISTRIBUTION STATEMENT  This document has been approved for public release and sale; its distribution is unlimited.			
13. SUPPLEMENTARY NOTES		14. SPONSORING MILITARY ACTIVITY US Army Foreign Science and Technology Center	
15. ABSTRACT  The book is dedicated to one of the youngest but rapidly developing fields of contemporary refrigeration engineering--that of thermoelectric cooling. The physical nature of thermoelectric cooling is set forth in an accessible format, with design and construction methods for thermoelectric cooling devices intended for various purposes. Various thermoelectric cooling devices are described which are intended for use in scientific practice and engineering. A large section of the book is devoted to the utilization of thermoelectric cooling in medicine.  This publication is intended for the wide group of readers engaged in the development and application of thermo-electric cooling devices, and also for students of refrigeration institutes.			

DD FORM 1473

REPLACES DD FORM 1473, 1 JAN 67, WHICH IS OBSOLETE FOR ARMY USE.

UNCLASSIFIED  
Security Classification

UNCLASSIFIED  
Security Classification

14 KEY WORDS	LINK A		LINK B		LINK C	
	ROLE	WT	ROLE	WT	ROLE	WT
thermoelectric pile n-type conductivity hole mobility impurity conductor coefficient of performance refrigerating capacity heat transfer resistance cry o extractor silicon-controlled rectifier micro thermistor						

UNCLASSIFIED  
Security Classification